EXPLORING THE ROLE OF CD248/ENDOSIALIN/TEM-1 ON LYMPHOID STROMAL CELLS IN SECONDARY LYMPHOID ORGANS

by

NATHALIE PAULINE ELIZABETH STEINTHAL

A thesis submitted to the University of Birmingham for the degree of DOCTOR OF PHILOSOPHY

Institute of Inflammation and Ageing

School of Medical and Dental Sciences

University of Birmingham

September 2016

Abstract

CD248 is a pericyte-associated, mesenchymal stem cell (MSC) marker that is highly expressed during embryological life. This expression is down regulated during development, becoming restricted on lymphoid stroma to the capsule, but reappearing during inflammation, as well as in a number of disease states (Lax et al., 2007). CD248 has been shown to play a role in controlling the differentiation of MSC to osteoblasts, both in *vitro* and *in vivo*, achieving this effect by modulating PDGFRβ signalling, as treatment with the PDGFRβ inhibitor imatinib mesylate phenocopies the effects seen in the $CD248^{-/-}$ mouse (Naylor et al., 2012).

Here we present evidence that CD248 is involved in the differentiation of MSC, via PDGFRβ signalling, into lymphoid stroma progenitors both *in vitro* and *in vivo.* In adult mice expression of CD248 is detected on FDCs following immunisation. Using $CD248^{-/-}$ mice, we observe that FDC networks in $CD248^{-/-}$ mice do not form normally and lack the reticular, dendrite-like structure typical of FDCs. This defect associates with a reduction in the functionality of the germinal centres.

Embryonic development of lymph node stroma occurs in a stepwise manner with progressive upregulation of VCAM and ICAM on resident mesenchyme. In the adult stroma, recent work has established links between different stromal cell subtypes; Jarjour *et al*. (2014) used a fate mapping technique to discover that marginal reticular cells are able to differentiate to follicular dendritic cells in response to immune challenge. Contrasting evidence shows that FDC in the spleen derive from ubiquitous perivascular precursors, likely to be pericytes (Krautler et al., 2012).

Acknowledgements

I must begin by thanking my supervisors Dr Francesca Barone, Dr David Withers and Dr Jorge Caamaño for all of their help throughout this process. Thank you for giving me this opportunity and for the support you have given to help me complete this research. Special thanks must go to Francesca, for always believing in me, and for never letting me give up, and to Dave, for stepping up and being incredibly helpful while Francesca was on maternity leave. I must also take the opportunity to thank Prof. Chris Buckley for his advice and help, and for creating a group as helpful and considerate as the RRG.

Thanks must also go to all of the past and present members of the RRG for their support and help throughout the years. Some of these experiments would not have been possible without the advice and guidance I have received from members of the group, and I would like to take the time to thank Dr David Gardner, Dr Saba Nayar, Dr Amy Naylor, Dr Jennifer Marshall, Dr John O'Neil, Joana Campos, Mike Ridley, Dr Debbie Hardie, Dr Guillaume Desanti and Dr Martin Fitzpatrick for all of their help with various parts of this research. Many other people have also provided invaluable assistance, including Dr Kai Toellner and Dr Yang Zhang. These experiments would also never have been possible without the help of the BMSU staff, especially Ian Ricketts, Claire Willis, Claire Lyons and Tracey Ballinger. To everyone that has helped with this project, thank you so much for your assistance, it would not have been possible for me to get to this stage without you all.

I must also thank the RRG for being such a warm and welcoming group. You have all made me feel as though Birmingham is my home, and made sure that I was well supplied with cake at all times. Your friendship has helped me get through the tough times and has made those difficult times few and far between! I must thank Joana, Saba, Jane Falconer, Holly Adams, Martin, Jenny, John and Amy especially for always being there when I needed someone to talk to. I will miss working in such a wonderful environment.

Finally, I must acknowledge all of the emotional support that I have received in completing this thesis. To my partner, Andy Lakin; I could not have done this without you. Thank you for being my rock and for helping me to keep some sense of normality through this slightly crazy time. I must also thank my parents, Tony and Jan, my sister Julia, and the rest of my family for their support. To all of my wonderful friends, old and new, thank you all of your support and for keeping me supplied with plenty of gin!

Words cannot adequately express how grateful I am to each and every one of you, but hopefully this will go some way to thanking you all.

"A good writer possesses not only his own spirit, but also the spirit of his friends"

Frederich Nietzsche

List of Abbreviations

-/-	Knock-out
+	Positive
-	Negative
ABL	Abelson murine leukemia viral oncogene homolog 1
ADSCs	Adipocyte derived stromal cells
Ag	Antigen
AID	Activation induced cytidine deaminase
APC	Antigen presenting cells
APRIL	A proliferation-inducing ligand (Tnfsf13)
BAFF	B-cell activating factor (Tnfsf13b)
Bapx1	Bagpipe homeobox homolog 1
BCA	B cell attracting chemokine (CXCL13)
Bcl-6	B cell lymphoma-6
BCR	B-cell receptor
BEC	Blood endothelial cells
BER	Base excision repair
Blimp-1	B lymphocyte-induced maturation protein-1
BM	Bone-marrow
BP-3	Bone marrow stromal cell antigen-1
BRC	B-cell zone fibroblastic reticular cell
BSA	Bovine serum albumin
C/EBPα	CCAAT/enhancer-binding protein alpha
CCL	C-C motif chemokine ligand
CCR	Chemokine (C-C) motif
CD	Cluster of differentiation
Clec-2	C-type lectin-like receptor 2
CLP	Common lymphoid precursors
c-Fos	Subunit of the activator protein 1 transcription factor
CR	Complement receptor
CSR	Class switch recombination
CTLD	C-type lectin domain
CXCL	C-X-C motif chemokine ligand
CXCR	Chemokine (C-X-C motif) receptor
DCs	Dendritic cells
DL4	Delta like 4
DN	Double negative
DNA	Deoxyribonucleic acid
DNase	Deoxyribonuclease
DSBs	Double strand breaks
DZ	Dark zone
E	Embryonic development day
E2A	E-box protein enhancer

EBI2	Epstein-Barr virus induced molecule-2, or GPR183
EPCAM	Epithelial cell adhesion molecule
ERTR7	Clone of antibody that detects reticular fibroblasts and reticular fibres in lymphoid organs
FACS	Fluorescence activated cell sorting
Fas/Tnfrsf6	Tumour necrosis factor receptor suferfamily member 6/apototsis antigen-1
Fc	Fragment constant
FCS	Foetal calf serum
FDC	Follicular dendritic cells
FDC-M1	Clone of antibody that recognizes Mfge-8
FRC	Fibroblastic reticular cell
GC	Germinal centres
GCDC	Germinal centre dendritic cells
GL-7	Clone of monoclonal antibody that reacts with a cell-surface protein found on activated T and B lymphocytes
gp38	Glycoprotein 38/podoplanin
HCV	Hepatitis-C virus
HEV	High endothelial venules
hi	High
HSV	Herpes Simplex Virus
IC	Immune complex
ICAM-1	Intercellular adhesion molecule 1
Id-2	Inhibitor of DNA binding-2
IF	Immunofluorescence
Ig	Immunoglobulin
IκB	Inhibitor of kappa B
IL	Interleukin
ILC	Innate lymphoid cells
ILF	Inducible lymphoid tissue
int	Intermediate
Islet-1	Insulin gene enhancer protein-1
KIT/SCFR	Mast/stem cell growth factor receptor
KLH	Keyhole limpet hemocyanin
LCMV	Lymphocytic choriomenigitis
LEC	Lymphatic endothelial cells
LIGHT	Homologous to LT, inducible expression, competes with herpes simplex virus (HSV) glycoprotein D for HSV entry mediator (HVEM), a receptor expressed on T lymphocytes
LN	Lymph node
LPS	Lipopolysaccharide
LTα	Lymphotoxin alpha
LTα1β2	Lymphotoxin alpha 1 beta 2
LTβ	Lymphotoxin beta
LTβR	Lymphotoxin beta receptor
LTi	Lymphoid tissue inducer

LTo	Lymphoid tissue organizer
lo	Low
LZ	Light zone
Mac-2BP/90K	Galactin-3-binding protein
MADCAM-1	Mucosal vascular addressin cell adhesion molecule 1
MALT	Mucosa associated lymphoid tissue
MFGE-8	Milk fat globule-EGF factor 8
MHC	Major histocompatibility complex
mLN	Mesenteric lymph node
MMP-9	Matrix metallopeptidase 9
MMRN2	Multimerin 2
MRC	Marginal reticular cells
MSC	Mesenchymal stem cells
mRNA	Messenger ribonucleic acid
NFκb	Nuclear factor kappa b
NIK	NF-κB-inducing kinase
NK	Natural killer cells
Nkx2-5	NK2 homeobox 5
NO	Nitric oxide
Notch	Single-pass transmembrane receptor protein
NP	4-Hydroxy-3-nitrophenylacetyl
NP-CGG	4-Hydroxy-3-nitrophenylacetyl-chicken gamma globulin
PALS	Periarteriolar lymphoid sheath
PαS	PDGFRα+Sca-1+ cells
PD	Programmed cell death protein
PD-L	Programmed cell death-ligand
PDGF	Platelet derived growth factor
PDGFRα	Platelet derived growth factor receptor alpha
PDGFRβ	Platelet derived growth factor receptor beta
p.i.	Post-immunisation
pLN	Peripheral lymph nodes
plt	paucity of lymph node T cells
PNA	Peanut agglutinin
PNad	Perpheral node addressin
PP	Peyer's patch
PPARγ	Proliferator-activated receptor γ
Prox 1	Prospero homeobox 1
RA	Retinoic Acid
RALDH2	Retinaldehyde dehydrogenase 2
RANK	Receptor activator of nuclear factor kappa-B
RANKL	Receptor activator of nuclear factor kappa-B ligand
RelB	Rel-like domain-containing protein
RET	Receptor tyrosine kinase
RNA	Ribonucleic acid

RNase	Ribonuclease
RORγ	RAR-related orphan receptor gamma
RT-PCR	Reverse transcriptase polymerase chain reaction
Runx	Runt-related transcription factor
S1P	Sphingosine-1-phosphate
Sca-1	Stem cell antigen-1
SCS	Subcapsular sinus
SCSM	Subcapsular sinus macrophages
SHM	somatic hypermutation
SLOs	Secondary lymphoid organs
SSB	Single strand breaks
TEM-1	Tumour endothelial marker-1
T_{FH}	T follicular helper cell
TLS	Tertiary lymphoid structures
Tlx1/HOX11	T cell leukemia homeobox 1
Th cells	CD4+ T helper cells
TNF	Tumor necrosis factor
TNFR1	Tumor necrosis factor receptor 1
TRANCE	Tumour necrosis factor-related activation-induced cytokine
TRANCER	Tumour necrosis factor-related activation-induced cytokine receptor
TRAF-6	TNF receptor associated factor 6
TRC	T-cell zone fibroblastic reticular cells
UNG	Uracil DNA glycosylase
VCAM-1	Vascular cell adhesion protein 1
WAT	White adipose tissue
WT	Wild-type

List of Figures

List of tables

Table of contents

Chapter 1. Introduction

1.1. Structure and function of Secondary lymphoid organs

1.1.1 Secondary lymphoid organs

Secondary lymphoid organs (SLOs) represent the hub of the adaptive immune response. SLOs include the spleen, lymph nodes (LN), Peyer's patches in the gut, tonsils and other mucosa-associated lymphoid tissue (MALT) (Goodnow, 1997, Butcher et al., 1999, Butcher and Picker, 1996). SLOs are distributed throughout the body, but a large number are found concentrated in areas where antigen is likely to be encountered, for example at mucosal sites. SLOs hold a network of fibroblasts, vessels and nerves that embeds the large mobile leukocyte component and support the functions of immune surveillance and response to noxious agents (Mebius, 2003, Roozendaal and Mebius, 2011). This elegant organization shapes SLOs in a highly conserved and regulated process that largely occurs, in mice and humans, in the embryonic and early postnatal life (Randall et al., 2008, van de Pavert and Mebius, 2010). SLOs evolved simultaneously with the development of an adaptive immune system in vertebrates, with hundreds of LN being distributed at strategic sites, thereby providing a platform for immune cell clustering at well-defined areas. This enables rapid and more efficient adaptive immune responses that outpace pathogen replication, spread and therefore, pathology (Eberl, 2007).

Within the organs a high number of highly specialised cell types cooperate to achieve a specific function, permitting specific interactions between leukocytes, resulting in a mature adaptive immune response. In order to achieve this, the organs have a very specific anatomy with segregation between the different leukocyte zones maintained by a number of different resident stromal cell populations (Malhotra et al., 2013) . The chemokine gradients established by these stromal cells allow for efficient trafficking of lymphocytes through the lymph nodes, allowing for the successful completion of the

immune surveillance role played by these organs. The importance of secondary lymphoid organs has been extensively demonstrated in initiating and maintaining an antigen specific response to immune challenges (Mueller and Germain, 2009, Roozendaal et al., 2009).

1.1.2 Immunological function of SLOs

The specific function of the particular SLO appears to be dependent on the anatomical location of the organ. For example, the spleen is understood to mount an immune response against blood born infections (Singer, 1973, Diamond, 1969, Evans, 1985), whereas antigens found in lymph nodes are drained from the local environment. It is understood that the presence of lymph nodes is essential for the induction of an adaptive immune response, as mice lacking these organs are known to be unable to mount hypersensitivity reactions (Rennert et al., 2001) or fight LCMV infections (Ochsenbein et al., 2001). More recent understanding of the genetics involved in the development of the organs and of the lymphocytes lead to the appreciation of the fact that T cell responses are maintained in the periphery in mice without lymph nodes. Similarly, mice which lack the T cell lymph node homing chemokines CCL19 and CCL21 (Paucity of lymph node T cell mutation (plt) mice) have been shown to be able to produce robust CD4+ T cell responses, as indicated by the production of IL-2. These responses are slightly delayed in response to contact sensitisation with picryl chloride and also in response to subcutaneous chicken OVA immunisations, although these responses are maintained for a prolonged period, resulting in a decrease in resolution (Mori et al., 2001, Yasuda et al., 2007). Accordingly, in plt mice, CD8+ cytotoxic T cells are able to be primed to respond to infection outside of SLOs (Junt et al., 2002, Hofmann et al., 2010).

Unlike T cell responses, the humoral immune response is entirely dependent on the presence and full functionality of SLOs. Mice with a genetic defect resulting in defective SLOs formation, despite normal bone marrow development and normal naïve B cell production, are unable to produce antigen-specific

class-switched antibody responses to various challenges, including herpes simplex virus (HSV) and KLH antigen (Miyawaki et al., 1994, Banks et al., 1995). Antigen specific humoral responses to NP-CGG immunisation with alum adjuvant has also been shown to be dependent on the presence of SLOs, as indicated by studies investigating the LTβR-/- mice, that lack functional lymph nodes but maintain a disorganised spleen (Futterer et al., 1998).

The presence and function of SLOs is essential for the establishment of antibody response as adoptive transfer of WT leukocytes into mice completely lacking all SLOs (the LTα-/- mouse) is unable to recapitulate the B cell responses and form germinal centres (Fu et al., 1997, Fu et al., 2000). This defective B cell response has been shown to be due to the lack of the SLOs as there are circulating immature B cells in the LTα-/- mice, indicating that these B cells are still able to produce antibodies. Expression of an IgM+ BCR is a prerequisite for the egress of immature B cells into the periphery, therefore if B cells can be detected in the circulation, the cells must have the intrinsic ability to produce antibody (Greter et al., 2009).

A number of studies have indicated that in mice unable to develop lymph nodes (LTα-/- mice, which will be discussed in detail) due to a defect in the inducer cells, the ability to clear viral infections is not completely compromised. This is due to these mice maintaining the ability to develop inducible lymphoid structures (or tertiary lymphoid structures; TLS) which can support germinal centre reactions. This data indicates that a different mechanism governs the development of TLS and SLO (Lund et al., 2002, Lee et al., 2000, Moyron-Quiroz et al., 2004).

1.1.3 Segregation of lymphocyte zones

Lymph nodes have a defined structure which allows for their efficient function. The kidney-shaped organs consist of an outer cortex and an inner medulla, for a diagram of the lymph node structure, see figure 1.1.

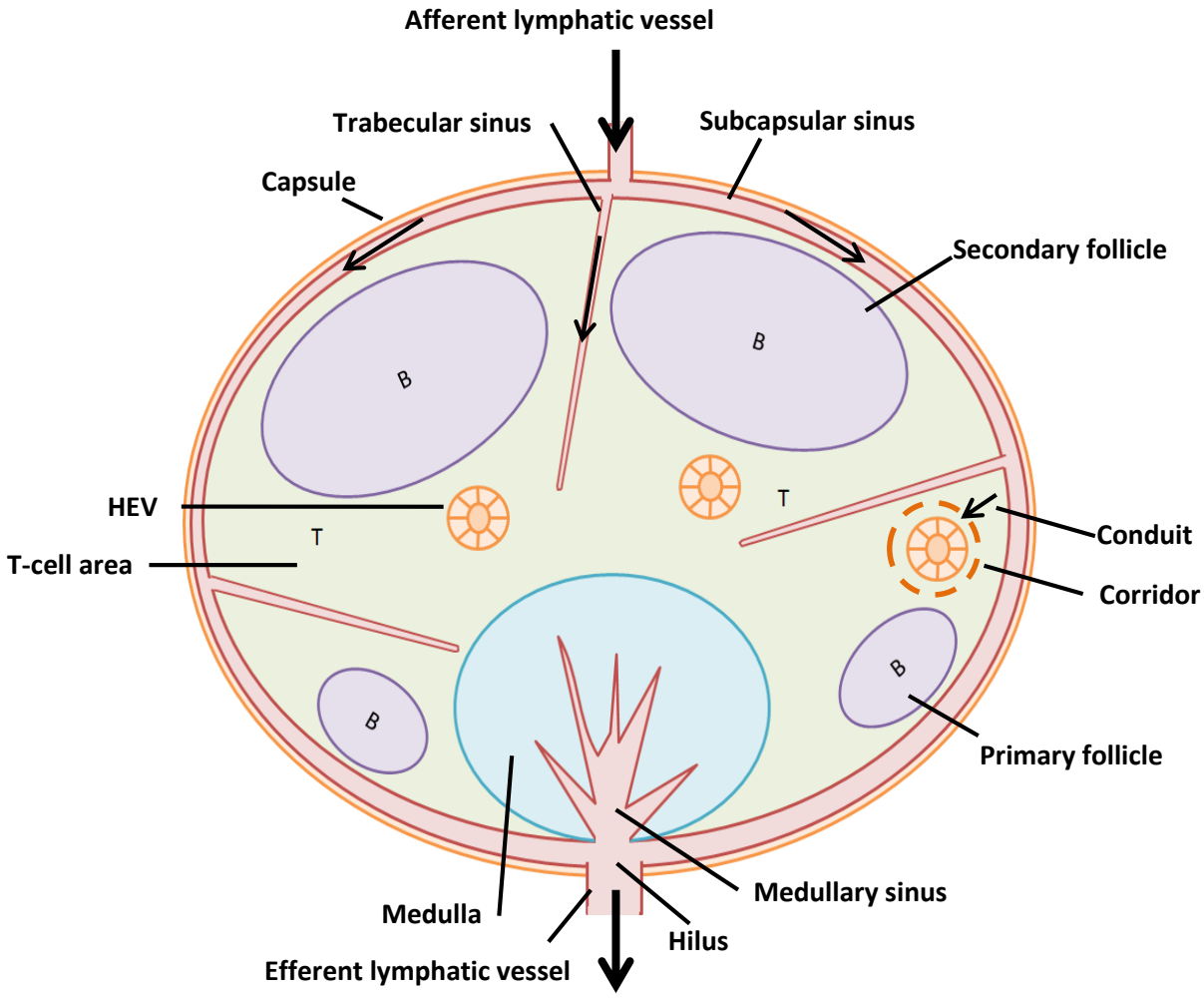

Figure 1.1 Schematic representation of the structure of a lymph node, depicting the cardinal features of the organ. Adapted from (Aloisi and Pujol-Borrell, 2006, Butcher and Picker, 1996)

LNs are connected to the cardiovascular system via afferent and efferent blood vessels which enter and leave the organ in the medullary region, leading into the medullary sinus. As well as being connected to the blood circulation through these large vessels, smaller capillaries also pass through the paracortical zone; these are referred to as high endothelial venules (HEVs). HEVs have specialised

endothelium that promote leukocyte trafficking by upregulation of adhesion molecules, especially VCAM-1 and ICAM-1 and expression of chemokines, such as CCL19, CCL21, CXCL12 and CXCL13 that attract naïve lymphocytes into the lymph node (Mueller and Germain, 2009, Girard and Springer, 1995). LNs are also connected to the lymphatic vasculature via afferent and efferent lymphatic vessels. The afferent lymphatic vessel opens into the subcapsular sinus, located in the cortex; just below the capsule of the organ; and the efferent lymphatic exits the organ from the medulla (von Andrian and Mempel, 2003). The cortex of lymph nodes is the location of maintenance of naïve lymphocytes, allowing for lymphocyte maturation in the presence of an immune stimulus. In the paracortical area of medullary follicles, the dominant leukocyte cell type is the T cell. The outer cortex of the LN is arranged into follicles containing B cells. These follicles can be primary follicles containing mainly naïve B cells, or secondary follicles which contain germinal centres.

1.1.4 Germinal centre structure and function

B cells develop in the bone marrow from hematopoietic stem cells (Kondo, 2010). These cells first undergo positive selection assessing the binding of the B cell receptor (BCR) to the ligand, and BCRs that are not able to bind undergo “death by neglect” (Martensson et al., 2010, LeBien and Tedder, 2008). A negative selection step then eliminates self-reactive BCRs by triggering apoptosis in cells that bind self-antigens with high affinity (Sabouri et al., 2014). Immature B cells generated by these processes enter the circulation and travel to SLOs where they undergo the reprogramming that is the main function of the germinal centre. This reaction results in the generation of cells capable of producing high-affinity class-switched antibodies (Nossal, 1994).

Germinal centres form in follicles rich in $IgM^{+}IgD^{+}$ naïve B cells. The germinal centre is segregated into two major structures based on their different histology. These are described as the light zone (LZ) that

includes FDCs and T follicular helper cells (T_{FH} cells) and the dark zone (DZ) that consists of proliferating B cells. Cells in the light zone and the dark zone are referred to as centrocytes and centroblasts, respectively.

The initiation of the germinal centre reaction begins with mature B cells encountering antigen within the B cell follicle (Batista and Harwood, 2009). These activated B cells then travel to the border of the B cell follicle via CCR7 upregulation in order to seek a cognate antigen-specific T cell (Okada et al., 2005, Qi et al., 2008, Garside et al., 1998, Reif et al., 2002). The interactions between these cell types via CD40 on the B cells and CD40L on the T_{FH} cells results in B cell proliferation, driving the formation of the GC (Foy et al., 1994, Han et al., 1995). The cells with the highest antibody specificities move to medullary chords and do not enter the germinal centre reaction, but differentiate into plasmablasts, a short-lived cell type capable of secreting low affinity antibodies which have not undergone somatic hypermutation (Jacob and Kelsoe, 1992). It appears that the B cells with the highest affinity antibodies preferentially differentiate into these plasmablasts, which upregulate CXCR4, and downregulate CXCR5, allowing the cells to traffic towards CXCL12 expression, moving to the interfollicular space, or the splenic marginal zone (Paus et al., 2006, O'Connor et al., 2006, Chan et al., 2009, Hargreaves et al., 2001). A subset of the remaining B cells which have received the T cell help then enter into the GC reaction. It appears that of this subset, only those B cells with the highest relative antibody affinity are able to access the GC, thanks to interclonal competition for the signals provided by the T cells (Dal Porto et al., 2002, Shih et al., 2002, Schwickert et al., 2011). Therefore, the multiple different B cell clones that are generated by the GC reaction is established in advance of the formation of the structure itself (De Silva and Klein, 2015). Upregulation of EBI2 (Epstein-Barr virus induced molecule-2, or GPR183), leads to movement of naïve B cells to the extrafollicular space, where they encounter their cognate T_{FH} cells. This molecule is then downregulated, allowing for the B cells to transport into the germinal centre (Gatto et al., 2009, Pereira et al., 2009).

Two-photon intravital microscopy has revealed that upregulation of the master regulator of the germinal centre for both the T and B cells; B cell lymphoma 6 (Bcl-6), occurs within one day following immunisation on the T_{FH} cells, although this marker can only be observed on the antigen-engaged B cells at 2 days post-immunisation (p.i.) (Kitano et al., 2011, Kerfoot et al., 2011, Baumjohann et al., 2011). Expression of Bcl-6 occurs after the upregulation of the lymphocyte activation factors GL-7 and Fas (Kitano et al., 2011). Upregulation of this factor has been shown to essential to allow migration of the B cells into the developing GC, this migration appears to be controlled by controlling the upregulation of EBI2 (Kitano et al., 2011). The earliest point at which developing GCs can be visualised by standard microscopy techniques is at 4 days after immunisation, when rapidly dividing B cell blasts are observed in the B cell rich areas of the SLOs (MacLennan, 1994). The structure grows as the number of B cell blasts increases, from 5 – 7 days post immunisation, when the germinal centre establishes its final organisation with two major microenvironments (Victora and Nussenzweig, 2012). These two structures were identified based on their different histological appearances, the light zone (LZ) and dark zone (DZ). The dark zone consists of rapidly proliferating B cells known as centroblasts with densely packed nuclei resulting in the dark appearance when examined under the microscope. These centroblasts downregulate their surface expression of immunoglobulins (Nieuwenhuis and Opstelten, 1984). The light zone is so called as the cells are less densely collected, and the B cells found in this region are known as centrocytes. Centrocytes tend to be smaller than centroblasts, with a more irregular nuclear morphology. Functionally, light zone centrocytes are characterised by the expression of the activation markers CD80 and CD86, upregulated cell surface immunoglobulin expression, low levels of CXCR4, but high CXCR5 expression (Allen et al., 2004, Caron et al., 2009). Upregulation of CXCR4 on centrocytes enables the movement of the centrocytes into the CXCL12+ dark zone to become centroblasts (Bannard et al., 2013). Stromal cell which express CXCL12 (CXCL12-expressing reticular cells, CRCs) have been recently identified in the dark zone. These cells are fate mapped by both CCl19 and CD21-cre mice (Rodda et al., 2015). The light zone is defined by the presence of FDCs, as well as containing T_{FH} and macrophages (Victora and Nussenzweig, 2012).

The main functions of the germinal centre reaction are somatic hypermutation (SHM) and class switch recombination (CSR). Circulating naïve B cells express mainly IgM and some IgD, as these are the first segments in the heavy chain locus (Stavnezer et al., 2008). The heavy chain exons of the immunoglobulin domains are organised in order, from the IgM cluster (Cμ) to the IgA cluster (Cα). In mice, these clusters are organised in a specific order; Cμ, Cδ, Cγ, Cε and Cα, corresponding to immunoglobulins which are therefore expressed in the order IgM, IgD, IgG, IgE and IgA (Xu et al., 2012). In order for the other immunoglobulin subtypes to be expressed, the Cμ and Cδ subunits must be excised from the immunoglobulin heavy chain (Stavnezer et al., 2008). This recombination occurs via the action of activation induced cytidine deaminase (AID). This enzyme acts on the S regions found between each exon of the heavy chain locus, converting the cytosines to uracils (Muramatsu et al., 2000, Revy et al., 2000, Chaudhuri et al., 2003). The repair of this uracil residue results in the generation of single strand breaks (SSBs) by the base excision repair (BER) pathway. These SSBs are converted to double strand breaks (DSBs) by the mismatch repair pathway (MMR) in the S regions, which are then recombined, resulting in intrachromosomal DNA recombination (Dickerson et al., 2003, Pham et al., 2003, Stavnezer et al., 2008). AID is also involved in the process of SHM, whereby the antibodies undergo mutations in order to develop higher antigen affinity and specificity. The hypermutations are generated in the hypervariable region of the immunoglobulin genes, whereby AID deaminates the deoxycytidine bases in both the heavy and light chains. These bases are then excised by the action of uracil DNA glycosylase (UNG), and the "gaps" generated by this reaction are replaced by an error-prone DNA polymerase, resulting in random insertions and therefore high mutation rates in the variable regions changing the BCR affinity and specificity (Gearhart and Wood, 2001). Both of these reactions occur during the rapid proliferative phase of the dark zone of the germinal centre. The mutated cells then traffic to the light zone and encounter the immune complexes displayed on the surfaces of the FDCs, where the BCR is tested for antigen affinity and specificity, as the random mutations are not guaranteed to increase the specificity of the antibodies (Gatto and Brink, 2010). The centrocytes also receive co-stimulatory signals via the MHC complex from cognate T_{FH} cells (Victora

and Nussenzweig, 2012). If these processes are not separated by the polarisation of the dynamic structure of the GC, it is understood that the accuracy of the selection is compromised (De Silva and Klein, 2015, Victora et al., 2012).

Selected high affinity B cells display the highest density of BCR on their surface, thus allowing strongest and longest-lasting functional contacts with the T_{FH} (Victora et al., 2010, Shulman et al., 2014). The B cells that receive the greatest T cell help in the light zone undergo higher number of replication rounds as compared than their competitors when returned to the dark zone (Gitlin et al., 2014). This proliferation results in higher levels of mutation, favouring the generation of a large pool of polyclonal BCRs, all with high affinities for the antigen very rapidly following GC initiation (Di Noia and Neuberger, 2007, De Silva and Klein, 2015). The selection pressure created by the assistance of T_{FH} is complemented by antigen masking of the antigen displayed on FDCs, where the early antibodies produced by plasma cells bind to the antigen on the FDCs, preventing all but the highest affinity, newly generated BCRs to be able to bind. This allows the GC to maintain a selection pressure on the BCRs, leading to antibody affinity increasing over time (Zhang et al., 2013).

Once the B cells have undergone the GC reaction and are able to express high levels of high-affinity, class-switched antibodies, the cells differentiate into either plasma cells or memory B cells (Gatto and Brink, 2010). Memory B cells generated by the GC reaction persist in the lymphoid tissues for prolonged periods of time. Upon secondary encounter of the antigen, these memory cells are able to proliferate rapidly and secrete high levels of antigen-specific antibodies (McHeyzer-Williams et al., 1991). The class-switched memory B cells have been shown to be capable of differentiating to plasma cells during a secondary immune response (Dogan et al., 2009). The plasma cells generated by the GC reaction are distinct from the plasma cells that are generated before the formation of the GC reaction, as these cells have undergone high affinity maturation. Differentiation of GC B cells into the plasma cell lineages is completely dependent on the actions of B lymphocyte-induced maturation protein-1

(Blimp-1) (Piskurich et al., 2000, Schliephake and Schimpl, 1996). This marker is suppressed by Bcl-6 during the GC reaction, and the differential expression of these two markers contributes to the generation of the two distinct mature B cell subsets (Angelin-Duclos et al., 2000, Shaffer et al., 2000). The long-lived plasma cells reside in the bone marrow and can be persist for up to 90 days after immunisation and are capable of secreting high titres of the high affinity antibodies (Manz et al., 1997). The factors governing whether the B cells continue to express Bcl-6 and become memory B cells, or whether they upregulate Blimp-1 and become plasma cells are currently unclear (Zhang et al., 2016). There is some evidence that the GC B cells with the highest affinity BCR preferentially differentiate into plasma cells, rather than the memory B cells (Phan et al., 2006, Smith et al., 1997). There are also indications that costimulatory signals via the complement receptor 2 (CR2) are able to stimulate plasma cell differentiation, although CR2-/- mice are still able to produce high affinity antigen-specific antibody responses (Gatto et al., 2005). Memory B cells can also be generated independently of the GC reaction (Takemori et al., 2014). CD40L+ memory T cells can promote the differentiation of B cells into a memory phenotype, by upregulating CD80 and CD273 (PDL2) (Zuccarino-Catania et al., 2014, Casamayor-Palleja et al., 1996). However, the exact mechanisms governing whether dark zone centroblasts exit the GC as plasma cells of memory B cells, or whether the cell recirculate through the GC to undergo further affinity maturation have yet to be resolved.

1.2 Embryonic development of secondary lymphoid organs

The location and organisation governing the development of SLOs is closely regulated during embryological development. This development has been investigated closely at various stages of the development of the embryo, and the stages at which various genes are essential for this development have been established using a number of knockout mice (Mebius, 2003). These studies have shown that the cross-talk between two cell types, the hematopoietic lymphoid tissue organiser cells (Lti cells) and the mesenchymal stromal organiser cells (Lto cells), via LTα1β2 and LTβR is critically important for SLOs development. These interactions are further discussed in the next section.

1.2.1 Lymphoid tissue inducer cells and lymphoid tissue organiser cells

In order to develop a number of secondary lymphoid organs (LNs), such as lymph nodes, Peyer's patches (PPs)and inducible lymphoid follicles (ILFs), the actions of two cell types have been shown to be very important: $CD45^{+}CD4^{+}CD3^{-}$ hematopoietic lymphoid tissue inducer (LTi) cells (Eberl et al., 2004) and stromal organiser (LTo) cells (Cupedo et al., 2009). These cells are the earliest cell type found within the developing anlage (Mebius, 2003). The interactions of the LTi and LTo cells governed by the cross-talk between the LTα1β2-expressing hematopoietic cells and the LTβR+ stromal organiser cells has been shown to be essential in the formation of all secondary lymphoid tissues, including the lymph nodes (van de Pavert and Mebius, 2010).

Common lymphoid precursors (CLPs) CD45+KIT^{mid} IL-7Rα+CD3-CD4- expressing α4β7 integrin in the foetal liver have been shown to give rise to LTi, which appear to be more closely related to NK cells than to T cells, although the progenitor can differentiate to any of these cell types (Yoshida et al., 2001, Mebius et al., 2001, Spits and Di Santo, 2011, Cherrier et al., 2012, Mebius et al., 1996). The transcription factors that have been shown to be important in the generation of these cells, including

Runx1 (Tachibana et al., 2011), Id2 (Yokota et al., 1999), Tox (Aliahmad et al., 2010) and TRANCE, although to a lesser extent (Kong et al., 1999). Expression of other transcription factors have been shown to be important at other stages of the Lti development, for example, in Id2-deficient mice, the numbers of α4β7 CLPs is significantly reduced, indicating that this signalling is essential for the upstream generation of the LTi precursors, by encouraging suppression of the expression of E2A-encoded proteins to allow for the development of these precursors (Boos et al., 2007). However, the most important transcription factor associated with the development of Lti is RORγt. During embryological development, this transcription factor has been shown to be exclusively expressed in these LTi cells, and essential for the production of this cell type (Eberl et al., 2004, Sun et al., 2000).

These cells are understood to persist into adulthood, where they have been identified as part of the novel an innate lymphoid cell subtype, the RORγt+ innate lymphoid cells (ILC3s) (Sonnenberg and Artis, 2015). Notch ligand engagement is also required to generate α4β7+ CLPs, the RORγt- Id2+ LTi precursors. However, if this Notch signalling is prolonged, half of the cells which derive from these precursors become T cells. If Notch signalling is inhibited, the majority of α4β7+ precursors become the RORγt+ LTi cells (Cherrier et al., 2012). The expression of the transcription factor RORγt has been conclusively demonstrated to be essential for the maturation of the LTi cells from their circulating precursor and, in absence of RORγt, lymph nodes do not form (Eberl et al., 2004).

The lymphoid tissue organisers (LTo) are stromal cells, descended from a tissue-resident mesenchymal precursor. LTo expand in response to the influx of LTi cells, due to the engagement of VCAM-1 expressed on the LTo cells, and in turn contribute to further infiltration of the LTi cells. The incoming LTi cells provide the LT signal required to maintain these cells (White et al., 2007). Utilizing a CCL19 Cre dependent LTβR ablation (Ccl19-cre × Ltbrfl/fl mice), Ludewig and colleagues have recently shown that CCL19+ myofibroblastic stromal cell precursor cells can develop basic LN infrastructure even in absence of LTβR triggering (Chai et al., 2013). Nonetheless, fibroblastic LTo cells require LTβR signalling

to reach full maturation and immunological competence that includes strong expression of ICAM-1, VCAM-1, CCL19, CCL21, IL-7 and RANKL (Benezech et al., 2010, Chai et al., 2013, Vondenhoff et al., 2009). Embryonic LTo cells in PP, mesenteric and peripheral LN show transcriptional differences as well as differential cellular and molecular requirements suggesting that LTo responsible for the aggregation of different lymphoid tissues are not uniform (Yoshida et al., 2002, Cupedo et al., 2004).

1.2.2 Embryological development of lymph nodes

Development of lymph node begins during embryogenesis at around mouse embryonic day 9.5 (Mebius, 2003). Importantly, the initiation of lymph node development has been shown to happen in a sequential manner, progressing from the anterior to the posterior side of the developing embryo (Yoshida et al., 2002). The mesenteric lymph node developing earliest, with the initial structures observed at E11, whereas the popliteal lymph node has been shown to begin to develop last, at E16 (Rennert et al., 1996).

The initial step in the development of the stromal lymph node compartment is the initial attraction of circulating IL-7Rα+ LTi cells out of the early vessels to develop the early clusters of cells. This initial attraction has been shown to occur in the absence of LTα1β2 or the LTα1β2, as the surrounding mesenchyme is able to upregulate ICAM-1 and VCAM-1, CXCL13 and IL-7, regardless of the presence of the LT stimulation (Yoshida et al., 2001, Vondenhoff et al., 2009, Eberl et al., 2004, Coles et al., 2006, Benezech et al., 2010). Nonetheless, LTα1β2 is required for the further up-regulation of adhesion molecules and the production of lymphoid chemokines in a process that is dependent on the activation of the alternative pathway of the NF-κB cascade (Mebius, 2003, Randall et al., 2008).

The origin and identity of the signals that induce specification of the mesenchymal progenitor cells prior to LTi arrival remain largely unknown. The current evidence appears to indicate that the signals

which initiate the development of the anlage are produced by cells resident in the location in which the LN anlage will begin to develop. It is clear that a close anatomical and functional connection between immune cells, mesenchyme and vascular structures is critical for the establishment of the anlage. For example, these organs have been shown to preferentially develop at the sites of large blood vessel branching where nerves are also developing (Yoshida et al., 2001). There is evidence that the retinoic acid (RA) derived from developing nerves, or possibly from the Lti cells, is able to induce the expression of CXCL13 in the local mesenchymal stem cells (van de Pavert et al., 2009). The production of retinoic acid from vitamin A is dependent on the action of the irreversible enzymes retinal dehydrogenases (RALDHs). Accordingly, RALDH2 has been shown to be essential in embryonic lymph node development, with RALDH2-/- mice unable to form the initial clusters of Lti cells which go on to develop into the LN anlage (van de Pavert et al., 2009).

This expression of CXCL13 by mesenchymal stem cells (MSCs) at the site of the developing lymph node anlage (Ohl et al., 2003) has then been shown to be able to attract $CD45^{+}CD4^{+}CD3^{-}$ IL-7Rα^{d} LTi out of peripheral blood vessels. These CXCL13 expressing MSCs are the proposed precursor of stromal organiser cells (LTo) (Luther et al., 2003). There is also evidence that these precursors express IL-7Rα, and that engagement of this receptor contributes to the induction of the expression of the LTα1β2 on the LTis (Yoshida et al., 2001, Yoshida et al., 2002, Honda et al., 2001). The local endothelium has also been shown to express other markers involved in attracting the LTi cells to the developing lymph node anlage, such as CCL21 (Ohl et al., 2003). These endothelial cells are also able to express LTβR, which has been shown to be important in controlling the location of peripheral lymph node development (Onder et al., 2013). There is evidence that the expression of VCAM-1 is essential for retaining the LTi cells in the developing anlage allowing the increase in cell number. The interaction with VCAM-1 is dependent on the expression of active β1 integrin, which appears to be dependent on CXCL13 binding to CXCR5 on the CD3-CD4+CD45+ LTi cells, as CXCR5-/- embryos reveal significant reductions in the VCAM-1+ clusters associated with LN development (Finke et al., 2002). This binding of CXCR5 to

CXCL13 has been shown to initiate a conformational change in β1 integrin on the stromal cells, which appears to be essential to promoting the binding of VCAM-1 with LTβR also expressed on the stromal cells (Finke et al., 2002). The importance of this interaction has been further demonstrated in transgenic mice overexpressing CXCL13, which can induce development of lymphoid tissues in extra-lymphoid locations. This development is still dependant on LTβR signalling, indicating that the action of CXCL13 is able to induce sufficient LTα1β2 expression (Luther et al., 2000). Other lymphoid chemokines such as CXCL12, CCL19 and CCL21 are also able to induce formation of lymphoid aggregates, with CCL21 producing the most highly organised aggregates (Chen et al., 2002, Fan et al., 2000, Luther et al., 2002). However, mice deficient for the receptor of these chemokines, CCR7, develop lymph nodes normally, indicating that neither CCL19 nor CCL21 are essential for the formation of lymphoid tissue (Nakano et al., 1997, Gunn et al., 1999, Vassileva et al., 1999, Luther et al., 2002, Forster et al., 1999).

LTα1β2 has been shown to binds specifically to LTβR, while TNFα and LTα3 bind to the TNF receptors TNFR1 and TNFR2 (Mebius, 2003, Randall et al., 2008). The importance of activation of LTβR signalling cascade in lymphoid formation has been shown by the complete absence of LN in knockout mice lacking components of this pathway (Futterer et al., 1998, De Togni et al., 1994, Banks et al., 1995, Alcamo et al., 2002). LTβR can be also bind to LIGHT (Blum and Pabst, 2006). This ligand is less important in controlling lymph node development, as LIGHT-/- mice have been shown to develop the majority of secondary lymphoid organs normally, although there is evidence that the mesenteric lymph node development is disrupted (Scheu et al., 2002) The combined activation of TNF receptors and LTβR signaling pathways leads to the activation of both the canonical and non-canonical NF-κB pathways. LTβR signalling via the NIK-dependent non-canonical pathway is known to regulate the expression of various chemokines, such as CCL19/21, CXCL13, survival factors (BAFF), whilst activation of the degredation of IκB proteins in the canonical NF-κB pathway is required for the production of adhesion molecules such as VCAM-1, MadCAM and ICAM-1 (Dejardin et al., 2002, Drayton et al., 2006,

Katakai et al., 2004, Katakai et al., 2008, Yoshida et al., 2002, Ruddle and Akirav, 2009). The activation of the non-canonical pathway, as indicated by expression of NIK and the transcription factor RelB, is a specific requirement for the activated mesenchyme to mature in a lymphoid tissue organiser cell (LTo) (Mebius, 2003, Randall et al., 2008, Roozendaal and Mebius, 2011).

Maturation of the LTos facilitates, in turn, further attraction and retention of more LTi cells through the binding of CXCR5, CCR7, $\alpha4\beta1$, $\alpha4\beta7$ and $LT\alpha1\beta2$ to their respective ligands (Randall et al., 2008, Roozendaal and Mebius, 2011). These steps coincide with the invasion of the endothelial bud by the surrounding mesenchyme (Benezech et al., 2010, Cupedo and Mebius, 2005, White et al., 2007, Peduto et al., 2009). The physical interaction between hematopoietic LTi and stromal LTo cells establishes a positive feedback loop that reinforces the formation of the cluster and leads to the stabilization of the anlagen with vascular differentiation, development of HEVs and eventually attraction and compartmentalization of mature lymphoid and myeloid cells (Randall et al., 2008, van de Pavert and Mebius, 2010, Roozendaal and Mebius, 2011).

Other members of the TNF superfamily are also involved in the full development of lymph nodes. The hierarchy of requirement of these family members in physiological lymphoneogenesis is clear with $LT\alpha-/-$ mice, which lack both LTα3 and LTα1β2 expression, and which gives the most severely affected phenotype, characterized by lack of all LNs and PPs, and disorganized splenic white pulp (Banks et al., 1995, De Togni et al., 1994). In contrast, $LT\beta-/-$ mice which specifically lack LTα1β2 function alone, retain mLNs and cervical LNs, and their splenic defects are less pronounced than those of $LT\alpha-/-$ mice (Alimzhanov et al., 1997, Koni et al., 1997). A similar phenotype is observed in pregnant mice treated with LTβR-Ig fusion protein, whose progeny lack most peripheral LNs, but retain mLNs (Rennert et al., 1997, Rennert et al., 1996, Rennert et al., 1998). Receptor activator of NF-κB ligand (RANKL, otherwise known as TRANCE), which is known to signal via TRANCER, is also understood to play a role in the development of lymph nodes. Knockout mice lacking either the receptor or ligand completely lack all

lymph nodes, although the development of other mucosa-associated lymphoid tissue continues as normal (Kong et al., 1999, Dougall et al., 1999, Kim et al., 2000, Harmsen et al., 2002). TRAF6 is an essential component of this signalling pathway, and Traf6-/- mice are also unable to develop lymph nodes (Naito et al., 1999). Engagement of TRANCER has been shown to cause upregulation of LTα1β2, although it is understood to have another role in lymph node organogenesis as addition of LTβR agonist *in utero* is unable to recapitulate the development (Kim et al., 2000).

In SLOs, the resident mesenchyme is unable to maintain the durable production of survival factors and chemokines if TNFR or LTβR engagement is missing and only a few disorganised LN form in LTα-/- or LTβR-/- mice (Futterer et al., 1998, Chai et al., 2013). Accordingly, the prolonged treatment of adult wild type mice with LTβR-Fc leads to de-differentiation of FDC and HEV and reduced lymphocyte compartmentalization (Browning et al., 2005).

1.2.3 Development of the lymphatic system

The formation of the lymphatic endothelium early lymph sacs budding from the pre-existing vessels was originally described over 100 years ago (Sabin, 1902, Sabin, 1904). These observations were then not able to be further proved until relatively recently. The established model for the formation of lymph sacs is that the endothelial cells which make up the wall of the surrounding blood vessels begin to form a bud. The location of this developing bud can be identified by expression of Prox1 on the vessel endothelial cells which is first observable at about embryonic day 9.5. this expression becomes increasingly polarised as the bud forms and eventually the lymph sac separates completely from the blood vessel (Wigle and Oliver, 1999). The lymphatic vasculature then develops from these buds by sprouting of the lymphatic vessels (Bailey and Weiss, 1975, Eikelenboom et al., 1978). The lymph sac then wraps around the developing lymph node anlage at around E18.5, inverting the mesenchymal LN

anlage and endothelial lymphatics (Benezech et al., 2010). These two separate cell types can be identified by their differential expression of gp38 on the endothelium and PDGFRα, fibronectin and ER-TR7 on the mesenchyme (Benezech et al., 2010). The anlage is separated from the outer layers of fibroblastic cells by a thin Perlecan+ basement membrane (Peduto et al., 2009, Benezech et al., 2010) Interestingly, LN development is associated with but not fully dependent on a functional lymphatic vasculature network. Prox-1^{null} and Prox1 conditional mutant embryos fail to form mature LN but develop a hypoplastic anlagen and small LTi clusters in areas of activated mesenchyme (Vondenhoff et al., 2008b). Similarly, Clec-2 knockout mice, that exhibit a defect in lymphatic endothelial cell proliferation late in embryogenesis, form hypoplastic LNs with a mixture of blood and lymphatic flow and reduced LTi and LTo numbers (Benezech et al., 2014).

1.2.4 Final stages of lymph node development

After birth, the lymph node is a completely encapsulated organ, the structure of which has been described in detail previously in this chapter. Expansion and development of the lymph node continues post-partum and naïve lymphocytes begin to infiltrate the organ, attracted by their respective chemokine gradients. Naïve T cells expressing CCR7 are attracted through the HEVs to the T cell zone by expression of CCL21. As the HEVs develop further in adult life, the embryological LN-specific phenotype develops due to the downregulation of mucosal addressing cell-adhesion molecule 1 (MADCAM-1) and the upregulation of peripheral node addressin (PNAD) (Mebius et al., 1996). B cell traffic into the node is mostly dependent on CXCL12:CXCR4 interactions, with CXCL13 interactions playing a more minor role (Ansel et al., 2000, Muller et al., 2003).

The T cells chemokines are produced in part by the T cell zone fibroblastic cells described later in this introduction. Interdigitating dendritic cells within the lymph node are also able to produce CCL19 and CCL21 to attract the T cells out of the circulation, as well as causing the influx of more DC from the

circulation into the organ (Aloisi and Pujol-Borrell, 2006, Acton and Reis e Sousa, 2016). These DCs are also involved in the dynamic maintenance of the lymphatic vasculature, and interactions between the DCs and the HEVs are essential to support the phenotype of these cells. In the absence of DCs and the LTβR signals they provide, the endothelium has been shown to lose the HEV phenotype and is unable to support leukocyte migration (Moussion and Girard, 2011). Importantly, this expression of LTβR has been shown to be able to induce endothelial transformation to HEVs in ectopic sites, indicating an intimate link between the cell types (Kratz et al., 1996, Fan et al., 2000, Luther et al., 2002, Chen et al., 2012). Dendritic cells may also be found within the germinal centre (GCDC), and these cells are able to produce the CXCL13 required for B cell homing to the follicles and subsequent GC formation (Vissers et al., 2001).

The influx of these leukocytes is able to support the further development and maturation of the lymph node stromal cells. The leukocytes produce LTα1β2, which acts on the LTβR previously established as being an essential interaction involved in the maintenance of the lymphoid tissue (Ware, 2005). The positive feedback loop developed by this interaction ensures that high expression of the chemokine and its receptor results in high expression of the downstream products of this signalling cascade, including adhesion molecules and lymphoid chemokines, ensuring dynamic maintenance of the structures (Ansel et al., 2000, Vondenhoff et al., 2009, Oeckinghaus et al., 2011)

Another important feature of the lymph node which develops postnatally is the sub capsular sinus (SCS). This channel surrounds the periphery of the lymph node, and the afferent lymphatics empty into this channel. Macrophages line the floor of this channel and function to capture and transport the small antigens which travel in the lymph fluid towards the lymph node into the B cell follicles, allowing antigen-specific immune responses (Junt et al., 2007, Kuka and Iannacone, 2014, Gray and Cyster, 2012).

1.2.5 Peyer's patch development

The molecules involved in the development of these organs are similar to those of the development of lymph nodes but with a few notable differences. Peyer's patch development is a three step process that was examined extensively by whole mount immunohistochemistry by (Adachi et al., 1997). This group identified spots of VCAM-1 expression, which could be observed in co-localisation with ICAM-1 expression at embryonic day 15.5 within the intestine at site of PP development (Mebius, 2003). The development of PP can be tracked progressing along the intestine, from the proximal end of the tissue to the distal end (Adachi et al., 1997). Administration of either LTαR Ig-fusion protein or a blocking antibody against IL-7R has been shown to be able to inhibit the formation of these "spots", resulting in a lack of Peyer's patches in the adult mouse (Rennert et al., 1996, Yoshida et al., 1999). IL-7 receptor signalling pathway components have been shown to be essential for the full development of Peyer's patches (Cao et al., 1995, Park et al., 1995, Ansel et al., 2000, Adachi et al., 1998). When IL-7-/- mice are engineered to overexpress IL-7 in the gut alone, new Peyer's patches can develop in the adult mouse (Laky et al., 2000). The second stage of Peyer's patch development begins at E16.5, and consists of the initial spots of adhesion molecules being colonised by hematopoietic cells which can express CD4 and IL-7R. These cells exhibit a random pattern of migration before their aggregation into the Peyer's patch primordia, with a receptor tyrosine kinase (RET) ligand being shown to be a strong gut hematopoietic cell attractant (Veiga-Fernandes et al., 2007). Once these initial cells invade the early regions, this step is followed by lymphocyte infiltration (Adachi et al., 1997).

1.2.6 Spleen development

More ancient evolutionarily than LNs is the spleen that, together with GALT (gut-associated lymphoid tissue), represents the oldest SLO. The spleen is present in bony fish, amphibians and reptiles, although the organisation of these organs is less complex than that observed in mammals (Boehm et

al., 2012, Brendolan et al., 2007). Due to the different structure of the organ with different zones, the development of the organ is more complicated than lymph node development. The murine spleen can initially be observed as an anlage at embryonic day 10.5 as clusters of progenitors collecting within the dorsal mesogastrium, closely associated with the dorsal pancreatic mesenchyme (Thiel and Downey, 1921). This close association can make the two structures difficult to separate, with the separate morphologies observable from E12.5. Recent investigations have revealed that various transcription factors can be used to separate the cells of the two developing organs, with the splenic primordia expressing Tlx1 (otherwise known as HOX11), Bapx1 and Nkx2-5, among others (Roberts et al., 1994, Dear et al., 1995, Tribioli et al., 1997, Tribioli and Lufkin, 1999, Kanzler and Dear, 2001). Bapx1 has been shown to be essential for separating the developing spleen from the pancreatic cells, and in the absence of this gene, the spleen remains in direct contact with the pancreas and the structure is disorganised (Asayesh et al., 2006, Hecksher-Sorensen et al., 2004). Mice lacking Tlx1 are completely unable to develop spleens, although the animals are viable and do not appear to present with any other developmental defects (Roberts et al., 1994, Dear et al., 1995, Kanzler and Dear, 2001). The asplenia observed in these mice appears to be due to a deficiency in the mesenchymal cells to proliferate once the initial clusters have formed (Dear et al., 1995, Brendolan et al., 2005). Interestingly, recent work has established a potential link between splenic development and lymph node development, as Tlx1 has been shown to be able to control retinoic acid metabolism, a factor hypothesised to be involved in lymph node development. This data indicates that inhibition of RA is essential to allow splenic development (Lenti et al., 2016).

The development of the splenic white pulp cords, that starts at birth in mice (Endres et al., 1999, Fu et al., 1998, Ngo et al., 2001, Vondenhoff et al., 2008a) and after 15 weeks of gestation in humans (Timens et al., 1987) does not require LTi cells or LTα1β2 (Boehm et al., 2012, Brendolan et al., 2007, Futterer et al., 1998, Sun et al., 2000). However, as observed in the LN, stromal cell maturation, chemokine expression and lymphocyte compartmentalization still require LTα1β2 and, possibly TNFα

(Coles et al., 2010, Coles and Veiga-Fernandes, 2013, Cook et al., 1998, Cyster et al., 2000, Mebius, 2003, Ngo et al., 1999, Randall et al., 2008). Those ligands are likely to be provided by B cells and, as a consequence, B cell deficient mice display smaller spleens, with poorly developed T zones (Ngo et al., 2001). In conclusion, spleen and LN development depend on different types of inducer cells, but show a similar hematopoietic-mesenchymal cell interaction, which eventually leads to a similar pathway of fibroblast maturation.

1.3 Stromal cells in secondary lymphoid organs

Fibroblasts are ubiquitous cells found within many tissues. At a steady state, all organs of the body contain fibroblasts that provide structure and mechanical strength, as well as contributing to the production and maintenance of the extracellular matrix. Fibroblast phenotype and function greatly differ between various anatomical sites, as shown by the extensive transcriptional differences detected in fibroblasts isolated from different compartments or tissues in diverse locations of the body (Chang et al., 2002). This specialisation is further enhanced by the specific ability of fibroblasts to respond to a series of cytokines and inflammatory stimuli which increase fibroblast proliferative capacity and induce functional adaptations to the environment (Buckley, 2011, Rinn et al., 2007, Malhotra et al., 2012, Fletcher et al., 2010, Yang et al., 2014). The identification of different fibroblastic cell types is based on their distinctive morphology and lack of markers specific to other cell types, such as epithelial cells, and they also display plastic adhesive characteristics.

Mature SLOs are characterized by the complex anatomical organization of lymphocytes in segregated areas. This is regulated by the specialization of resident stroma or fibroblastic reticular cells (FRC) in functional subsets. FRCs are highly specialised and provide gradients of chemoattractants as well as survival factors for specific leucocyte populations. FRC exist in distinct subsets, of which the ones to be discussed in detail in this thesis include T cell reticular cells (TRCs), B cell reticular cells (BRCs), follicular dendritic cells (FDCs) and marginal reticular cells (MRCs). These subtypes can be defined by phenotype, anatomical location and function (Brown and Turley, 2015, Chang and Turley, 2015, Mueller and Germain, 2009, Roozendaal and Mebius, 2011, Usui et al., 2012, Munoz-Fernandez et al., 2006) (Figure 1.2).

There is some confusion in the literature about the terminology regarding these different stromal cell populations, namely as to whether the term FRC refers to the total myofibroblastic lymphoid stromal cells, or whether the FRCs are specifically the T cell zone reticular cells. In this thesis, the term TRC will

be used to refer to the T cell zone fibroblasts, to differentiate between these cells and the BRCs, the FDC and the MRC. However, these cell types appear to be intimately associated, with evidence of a shared origin and the potential for these cells to mature from one subtype to another (Jarjour et al., 2014). Fibroblastic reticular cells are the largest stromal cell population in the lymph node, and make up between 20-50% of the non-hematopoietic component of the organ (Link et al., 2007, Fletcher et al., 2011). The three-dimensional structure of the organ is dependent on the cell-cell contact established by these FRCs, forming a network on which the leukocytes are able to migrate (Bajenoff et al., 2006, Katakai et al., 2008). As well as these fibroblastic stromal cells, there are also a number of endothelial cell types that contribute to the stromal cell population within the lymph node, including blood endothelial cells (BEC), lymphatic endothelial cells (LEC) and high endothelial venules (HEV). The distribution of these different stromal cell types is illustrated in figure 1.2.

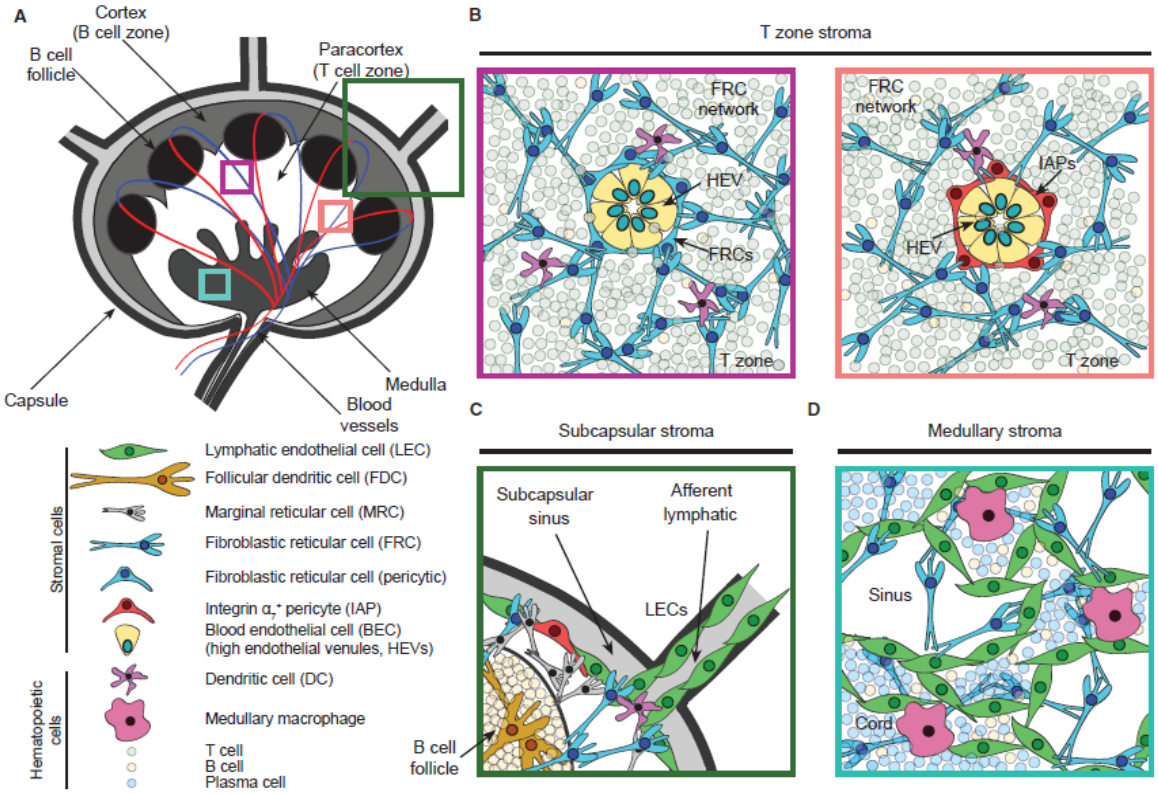

Figure 1.2 Diagrammatic representations of the stromal cell compartments in the lymph node. A) An overview of the structure of the whole organ with more detailed areas colour-coded and depicted in **(B-D)**. Diagram taken from (Malhotra et al., 2013)

The development of the fibroblastic components of the lymph node has been extensively studied, both during early formation of the organ and during the extensive remodelling that occurs following inflammation. To that end, a dual model of fibroblastic stromal cell development has been proposed, whereby these cells can develop *in utero*, and can also be supplemented by cells developing in response to inflammation (Fletcher et al., 2015). The total stromal component of the nodes is believed to develop from the LTo precursor cells discussed previously. These cells are understood to be the direct precursors of the MRC population (Katakai, 2012), and evidence is collecting that these MRCs are the precursors of other stromal cell compartments, with links having been established between the MRCs and FDCs (Jarjour et al., 2014). The development of other reticular cells, the BRC and TRC is less well established, although they are hypothesised to develop from the LTo cells via a FRC precursor (Fletcher et al., 2015). This two-step development of the FRCs has been demonstrated in mice with abnormal NF-κB non-canonical signalling pathway, for example NF-κB2-/- and Ikkα, as these mice are able to initiate lymph node development, but these organs are hypoplastic and unable to attract and retain B cells (Carragher et al., 2004, Drayton et al., 2004).

Novel evidence has indicated that the expansion of lymphoid stromal cells observed following immune challenge is thanks also to *de novo* differentiation of mesenchymal precursors in the adult. Lymph nodes have long been known to inhabit white adipose tissue (WAT), and the development of these two organs have been shown to be intimately linked during embryogenesis. The localisation of these fat pads is highly evolutionarily conserved (Benezech and Caamano, 2013, Pond and Mattacks, 2002, Pond, 2003). Adipocyte differentiation has been extensively studied, and it is well-established that mesenchymal stem cells differentiate to adipocytes via a pre-adipocyte intermediate. The pre-adipocyte is a cell which is morphologically indistinct from its mesenchymal precursor, but have been determined to differentiate to the adipocyte lineage (Rosen and MacDougald, 2006). This differentiation is dependent on expression of CCAAT-enhancer-binding protein α (C/EBPα) and proliferator-activated receptor γ (PPARγ) (Rosen and MacDougald, 2006, Suh et al., 2006). Expression

of these factors has been shown to inhibit the action of osteoblast differentiation pathways such as the action of PPARγ in downregulating the RUNX2 expression required for osteogenesis (Akune et al., 2004, Ali et al., 2005, Kawaguchi et al., 2005). Organs formed from mesenchymal cells have been shown to maintain a population of multipotent stem cells which persist into adulthood – notably pre-adipocytes in the adipose tissue and PDGFRα+Sca-1+ (PαS) cells in long bones (Houlihan et al., 2012). Interestingly, although the division between adipose stroma and osteoblasts seems to be binary, the adipose tissue and lymphoid stroma seem to be much more intimately linked. Recent publications have indicated that the pre-adipocytes in the adult fat pad can be reprogrammed into a stromal cell phenotype. The stimulation of the LtβR by a receptor agonist, alongside concurrent activation of the canonical NF-κB pathway by TNF-α has been shown to be able to stimulate the cells to upregulate the adhesion molecules VCAM-1 and ICAM-1 (Benezech et al., 2012). This upregulation occurs in a stepwise manner, so the cells differentiate from a VCAM-ICAM- population through a $VCAM^{int}ICAM^{int}$ population and to a $VCAM^{hi}ICAM^{hi}$ population. In the adult immune response, the fibroblastic cells of the lymph node have been shown to consist of a number of cells derived from this pre-adipocyte origin, with up to 60% of the total lymphoid stromal populations deriving from this pre-adipocyte source (Benezech et al., 2012, Benezech and Caamano, 2013). This source of mesenchymal stem cells in the adult gives a mechanism by which the lymphoid stroma is able to respond quickly to infection and the nodes are able to expand, allowing for increased leukocyte influx and maturation. Signalling via the LTβR has been shown to be essential for the development of FRCs, and the commitment of these cells to the multiple lineages essential for lymph node function (Onder et al., 2013)

1.3.1 Fibroblastic Reticular Cells (TRCs and BRCs)

T zone fibroblastic reticular cells (TRCs) classically inhabit the T cell cortex in lymph nodes and are characterized by the expression of gp38/podoplanin, extracellular matrix proteins ERT-7 and collagen-I and the lack of the vascular marker CD31 (Chai et al., 2013, Malhotra et al., 2012). TRCs are responsible for the recruitment, retention and movement of naïve T lymphocytes and DCs via their expression of CCL19 and CCL21. This is a dynamic environment, with the T cells and DCs constantly migrating around the zone, crawling over the TRC (Malhotra et al., 2012, Malhotra et al., 2013, Bajenoff et al., 2006) The expansion and subsequent contraction that the lymph node in response to immune challenge is also due to the contractile nature of the FRCs (Link et al., 2007, Katakai et al., 2004, Malhotra et al., 2013). These cells are also responsible for the production of a number of extracellular matrix components, which form the conduit network of the organ which allows for transport of soluble antigens and other molecules throughout the lymph node parenchyma (Roozendaal et al., 2009, Gretz et al., 2000, Malhotra et al., 2013).

Recruitment and maintenance of naïve T cells from the circulation, into the T cell zone is dependent on cytokines and chemokines produced by the TRCs. These cells produce CCL19 which binds to CCR7 expressed by naïve T cells, to attract the lymphocytes out of circulation into the lymph node and retain these cells within the T cell zone. These cells also produce IL-7 to promote survival of naïve T cells within the organ (Link et al., 2007). TRCs are intimately associated with a conduit system that supports the structure of the lymph node. These conduits are essential for allowing the trafficking and mobilization of soluble molecules within the lymph node. The penetration of the conduits deep into the lymph parenchyma, ensures that migratory DC are able to access the entire T cell region of the lymph node (Sixt et al., 2005, Gretz et al., 2000). Following immune challenge, the number of antigen-loaded DCs infiltrating the lymph node increases via engagement of the CCR7 receptor on the DC by the FRC-secreted CCL19 and CCL21 (Itano et al., 2003, Schumann et al., 2010, Marsland et al., 2005).

Small antigens can also be carried within the lymph fluid, and these Ag are able to penetrate the organ (Sixt et al., 2005, Itano et al., 2003).

FRCs that inhabit the outer B zone, also termed B cell zone FRCs (BRC), are characterised by high levels of BP-3 and podoplanin expression but lack FDC markers like CD21/35. BRC represent an important source of oxysterol chemoattractants, BAFF, CXCL13, and the Notch ligand DL4 (Cremasco et al., 2014, Fasnacht et al., 2014, Yi et al., 2012). Induction of these cells in response to inflammation has been shown to be dependent on LTβR stimulation provided by B cells, to trigger the upregulation of CXCL13 (Mionnet et al., 2013). These cells have been observed both in the lymph node and the spleen, indicating that they play an important role in supporting all B cell responses (Cremasco et al., 2014, Fasnacht et al., 2014). It appears that these cells alone are important for supporting the organisation of the lymphoid follicles and B cell viability, independently of the FDC (Cremasco et al., 2014, Wang et al., 2011). The presence of these cells has been shown to be important in supporting the ability of an organism to mount an influenza infection (Denton et al., 2014). These cells are a relatively newly described subtype, and so have not been examined in detail as yet.

Pericytic FRCs have also identified surrounding and supporting the HEVs. These FRCs have been shown to interact with the platelets as they leave the vessels. This interaction occurs via the FRC-expressed gp38 and CLEC-2 expressed on the platelets and functions to maintain the integrity of the HEVs (Benezech et al., 2014). The release of sphigosine-1-phosphate by these platelets is also responsible for maintaining the junctions between the endothelial cells (Girard and Springer, 1995). In the absence of either of these markers, the lymphatic vasculature does not develop properly, and gp38-/- lymph nodes exhibit severe infiltration with erythrocytes resulting in an embryonic lethal phenotype (Schacht et al., 2003).

1.3.2 Follicular Dendritic Cells

The structure of FDCs has been established using both light and electron microscopy techniques and the cells have been shown to have a structure that uniquely define their role as professional antigen presenting cells (APCs). These cells are identified as having many fine dendritic processes that can extend and form intimate interactions with neighbouring cells. These processes can take two different major forms; one being smooth, finger-like dendrites and the other appearing like “beads on a string”, the “beads” are called iccosomes – due to their composition of high numbers of immune complex bodies. Smoother processes are able to transform into iccosome rich networks after delivery of antigen (El Shikh and Pitzalis, 2012). FDC dendrites can be highly variable in both length and thickness of the processes, ranging from non-uniform, short dendrites with folds and thickenings, to narrow, elaborate arrangements. The ICs are displayed on these dendritic processes. Due to their high surface area, FDC display very little cytoplasm, and have a distinctive irregular nuclei, which can be bilobed and contain distinct nucleoli (Sukumar et al., 2008, Sukumar et al., 2006). The evidence that these cells may be binucleate has lead to the hypothesis that FDCs are formed by the fusing of CD35+B220+ cells with CD45- CD35- stromal cells (Murakami et al., 2007), however, there is currently no conclusive evidence for this.

The expression of CD21/35, otherwise known as complement receptor 1 (CR1) and complement receptor 2 (CR2), on FDCs is essential for their function in presenting immune complexes for B cell recognition (Barrington et al., 2002, Roozendaal and Carroll, 2007). FDCs are able to retain these ICs on their surfaces long-term, but are unable to phagocytose and process antigen themselves. The ICs are conserved on the surface of the FDCs mainly via CD21/35, although expression of low affinity Fc receptors FcγRIIB (CD32) and FcεRII (CD23) and factors such as iC3b, C3d and C3dg from complement 3 are also important to allow this function to occur (El Shikh and Pitzalis, 2012). FDCs are able to present proteins in their native form across multimerised ICs. This allows the cross-linking of the B cell

receptors (BCRs) resulting in more efficient B cell activation and initiation of the germinal centre response (Sukumar et al., 2008).

Due to their anatomical localisation, FDCs are not in close contact with any circulatory systems and so the mechanisms by which antigen is delivered to these stationary cells for presentation to B cells are widely debated (Imazeki et al., 1992). Antigen can be identified within the follicle as soon as 1 minute after administration (El Shikh and Pitzalis, 2012). Recent work has shown that immunisation with proteins can activate circulating complement factors, so that complement factor C3 binds to the antigen. This complex can then be transported through the circulation into lymphoid organs within SCS macrophages (SCSM). The formation of this complex is essential for the trafficking of large antigens into the lymph nodes (Zhang et al., 2016). Once inside the LN, the SCSMs can transfer the C3:antigen complex onto naïve B cells, where they bind via CR1/2-CD32; B cells can then migrate along their chemokine gradient to the developing FDC networks within B cell follicles (Phan et al., 2007).

In the spleen, a similar process occurs where antigen is trafficked by marginal zone B cells which traffic between the centre of the follicle and the marginal zone macrophages (Arnon et al., 2013). Once inside the B cell follicle, the C3:Ag complex can be recognised by pre-existing specific antibodies (during a secondary immune response), or by innate recognition molecules including IgM, C-type lectins and pentraxins. These factors can then opsonise this complex, further activating complement, which allows binding of the C3 coated immune complexes to the CR1/2 receptors expressed on FDCs (Cyster, 2010, Gonzalez et al., 2011). The transfer of immune complexes onto the FDCs occurs via CR1/CR2 engagement, and the immune complex is then rapidly internalised by actin polymerisation (Heesters et al., 2013). Both the macrophages and the B cells are able to bind the C3:antigen complex simultaneously via different complement receptors (Heesters et al., 2014). FDC maturation results in the cells upregulating various molecules important for anchoring ICs to the cell and ensuring that B

cells are able to receive a sufficient stimulation, including adhesion molecules such as VCAM-1, ICAM-1 and MAdCAM-1, and low affinity Fc receptors that anchor the B cell and provide the costimulatory signals required for full B cell activation. FDCs are also responsible for marking apototic B cells with milk fat globule-8 (MFGE-8, recognised by the antibody clone FDC-M1) for uptake and clearance by the tingible body macrophages that patrol the germinal centre clearing lower affinity B cells (Kranich et al., 2008, Aguzzi et al., 2014).

The identification of progenitor cells for FDCs and the mechanism governing the development of this stromal cell subtype has previously proved difficult (Kasajima-Akatsuka and Maeda, 2006). Induction of FDC maturation is strictly dependent on the expression of TNF and lymphotoxin (LT), as mice that are deficient in the expression of these molecules or in their downstream signalling pathways are unable to develop FDCs and GCs within their SLOs (Allen and Cyster, 2008). The cells responsible for providing this stimulus are the B cells, and it has been shown that soluble TNF produced by these cells is more important for FDC maturation than membrane-bound TNF (Tumanov et al., 2004). As naïve B cells are responsible for providing the TNF required for FDCs to mature; and FDCs are essential to provide the maintenance and differentiation factors required for maturation of the naïve B cells, these two cell types therefore function in a positive feedback loop (El Shikh and Pitzalis, 2012). FDCs express CXCL13, which signals via CXCR5 expressed on naïve B cells and attracts them to the nascent follicle. Accordingly, CXCR5- B cells are able to migrate into the splenic white pulp, but are unable to traffic to the follicle and so induce FDC in atypical locations. Stimulation of the B cells via CXCR5 causes them to express LT and TNF, inducing the maturation of FDCs as described previously (Forster et al., 1996, Voigt et al., 2000, Ngo et al., 1999). Removal of FDCs during the germinal centre reaction completely disrupts the architecture of the follicles and destroys the germinal centre response by eliminating the germinal centre B cells and simultaneously increasing the density of T cells and DCs (Wang et al., 2011).

Recently, a great deal of research has been carried out in order to attempt to resolve the identity of the FDC precursor. Initially, expression of FDC markers (MFGE-8 and CXCL13 transcripts) was observed surrounding the splenic vasculature, on PDGFRβ+NG2+ perivascular cells (Krautler et al., 2012). The authors of this paper have indicated that the perivascular precursors upregulate MFGE-8 in response to LTβR signalling to become a pre-FDC subtype, which then mature to fully functional FDCs upon lymphocyte stimulation. (Krautler et al., 2012) Another group investigating the splenic stromal development have indicated the transcription factors Nkx2-5 and Islet1 are important for the development of the splenic mesenchyme (Castagnaro et al., 2013). Lineage tracing experiments have indicated that many of the adult stromal cell compartments in the spleen are derived from these Nkx2-5^{+}Islet1^{+} mesenchymal precursors, notably the TRC, MRC and FDC (Castagnaro et al., 2013). These findings have supported previous evidence indicating that the FDCs appear to differentiate from a mesenchymal precursor, although the mechanism by which this is able to proceed was unclear (Aguzzi and Krautler, 2010, Wilke et al., 2010, Mabbott et al., 2011). On the other hand, the Nkx2-5^{+}Iselt1^{+} lineage have been shown to play no role in the generation of either LN or Peyer's patch stroma (Castagnaro et al., 2013). Therefore, a more recent study investigated the origin of FDCs in the lymph node using elegant multicolour fate mapping experiments (Jarjour et al., 2014). This study was able to indicate that FDCs which expand in response to inflammation differentiate from a tissue-resident precursor which the group identified as the marginal reticular cells (MRCs). The cells mature via an intermediate CD21/35^{+}RANKL^{int} population which can be observed close to the subcapsular sinus, which then passage further into the centre of the follicle and upregulate CD21/35, while downregulating RANKL, developing into mature FDC (Jarjour et al., 2014). These data indicate that the FDCs in different anatomical locations derived from different precursors. However, as evidence has indicated that the MRC are derived from the LTo mesenchymal precursor, all FDCs appear to differentiate from mesenchymal stem cells, although the manner in which this differentiation occurs appears to vary in different organs., and also depends on the immunological activation.

1.3.3 Marginal Reticular Cells

MRCs are the most recently identified and the smallest currently described population of lymphoid stromal cells (Katakai, 2012). These cells are located in the outer margin of the cortex, just below the subcapsular sinus of the lymph node where they form a thin layer of reticulum between the SCS and the paracortical region. MRC are identified as being CXCL13+ and MAdCAM-1+, but CCL21-, indicating that they are distinct from the FRC, and CD21/35$^{lo/}$, indicating that these cells are not FDCs. As previously discussed, these cells appear to be the direct descendants of the LTo cell that directs the development of the lymph node anlage (Eberl et al. 2004; Finke et al. 2002; Cupedo et al. 2004; Katakai et al. 2008). Importantly, these cells express RANKL and TRANCE, both of which are essential for LN development, meaning that they were a distinct subset and so were defined as MRCs (Katakai et al. 2008). These cells have been observed in the periarteriolar lymphoid sheaths within the spleen, and similar cells have been found in the subepithelial dome in MALT (Knoop et al. 2009).

Due to the anatomical location of MRC within the secondary lymphoid organs, it is believed that they play a role in controlling the influx of antigen into the tissue. MRCs have been shown to be capable of forming a conduit network underneath the subcapsular sinus, allowing soluble antigens to transport from the exterior of the follicle to the centre of the follicle and the FDCs (Bajenoff and Germain, 2009, Roozendaal et al., 2009). These MRCs may also have a supportive role towards to CD169+ macrophages which are responsible for the capture and transport of small particles from the afferent lymphatics into the follicles (Phan et al., 2009). This role of the MRCs may be especially relevant in the Peyer's patch, as the development of the M cells which are responsible for the uptake of antigen from the gut lumen has been shown to be dependent on RANK:RANKL signalling, possibly provided by these cells (Knoop et al., 2009). Finally, MRC might also play a role in the remodelling of the secondary lymphoid organs following immune challenge. This process progresses in a similar way to the initial development of the SLOs. It is known that the MRCs are very closely related to the LTo cells, indicating

that these cells may be able to communicate with the LTi cells (ILC3s) present in the adult mouse allowing for this remodelling (Kim et al., 2003, Scandella et al., 2008).

1.3.4 Endothelial stromal cells in lymphoid organs (Blood Endothelial Cells, Lymphatic Endothelial Cells and High Endothelial Vessels)

Specialised vascular structures known as high endothelial venules (HEVs) permeate the lymph nodes, these blood vessels are formed by a population of specialised "plump" blood endothelial cells (BECs). The expanded size of the endothelium results in a reduced vascular lumen to and the BEC also express high levels of adhesion molecules such as VCAM-1, ICAM-1 and MAdCAM, as well as the chemokine CCL21. The combination of these two features allow for efficient trafficking of naïve lymphocytes out of the circulation and into the lymph node to generate mature adaptive immune responses. In contrast, the lymphatic endothelial cells make up the walls of the lymphatic vessels, as well as being found in the interfollicular regions and the T cell zones (Mueller and Germain, 2009). As these cell types are both endothelial, they both express CD31, with LECs also expressing gp38, whereas BECs do not (Link et al., 2007).

Current evidence points to there being three distinct subsets of LECs, which are defined by their anatomical location and differential expression of markers. LECs can be either subcapsular LECs (S-LECs), cortical LECs (C-LECs) or medullary LECs (M-LECs) (Kedl and Tamburini, 2015). S-LECs are PD-L1^{hi}ICAM-1^{hi}MadCAM-1^{+}LTβR^{lo}, and line the subcapsular sinus and play a role in controlling the antigen uptake from the incoming lymphatic fluid (Kedl and Tamburini, 2015). M-LECs are found in the lymph node medulla, at the efferent lymphatic junction, where they are notable for their high expression of PD-L1, ICAM-1 and LTβR (Grigorova et al., 2010, Roozendaal et al., 2008, Sinha et al., 2009). The C-LECs form conduits which permeate the lymph nodes and come into contact with both other subsets

of the LECs and express LTβR and intermediate levels of PD-L1 and ICAM-1 (Tewalt et al., 2012, Cohen et al., 2014). These cells are all involved in the control of the flow of lymphatic fluid as it enters and exits the lymph node, and also contribute to the chemokine gradients established within the lymphoid organ (Schumann et al., 2010, Kabashima et al., 2007, Qu et al., 2004). Importantly, LECs have been established as the main source of sphingosine-1-phosphate (S1P), the G-protein coupled receptor essential for the movement of lymphocytes from the SLOs into the lymphatics (Matloubian et al., 2004, Pham et al., 2010). Proliferation of LECs in response to inflammatory challenge is also essential to allow for the influx of lymphocytes that occurs following this challenge (Tamburini et al., 2014). A novel role for these cells has recently been proposed, by which they are able to maintain antigen within the SLO for prolonged period of time following inflammation. The prolonged presence of antigen was established as being independent of the presence of FDCs, as the antigens can persist in B cell -/- mice or CR2-/- mice (Tamburini et al., 2014). Tamburini et al. (2014) were able to establish that the antigen was being captured and maintained by LECs for a significant amount of time following immunisation using fluorescence labelled antigen. From this data, the group established that LECs were responsible for archiving antigen for prolonged periods of time following immune challenge, assisting in the faster and stronger immune response generated upon secondary exposure to the antigen (Kedl and Tamburini, 2015).

1.4 CD248

1.4.1 Structure

CD248 is otherwise known as endosialin or tumour endothelial marker-1 (TEM-1). It has a number of different names because it was identified via a number of different studies and subsequently found to be the same molecule (Christian et al., 2001, MacFadyen et al., 2005, MacFadyen et al., 2007, Christian et al., 2008).

CD248 is a glycoprotein with a 95kDa protein core surrounded by 95kDa of highly sialylated O-linked oligosaccharides. Because of the high levels of glycosylation, the crystal structure has not been fully resolved, although a putative domain structure has been published (Christian et al., 2001). According to this structure, CD248 is hypothesised to be a type 1 C-type lectin membrane receptor that shares 33% sequence identity with human C1qR complement receptor and 39% identity with human thrombomodulin (CD141), an endothelial cell receptor and CD93 (otherwise known as C1qRp), a protein involved in cell adhesion and regulating inflammation (Valdez et al., 2012). The human CD248 gene is 2274 base pairs in length and does not have any intron. This gene is located on chromosome 11 in humans, whereas the murine counterpart is found on chromosome 19. The resulting protein consists of 757 amino acids, with a number of different domains. The N terminal domains between the different members of the family are very similar with a globular C-type lectin domain (CTLD), which is 157 amino acids long in CD248. This is attached to a complement control protein or SUSHI domain, which is then followed by three epidermal growth factor (EGF) repeats, a mucin-like domain and then a 51 amino acid cytoplasmic tail at the C-terminal (Christian et al., 2001). This C-terminal has also been proposed to be responsible for clustering of protein complexes and anchoring transmembrane proteins to the cytoskeleton, however, there is currently no evidence that CD248 has this functional role, and this has just been hypothesised from the proposed structure. The murine CD248 protein

shares 77.5% sequence homology with the human protein, with the transmembrane and cytoplasmic domains being mostly highly conserved (Opavsky et al., 2001).

1.4.2 Known expression and interactions

CD248 is a relatively new molecule that has been identified as having a role in promoting the growth and invasiveness and metastasis of tumours (Valdez et al., 2012, Maia et al., 2011), as well as having been identified on a number of stromal cell markers, making this molecule an interesting target in cancer and in other inflammatory diseases. The expression of CD248 has been shown to be mainly on fibroblasts and pericytes, and in the lymph node capsule, as previously mentioned (MacFadyen et al., 2005, Virgintino et al., 2007, Christian et al., 2008, Simonavicius et al., 2008, Tomkowicz et al., 2010, Simonavicius et al., 2012).

Studies using the CD248 knockout mouse to investigate the role of this molecule in the progression of cancer have found that these mice exhibit reduced cancer growth following implantation of cancerous cells, compared to wild type animals (Nanda et al., 2006). Investigation of the expression of CD248 within tumours have found that CD248 is expressed on pericytes that surround the tumour vasculature, and so may it may potentially play a role in supporting tumour angiogenesis and growth (Bagley et al., 2009, Tomkowicz et al., 2007, MacFadyen et al., 2005, MacFadyen et al., 2007). An article published by Nanda *et al*. (Nanda et al., 2006) has shown that the progression of tumour development in different tumour models in both immunocompromised and immunocompetent mice was compromised in the absence of CD248. In this study, $CD248^{-/-}$ nude mice not only had an increased survival compared to the WT counterparts, but also increased incidence of metastases. This study found expression of CD248 on the tumour vasculature in the WT mice, and hypothesised that it is involved in angiogenesis, as the authors also observed abnormal tumour development, with the

CD248$^{-/-}$ mice developing much longer, flatter and less rounded tumours which had a decreased invasiveness compared to the WT mice. Importantly, the authors were unable to find any evidence for a defect in s.c. vascularisation in a wound healing model. This differential response in the normal angiogenesis and in the development of the tumour vasculature indicates that CD248 plays an interestingly varied role in these different disease processes. However, the authors were unable to explain how CD248 is able to produced this nuanced response (Nanda et al., 2006). Interestingly, the lack of CD248 appears to result in a significant increase in the migratory velocity of cells, this was observed both in CD248$^{-/-}$ MEF, but also when the human osteosarcoma cell line is transfected with CD248, the migratory velocity of the CD248-expressing cells in significantly increased (Lax et al., 2010). This is relevant when compared to the decreased invasiveness observed by Nanda *et al*. (Nanda et al., 2006).

Expression of CD248 has also been studied in human disease states, and it has been found on fibroblasts in the synovium from rheumatoid arthritis patients and in chronic kidney disease. Other diseases that are associated with an increased expression of CD248 include cirrhotic end stage liver disease, where CD248 mRNA has been identified on the hepatic stellate cells (HSC) (Wilhelm et al., 2016). In a variety of human tumours, including small intestine, renal cell carcinoma, melanoma and brain metastasis, CD248 expression has been found to be highly upregulated when compared to the very low resting expression (MacFadyen et al., 2005).

CD248 is expressed in the developing embryo in a number of different developing tissues at different stages of development, as early as embryonic day 8.5 (Opavsky et al., 2001). Weak expression can be observed in the heart at E10 (Huang et al., 2011) and in the developing vessels surrounding the brain (Rupp et al., 2006). Expression on mesenchymal cells and in the developing lymphoid organs can be observed from embryonic day 15 onwards, with the expression becoming restricted specifically to lymphoid structures as development progresses (MacFadyen et al., 2007, Lax et al., 2007).

Mesenchymal cells expressing CD248 are able to differentiate into various lineages, including adipose tissue and bone (Naylor et al., 2012, Bechar, 2012). The importance of the CD248 expression by these cell types is evidenced by work done by this laboratory, which has shown that the CD248 knockout mice develop stronger bones than their wild type counterparts at the expense of the development of adipose tissues, resulting in stronger bones and less fat in the CD248 knockout mice (Naylor et al., 2012, Bechar, 2012). However, the role of CD248 in maintaining the balance of these three distinct lineages requires further investigation in order to fully understand the differentiation of these cell types. In vitro cultured cells are also understood to express CD248, notably mouse embryonic fibroblasts and other mesenchymal stem cells as well as pericytic cells (Christian et al., 2008, Bagley et al., 2009). Expression of CD248 cannot be observed on human umbilical vein endothelial cells, even upon stimulation with a variety of different factors (Rettig et al., 1992, MacFadyen et al., 2005, Carson-Walter et al., 2009). The stromal cell scaffold of lymphoid organs has been shown to be derived from mesenchymal stem cells (Castagnaro et al., 2013). Interestingly, during lymph node embryogenesis, CD248 is highly expressed in the spleen, thymus and lymph node. This expression becomes progressively restricted to the capsule (Lax et al., 2007). After birth in resting conditions, the capsule is the only $CD248^{+}$ structure in the organ, excluding the pericytes that surround bloods vessels that express CD248 in the secondary lymphoid organs (MacFadyen et al., 2005, Lax et al., 2007, Teicher, 2007, Armulik et al., 2011). This would indicate that CD248 plays some role in controlling the development of the lymphatic tissue, although the mechanism by which this is able to proceed is not understood.

During the immune response, the expression of CD248, which is restricted to the lymph node capsule in homeostatic conditions, has been shown to be significantly upregulated throughout the spleen in response to salmonella infection (Lax et al., 2007). Further investigation into this mechanism, exploiting the CD248-/- mice has demonstrated that expansion of popliteal lymph nodes (pLN) in response to paw pad immunisation with NP-CGG is compromised, resulting in a significant reduction

in the size of these LN at the peak of the immune response. Interestingly, the authors were unable to identify any defects in the immune response, most notably with normal antibody production in the CD248-/- mice (Lax et al., 2010). The role of CD248 in other inflammatory processes was investigated in a model of liver inflammation following carbon tetrachloride (CCl_4) injury (Wilhelm et al., 2016). The authors found no difference in the inflammatory response to this stimulus as there was no significant difference in the expression of hepatic CD45. The $CD248^{-/-}$ mice also demonstrated a significant reduction in the levels of fibrosis compared to WT mice, a key regulator of which is understood to be the cytokine TGF-β, which was shown to be reduced in the WT mice compared to the $CD248^{-/-}$. However, there is no difference in a number of other pro-fibrotic factors, including matrix metalloproteinase-2 (MMP-2), MMP-9 and tissue inhibitor of matrix metalloproteinase-1. This reduction in TGF-β appears to result in a significant reduction in the accumulation of collagen in the portal area of the liver, as well as a reduction in the mRNA expression of procollagen α-1, which combine to result in a significant reduction in liver fibrosis in $CD248^{-/-}$ mice. However, the resolution of fibrosis following injury shows no significant difference between the WT and $CD248^{-/-}$ mice. This data is particularly interesting as it appears to show that CD248 plays a very subtle role in the progression of this disease, as inflammation is unaffected in the CD248-/-, whereas there is a reduction in the level of fibrosis, which was thought to be a product of the inflammation. This interestingly nuanced role of CD248 was also reported on in previous work published by this group (Lax et al., 2010), and also in the context of cancer progression as discussed before in the report by Nanda *et al*. (Nanda et al., 2006).

1.4.3 Binding partners and hypothesised signalling pathways

The extracellular domain of CD248 is currently being investigated widely and several potential ligands have been identified. CD248 is understood to bind to extracellular matrix components such as

fibronectin, collagen type I and collagen type IV. The binding of CD248 to these molecules appear to play an active role in controlling the remodelling of tissues, notably in regulating the invasiveness of tumour microvasculature by enhancing the activity of matrix metalloproteinase 9 (MMP-9) (Tomkowicz et al., 2007). CD248 has also been shown to be able to control metastasis of different tumour cells *in vitro* via its binding to the C terminal core protein of the galectin 3 binding protein Mac-2BP/90K (Becker et al., 2008). This binding may initiate a repulsive signal, similar to the Ephrin-receptor binding which has been thoroughly examined in angiogenesis and neural crest patterning (Cheng et al., 2002). The repulsive signal observed here may then contribute to distant metastasis of cancer cells throughout the organism (Valdez et al., 2012).

CLEC14A, another member of the CD93 superfamily that includes CD248 is known to control sprouting and splitting angiogenesis via binding to the axtracellular matrix component MMRN2 (Noy et al., 2016). CD248 itself is also known to play a role in sprouting but not splitting angiogenesis in skeletal muscle, indicating a functional and possible binding partner link between these two members of the family (Naylor et al., 2014).

The binding of the intracellular domain and the subsequent signalling promoted by this molecule is proving elusive to establish. The cytoplasmic tail is very short, although it has been shown to play a role in inflammatory disorders, with mice lacking the cytoplasmic domain of CD248 alone exhibiting reduced arthritis progression mimicking the full CD248-/- (Maia et al., 2010). The lack of the cytoplasmic domain also reduced the growth of tumours in a number of murine cancer models (Maia et al., 2011). A recent study investigating the signalling of CD248 has shown that in CD248-/- cells, PDGF-BB stimulation of ERK phosphorylation and c-Fos transcription is inhibited (Tomkowicz et al., 2010). This indicates a role in controlling PDGFRβ signalling, however, this effect does not appear to be directly related to the action of CD248 on PDGFRβ itself. Further investigation of this signalling pathways showed that PDGF-BB stimulation is unable to promote cell proliferation in CD248-/-

osteoblasts in comparison to their WT counterparts (Naylor et al., 2012). CD248-/- hepatic stellate cells also exhibit a defective proliferative response to PDGF-BB stimulation, as compared to their WT counterpart (Wilhelm et al., 2016).

This link between CD248 and PDGFR has also been investigated by using the PDGFR signalling inhibitor imatinib mesylate. This drug is used widely in the treatment of a number of cancers, including chronic myeloid leukaemia, and a number of solid state cancers such as gastrointestinal stromal cancers (Demetri et al., 2002, Wang and Li, 2015). Imatinib mesylate is understood to inhibit the action of several tyrosine kinase oncogenes, responsible for the transformation into malignant cells. For example, it has been shown to be able to inhibit the BCR/ABL tyrosine kinase pathway by enhancing MAP kinase activity in CML CD34+ cells (Chu et al., 2004). Work carried out in this laboratory has shown that treatment with imatinib mesylate is able to mimic the defect in sprouting but not splitting angiogenesis observed in the CD248-/- cells (Naylor et al., 2014). However, this investigation has still not revealed the direct mechanism by which CD248 is able to interact with the PDGFRβ signalling pathway.

1.5 NP-CGG immunisations

The immune response generated in response to the antigen 4-hydroxy-3-nitrophenyl acetyl (NP) conjugated to chicken gamma globulin protein (NP-CGG) has been extensively studied (Luther et al., 1997, Toellner et al., 1998). This antigen has been shown to generate a robust, germinal centre-dependant immune response. Luther *et al.* were able to demonstrate that mice immunised s.c. into the paw pad with NP-CGG were able to generate specific IgG antibodies, which were detectable from day 5, peaking around day 8, with the titres remaining constant through until day 30, when the experiment ended. The authors also reported a significant expansion in the total numbers of $B220^+$ B cells in response to the immunisation, and formation of germinal centres by day 5 post-immunisation (p.i.) (Luther et al., 1997). This observation was confirmed in a later publication by Toellner *et al.* (Toellner et al., 1998). Antigen was observed on the surface of FDCs at day 8 p.i., demonstrating that this immunisation protocol was sufficient and appropriate for studying germinal-centre dependent responses. Further investigations into the mechanisms of the immune response generated by NP-CGG immunisation demonstrated that significant immunoglobulin class-switching was observed following immunisation, with 40% of all NP-specific cells having undergone class-switching (Toellner et al., 1998). This data indicates that NP-CGG immunisation is able to generate a strong, germinal centre-driven response, and that this response can be measured by directly investigating antigen-specific B cells by flow cytometry and by measuring antigen specific antibody responses.

This immunisation protocol has previously been used within this group in order to investigate the immune response in the $CD248^{-/-}$ mice (Lax et al., 2010). This study investigated the response generated in the popliteal lymph node in response to this immunisation in the CD248-/- mice. The authors demonstrated that CD248 was essential for the expansion of the LN, but were unable to describe the CD248-espressing LN stromal cells which contribute to this mechanism. In this thesis, I have endeavoured to further develop these data in an attempt to understand which lymphoid stromal

cells express CD248, and also whether there are any differences in the stromal cell compartments in different lymphoid tissue. This, taken together with the fact that NP-CGG immunisations generate a robust and well-characterised germinal centre response, encouraged the selection of this immunisation protocol for this thesis in order to characterise the role of CD248 in controlling the function of different lymphoid stromal cell compartments during the germinal centre reaction.

1.6 Project Hypothesis

CD248 has been shown to be a molecule with a wide variety of functions in a number of disease states. Previous work in this laboratory has explored the role of CD248 in modulating the differentiation of mesenchymal stem cells (MSCs) into different lineages. The body of work described in this thesis endeavours to further investigate this role of CD248 in controlling the differentiation of MSCs to the lymphoid lineage. There is previous evidence that this lineage is linked to the development of the adipocyte lineage (Benezech et al., 2010) and in this thesis I intend to further investigate the links between these different lineages, based on the previous work indicating that CD248 is involved in the differentiation of preadipocytes (Bechar, 2012, Naylor et al., 2012). Additional previous work has shown that CD248 is highly expressed in lymphoid tissues during the immune response (Lax et al., 2010). In this thesis I will also attempt to further develop this work and identify the CD248-expressing stromal cells which expand in response to immunisation and also to discover what role these cells play in the establishment and maintenance of the immune response.

1.7 Project Aims

- To explore the role played by CD248 in controlling the differentiation of mesenchymal stem cells and the development of embryological lymph nodes, and the signalling pathways involved in this differentiation.
- To evaluate the expression of CD248 on adult lymphoid stromal cells in an attempt to understand the dynamic interactions between the stromal cell subsets and to exploit this expression to further delineate lymphoid stromal cell subsets.
- To exploit the CD248 deficient mice in order to understand the function of CD248 in the establishment and maintenance of an adaptive immune response.

Chapter 2. Materials and methods

2.1 Mice

The generation and genotyping of CD248$^{-/-}$ mice has previously been described (Nanda et al., 2006), these animals were generated on the C57BL/6 background. B cell knockout mice lacking the µ chain of the IgM isotype, preventing the pre-B cells differentiating further and exiting the bone marrow (Kitamura et al., 1991) were kindly provided by Kai Toellner. All wild type C57BL/6 animals were purchased from Harlan or Charles River, UK. Mice were bred and maintained by the Biomedical Services Unit, University of Birmingham, and kept under pathogen-free conditions according to Home Office Regulations. Mice were housed in individually ventilated cages in groups of 2-7 individuals on a 12-hour light-dark cycle.

Experiments were carried out at the University of Birmingham (project licence number 70/8003) following guidelines governed in the UK by the Animal (Scientific Procedures) Act 1986, and approved by the ethics committee (Birmingham Ethical Review Subcommittee).

2.1.1 Preparation of NP-CGG in alum

Nitrophenol conjugated to chicken γ-globulin at a ratio of 10-19 (NP-CGG) (2b Scientific) was reconstituted in sterile PBS (SIGMA) to 5mg/ml. NP-CGG and 9% aluminium potassium sulphate solution (SIGMA) (diluted in sterile dH_2O) were mixed in a 1:1 ratio, the pH was adjusted to 6.5 by addition of 10M NaOH stock solution, and the solution was incubated in the dark for 30 min at room temperature. The precipitate was then washed twice in sterile PBS (4 min at 2000 rpm), before resuspension in sterile PBS at 1mg/ml for administration.

2.1.2 Immunisation

Mice at 6-12 weeks of age were immunised either via an intraperitoneal route or by subcutaneous injection into the base of the front paw pads with NP-CGG/alum in sterile PBS prepared as described. Control mice were immunised with PBS alone following the same routes.

The primary immunisations were carried out on day 0, with secondary and tertiary rechallenges carried out on day 21 and day 41 respectively. Animals were then sacrificed by exsanguination at 8 days after final immunisation (day 8, day 30 and day 50) (Nishimura et al., 2011). The appropriate organs were then dissected out and processed for cryosectioning or flow cytometry as outlined below

2.1.3 Treatment with imatinib

Administration of imatinib mesylate at a therapeutic dose *in vivo* has already been described (Schultheis et al., 2012). Mice were dosed at 150mg/kg/day imatinib mesylate. This was achieved by giving imatinib daily for 7 days, beginning one day before final immunisation until the end of the experiment. Imatinib mesylate was administered at a concentration of 15mg/ml in deionised sterile H_2O by gavage.

2.1.4 Isolation of embryological lymph nodes

Female mice were timed-mated to be able to date the embryological stages of development. Pregnant mice were sacrificed by cervical dislocation at E18, and the pups were dissected out of the mother. These embryos were culled by decapitation. New born mice were culled by decapitation.

Lymph nodes anlage were dissected out of the embryos with the help of a stereo microscope (Leica, Bucks, UK). The organs were then stored on ice cold RPMI with 2% foetal calf serum.

2.2 *In vitro* culture

2.2.1 Isolation of mouse embryonic fibroblasts

Pregnant mice at E15 were culled and the embryos dissected out of WT and CD248-/- female mice. The embryos were culled by decapitation. The total skin from the embryos was harvested and mashed in sterile PBS. The resulting tissue was then digested for 15 minutes at 37°c with constant agitation in 2ml Trypsin-(5%) EDTA (2%). The enzyme reaction was stopped with 3.5ml RPMI (10% FCS), and the resulting samples were centrifuged at 300xg for 5 minutes. The resulting pellet was resuspended in 10ml DMEM (10% FCS, 1% GPS) and incubated at 37°c in 5% CO_2 in two T25 cell culture flasks. Non-adherent cells were washed off with a change of media, and the flasks then grown to confluence before being passaged and frozen as outlined below.

2.2.2 Isolation of adipose derived stem cells

Subcutaneous inguinal adipose tissues were dissected from adult WT and CD248-/- mice and rinsed in sterile PBS before being placed into sterile 1.5ml eppendorfs. 700µl collagenase solution (collagenase II (GIBCO) 1mg/ml solution in sterile PBS) and 70µl CaCl (30mM) was added and the tissue was finely minced using scissors. Once minced, tissue samples were incubated in digestion buffer at 37°c with agitation for 45mins – 1hour, with frequent pipetting to ensure disruption of the tissue. The digested tissue was then forced through a 100µm cell sieve with a syringe plunger and washed through with sterile DMEM. The resulting cells were pelleted by centrifugation for 5 minutes at 300g, and the supernatant was removed. The cells were resuspended in sterile DMEM and then filtered twice more. Cell pellets were resuspended in red blood cell lysis buffer (SIGMA) for 5 minutes at room temperature, before being washed in sterile PBS. Resulting cells were then counted and seeded in T75 cell culture flasks at 10,000cm^2, and then incubated overnight at 37°c. Non-adherent cells were washed out of culture with sterile PBS and fresh media was then added and cells were cultured as below.

2.2.3 Culture of MEFs and ADSCs

Confluent cells were harvested from flasks using trypsin (5%)-EDTA (2%) enzyme solution (SIGMA) for 5 minutes at 37°c at 5% CO_2. Cells were then either frozen or reseeded into additional or larger flasks and incubated at 37°c in 5% CO_2 until confluent. Cells were frozen at -80°c in foetal calf serum (FCS) with 10% DMSO before being transferred to liquid nitrogen stores for long term storage.

2.2.4 *In vitro* stimulation

MEFs and ADSCs harvested and cultured as described were then seeded at $1x10^6$ cells/well in a 6 well plate and rested overnight before stimulation with LTβR agonist antibody (clone 4H8, Novus Biologicals) at 2µg/ml concentration (Banks et al., 2005, Dejardin et al., 2002) and murine TNF-α (Thermo Scientific) at 10ng/ml following a previously established protocol (Benezech et al., 2012). Cells were kept in stimulation media as long as indicated (1 hour and 72 hours), before being prepared for analysis as described below.

2.3 Flow cytometry

2.3.1 Tissue digestion

Harvested tissues were kept in 5ml ice-cold RPMI until ready for processing. The tissues were then placed in 2ml of digestion buffer (RPMI 2% FCS with 0.8mg/ml Collagenase/Dispase (Roche), 0.2mg/ml Collagenase P (Roche) and 0.1mg/ml DNase1 (SIGMA)) and the organ structure was mechanically disrupted using scissors. The tubes were then incubated at 37°c with constant agitation for 20 minutes. The samples were repeatedly pipetted using p1000 during the incubation time to increase separation. After 20 minutes, the supernatant was removed from the samples and filtered through a 70µm cell strainer into 10ml ice cold MACS buffer (PBS, 1% BSA, 0.2mM EDTA), and then kept on ice. 2ml fresh digestion buffer was then added to each sample, which were incubated for 10 minutes at 37°c with constant agitation. Samples were pipetted regularly during the incubation to increase the separation of the cells. After 10 minutes, the samples were filtered through 70µm cell strainer into the 10ml ice cold MACS buffer and washed through with another 10ml MACS. Further digestion steps can be undertaken until all fragments are completely digested. The MACS buffer should now contain the entire cell fraction of the organs. The cells were then pelleted by centrifuging samples at 300xg for 4 minutes at 4°c. The resulting cells were then counted and stained in appropriate amount of antibodies as below.

Purified collagenase enzymes are used for this digestion in preference to traditional collagenase preparations taken from different fractions of bacterial supernatants because of the reduction in composition variability and the increase in stability of the preparation (Cavanagh et al., 1997). The collagenase fractions also present higher levels of endotoxins, which may cause activation of the immune cells, affecting the validity of the assay (Vargas et al., 1997, Eckhardt et al., 1999, Vargas et al., 1998). The selection of digestion method to study the stromal compartment is also based on the yield of cells required. The different collagenase enzymes can be classified based on their activity.

Collagenase D has a much higher activity than Collagenase P. Because of this increased activity, Collagenase D is more successful at disrupting the bonds between the cells, allowing for better separation of the cell populations. However, use of this method also requires Collagenase Dispase enzyme to be used separately, adding time to the protocol. The strength of the enzymes might also compromise the preservation of some of the cell surface markers, thus making difficult in the assessment of the cells by flow cytometry and limiting the markers that can be used to differentiate the cells.

Collagenase P requires a slightly longer time to separate the cells, although this enzyme can be used in conjunction with the Collagenase Dispase enzyme, making this method comparable in duration to the Collagenase D digestion protocol. This milder digestion presents the advantage of better preservation of the markers, reducing the loss of cell surface markers necessary for the flow cytometric analysis. Collagenase P digestion was used throughout this thesis as the retention of cell surface markers was considered essential. Representative plots are shown in figure 2.1, indicating that collagenase P is far better at retaining cell surface gp38 expression that collagenase D.

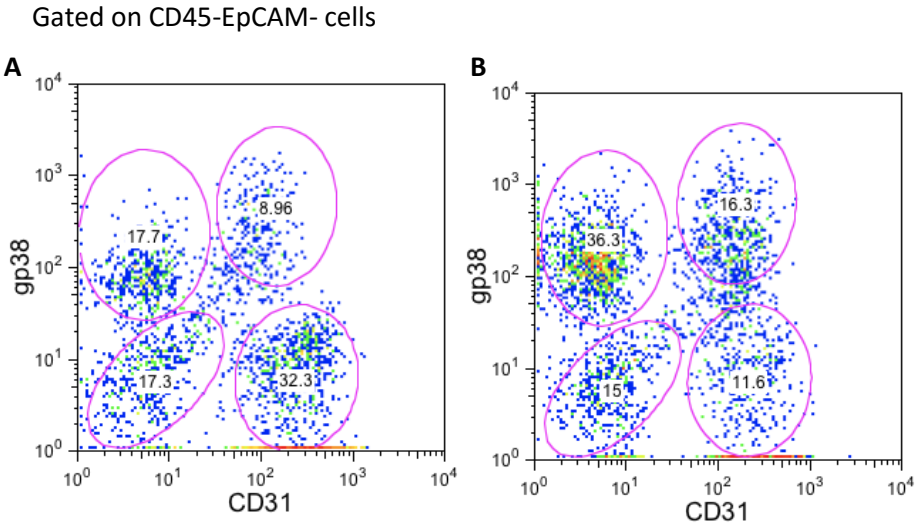

Figure 2.1 Comparison of the lymph node stromal populations generated by different digestion methods. Comparisons of the classical lymph node stromal cell populations achieved following different digestion protocols, with the results for Collagenase D digestion shown in **(A)** and the results from Collagenase P digestion shown in **(B)**

2.3.2 Embryological tissue digestion

Embryological lymph node anlage were isolated as outlined above and then digested for flow cytometry analysis. These organs were placed into 500µl digestion buffer (RPMI 2% FCS, Collagenase/Dispase 2.5mg/ml (Roche), DNase1 100µg/ml (SIGMA)) and incubated at 37°c with constant agitation for 30 minutes. These samples were pipetted several times during incubation to ensure thorough separation. 50µM EDTA was then added to each sample, which were incubated at 37°c for a further 5 minutes. Cells were centrifuged at 300xg for 4 minutes at 4°c. The resulting pellet was then resuspended in sterile RPMI (10% FCS, 1% GPS) and the samples were incubated overnight at 37°c in 5% CO_2 on a 6 well plate. The following day the cells were scratched off the plate and washed out of RPMI before staining in antibodies as outlined below.

2.3.3 Lymphocyte separation

Lymphocytes were prepared from the spleen by disruption and filtration through a 70µm cell strainer. The single cell suspensions produced were washed thoroughly in MACS buffer (PBS 1% BSA, 0.2mM EDTA). Erythrocytes were removed from the suspension by incubation for 5 minutes in 1ml red blood cell lysis buffer (SIGMA). Cells were then washed in PBS, before being centrifuged at 300xg for 4 minutes at 4°c. The resulting cell pellet was then cell pellet was then resuspended in MACS buffer for staining in antibodies as outlined below.

2.3.4 Preparation of *in vitro* cells for flow cytometry

Cells were removed from the incubators and were scratched off the plastic to prevent loss of cell surface markers. These cells were then washed out of media in sterile PBS at 300xg for 4 minutes at 4°c. The resulting cell pellet was then resuspended in MACS buffer for staining in antibodies as outlined below.

2.3.5 Enrichment of stromal cell population using MACS™ beads

Lymphoid stromal cells are understood to make up between 1-5% of the total lymph node cellularity (Malhotra et al. 2012). In order to enrich this population and allow for better separation of the resulting stromal populations, the digested cells were incubated with CD45+ MACS (Miltenyi Biotec) beads at 10µl per 10^7 cells for 15 minutes at 4°c. LD columns (Miltenyi Biotec) were placed onto a Quadro MACS separator and then preactivated with buffer. Cells were then run through the columns the effluent collected. The columns were washed through twice to ensure all negative cells were washed through. The resulting cells were then centrifuged at 300xg for 4 minutes at 4°c. The resulting cell pellet was then cell pellet was then resuspended in MACS buffer for staining in antibodies as outlined below.

2.3.6 Staining

The cells were then stained for 30 minutes at 4°c in the dark in 100µl MACS buffer with antibodies diluted to the correct concentration as shown in table 2.1. Following washing in MACS buffer as above, the cells were then incubated in fixation/permeabilisation (1:4 fixation/permeabilisation concentrate:diluent, both from eBioscience) for 30 minutes at 4°c in the dark. These cells were then washed out of fixing solution using eBioscience wash buffer and resuspended in MACS buffer for acquisition. In order to ensure compensation was set correctly, compensation controls were used. For these controls, BD™ CompBeads were stained with single antibodies. Fluoresence minus one (FMO) controls were also used in order to eliminate false positives in the two-step staining protocols.

Cells were analysed using a CyAn™ ADP Analyzer (Beckman Coulter) with forward/side scatter gating to exclude non-viable cells. Data were then analysed using FlowJo v7 software (Tree Star). For cell sorting, stained ells were sorted using a MoFlo-XDP (Beckman Coulter). The purity of sorted stromal cell populations routinely exceeded 96%.

Table 2.1 Antibodies used for flow cytometry

Antibody (clone)	Format	Working Dilution	Isotype	Supplier
CD45 (30-F11)	APC	1:200	Rat IgG2b	eBiosciences
CD31 (390)	FITC	1:200	Rat IgG2a	eBiosciences
gp38 (ebio8.1.1)	PECy7	1:200	Hamster IgG	eBiosciences
ICAM-1/CD54 (YN1/1.7.4)	PE	1:200	Rat IgG2b	eBiosciences
VCAM-1/CD106 (MVCAM.A)	PERCPCy5.5	1:50	RatIgG2a	Biolegend
CD3ε (145-2C11)	FITC	1:100	Hamster IgG	BD Biosciences
B220 (RA3-6B2)	eFluor 450	1:100	Rat IgG2a	BD Biosciences
CD35 (8C12)	biotinylated	1:100	Rat IgG2a	BD Biosciences
CD4 (RM4-5)	eFluor 450	1:50	Rat IgG2a	eBiosciences
CD157 (BP-3)	APC	1:200	Mouse IgG2b	Biolegend
GL-7 (GL7)	Alexafluor 647	1:100	Rat IgM	eBiosciences
CD95/Fas (15A7)	biotinylated	1:100	Mouse IgG1	eBiosciences
CD19 (eBio1D3)	FITC	1:200	Rat IgG2a	eBiosciences
Ter119 (ter-119)	FITC	1:100	Rat IgG2a	eBiosciences
CD11b (M1/70)	FITC	1:100	Rat IgG2b	eBiosciences
Streptavidin	PECy7	1:200		eBiosciences

2.4 Histology

2.4.1 Tissue harvesting

After dissection, half of an immunised spleen or a whole lymph node was retained for histological analysis. Freshly dissected tissue was placed in a cryomold (Sakura Finetek) and embedded in OCT compound (Sakura Finetek) before being snap frozen in dry ice or liquid nitrogen and stored for cryosectioning at -80°C.

2.4.2 Cryosectioning

Tissues were mounted for sectioning using OCT compound (Sakura Finetek). 6µm sections of tissue were cut using a Leica cryostat at -20°c (Leica, Bucks, UK) and mounted on 4 spot histology slides. Slides were dried thoroughly being fixed for 20 minutes in histological grade acetone (SIGMA) at -20°c. Slides were removed from acetone and dried before being wrapped individually in foil and stored at -80°c for future use.

When microdissection was planned, sectioning was carried out using the same cryostat. However, prior to use, the cryostat was cleaned using Cryofect disinfectant (Leica), and then irradiated under UV light for 40 minutes. PALM membrane PEN slides were activated with UV light and then chilled to -20°c before 8µm sections were cut and mounted onto the slides. Membrane slides were then stored on dry ice for further use.

mRNA was also isolated from whole sections, also using the same cryostat, cleaned before use as for microdissection. 5 sections of 20µm thickness were collected into an RNase-free eppendorf tube using sterile needles. These samples were also stored at -80°c for future use.

2.4.3 Immunofluorescence

When ready for staining, the slides were defrosted thoroughly and then washed in PBS (Phosphate buffered saline tablets, pH7.0, Oxoid). The slides were blocked for 15 minutes in 10% Horse Serum (SIGMA, UK) made up in PBS 1%BSA (SIGMA, UK) (PBS BSA). Excess blocking solution was then aspirated and replaced with primary antibodies. All blocking and staining steps were carried out at room temperature in dark, humid conditions. Antibodies are listed in appendix table 1, with primary antibodies being incubated for 1 hour, and secondary, tertiary, quaternary and quinternary antibodies were incubated for 30 minutes as required. 10 minute washes in PBS were carried out between each incubation step. Following the final wash, the slides were mounted with Prolong Gold Antifade reagent (Invitrogen). The slides were then stored at -20°c until visualisation by confocal microscopy.

Confocal images were acquired using a Zeiss LSM 780 Zen confocal microscope using water immersion objectives as described on each image.

2.4.4 Quantification of immunofluorescence images

Quantification of confocal images was achieved using Zeiss Zen 2010 software to select the appropriate regions. For B cell/ germinal centre analysis, the area was calculated by the software. For quantification of the FDC regions the number of red pixels within the regions were counted and expressed as mean fluorescence intensity per unit of area.

An imagej macro was created to analyse the percentage of area of the germinal centre zone that was covered by FDC-M1 positive pixels. At least two non-overlapping areas within the germinal centre of at least 3000 pixels2 were selected and the area of red was quantified as a % of the total area. Full macro details are described in figure 2.2.

```
title = getTitle;
i   dir = getDirectory("image");
    threshold=50;
    radius=20;
ii  size=50;
iii run("Split Channels");
    close();
    close();
iv  roiManager("select", 0);
    setBackgroundColor(0, 0, 0);
    run("Clear Outside");
v   setThreshold(0, threshold);
    run("Convert to Mask");
    run("Remove Outliers...", "radius=" + radius + " threshold=“ + threshold + “ which=Dark");
vi  run("Invert");
    run("Analyze Particles...", "size=" + size + "-Infinity display clear");
    roiManager("measure");
vii roiManager("delete");
    saveAs("Results", dir + title+ "-Results.xls");
```

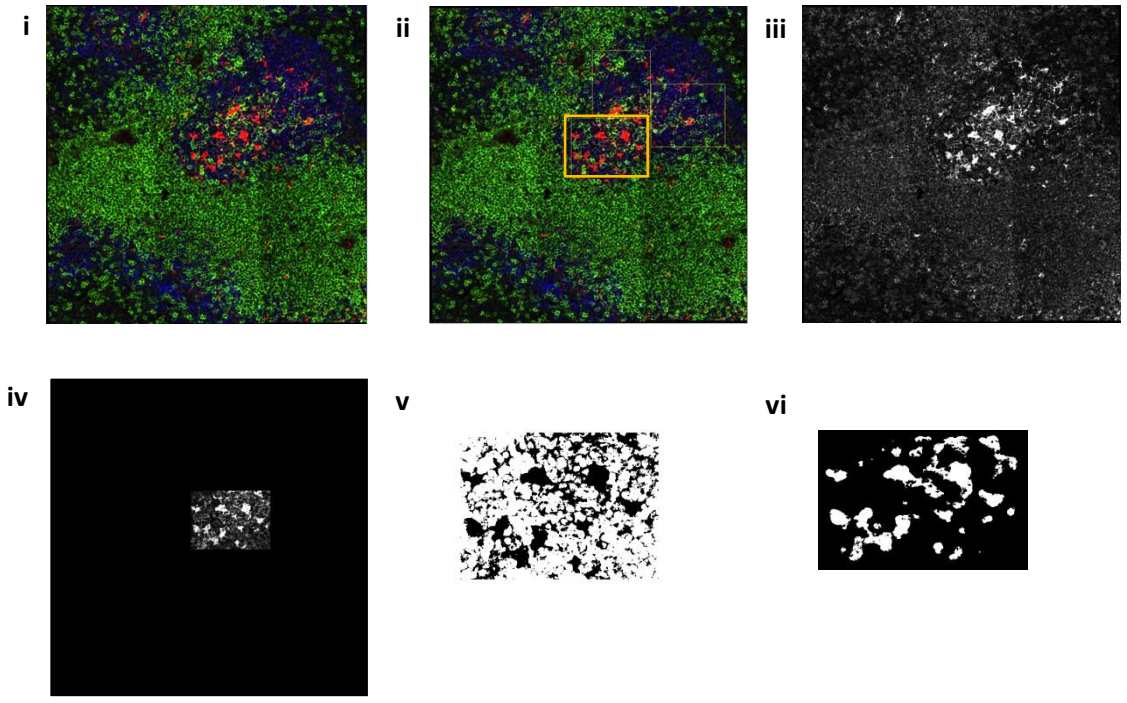

Figure 2.2 Imagej macro designed to quantify the percentage coverage of germinal centre with FDC-M1 positive staining. The macro is designed to quantify this defect by **(i)** selecting the image of interest from the file **(ii)** selecting a region of interest (ROI) within the germinal centre of at least 300px^2 (3 ROI were analysed per image) **(iii)** Splitting the channels to analyse only the FDC-M1 red channel **(iv)** selecting the ROI alone **(v)** enlarging the ROI and creating a mask **(vi)** removing outliers with a radius below the detectable range, and finally **(vii)** measuring the white (stained) area and the total area and generating a excel sheet describing the results. The appropriate regions of code are indicated and the results generated are also described graphically.

Table 2.2 Primary antibodies used for immunofluorescence

Antibody (clone)	Format	Working Dilution	Isotype	Supplier
Anti-CD248 (p13)	Purified	1:400	Rabbit polyclonal	Gift from Professor C Isacke, CRUK, London
Anti-FDC-M1 (FDC-M1)	Purified	1:50	Rat IgG2c	BD Pharmingen
Anti-CD35 (8C12)	Biotinylated	1:50	Rat IgG2a	BD Pharmingen
Anti-CD3e (145-2C11)	FITC Biotinylated	1:200	Hamster IgG	eBioscience
NG2 (132.38)	Purified	1:50	Mouse IgG1	BD Biosciences
α-SMA (1A4)	Purified	1:50	Mouse IgG2a	SIGMA
Anti-CD4 (RM4-5)	Alexa Fluor 647	1:150	Rat IgG2a	BD Pharmingen
Anti-CD19 (eBio 1D3)	eFluor 660	1:200	Rat IgG2a	eBioscience
Anti-CD45 (30-F11)	APC	1:100	Rat IgG2b	eBioscience
Anti-Bcl6 (K112-91)	Alexa Fluor 488	1:25	Mouse IgG1	BD Pharmingen
Anti-CXCL13	Purified	1:100	Goat polyclonal	R&D Systems
Anti-CCL21	Purified	1:100	Goat polyclonal	R&D Systems
RANKL (Iκ22/5)	PE	1:50	Rat IgG2a	BD Pharmingen

Table 2.3 Secondary antibodies used for immunofluorescence

Antibody (clone)	Format	Working Dilution	Isotype	Supplier
Anti-rabbit IgG (H+L)	Alexa Fluor 488	1:100	Goat IgG	Invitrogen
Anti-rat IgG2c	Biotinylated	1:100	Mouse IgG	Southern Biotech
Anti-FITC	Purified	1:200	Rabbit IgG	Invitrogen
Anti-Alexa Fluor 488	Purified	1:200	Rabbit IgG	Invitrogen
Anti-rabbit	FITC	1:100	Goat IgG	Southern Biotech
Anti-FITC	Alexa Fluor 488	1:200	Rabbit IgG	Life Technologies
Anti-goat IgG	FITC	1:100	Donkey IgG	Invitrogen
Streptavidin	Alexa Fluor 555	1:500		Invitrogen
Streptavidin	Alexa Fluor 488	1:100		Invitrogen
Hoescht		1:1000		Invitrogen

2.5 Relative quantification of gene expression

2.5.1 Microdissection

Snap frozen tissue samples were cut at 8µm thick sections using a sterilised Leica (Bucks, UK) cryostat onto UV activated PALM membrane slides (Leica 1.0 PEN slides). The slides were then stained with Cresyl Violet acetate (SIGMA) dissolved to 0.1% w/v solution in 100% ACS grade ethanol (SIGMA). Slides were stored at -80°c until ready for microdissection. 20µl RLT buffer (Qiagen) was added to adhesive capped tubes (Leica) and kept on dry ice. Areas of interest were selected using PALM microbeam microscope and dissected onto adhesive capped tubes. These samples were frozen at -80°c in RLT buffer before RNA was extracted from the samples following the manufacturer's protocol outlined below.

2.5.2 RNA extraction

RNA was extracted from tissues using RNeasy mini kits (Qiagen) following the manufacturer's instructions for sectioned samples. RNA was extracted from microdissected and whole cell samples using RNeasy micro kits (Qiagen). Whole tissues sectioned in the cryostat as mentioned above and, once thawed, lysed in 200µl RLT Buffer (Qiagen) with 10% of β-mercaptoethanol (Sigma Aldrich). Samples were vortexed and centrifuged for 1 minute at 13000rpm, followed by 200µl of ice-cold 70% ethanol (ratio 1:1 to RLT Buffer). After mixing by pipetting, samples were transferred to RNeasy mini spin columns and centrifuged for 2 minutes at 13000rpm. Solution in collection tube was discarded and 350µl of Buffer RW1 was added and centrifuged once again. 80µl of DNase I (previously prepared with 10µl of DNase I to 70µl of Buffer RDD) was added directly to the column membrane and incubated for 15 minutes at room temperature. After DNase I incubation, centrifugation with 350µl of Buffer RW1 was repeated, followed by 500µl of Wash Buffer RPE and a one minute spin, twice. The collection tube was discarded; pink columns were placed in new 2ml collection tubes and centrifuged for 5 minutes at 13000rpm in order to dry the membrane. Columns were then placed in new 1.5ml

collection tubes and 12.5µl of RNase-free water was directly added to the membrane, twice, in order to elute the extracted RNA.

To isolate total RNA from microdissected tissues, the RNeasy Micro Kit (Qiagen) was used according to manufacturer's instructions. This protocol was similar to the whole tissue extraction, although DNase I was not used, and the sample was eluted in 12.5µl RNase free water twice.

To isolate total RNA from sorted cells the RNeasy Micro Kit (Qiagen) was used according to manufacturer's instructions. In brief, there were three key differences to the protocol of RNA extraction from tissues. After adding 200µl of RLT Buffer to each sample, a 19G needle and a 2ml syringe was used to break up the cells further. Secondly, instead of a second wash with Wash Buffer RPE, 500µl of ice-cold 80% ethanol was added and centrifuged at 13000rpm for 2 minutes. Lastly, at first RNA was eluted with 12.5µl of RNase-free water and after centrifugation the eluted 12.5µl of RNA were put through the membrane again to ensure a higher concentration of RNA.

2.5.3 cDNA amplification

A cDNA library was synthesised from extracted RNA immediately after isolation. This was carried out using High Capacity cDNA Reverse Transcription Kit (Applied Biosystems), according to the manufacturer's instructions. RNA samples were added to a 96-well plate and then mixed in a 1:1 ratio with a master mix of 10X RT Buffer, 10X Random primers, 100nM dNTP mix, reverse transcriptase enzyme and RNase-free H_2O. The plate was sealed with Clear Adhesive Film (MicroAmp, Applied Biosystems). The PCR reaction was carried out on a Techne TC-Plus thermal cycler with the cycles as follows: 25°c for 10 minutes, 37°c for 2 hours and 85°c for 5 minutes. Once the reaction was completed, the resulting cDNA was diluted 1:1 with RNase-free water and stored at -20°c.

2.5.4 Quantitative real-time qPCR analysis

The diluted cDNA was then plated out on 384 well plates with Taqman gene expression assays primers and probes and master mix. The primers and probes were prelabelled with 6-FAM™ and were then combined at their reported optimal concentration with Taqman Master Mix (Applied Biosystems) in a ratio of 1:0.1µl and mixed 1:1 with the cDNA, as specified in the manufacturer's instructions. The samples were then added to the plates in duplicate at a final volume of 5.1µl. The plates were then sealed with a MicroAmp™ Clear Adhesive Film (Applied Biosystems) and spun for 2 minutes at 1200rpm.The plates were then run on a 7900 HT Applied Biosystems qPCR machine with standard thermal cycling conditions (40 cycles of: 2 minutes at 50°c for UNG activation; 10 minutes at 95°c for Taq polymerase enzyme activation; denaturation for 15 seconds at 95°c; and 1 minute at 60°c for annealing). The results were then analysed with Applied Biosystems RQ Manager 1.2 software and Ct values were determined within the logarithmic phase of the PCR reaction, which correspond to the cycle number at which the amplification plot crosses the defined fluorescence threshold. The two technical replicates were then used to calculate a mean Ct value for each sample and gene, for both endogenous controls (β-actin and PDGFRβ) and targets. ΔCt was determined by subtracting the Ct of the endogenous control from the Ct of the gene of interest. Relative expression (RQ) of the target gene as compared to the endogenous control was calculated as $2^{-\Delta Ct}$.

All target genes were normalised to β-actin, except for stromal cell dependent genes that were normalised to PDGFRβ to account for possible differences in the percentages of stromal cells per lymphoid organ.

A list of primers used for qPCR analysis is shown in table 2.4.

Table 2.4 Taqman Primer/probes used for RT-qPCR analysis

Gene	mRNA Accession number	Assay ID	Supplier
β-actin	NM_007393.3	Mm01205647_g7	Applied Biosystems
PDGFRβ	NM_001146268.1	Mm00435546_m1	Applied Biosystems
APRIL (Tnfsf13)	NM_003808.3	Mm00840215_g1	Applied Biosystems
BAFF (Tnfsf13)	NM_033622.1	Mm00446347_m1	Applied Biosystems
CXCL12	NM_001012477.2	Mm00445553_m1	Applied Biosystems
CXCL13	NM_018866	Mm00444533_m1	Applied Biosystems
CCL19	NM_011888	Mm00839967_g1	Applied Biosystems
CCL21b	NM_011124.4	Mm03646971_gH	Applied Biosystems
VCAM	NM_011693.3	Mm01320970_m1	Applied Biosystems
ICAM	NM_010493.2	Mm00516023_m1	Applied Biosystems
LTα	NM_010735.2	Mm00440228_gH	Applied Biosystems
LTβR	NM_010736.3	Mm00440235_m1	Applied Biosystems
NG2 (Cspg4)	NM_139001.2	Mm00507257_m1	Applied Biosystems
α-SMA (Acta2)	NM_007392.3	Mm00725412_s1	Applied Biosystems
MFGE-8	NM_001045489.1	Mm00500549_m1	Applied Biosystems

2.6 Western Blotting

2.6.1 Harvesting cells

Stimulated cells were removed from the incubator and placed on ice. Media was removed and the plates were washed in Tris-buffered saline (TBS). The cells were then lysed using RIPA buffer with 10% phosphatase and 10% protease inhibitors (Thermo Fisher). Cells were then scraped using cell scraper and then collected into a tube and stored at -20°c for later analysis.

2.6.2 Determining protein concentration

Samples were shredded using QIAshredder columns (QIAGEN) at 4°c for 1 minute at 13000rpm. Protein concentrations were then determined using a Biorad protein assay (Bradford Assay) with bovine serum albumin (BSA) standards. The 96 well Nunc Immulon ELISA plate was then read at 595nm on BioTek plate reader.

2.6.3 Loading and running samples on gel

Biorad Criterion TGX protein gels were prepared according to manufacturers instructions. Volumes of samples were calculated to give 50µg of each sample and then diluted 1:4 with loading buffer and then denatured by heating to 95°c for 5 minutes, before being loaded onto the gel, alongside 5µl of rainbow protein ladder. The samples were run at 100V for 90 minutes.

2.6.4 Transferring gel to membrane

The gels for blotting were transferred onto Trans-Blot Turbo transfer system (Biorad). Trans-Blot Turbo Midi PVDF Tansfer Packs (Biorad) were prepared by incubating the PVDF membrane with methanol and then the blotting paper, membrane and gel were layered, with the gel towards the anode and the membrane towards to cathode. The protein was then transferred on the membrane using Biorad Transblot protein transfer block was then run for 7 minutes.

2.6.5 Probing membrane with antibodies and detection

Membrane was removed from the Transblot system and then blocked using 5% BSA/TBSTween20 buffer for 1 hour on with agitation. Blocking buffer was then removed, and the primary antibody was added diluted in blocking buffer at the dilutions shown in table 2.3. The membrane was then incubated at 4°c overnight with constant agitation. The primary antibody was then washed off the membrane 3 times, the membrane was then incubated for 1 hours with agitation with secondary antibodies according to the antibodies in table 2.3. The membrane was then washed three times, and then the sample was detected using ECL solution (Biorad) for 1 minute. The membrane was then exposed using a chemidoc to detect the presence of protein.

Table 2.5 Antibodies used for western blotting

Antibody (clone)	Working Dilution	Host Species	Manufacturer
β-actin (Ac-74)	1:5000	Mouse IgG	SIGMA
p44/42 (ERK 1/2) (9102)	1:1000	Rabbit IgG	Cell Signalling
Phospho-p44/42 (ERK1/2) (4377)	1:1000	Rabbit IgG	Cell Signalling
IκBα (9242)	1:1000	Rabbit IgG	Cell Signalling
p50/105 (3035)	1:1000	Rabbit IgG	Cell Signalling
RelB (10544)	1:1000	Rabbit IgG	Cell Signalling

2.7 NP-specific immunoglobulin ELISA

Nunc immulon 96-well plates were coated overnight at 4°c in NP15-BSA (5µg/ml) and NP2-BSA (5µg/ml) in 0.1M carbonate-bicarbonate buffer (SIGMA, UK) at 100µl/well. They were then washed 3x in PBS with 0.05% Tween 20 (Fisher) and blocked in 100µl/well PBST 1% BSA at 37°c for 2 hours. The blocking solution was then washed off the plate 3x and mouse sera were diluted to 8 serial dilutions in PBST 1%BSA and added to the plates at 100µl/well before being incubated at 37°c for 1 hour. The plates were then washed and goat anti-mouse total IgG or IgM alkaline phosphatase conjugated antibodies (Southern Biotech) 1/1000 dilution was added before being incubated at 37°c for 1 hour. After another wash, the p-Nitrophenyl phosphate substrate (SIGMAFAST tablets, SIGMA, UK) was added and the colour left to develop for 20 minutes at 37°c, before the plate was read on a plate reader at a wavelength of 405nm.

2.8 Statistical analysis

Statistical analysis was performed using GraphPad Prism and difference between groups assessed using appropriate statistical tests as indicated on the appropriate figure. Significance was accepted at $p \leq 0.05$. All graphs are presented as mean ± SEM.

Chapter 3. Exploring the role of CD248 in determining the differentiation fate of mesenchymal stem cells

3.1 Chapter aims

- To explore the role played by CD248 in controlling the differentiation of mesenchymal stem cells and the development of embryological lymph nodes, and the signalling pathways involved in this differentiation.

3.2 Introduction

CD248 is c-type lectin that regulates growth and invasiveness of tumours metastasis (Bagley et al., 2009), During embryogenesis CD248 is broadly expressed on lymphoid associated mesenchyme (Lax et al., 2007). It is known that mesenchymal stem cells (MSCs) are able to differentiate into various lineages, including lymphoid stroma, adipose tissue and bone (Dimarino et al., 2013, Caplan, 2008, Bonfield and Caplan, 2010, Pittenger et al., 1999, Dennis et al., 1992). The importance of the CD248 expression by these cell types is evidenced by work done by our laboratory (Naylor et al. 2012), which has shown that the CD248 knockout mice develop stronger bones than their wild type counterparts at the expense of the development of adipose tissues, resulting in stronger bones and less fat in the CD248 knockout mice. Lax et al. (Lax et al., 2007) also described widespread expression of CD248 on the early stroma compartment of the embryonic lymph node anlagen, suggesting a potential role for CD248 in the early determination of MSCs to specialised stroma.

The mechanism by which CD248 functions is currently unknown. Current evidence appears to suggest that CD248 has some role to play in the regulation of the PDGFRβ pathway (fig.3.1). Whilst initial phosphorylation of PDGFRβ appears to be normal in $CD248^{-/-}$ cells, the phosphorylation of

downstream targets such as ERK (extracellular signal-regulated kinase) is markedly reduced in CD248$^{-/-}$ cells (Tomkowicz et al., 2010, Naylor et al., 2014). This suggests the possibility that the two signals co-operate intracellularly (figure 3.1). However, identification of the exact subunits in the PDGFRβ signalling pathway with which CD248 is able to interfere with has proved difficult. This is due to the structure of CD248, which includes a very short intracellular domain of only 49 amino acids, with no apparent consensus signalling motif in this cytoplasmic tail (Valdez et al., 2012, Maia et al., 2010). Current evidence has indicated that CD248 is able to modify phosphorylation of ERK in response to stimulation with the recombinant homodimer PDGF-BB, a potent stimulator of the PDGFRβ signalling pathway. ERK is also known to feature in a number of different signalling pathways, apart from the PDGFRβ pathway. Evidence that CD248 is not essential for PDGFRβ signalling is that the phenotype of CD248$^{-/-}$ mice is non-lethal, unlike the PDGFRβ$^{-/-}$ mice, and they demonstrate mostly normal development of vascular smooth muscle cells and pericytes, two cells types known to be dependent on PDGFRβ (Leveen et al., 1994). PDGFRβ signalling is known to control the differentiation of the lymphatic vessels which enervate the lymph nodes (Cao et al., 2004).

Embryonic lymph node development is a tightly regulated and orchestrated procedure that is extensively discussed in chapter 1. The location at which LN develop is stereotyped and determined, at least in part, by the endothelial expression of the lymphotoxin β receptor (LTβR) (Onder et al., 2013). Activation of the LTβR signalling pathway in endothelial cells enables the recruitment, extravasation and clustering of LTβ^{+}TRANCE^{+}RORγt^{+}CD45^{+}CD4^{+}CD3^{-} hematopoietic lymphoid tissue inducer (LTi) also known as type 3 innate lymphoid cells (ILC3) (Randall et al., 2008, van de Pavert and Mebius, 2010) . The origin and identity of the signals that induce specification of the mesenchymal progenitor cells prior to LTi arrival remain largely unknown. This signalling pathway is known to activate NF-κB signalling pathways, both the NIK-dependant non-canonical pathway, causing upregulation of CXCL13, and the p50-RelA heterodimer- dependent canonical pathway involved in upregulation of adhesion molecules. Expression of these chemokines and adhesion molecules allow

LTo cells to mature, and, in turn, facilitates further attraction and retention of more LTi cells through the binding of CXCR5, CCR7, $\alpha4\beta1$, $\alpha4\beta7$ and $LT\alpha1\beta2$ with their respective ligands (Randall et al., 2008, Roozendaal and Mebius, 2011). The physical interaction between hematopoietic LTi and stromal LTo cells establishes a positive feedback loop that reinforces the formation of the cluster and leads to the stabilization of the anlagen with vascular differentiation, development of HEVs and eventually attraction and compartmentalization of mature lymphoid and myeloid cells (Randall et al., 2008, van de Pavert and Mebius, 2010, Roozendaal and Mebius, 2011). Utilizing a CCL19 Cre dependent LTβR ablation (Ccl19-cre × $Ltbr^{fl/fl}$ mice), Ludewig and colleagues recently shown the ability of CCL19+ myofibroblastic stromal cell precursor cells to generate basic LN infrastructures even in absence of LTβR triggering (Chai et al., 2013). Nonetheless, fibroblastic LTo cells require LTβR signalling to reach full maturation that includes strong expression of ICAM-1, VCAM-1, CCL19, CCL21, IL-7 and RANKL, as well as immunological competence (Benezech et al., 2010, Chai et al., 2013, Vondenhoff et al., 2009). Embryonic LTo cells in PP, mesenteric and peripheral LN show transcriptional differences as well as differential cellular and molecular requirements suggesting that LTo responsible for the aggregation of different lymphoid tissues are not a uniform (Yoshida et al., 2002, Cupedo et al., 2004). Mice with deficiencies in subunits of the LT-βR signalling pathway demonstrate significantly dysregulated lymph node development. For example, $LT\beta R^{-/-}$ mice completely lack peripheral lymph nodes and have some structural abnormalities in both the spleen and the thymus (Futterer et al., 1998, Venanzi et al., 2007, Boehm et al., 2003). Peripheral lymph nodes are also completely absent in $Nik^{-/-}$ mice (Yin et al., 2001), whereas $NfκB1^{-/-}$ and $NfκB2^{-/-}$ mice lack only inguinal lymph nodes (Lo et al., 2006) and $Relb^{-/-}$ mice have normal lymph node distribution, with a slight depletion in the number of lymphocytes (Weih et al., 1995).

As illustrated by Bénézech *et al.* (2010), the adult source of mesenchymal stem cells known as adipose derived stem cells (ADSCs), or preadipocytes, can be stimulated in vitro to differentiate to a population that resembles a lymphoid stromal phenotype, which express high levels of the adhesion molecules

VCAM-1 and ICAM-1. This differentiation is dependent on engagement of LTβR, resulting in activation of the non-canonical NF-κB pathway and concurrent engagement of the canonical NF-κB pathway by stimulation with TNF-α.

The distribution of CD248 on MSC and its suggested role as element involved in mesenchymal specification prompted us to address the role of this pathway and its interaction with PDGFRβ and LTβR in the context of lymphoid stromal cell *in vitro* and *in vivo*.

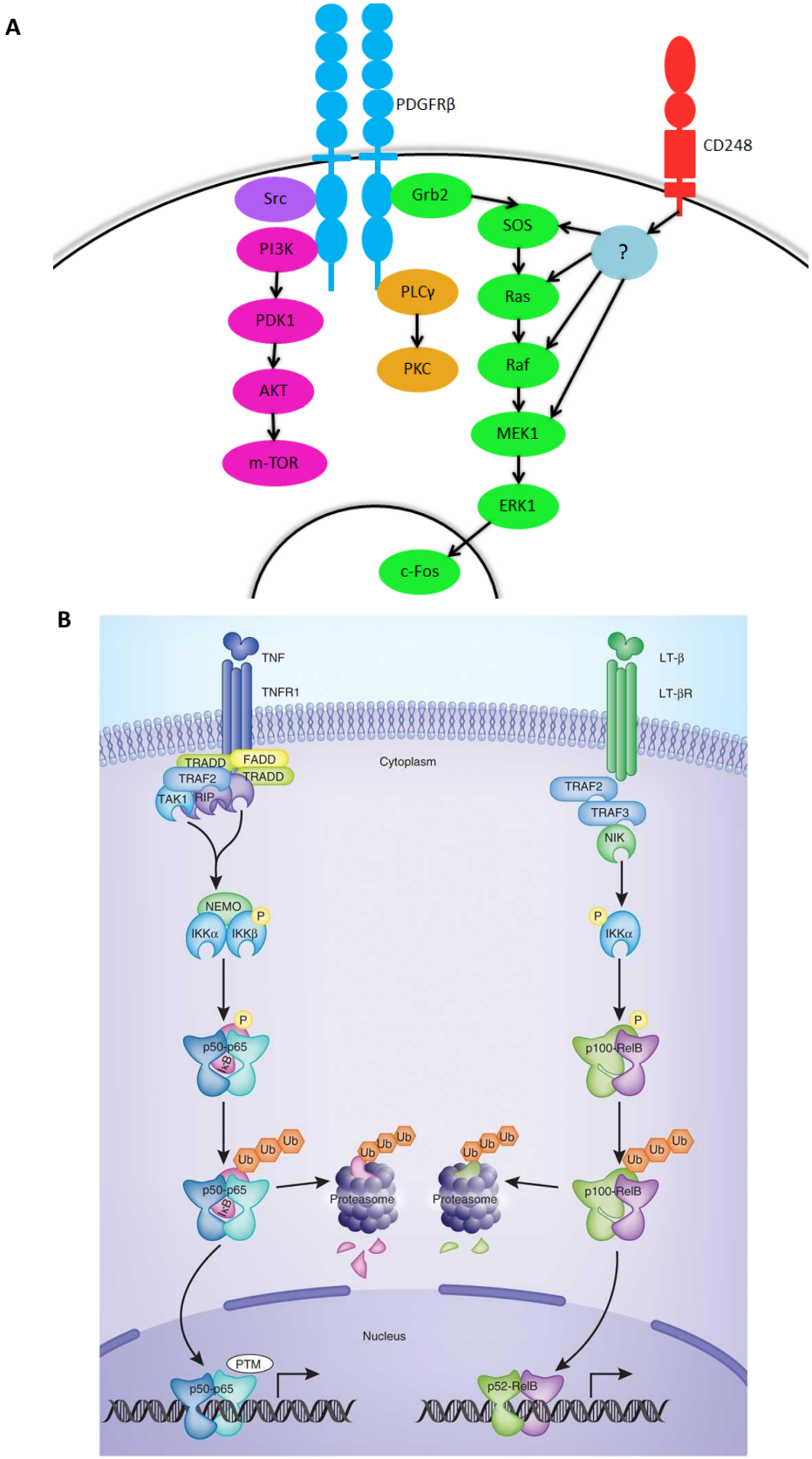

Figure 3.1 Schematic representations of the PDGFR and NF-κB signalling pathways discussed in this chapter. A) Representation of the PDGFRβ signalling pathway and the potential interaction of CD248 with the subunits. Adapted from (Demoulin, 2010, Kok et al., 2014) **B)** Schematic representation of the canonical and non-canonical NF-κB signalling pathways. Taken from (Oeckinghaus et al., 2011)

3.3 Results

3.3.1 Impairment of lymphoid stroma differentiation in absence of CD248

Lymphoid stromal cells can be differentiated from MSCs by stimulation with LTβR agonist and TNFα (Benezech et al., 2012). Successful differentiation involves upregulation of VCAM-1 and ICAM-1 on stimulated cells in a stepwise manner, with the generation of 3 different populations; a negative population, an intermediate-expressing population and a high-expressing population (figure 3.2a).

I investigated whether CD248 played any role in this differentiation by investigating the ability of $CD248^{-/-}$ mouse embryonic fibroblasts (MEFs) to differentiate to lymphoid precursors. As shown in figure 3.2, both WT and $CD248^{-/-}$ MEFs were able to upregulate VCAM-1 and ICAM-1 in a stepwise manner, resulting in the generation of three different populations with different VCAM-1 and ICAM-1 expression (figure 3.2 b - d). $CD248^{-/-}$ cells are able to respond to the stimulation and significantly upregulate their expression of both VCAM-1 and ICAM-1 in the same manner as the WT cells (fig. 3.3 b – d). However, at resting conditions MEFs isolated from $CD248^{-/-}$ mice displayed a significantly higher expression of ICAM and VCAM, (fig. 3.2 b – d), at a level comparable to the intermediate population.

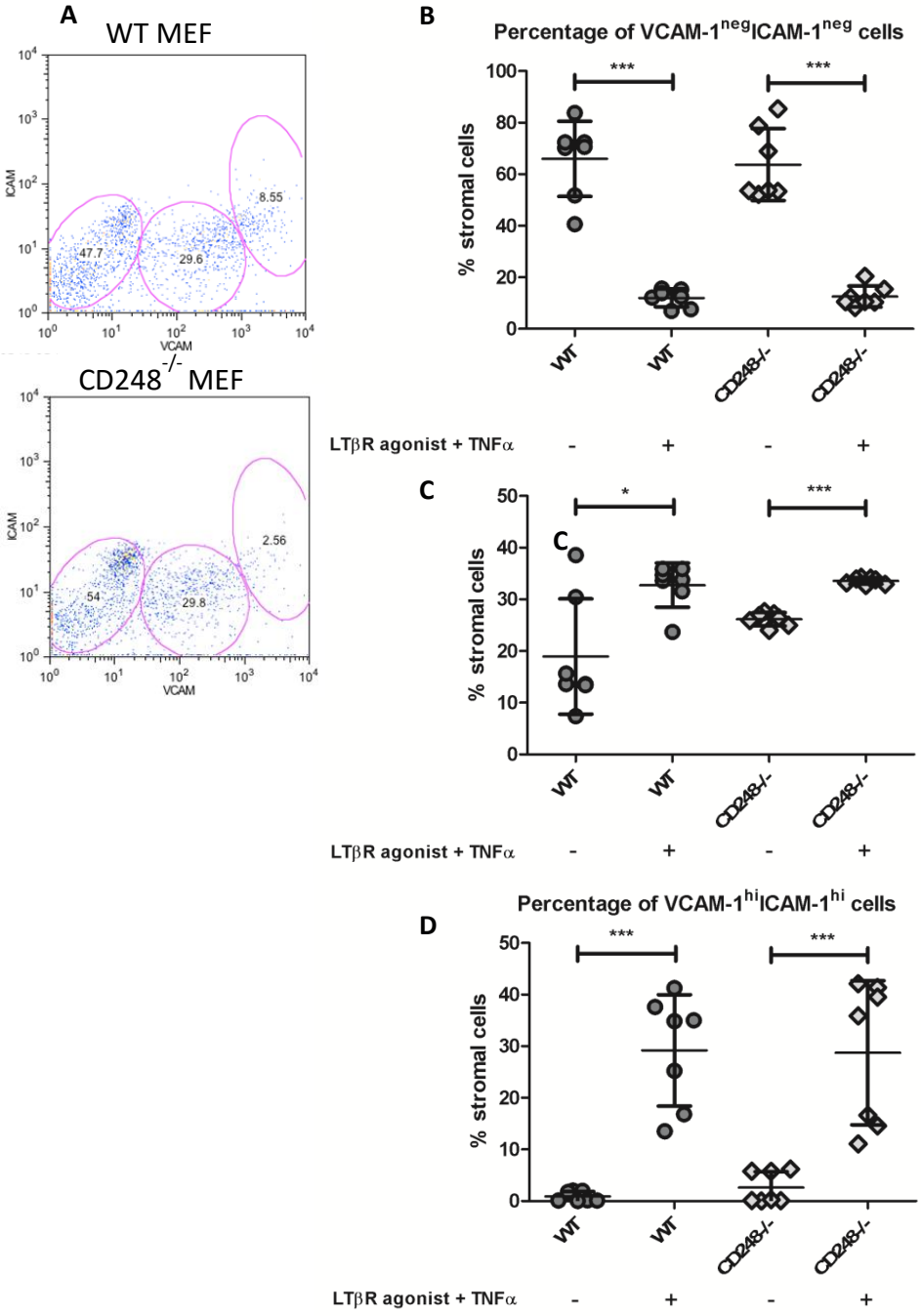

Figure 3.2 Differentiation of mouse embryonic fibroblasts to lymphoid precursors. A) Flow cytometry gating strategy employed to analyse the expression of ICAM-1 and VCAM-1 following stimulation with LTβR agonist and TNF-α. The percentages of cells in three different VCAM-1/ICAM-1 expressing populations, including $VCAM^{hi}ICAM^{hi}$ **(B)**, $VCAM^{int}ICAM^{int}$ **(C)**, and $VCAM^{-}ICAM^{-}$ **(D)** were analysed following stimulation. Data shown is representative of two independent experiments with n = 6. Significance was calculated using a Mann-Whitney Unpaired t test with $p < 0.05$ = *, $p < 0.005$ = **, and $p < 0.0005$ = ***.

The upregulation of ICAM and VCAM was calculated as a fold change upon stimulation with LTβR agonist and TNF-α, because of the higher resting expression in the $CD248^{-/-}$. This data is shown in figure 3.3a. As shown, the upregulation of both adhesion markers was found to be defective in the $CD248^{-/-}$ cells compared to the WT counterparts.

This analysis was also carried out in ADSCs, as these cells have previously shown to be capable of reprogramming to lymphoid stromal cells when stimulated in this manner (Benezech et al., 2012). As shown in fig 3.3b, the fold change increase in the percentage of cells in $VCAM^{int}ICAM^{int}$ population in response to stimulation is not significantly affected in the $CD248^{-/-}$. However, a significant reduction in the $VCAM^{hi}ICAM^{hi}$ population was observed. It is important to highlight that upregulation of adhesion molecules upon stimulation was less significant in the ADSCs than in the MEFs, thus suggesting that lineage differentiation in already committed cells is a more complex phenomenon that might require slightly different conditions and, potentially, prolonged stimulation (fig. 3.3a & 3.3b).

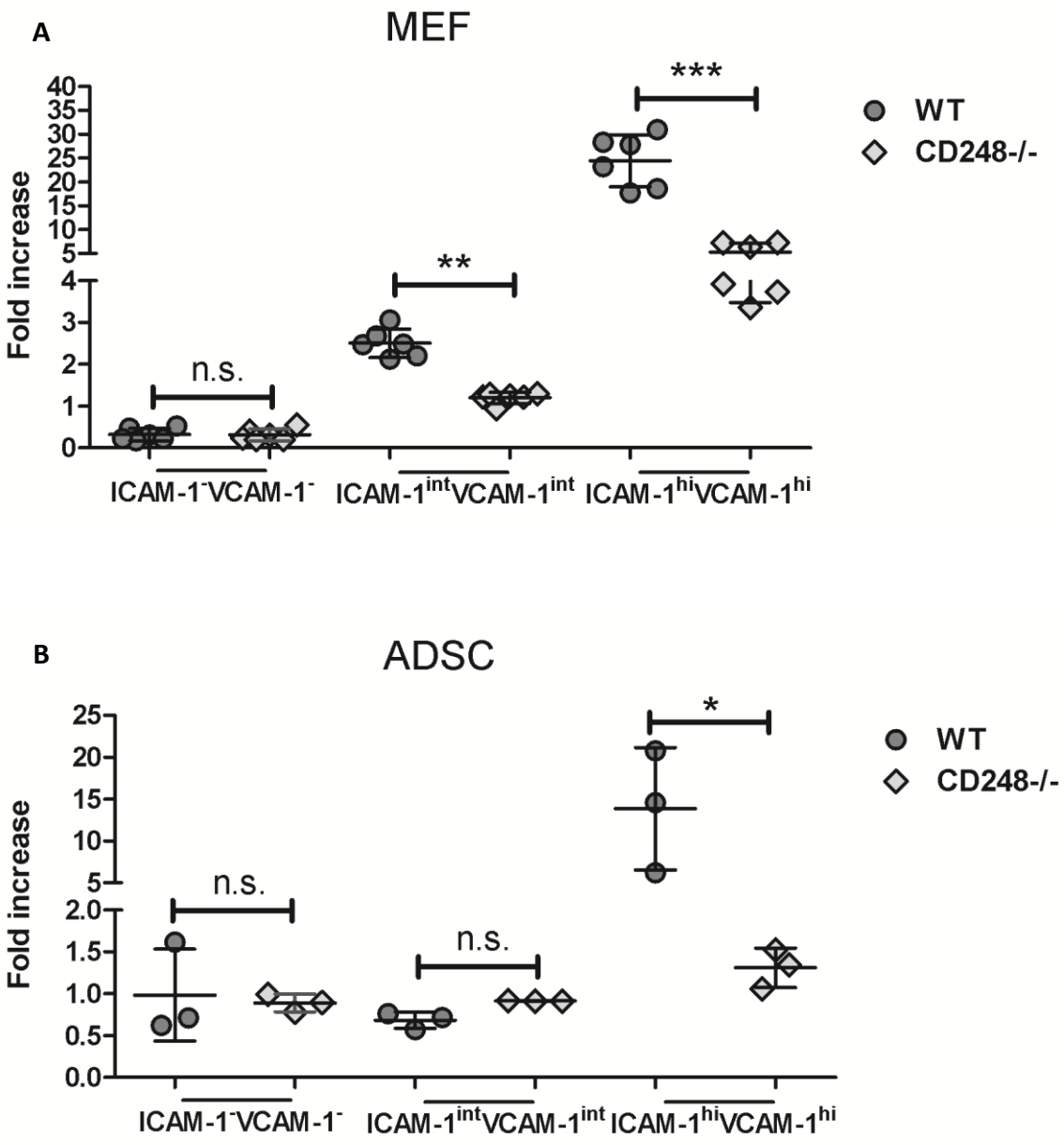

Figure 3.3 Mesenchymal stem cells from different origins were differentiated to lymphoid precursors. The expansion of the ICAM-1, VCAM-1 populations is expressed as a fold change increase for the ICAM-1intVCAM-1int and ICAM-1higVCAM-1hig populations and shown for MEFs **(A)** and stimulated ADSCs **(B).** Data shown is representative of two independent experiments with n = 3 - 6 and is described as the mean ± SD. Significance was calculated using a one-way ANOVA, with $p < 0.05$ = *, $p < 0.005$ = ** and $p < 0.0005$ = ***.

3.3.2 Investigating the interaction between CD248 and the PDGFRβ signalling pathway

CD248 has long been understood to signal via the PDGFRβ signalling pathway, as stimulation with recombinant PDGF-BB has been shown to be unable to trigger a response in CD248$^{-/-}$ cells (Naylor et al., 2012). However, the mechanism by which this interaction occurs is currently not well understood. In order to evaluate whether this mechanism was involved in the differentiation in to "lymphoid-tissue" phenotype cells, stimulation with LTβR agonist and TNFα was repeated in WT MEF, in the presence of the PDGFRβ signalling inhibitor imatinib mesylate. As shown in figure 3.4, WT cells treated with imatinib mesylate were significantly reduced in their ability to respond to this stimulation, with a reduction in the number of cells expressing intermediate (fig. 3.4a) and high levels of VCAM/ICAM (fig. 3.4b). When the upregulation of these markers was calculated as a fold change in response to stimulation as previously investigated, it was found significantly reduced (fig 3.4c). This defect mimics the effect observed in the CD248$^{-/-}$, suggesting the possibility that CD248 signalling via PDGFRβ may play a role in the differentiation of MSCs to lymphoid stromal cells.

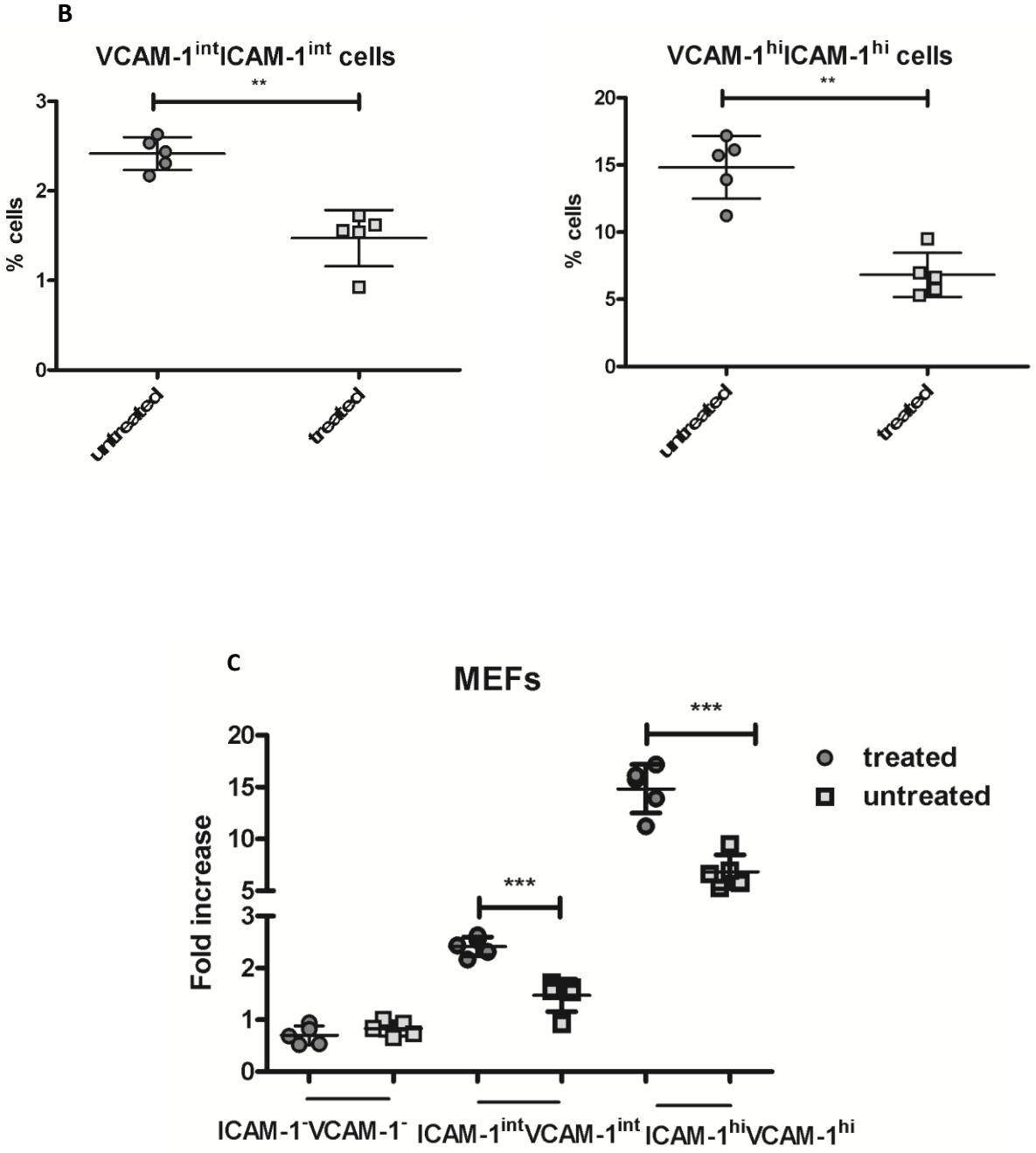

Figure 3.4 Differentiation of MEFs to lymphoid precursors is dependent on signalling via PDGFRβ. Percentages of cells expressing intermediate VCAM/ICAM levels **(A)**, and high VCAM/ICAM levels **(B)**. The proportions of cells in each population were calculated as a fold increase following stimulation and are represented in **(C)**. Data shown is representative of two independent experiments with n = 5 and is described as the mean ± SD. Significance was calculated using a Mann-Whitney Unpaired t test (A & B) and a one-way ANOVA (C), with $p < 0.005$ = ** and $p < 0.0005$ = ***.

Previous evidence generated within our laboratory (Naylor et al., 2012) indicated a significant difference in the levels of ERK phosphorylation in the CD248$^{-/-}$ as compared to WT mice. Western blot analysis was carried out to investigate whether ERK phosphorylation was relevant in this system. This data is very preliminary, and as such is based on only a very few replicates and as such, definite conclusions may not be drawn. As shown in figure 3.5a, the total amount of ERK in the CD248$^{-/-}$ unstimulated cells was comparable to the level observed in WT cells. however, at 1 hour post stimulation, the WT cells appear to have a higher concentration of total ERK compared to the CD248$^{-/-}$. This defect continues into 72 hours post stimulation (fig 3.5b).

Densitometry analysis was carried out to calculate the ratio of phosphorylated ERK to the total ERK concentration. There appears to be higher levels of phosphorylated ERK in resting CD248$^{-/-}$ unstimulated cells as compared to the WT (fig. 3.5c). Upon stimulation, whilst WT MEFs were able to respond to stimulation with LTβR and TNF-α and increase the levels of ERK phosphorylation, CD248$^{-/-}$ MEF were not (fig. 3.5c). However, as previously mentioned, this is very preliminary data, and requires much further investigation in order to confirm this observation.

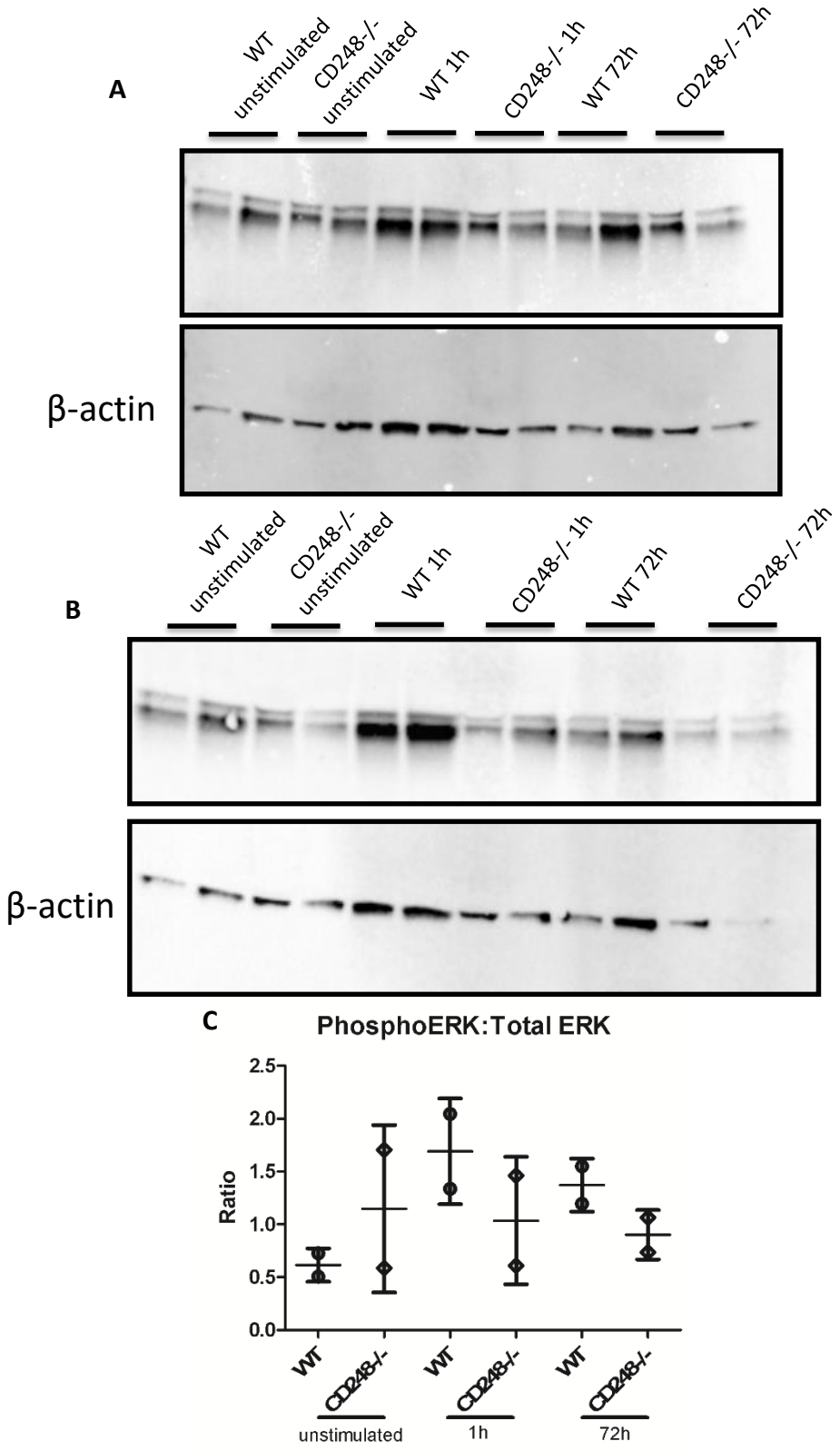

Figure 3.5 Investigation of the mechanism by which CD248 may function to inhibit differentiation. A) Amount of ERK present in MEFs both before and after stimulation at different time points was analysed by western blot, with β-actin as a loading control. **B)** Level of ERK phosphorylation in MEFs both before and after stimulation at different time points was analysed by western blot with β-actin as a loading control. **C)** Densitometry analysis of the blots was carried out and the ratio of phosphoERK to total ERK was calculated. Data shown is representative of mean ± SD with n = 2.

3.3.3 Investigating potential links between CD248/PDGFRβ and the canonical and non-canonical NF-κB pathways

LTβR and TNF-α are known to function via the NF-κB signalling pathways. TNF-α binding to TNFR1 signals via the canonical NF-κB pathway, whereas LTβR is known to activate the non-canonical NF-κB pathway. These two different pathways have different subunits, but are also able to interact with each other. These different pathways are outlined in figure 3.1b. Subunits within both of these pathways were analysed in order to investigate whether a novel role for CD248 can be identified in controlling NF-κB signalling.

Several subunits were selected to study both pathways, and their interactions, with IκBα selected as a subunit of the canonical pathway, RelB selected as a subunit of the non-canonical pathway, and P50/p105 subunits chosen as shared between the two pathways. This data is very preliminary, and as such, no definitive conclusions can be drawn. WT cells appear to be able to upregulate both p50 and RelB in response to NF-κB stimulation with 1 hour (fig 3.6b & 3.6c). However, $CD248^{-/-}$ cells do not seem to be able to respond as quickly. After 72h stimulation, an upregulation in the expression of NF-κB signalling may be observed in the $CD248^{-/-}$ cells, although the data is insufficient to comment on the degree of expression in these cells. IκBα is broken down upon stimulation (figure 3.6a) in WT cells within an hour from stimulation, once again, the response appears to be delayed in the $CD248^{-/-}$ cells. This is also very preliminary data, and has shown that the amount of these subunits can be studied using this methodology, although other conclusions cannot be drawn.

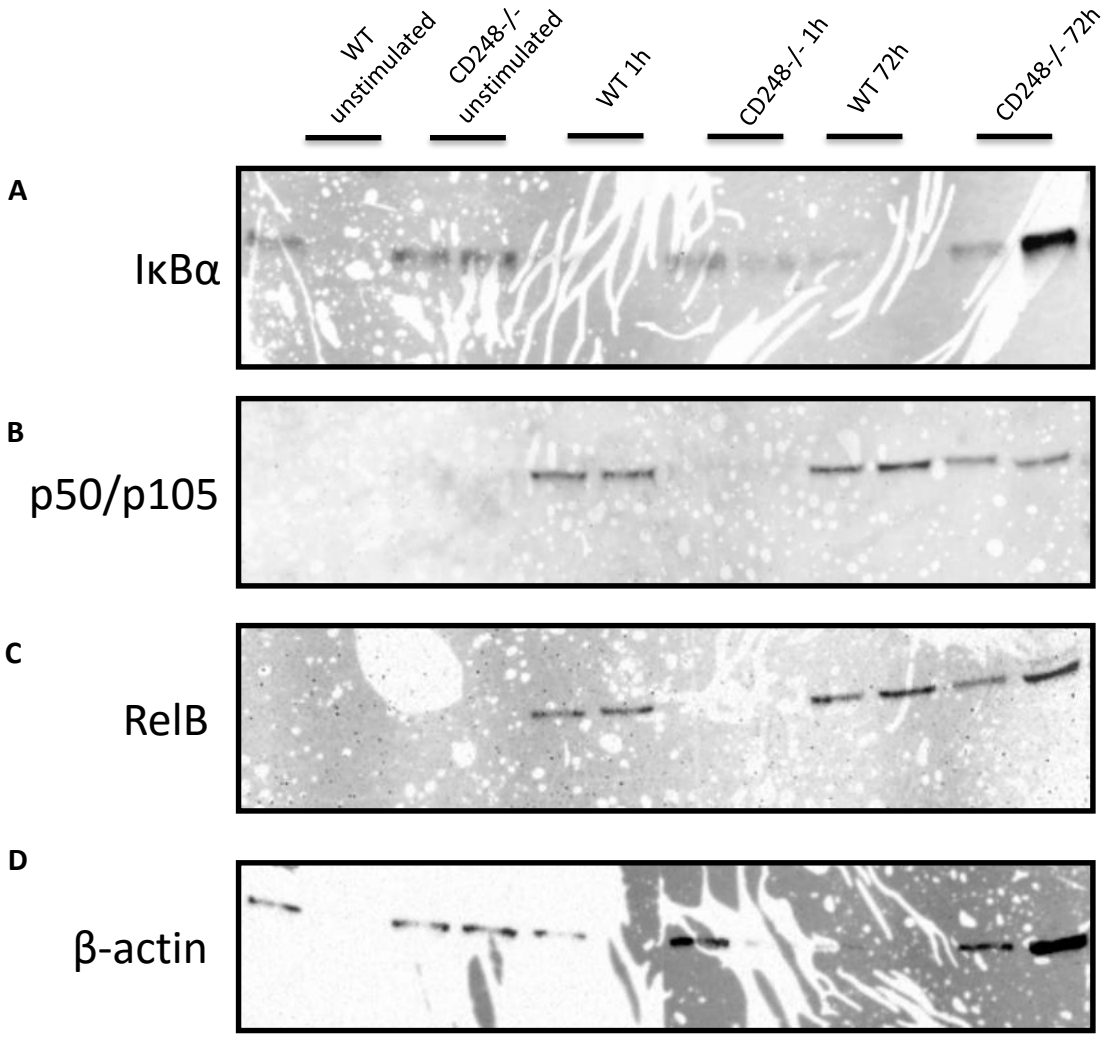

Figure 3.6 Investigation of abnormal NFκB signalling pathways in CD248-/- MEFs. Analysis of selected subunits of the NFκB signalling pathway by Western blotting **A)** IκBα **B)** p50/p105 **C)** RelB **D)** β-actin.

3.3.4 Investigating potential defective lymph node development in CD248$^{-/-}$ embryos

As previously discussed, development of embryonic lymph nodes is dependent on the interactions of lymphoid tissue inducer (Lti) cells and lymphoid tissue organiser (Lto) cells. In order to analyse the role of CD248 in the embryological development of these organs, the proportions of these cells in the WT and CD248$^{-/-}$ mice were compared at various stages of development. For this comparison, embryological inguinal and mesenteric lymph nodes were dissected from pups at different stages of development, from embryonic day 18 to new born day 1 (figure 3.7a). These organs were then digested according to the protocol described in chapter 2, allowing for the separation of the two cell types involved in embryological lymph node development. The separation of these cells is indicated in figure 3.7b, with Lti cells identified as CD45^{+}CD4^{+} cells, and the Lto cells identified as CD45^{-}CD4^{-} ICAM^{hi}VCAM^{hi}.

The proportions of the Lti and Lto cells in new born pups mesenteric lymph node and inguinal lymph node is shown in figures 3.7c – 3.7f, and the proportions of these cells in embryos at embryological development day 18 are shown in figures 3.8a – 3.8d. A significant reduction of Lto cells at embryonic day 18 (fig.3.8c) was observed in mesenteric lymph nodes, accompanied by a non significant reduction of LTi cells at new born stage in the same site (fig. 3.7e).

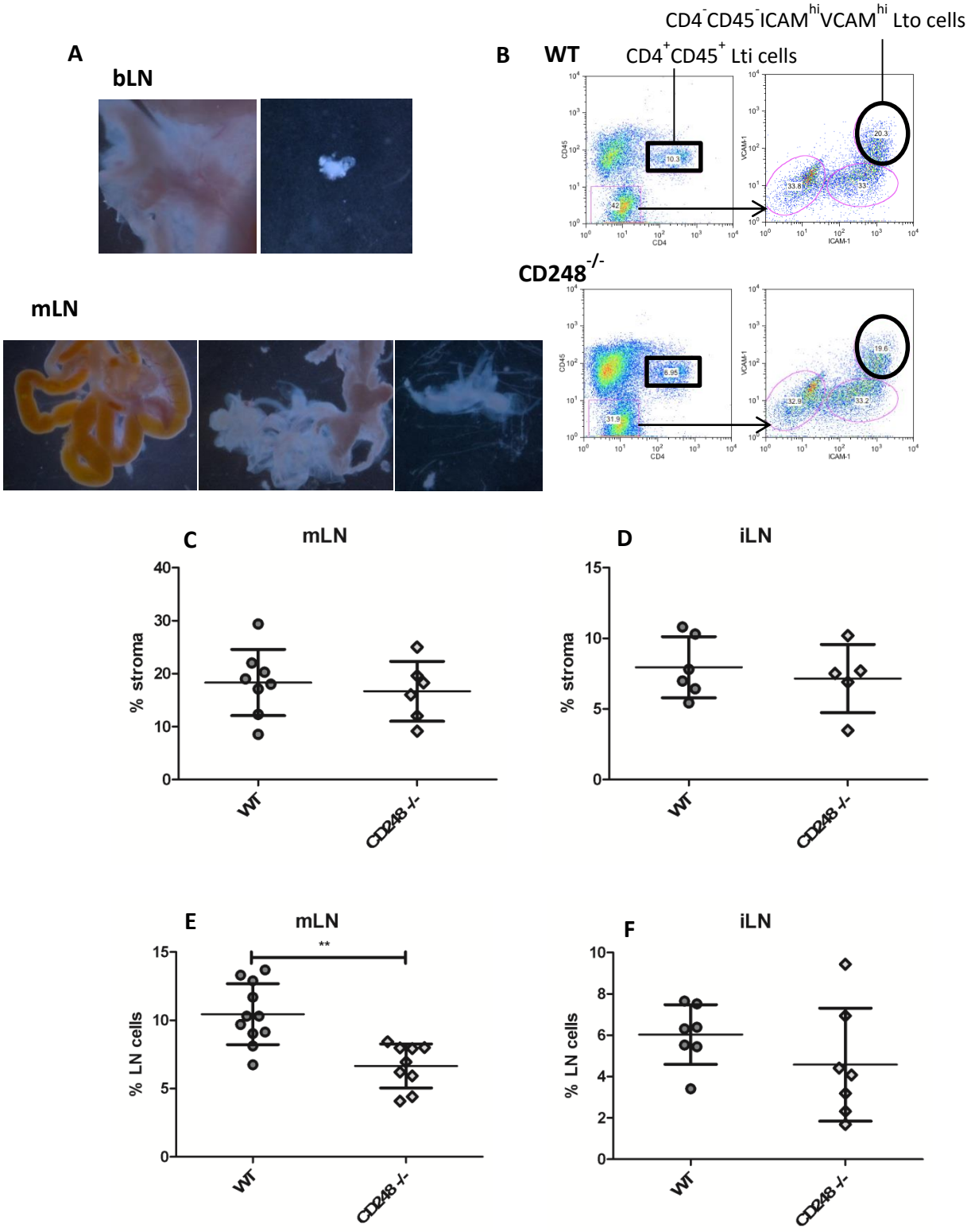

Figure 3.7 Analysis of lymph node development in CD248-/- newborn pups. A) Representative images of the brachial and mesenteric lymph nodes and their location within the developing pups. **B)** Flow cytometry plots showing the gating strategy employed in analysing the Lti and Lto cells. The populations of the Lto cells in the WT and CD248-/- were analysed in mesenteric **(C)** and inguinal **(D)** lymph nodes and the numbers of Lti cells in mesenteric **(E)** and inguinal **(F).** Data shown is representative of three independent experiments with n = 8 – 11 and illustrated with mean ± SD. Significance was calculated using a Mann-Whitney Unpaired t test with $p < 0.005$ = **.

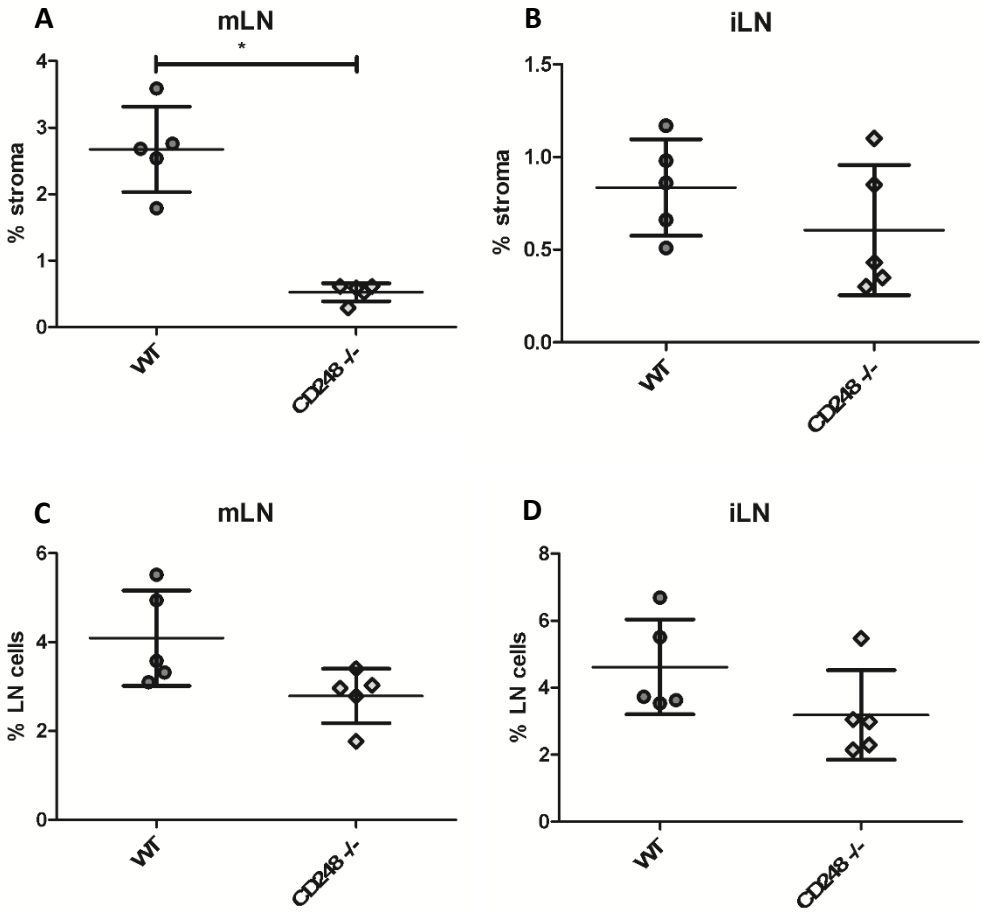

Figure 3.8 Analysis of lymph node development in CD248-/- embryological day 18 pups. The populations of the Lto cells in the WT and CD248-/- were analysed in mesenteric **(A)** and inguinal **(B)** lymph nodes and the numbers of Lti cells in mesenteric **(C)** and inguinal **(D).** Data shown is representative of three independent experiments with n = 8 – 11 and illustrated with mean ± SD. Significance was calculated using a Mann-Whitney Unpaired t test with $p < 0.05$ = *.

3.4 Discussion

3.4.1 Main findings

- The absence of CD248 on MEFs and ADSCCs reduces the ability of the cells to differentiate into lymphoid like stromal cells *in vitro*.
- *In vitro* analysis of the signalling pathways affected by the lack of CD248 was unable to adequately describe the mechanism by which CD248 exerts its influence.
- *In vivo* analysis of the stromal cells involved in the embryological development of the lymph node anlage demonstrated a reduction in the populations of both the hematopoietic Lti and the mesenchymal Lto cells in the $CD248^{-/-}$ embryos, although this is overcome as development progresses by an unknown mechanism.

3.4.2 In vitro differentiation of MSCs to adipocytes and lymphoid stroma is perturbed in absence of CD248

CD248 is expressed on mesenchymal stem cells (MSCs) during embryonic life, and is then down regulated as these cells become committed to specific lineages (Lax et al., 2007). Mesenchymal stem cells are pluripotent stem cells able to differentiate into multiple lineages, including adipose tissue, osteoid tissue and lymphoid stroma. The differentiation of mature adipose tissue from MSCs has been shown to occur via a preadipocyte precursor. This precursor has been shown to retain some pluripotent differentiation abilities, and is known to be able to differentiate to lymphoid stroma (Benezech et al., 2012). Previous work performed within the group indicated that CD248 plays a role in controlling the differentiation of MSCs in to the bone lineage, regulating osteoblast differentiation in vitro (Naylor et al., 2012). $CD248^{-/-}$ mice were shown to have stronger, thicker bones in vivo, and in vitro, osteoblast differentiation from $CD248^{-/-}$ MSCs was impaired. $CD248^{-/-}$ mice have also been

shown in our laboratory to have defective fat pad development, when compared to the WT (Bechar, 2012). In order to address the role of CD248 in mesenchymal differentiation, our laboratory has previously investigated the differentiation of MEFs to adipocytes in vitro. This data indicated that differentiation of these MSCs to pre-adipocytes was reduced in the $CD248^{-/-}$ cells compared to the WT cells.

The large distribution of CD248 in the lymph node anlagen, its expression on MSCs and its involvement in adipogenic differentiation prompted us to investigate the potential involvement of CD248 in the differentiation towards the lymphoid tissue lineage both *in vitro* and *in vivo*, the invovement of the PDGFRβ signalling in to this and the potential role of CD248 in mediating adipogenic versus lymphoid differentiation. Adipose tissue and lymphoid tissue are understood to be two very intimately linked cell types.Lymph nodes are known to develop concurrently with the fat pads in which they reside into adulthood. According to Bénézech *et al*., (2012) ADSCs could be reprogrammed into lymphoid-tissue mesenchyme precursors by stimulation with a LTβR agonist and TNF-α (for methods see chapter 2). This re-programming could be analysed by the concurrent upregulation of the adhesion markers VCAM-1 and ICAM-1 on activated mesenchyme, that represent a pre-requisite for TLO differentiation in the anlagen (Benezech et al., 2015). We used this assay to evaluate the role of CD248 in this development. Stimulation with LTβR agonist and TNF-α caused the contemporaneous upregulation of VCAM-1 and ICAM-1, with both the WT and $CD248^{-/-}$ upregulation progressing in a step-wise manner from a VCAM-ICAM- population to a an intermediate $VCAM^{int}ICAM^{int}$ population and a $VCAM^{hi}ICAM^{hi}$ population. $CD248^{-/-}$ cells were able to respond to stimulation in this manner, the strength of this response was significantly reduced when compared to the WT. The unstimualted $CD248^{-/-}$ cells seem to have a higher constitutive expression of VCAM-1 and ICAM-1 than the WT. This altered state could be supported by abnormal intracellular activation in the $CD248^{-/-}$ mice; I therefore investigated this possibility.

3.4.3 Investigation of the signalling pathways governing CD248 function in differentiation of mesenchymal stem cells

CD248 has previously been shown to modulate ERK phosphorylation in response to PDGF stimulation (Tomkowicz et al., 2010), although the precise way in which it is able to elicit an effect in the PDGFRβ signalling pathway is currently unknown. Our evidence suggested the possibility that CD248$^{-/-}$ cells exist in a "pre-activated" state. We therefore aimed to investigate whether this was assumption could be supported by a different basal intracellular activity of the PDGFRβ cascade and so we investigated the phosphorylative state of ERK. The phosphorylation of ERK has previously shown to be defective in the CD248$^{-/-}$ cells, resulting in a reduction in the expression of the transcription factor c-Fos (Tomkowicz et al., 2010, Naylor et al., 2012). Under normal circumstances, the amount of ERK phosphorylation should increase following stimulation.

By calculating the ratio of phosphoERK to total ERK, I intended to demonstrate whether the CD248$^{-/-}$ cells had a different level of ERK phosphorylation than their WT counterparts. However, the results are simply too preliminary to draw any definitive conclusions about the expression levels of the different subunits and require further investigation.

Imatinib mesylate, an inhibitor of the PDGFRβ signalling pathway was used to evaluate the relative importance of the PDGFR signalling in the effects observed. Imatinib is widely used in the treatment of several cancers (Demetri et al., 2002), thanks to its ability to inhibit the tyrosine kinase enzymes often described as oncogenes due to their ability to transform many cells into malignant cancers. This includes the BCR/ABL tyrosine kinase pathway known to be involved in chronic myeloid lymphoma transformation (Chu et al., 2004). Based on previous results indicating the lack of effect of stimulation with the recombinant PDGF homodimer PDGF-BB in CD248$^{-/-}$ cells (Naylor et al., 2012, Naylor et al., 2014), we believe that the phenocopying of the effect seen in CD248$^{-/-}$ cells by imatinib treated cells is due to abnormal PDGFR signalling, rather than signalling via another pathway.

Interestingly, the stimulation used in our assay is known to activate the canconical and non-canonical signalling pathway, but not the PDGFRβ pathway. This inability to respond appropriately would therefore indicate that either CD248 has an as-yet-unknown ability to modulate the NF-κB signalling pathways, or that the PDGFRβ signalling pathway is unexpectedly involved in the response to LTβR agonist and TNF-α stimulation. Upregulation of PDGFRβ expression and translocation of the NF-κB subunits p65 to the nucleus have been shown to be linked thanks to engagement of receptors by extracellular matrix components (Chung et al., 2009), this appears to be the main link between these two signalling pathways. Both of the theories outlined here would provide a new and interesting avenue to study, and, as NF-κB signalling is known to be essential in a large number of immunological functions (Oeckinghaus et al., 2011), would give a novel outlook as to why CD248 is upregulated in during inflammation.

In our hands it appeared that both the canonical and non-canonical NF-κB pathways are differentially regulated in the $CD248^{-/-}$ cells. These results require further investigation preliminary results would indicate that there is abnormal signalling transduction in the $CD248^{-/-}$. Whilst suggesting that both the NF-κB and the PDGF-Rβ pathway are impaired in absence of CD248, it does not provide indications on at which point in the intracellular signalling the 2 pathways interact. These results require further confirmation and validation. Chromatin immunoprecipitation could be used in an attempt to identify the interactions between the different subunits. Single subunits could also be inhibited in WT stimulated cells to recreate the results observed in the $CD248^{-/-}$ cells, providing key information about how this molecule is able to exert its effects.

3.4.4 Investigating the role of CD248 in embryological lymph node development

CD248 is known to be widely expressed in developing lymph nodes, and this expression becomes increasingly restricted after birth until it is only found on the capsule of adult LN (Lax et al., 2007). As this work has demonstrated that CD248 plays a role in controlling the differentiation of MSCs to lymphoid stromal cells in vivo, further work was carried out to identify whether this translated into an in vivo defect in the development of lymph nodes in CD248$^{-/-}$ pups. The development of the lymph nodes can be analysed by investigating the proportions of the LTi and LTo cells, as demonstrated in figures 3.8 and 3.9. The Lti cells are known to have a hematopoietic origin, whereas the Lto cells derive from mesenchymal precursors. Therefore, due to both the published data and the data presented here, one would assume that any defect would be observable in the Lto cells, but not the Lti cells, although due to the intimate association between these two cells types, a significant defect in one would be assumed to result in a defect in the other.

When investigating the role of CD248 at different time points during embryological development, it appears to be more influential earlier during development. The CD248$^{-/-}$ anlage have a greater reduction in both Lti and Lto cells at E18 than the lymph nodes taken from newborn pups. From previous observations that adult CD248$^{-/-}$ still present with functional lymph nodes, this is unsurprising. The apparent defect in early development seems to be reversible as the developmental stages proceed; likely indicating that CD248 is not controlling the development itself, rather affecting other factors involved in the development at different stages. This hypothesis is supported by the fact that the signalling pathway associated with CD248 function, the PDGFRβ pathway investigated here, is associated with lymphangiogenesis (Cao et al., 2004). CD248 may function as an intermediary between the two signalling pathways responsible for lymphatic vasculature and mesenchyme development in the developing lymph node.

LTβR$^{-/-}$ mice unable to activate the non-canonical NIK-dependent pathway of NFKB activation (Futterer et al., 1998). Analysis of the role of different NF-κB subunits in the development of lymph nodes has been carried out using knock out mice, and a range of phenotypes in defective lymph node development have been identified. These can range from complete absence of LN to reduced lymphoid organisation, as examined in the introduction to this chapter (van Delft et al., 2015, Yin et al., 2001, Weih et al., 1995). The evidence described here appears to indicate that these pathways in CD248$^{-/-}$ MEFs function abnormally, but not to the extent that these functions are completely abrogated. This is further supported by the fact that CD248$^{-/-}$ mice have a normal complement of lymph nodes and other lymphoid tissue. The involvement of CD248 is likely to present a high degree of redundancy, as indicated by the fact that CD248$^{-/-}$ mice are healthy and viable, and present an apparent normal lymphoid system. The data presented here gives further evidence that CD248 modulates the development of lymphoid tissue, indicating that it is able to modulate the function of both of these essential pathways, or that these pathways interact in a novel manner *in vivo*.

Chapter 4. Role of CD248 in controlling the lymphoid stromal remodelling in response to inflammation

4.1 Chapter aims

- To evaluate the expression of CD248 on adult lymphoid stromal cells in an attempt to understand the dynamic interactions between the stromal cell subsets and to exploit this expression to further delineate lymphoid stromal cell subsets.

4.2 Introduction

The structure and organisation of lymph nodes requires a supporting scaffold. This enables trafficking in the LN, the production of lymphoid chemokines and cytokines required to attract and trap the lymphocytes in the correct regions and to maintain lymphocyte survival and maturation. These cells are referred to as stromal cells. Fibroblastic reticular cells (FRCs) compromise most of the lymphoid stromal cells. FRCs can be divided into B cell zone reticular cells (BRCs), T cell zone reticular cells (TRCs), marginal reticular cells (MRCs) and follicular dendritic cells (FDCs) (Malhotra et al., 2013), see chapter 1 for a thorough review of the lymph node stromal cells. Follicular dendritic cells (FDCs) are located in the germinal centre and support the germinal centre reaction. The germinal centre is segregated into two major structure based on their different histological and functional features. The light zone (LZ) is the location of FDCs and T follicular helper cells (T_{FH} cells), whereas the dark zone (DZ) consists of proliferating B cells. Cells in the light zone and the dark zone are referred to as centrocytes and centroblasts, respectively. Centrocytes and centroblasts shuttle continuously between the two zones. Somatic hypermutation (SHM), class-switch recombination (CSR), proliferation and differentiation occurs during the GC reaction that contributes to the process of affinity maturation of the of the B cell

repertoire (Durandy, 2003, Gatto and Brink, 2010, Zaheen and Martin, 2011, Kracker and Durandy, 2011). The germinal centre reaction is explained in depth in chapter 1.

Mature FDCs display a defined location within lymphoid organs (described in Chapter 1). FDCs are stationary cells located in defined regions of the lymphoid tissue. Expression of specific markers and the unique structure of these cells with multiple fine dendrites are the factors used to characterise FDCs by histology. Initially described as binucleate (Sukumar et al., 2006), it was suggested that FDCs were formed by the fusing of CD35+B220+ cells with CD45- CD35- stromal cells (Murakami et al., 2007). No evidence of these cells has been observed outside of lymphoid organs. Thanks to the small number of these cells and the difficulties associated with separating these cells from their intimate association with the developing B cells, understanding of the development of these cells and identification of the progenitor cell of this stromal cell subtype has proved difficult (Kasajima-Akatsuka and Maeda, 2006).

Recent work has indicated that FDCs are not a dendritic cell population, but are in fact a specialised population of cells derived from the mesenchymal lineage (Aguzzi and Krautler, 2010, Mabbott et al., 2011). There is a degree of controversy about the origin of FDCs. Initially, the first group to investigate the origin of the FDCs observed that the cells could derive from perivascular precursors. This was evidenced by Mfge-8 expression, as well as CXCL13 transcripts, which could be observed in regions outside of the B cell follicles, surrounding the vasculature of lymphoid organs, by cells that express PDGFR-β (Krautler et al., 2012). These cells may be pericytes, a subtype of cells that surround and support blood vessels function and homeostasis. However, a more recent study has indicated that FDCs in the lymph node derive from marginal reticular cells (MRCs) in response to inflammation (Jarjour et al., 2014).

Induction of FDC maturation is strictly dependent on the expression of TNF and lymphotoxin (LT), as mice that are deficient in the expression of these molecules or in their downstream signalling

pathways are unable to develop FDCs and GCs within their SLOs (Allen and Cyster, 2008). The cells responsible for providing this stimulus are the B cells, and it has been shown that soluble TNF produced by these cells is more important for FDC maturation than membrane-bound TNF (Tumanov et al., 2004). As naïve B cells are responsible for providing the TNF required for FDCs to mature; and FDCs are essential to provide the maintenance and differentiation factors required for maturation of the naïve B cells, these two cell types function in a positive feedback loop (El Shikh and Pitzalis, 2012). FDCs express CXCL13, which signals via CXCR5 expressed on naïve B cells and attracts them to the nascent follicle. These B cells provide further lymphotoxin, resulting in further FDC maturation via a positive feedback loop. Accordingly, $CXCR5^{-/-}$ B cells are able to migrate into the splenic white pulp, but are unable to traffic to the follicle itself. Therefore, these cells contribute to induction of FDC development in atypical locations (Voigt et al., 2000). Stimulation of the B cells via CXCR5 causes expression of LT and TNF, inducing the maturation of FDCs as described previously (Forster et al., 1996, Voigt et al., 2000, Ngo et al., 1999). Removal of FDCs during the germinal centre reaction completely disrupts the architecture of the follicles and destroys the germinal centre response by eliminating the germinal centre B cells and simultaneously increasing the density of T cells and DCs (Wang et al., 2011).

Work carried out in this laboratory has shown that CD248 expression in the spleen is highly upregulated in response to salmonella infection (Lax et al., 2007). This increase in expression was further investigated, and $CD248^{-/-}$ lymph nodes have been shown to be unable to expand in response to inflammatory challenge (Lax et al., 2010). However, currently there is currently no appreciation as to which cell types might be expressing this CD248. Due to the fact that CD248 is understood to be expressed on pericytes (Tomkowicz et al., 2010, MacFadyen et al., 2005, MacFadyen et al., 2007, Naylor et al., 2012, Lax et al., 2010) and that this molecule functions via PDGFR-β (Naylor et al., 2012, Hardie et al., 2011, Tomkowicz et al., 2010) as well as being involved in early differentiation of the embryonic mesenchyme in the anlagen (Lax et al., 2007), we hypothesise that CD248 might be involved in FDC differentiation and function in the adult. Therefore, taking advantage of the $CD248^{-/-}$

mice which present seemingly normal lymphoid organs in the adult, in this chapter I have investigated the structure and function of FDCs in immunised CD248$^{-/-}$ lymphoid organs.

4.3 Results

4.3.1 CD248 expression has been identified on follicular dendritic cells

In order to investigate the expression of CD248 in activated lymphoid tissues, a well-described immunisation schedule was followed. The immunisation protocol employed in which NP-CGG is administered with alum adjuvant is fully discussed in the introduction to this thesis and in the materials and methods section. In these experiments, 100µg NP-CGG with alum adjuvant was administered as an intra-peritoneal injection (i.p.) on day 0 in order to induce an immune response in the spleen. In the rechallenge experiments, the mice were reimmunised on days 21 and 41, where appropriate. In order to investigate the immune response in the draining lymph nodes, 10µg NP-CGG in alum was administered as a sub-cutaneous injection (s.c.) into the foot pad of the mice at the same time points as mentioned for the i.p. immunisations. Using this immunisation schedule in order to investigate the expression of CD248 in activated lymphoid tissue, I was able to identify a population of cells with very high levels of CD248 expression within the inner part of the follicle and separated from the CD248+ capsule. These cells were located within the B cell zones of repeatedly challenged lymph nodes and further co-staining with follicular dendritic cell markers such as FDC-M1 revealed that these cells were in fact FDCs (fig. 4.1a).

As shown in figure 4.1b, the FDC network formed in response to immunisation in $CD248^{-/-}$ lymph nodes appear histologically normal. The FDCs in WT lymph nodes have been shown to express CD248, as shown in figure 4.1a. However, in the $CD248^{-/-}$ nodes, as shown in figure 4.1b, although there is no CD248 expression in the $CD248^{-/-}$ lymph nodes, as expected, the $CD248^{-/-}$ FDC networks have formed normally, and no abnormal histology is observed.

In the spleen following primary immune response, the follicular dendritic cell network form normally within the germinal centres (fig. 4.2a & b). However, as shown in figure 4.2d, following secondary immunisation, the FDC networks that form in the $CD248^{-/-}$ spleens display an abnormal histology, with aberrant interconnected network. As shown in figure 4.2d, the FDC networks formed in the $CD248^{-/-}$ spleens have a punctate histology, lacking the interconnected networks displayed in their WT counterparts shown in figure 4.2c. Interestingly, there is no abnormal structure in the $CD248^{-/-}$ following primary immunisation as shown in figure 4.2a. This is different to the expression seen in the $CD248^{-/-}$ lymph nodes in figure 4.1, demonstrating a differential role in different tissues.

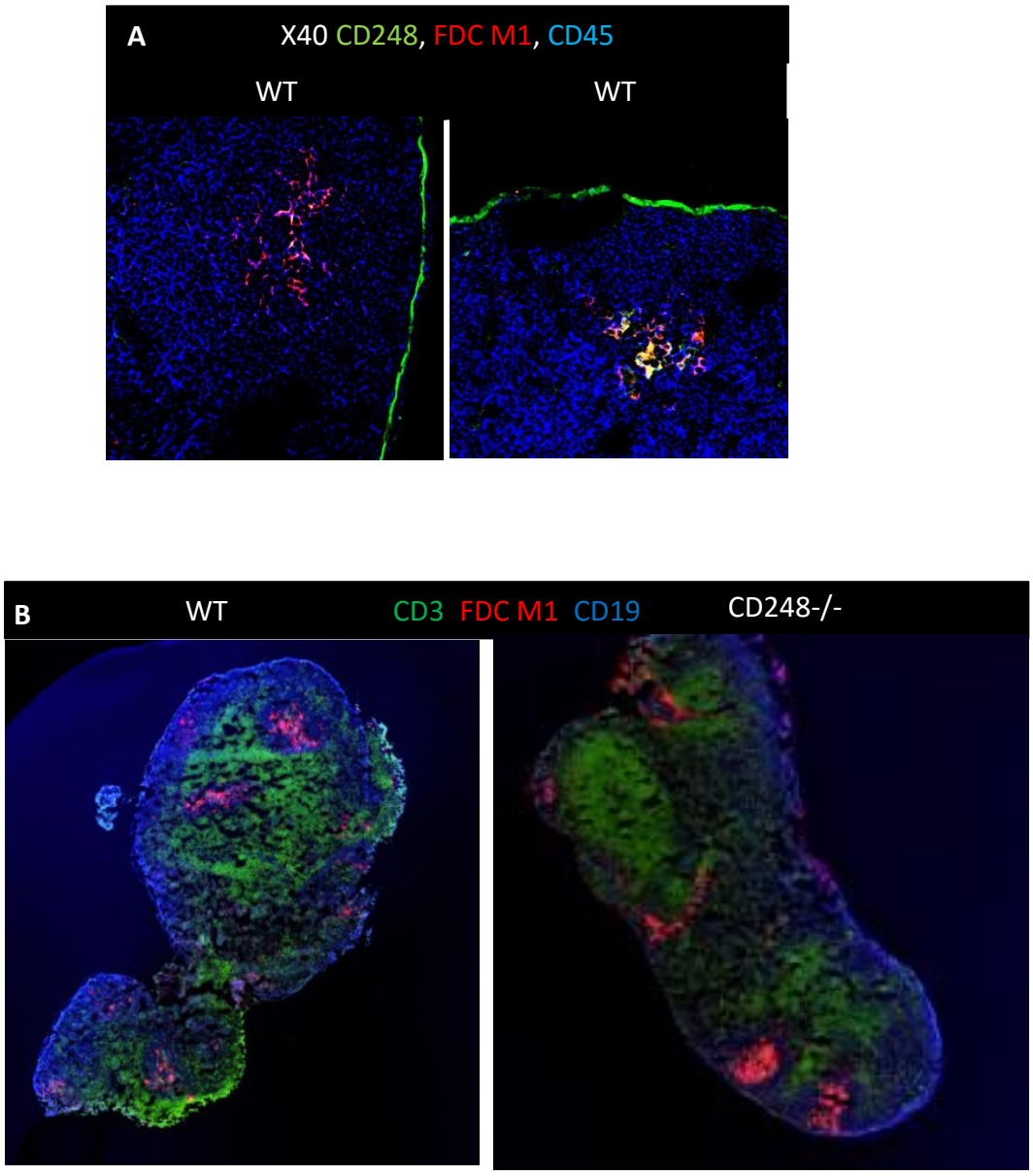

Figure 4.1 Analysis of FDC networks in immunised WT and CD248-/- draining lymph nodes. A) Identification of a population of CD248+ FDCs in WT LN as described by staining with CD248 (green), FDC-M1 (red) and CD245 (blue) at x25 magnification. **B)** Analysis of the effect of losing CD248 on the development of FDCs in the LN stained with CD3 (green), FDC-M1 (red) and CD19 (blue) at x10 magnification.

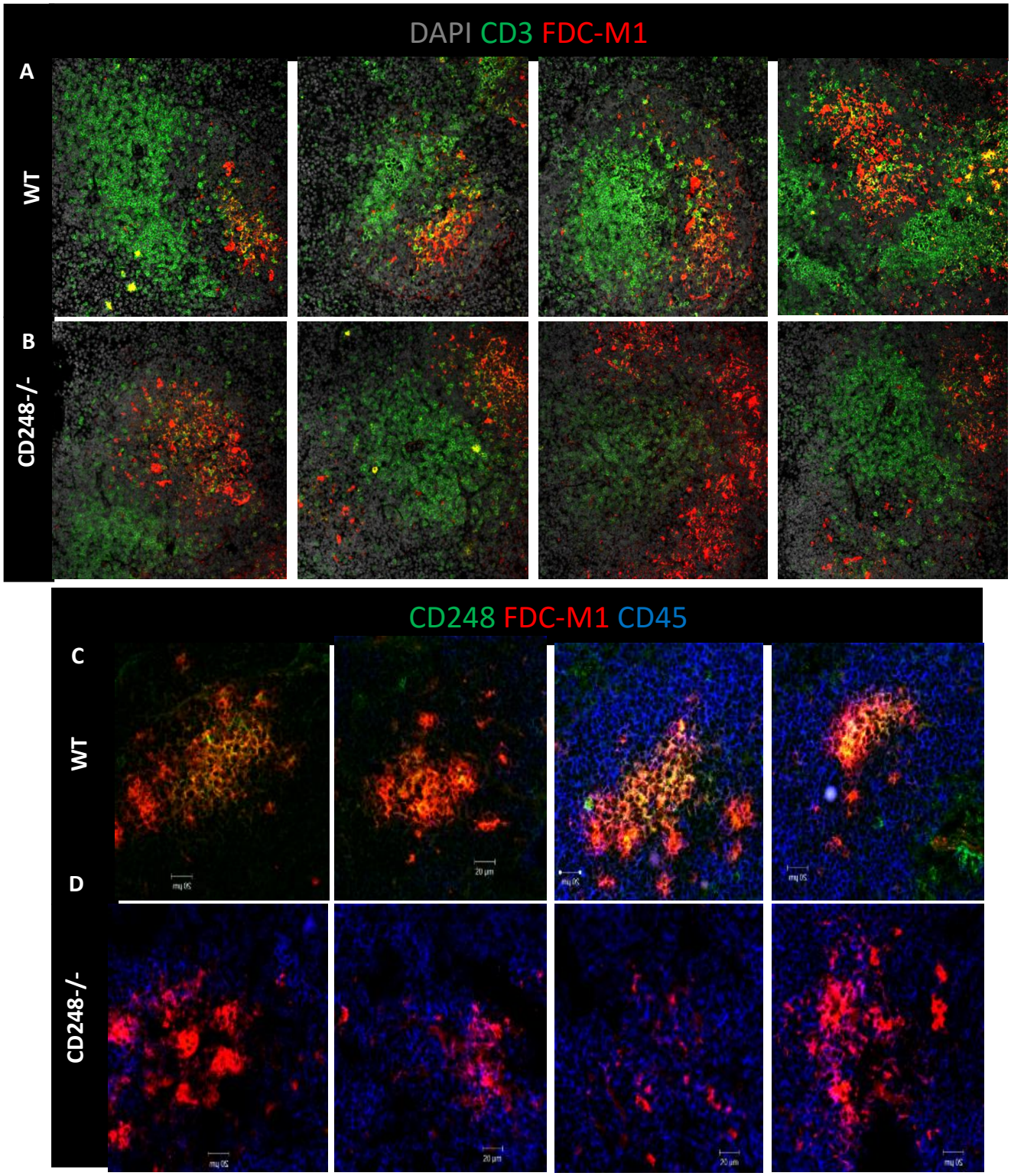

Figure 4.2 Analysis of FDC networks in immunised WT and CD248-/- spleens. FDCs in **A)** WT and **B)** CD248-/- primary immunised spleens were stained using DAPI (grey), CD3 (green), FDC-M1 (red). FDCs in **C)** WT and **D)** CD248-/- secondary immunised spleens were stained using CD248 (green), FDC-M1 (red) and CD45 (blue). Images all taken at x40 magnification.

This histological defect was further investigated throughout the whole spleens, using tile scans at multiple cutting levels and different staining protocols. Representative images are shown in figure 4.3. FDC morphology was analysed, staining the tissue with both FDC-M1 and CD35 using a number of different methods (fig. 4.3).

Spleens isolated from CD248$^{-/-}$ mice and stained with FDC-M1 showed abnormal FDC development with a complete absence of the interconnected networks demonstrated in the WT spleen in figure 4.3a, in agreement with the previous data demonstrated in figure 4.2. There also appears to be a reduction in the number of germinal centres across the whole spleen when compared to the WT. When the histology of the FDCs is analysed by staining with CD35 (fig. 4.3d), which is a different FDC marker, known to stain a functional molecule on the surface of the FDCs, the structures of the networks did not seem to be affected. The CD248$^{-/-}$ FDCs demonstrate the same structure as their WT counterparts, but the total size and number of FDC networks appears to be was reduced in comparison to the WT spleens shown in figure 4.3c.

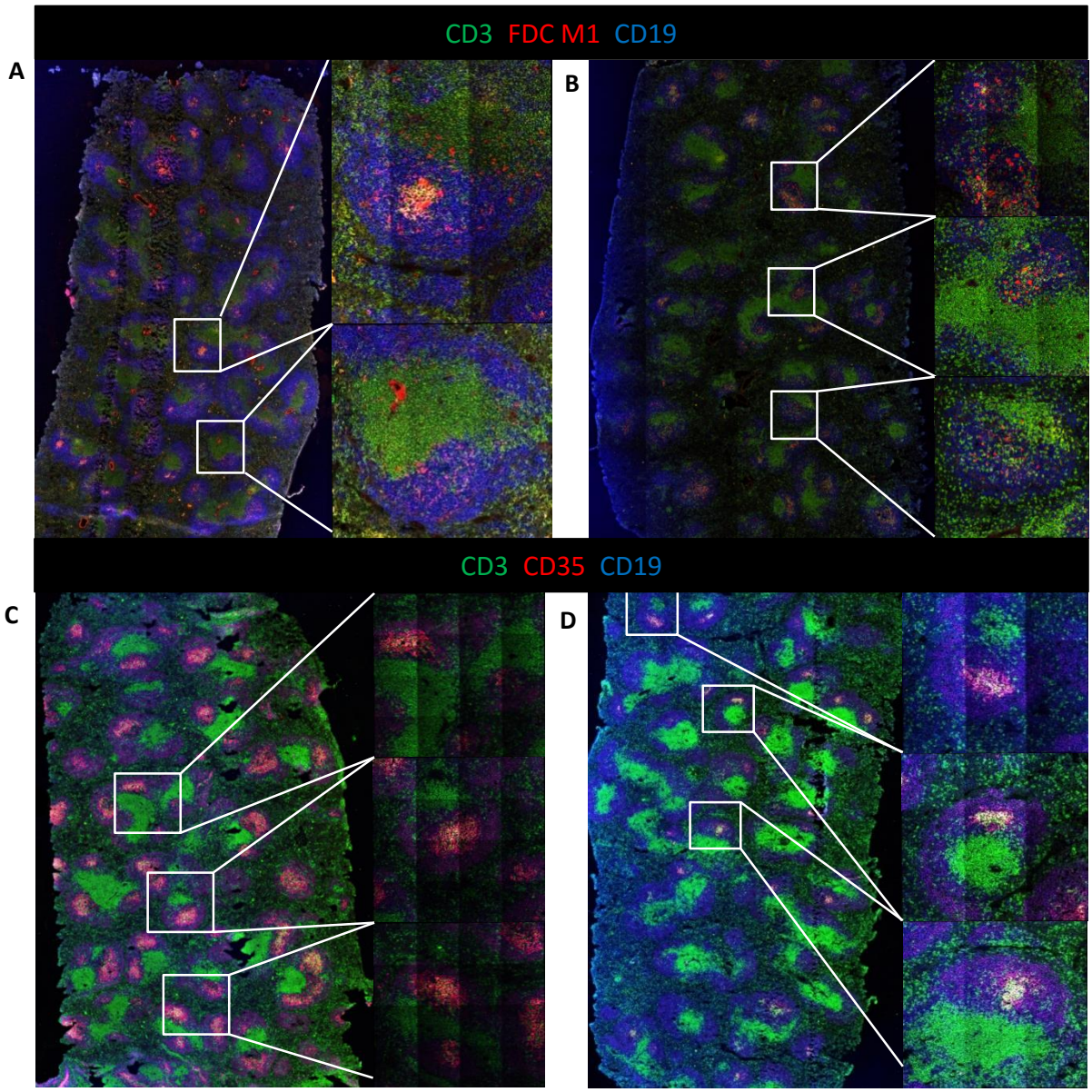

Figure 4.3 Identification of a defect in FDC networks of CD248-/- spleens. Representative images of WT and CD248-/- spleens stained with different markers as follows: **A)** WT and **B)** CD248-/- spleens stained with CD3 (green), FDC-M1 (red) and CD19 (blue) and **C)** WT **D)** CD248-/- spleens stained with CD3 (green), CD35 (red) and CD19 (blue). Overview images at 10x magnification with inserts at 40x magnification.

These defects were quantified using a number of methods. Initially, the size of the follicular dendritic cell networks was measured in μm^2, this revealed that the area covered by FDC-M1 positive staining within the germinal centre was reduced in the $CD248^{-/-}$ spleens compared to the WT (fig. 4.4a). This was also true of the area of CD35 positive staining, with a significant reduction in the size of the of the follicular dendritic cell areas in the $CD248^{-/-}$ when compared to the WT (fig. 4.4b). The defect in the FDCs when investigated using FDC-M1, as previously observed, was not a significant reduction in the size of the areas, rather a reduction in the development of processes and the interconnectivity of the cells. In order to further quantify this defective development, the pixel density of the FDC region was analysed. The FDC-positive stained area was selected using Zen software; this software then calculated the number of positive pixels within this region. Using this data, I was able to calculate the mean pixel density per unit area, therefore quantifying the distribution of the FDC-M1 positive staining and giving an indication of the interconnectivity of the dendritic processes and network formation. No significant difference in the mean number of FDC-M1 positive pixels between the $CD248^{-/-}$ and the WT was observed in mice immunised once (figure 4.4c). Following secondary rechallenge with the same antigen, however, the $CD248^{-/-}$ spleens revealed a significant reduction in the mean FDC positive pixel density per unit of FDC area compared to the WT (figure 4.4d). The defect in the immunised $CD248^{-/-}$ lymph nodes was also analysed in this manner, and as can be seen in figure 4.4e, there is no significant difference between the WT and $CD248^{-/-}$ nodes.

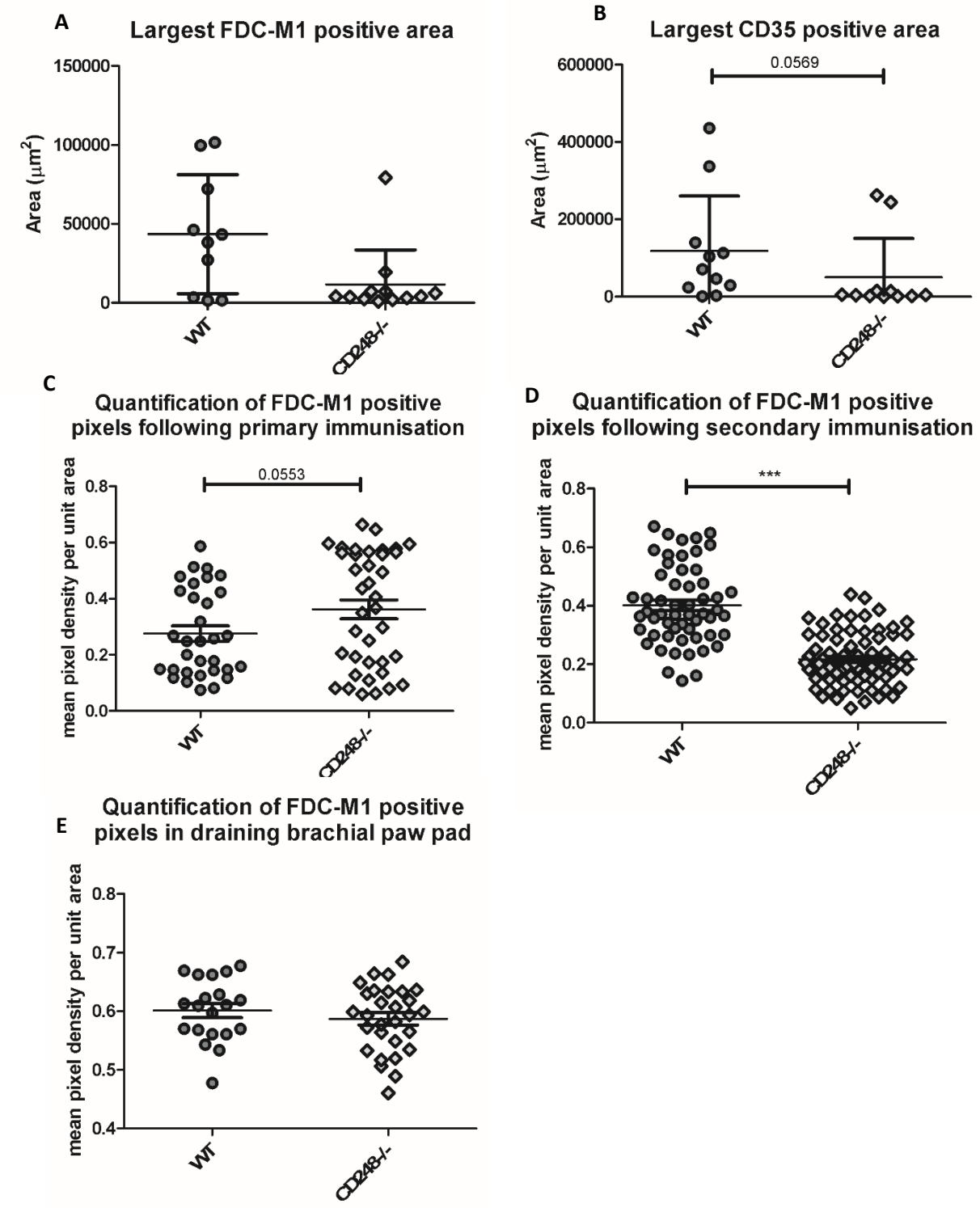

Figure 4.4 Analysis and quantification of the observed defect in FDC networks of CD248-/- spleens and LN. A) The area of the single largest FDC-M1 positive area was calculated using Zen software in μm^2. **B)** The area of the single largest CD35 positive area was calculated using Zen software in μm^2. Data shown in **A)** & **B)** is representative of 4 spleens, with 3 independent cutting levels per spleen. Error bars demonstrate the mean ± SD with significance calculated using a Student's t test. Mean pixel density per unit area of the germinal centre was calculated from 3 representative images per spleen, with 4 independent spleens used per group. This was calculated following primary immunisation (**C)** and secondary immunisation **(D)**. Error bars demonstrate the mean ± SEM, and significance was calculated using a Student's t test with $p < 0.0005$ = ***. Mean pixel density was also calculated for the germinal centres found within immunised bLN (E) (n = 24) and errors bars describe mean ± SEM

This analysis gave some interesting insights into the defect in the CD248$^{-/-}$ germinal centres, although it did not completely address the abnormal structure of the FDC networks observed in the CD248$^{-/-}$ spleens. Therefore, an imagej macro was designed in order to more fully understand the reduction in connections between the individual follicular dendritic cells. The steps in the macro analysis are described in figure 2.2, and also shown in fig. 4.5a. However, in brief, the percentage of GC covered by FDC-M1 positive staining was calculated. The aim of this analysis was to give a better representation of the defect in network formation by analysing the connections between the FDC-M1 positive regions. As shown in figure 4.5b, the CD248$^{-/-}$ spleens display a significantly reduced coverage over the germinal centre with follicular dendritic cells, again indicating that there is significant reduction in the interconnectivity of the networks.

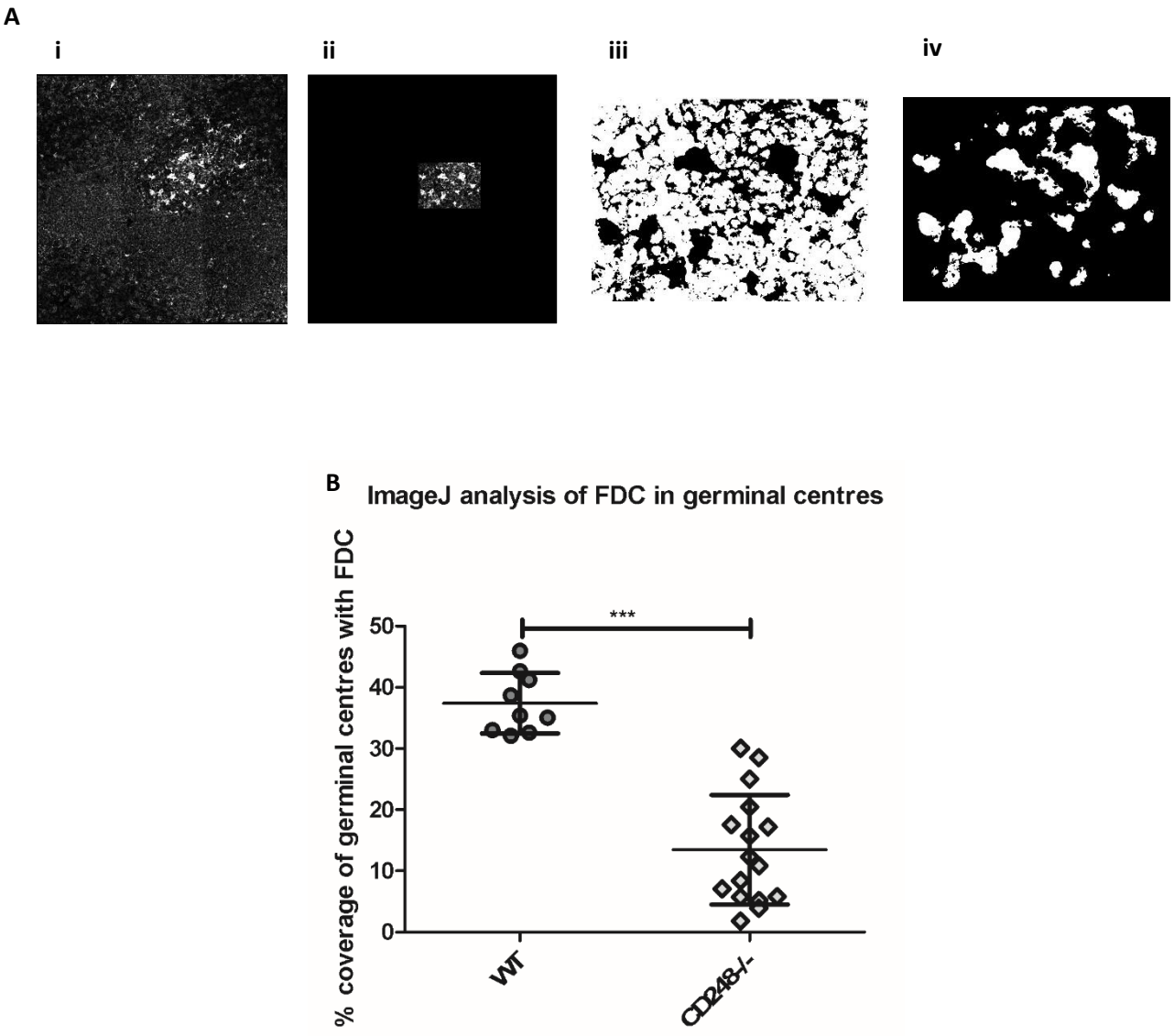

Figure 4.5 Design and use of an imageJ macro to quantify the defect in FDC networks of CD248$^{-/-}$ spleens. A) Description of the macro designed to analyse this FDC defect, described in detail in chapter 2. The analysis of the FDC networks in three times challenged spleens is demonstrated in **(B)** with error bars describing the mean ± SD. Significance was calculated using a Student's t test with $p < 0.0005$ = ***.

4.3.2 Investigating a developmental origin for follicular dendritic cells

There is some evidence that FDCs in the spleen derive from ubiquitous perivascular precursors (Krautler et al., 2012). CD248 is also known to be expressed on pericytes, with the evidence outlined in chapter 1. Naylor and al. (2014) demonstrated co-localization of CD248 with both NG2 and α-smooth muscle actin (α-SMA), two classical pericyte markers (Bergers and Song, 2005, Tomkowicz et al., 2007). We used these markers to characterise our immunized tissue, firstly addressing staining distribution in WT mice (top row of figure 4.6a). NG2 expression was detected in the FDC rich area that exceeded the CD248 staining (top left panel figure 4.6a) The abnormal FDC networks observed in the $CD248^{-/-}$ showed discrete positive NG2 staining, although this was reduced compared to the WT (fig.4.6a). The mean pixel density of the NG2 positive pixels within the GC was also calculated using the Zen software as before. Results are shown for this quantification that show reduced amount of NG2-positive staining in the $CD248^{-/-}$ spleens (figure 4.6b). The levels of expression of NG2 were also analysed by quantitative real time PCR on microdissected GC from WT and $CD248^{-/-}$ spleens, and revealed a reduction in the number of transcripts of NG2 in the $CD248^{-/-}$ as compared to the WT (fig. 4.6c). Similar analysis was performed for CD248 and α-SMA. As can be seen in the top panel of figure 4.7a, CD248-positive FDCs are also positive for α-SMA. A significant reduction in the expression of α-SMA was observed in the $CD248^{-/-}$ spleens, as shown in the bottom panel of figure 4.7a. However, PCR analysis was unable to confirm the observation at the protein level (fig.4.7b).

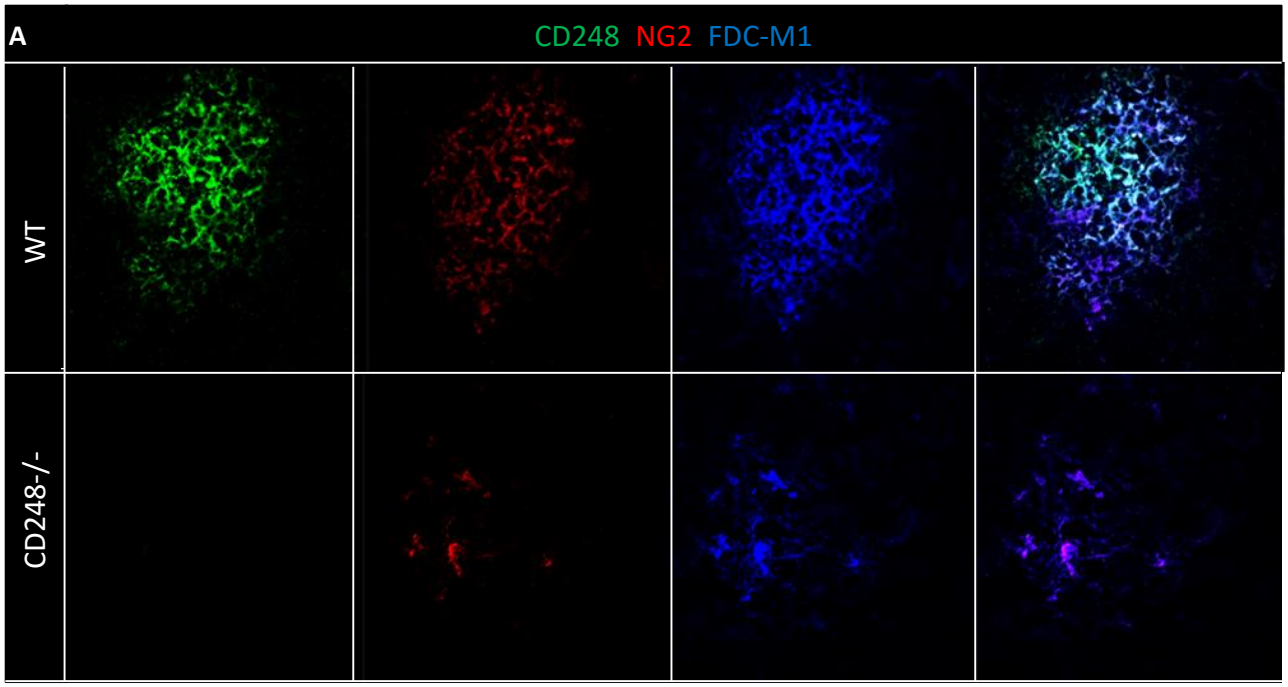

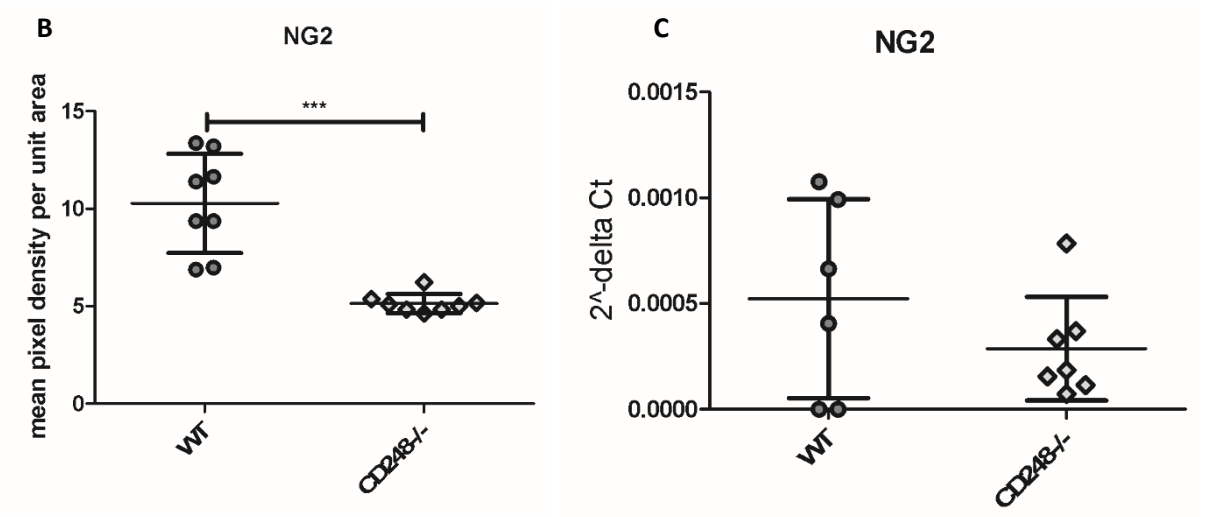

Figure 4.6 Analysis of expression of pericytes marker NG2 in immunised WT and CD248-/- spleens. A) Germinal centres in WT and CD248-/- spleens stained with CD248 (green), NG2 (red), and FDC-M1 (blue). Mean NG2 positive pixel density per unit area of the germinal centre was calculated from 2 representative images per spleen, with 4 independent spleens used per group **(B).** Error bars demonstrate the mean ± SEM, and significance was calculated using a Student's t test with $p < 0.0005$ = ***. The number of transcripts of NG2 in the germinal centres of microdissected spleens was analysed by RT-qPCR **(C)**. Data is represented with error bars demonstrating mean ± SD with n = 6. Significance was analysed using Mann-Whitney Unpaired t test.

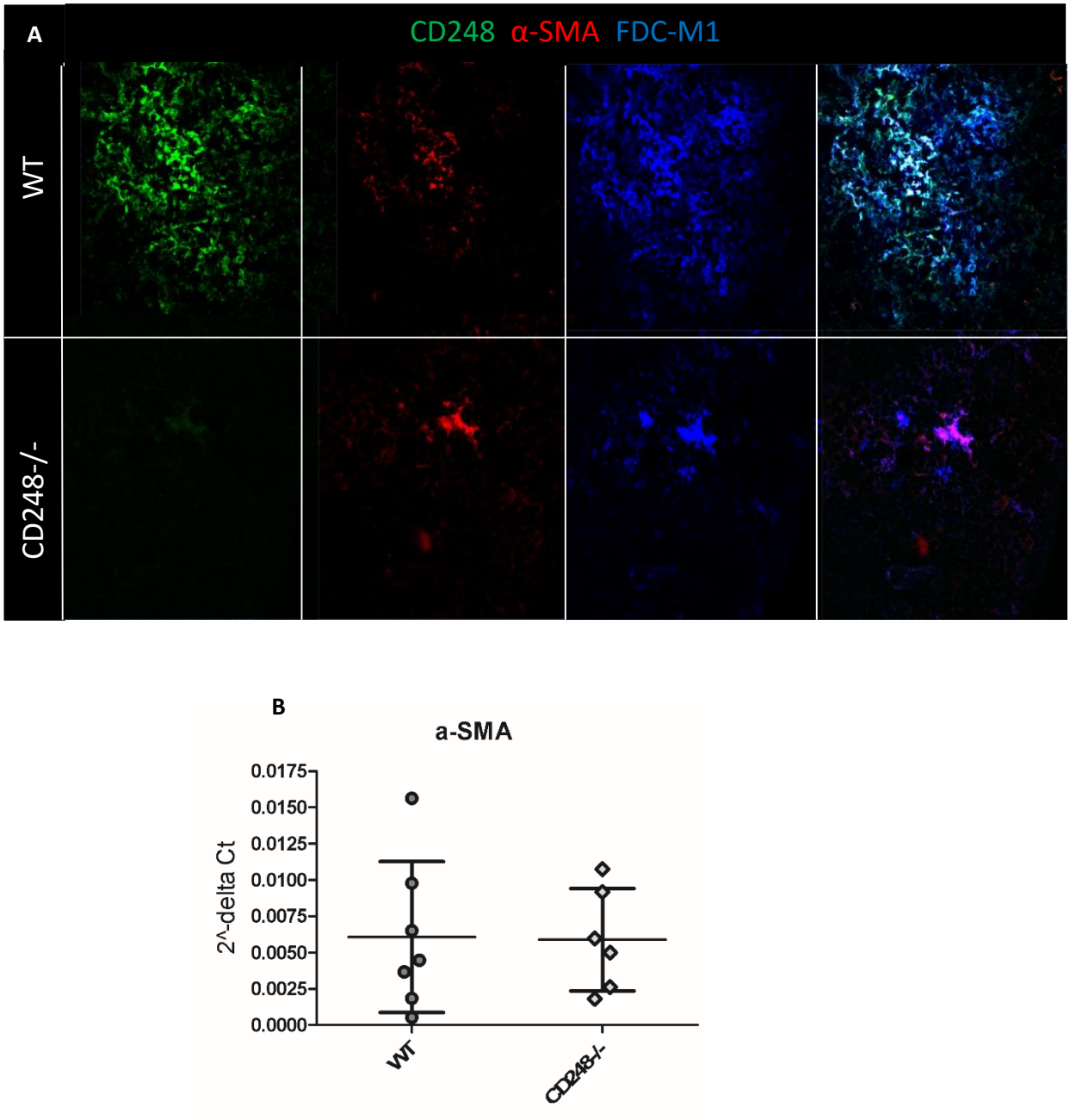

Figure 4.7 Analysis of expression of pericytes marker α-SMA in immunised WT and CD248-/- spleens. A) Germinal centres in WT and CD248-/- spleens stained with CD248 (green), α-SMA (red), and FDC-M1 (blue). The number of transcripts of α-SMA in the germinal centres of microdissected spleens was analysed by RT-qPCR **(B)**. Data is represented with error bars demonstrating mean ± SD with n = 6. Significance was analysed using Mann-Whitney Unpaired t test.

Jarjour et al. (2014) have recently proposed that FDCs in the lymph node which develop in response to inflammation do so from a marginal reticular (MRC) precursor. These cells are currently believed to derive directly from the LTo embryological precursor, giving a direct link between the LTo and the mature FDCs. The main markers that allow identification of the MRCs are CXCL13 and RANKL. The expression of these markers was investigated in the WT and CD248$^{-/-}$ spleens and lymph nodes. As can be seen in figure 4.8, the sizes of the B cell zones were significantly upregulated in both the WT and the CD248$^{-/-}$ immunised spleens. The expression of CXCL13 is found restricted to within the B cell zones, rather than outside of these areas. There does not appear to be any difference in the amount or localisation of the expression of CXCL13 in the CD248$^{-/-}$ spleens, indicating that these cells have a normal ability to recruit and retain B cells in follicles in response to immunisation. The expression of RANKL in the WT and CD248$^{-/-}$ spleens appears to be very limited. The level of staining observed in both spleens does not seem to be significantly above background (fig. 4.8a & b).

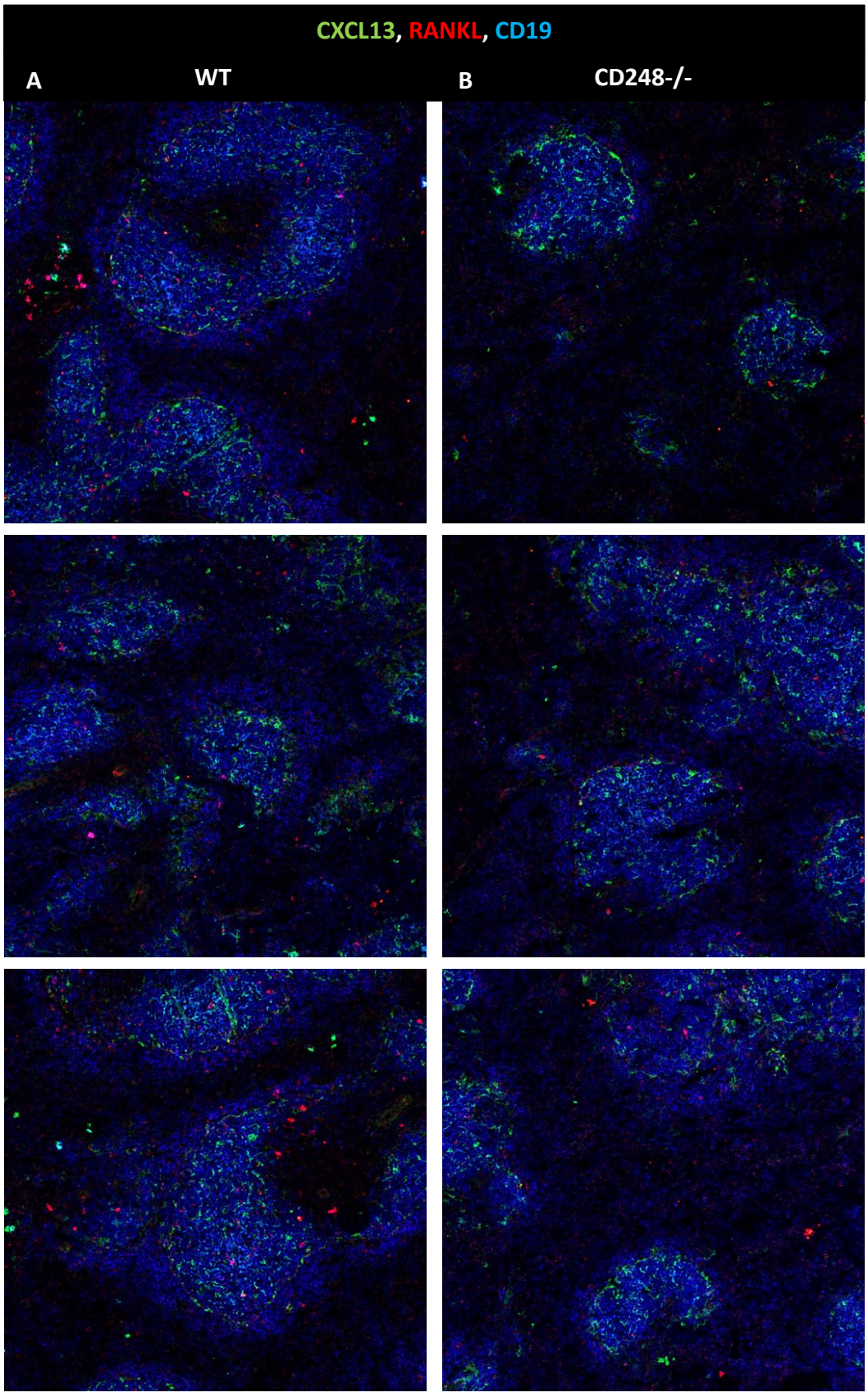

Figure 4.8 Analysis of MRC structures in immunised WT and CD248-/- spleens. A) WT and **(B)** CD248-/- immunised spleens stained with CXCL13 (green), RANKL (red), and CD19 (blue) at x40 magnification.

MRCs are known to localise to the cortical side of the subcapsular sinus of lymph nodes. Therefore, the expression of RANKL located around the capsule of lymph nodes was analysed by immunofluorescence. As can be seen in figure 4.9, expression of RANKL can be observed surrounding the cortex of both WT and CD248$^{-/-}$ lymph nodes. This was further examined by investigating the co-localisation of RANKL with CXCL13, as can be seen in figure 4.9a & b. As demonstrated in figure 4.9, expression of RANKL can be observed immediately below the subcapsular sinus. CXCL13 expression can be detected throughout the B cell follicles of the lymph nodes, but is also notably co-localised with the RANKL at the edge of the cortex (fig. 4.9). There does not seem to be any significant difference in the expression of either CXCL13 or RANKL in the CD248$^{-/-}$ lymph nodes. These CD248$^{-/-}$ lymph nodes also display the expected localisation of these markers within the organ.

Taken together, the observations made in both the lymph nodes and spleens appear that the CD248$^{-/-}$ lymphoid organs have apparently normal expression and distribution of marginal reticular cells when examined by histology.

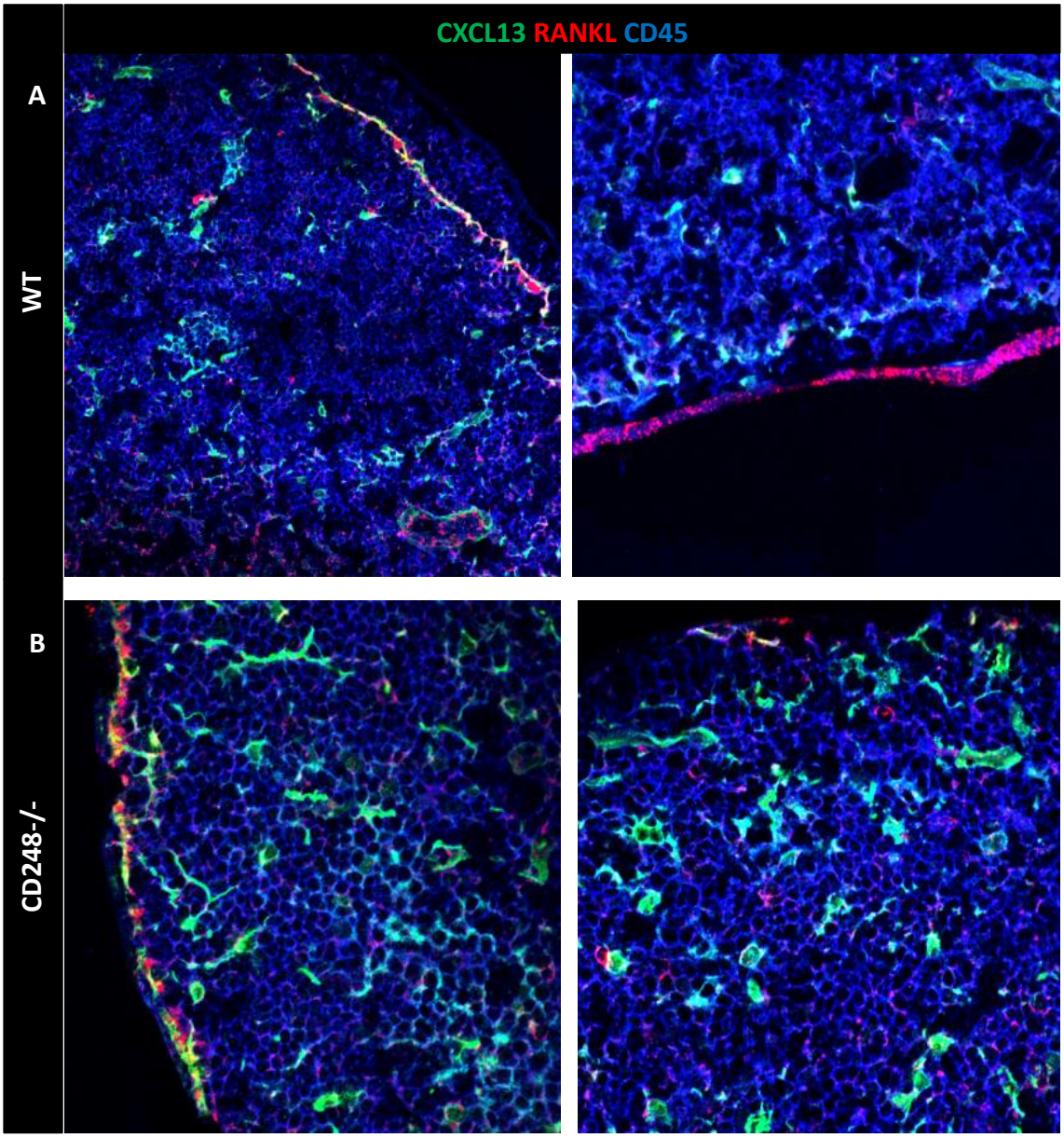

Figure 4.9 Analysis of MRC structures in immunised WT and CD248-/- draining lymph nodes. A) WT and **B)** CD248-/- immunised brachial lymph nodes stained with CXCL13 (green), RANKL (red), and CD45 (blue) at x40 magnification

4.3.3 Establishing a novel method for digestion and flow cytometry analysis of follicular dendritic cells

Follicular dendritic cells are an important cell type in the development of the germinal centre response, but understanding of these cells has previously been limited. Based on the data presented in this chapter, notably the appearance of CD248 on a discrete population within the FDC network and the presence of evident FDC defects in the spleen but not in the LNs, we hypothesised the presence of a certain degree of heterogeneity in this population in different lymphoid organs. In order to address this complex scenario, we seek to digest FDC networks upon immunization and to use flow cytometry to investigate FDC phenotype more accurately. The digestion and staining protocol established is outlined in figure 4.10. The large and irregularly-sized stromal cells were selected based on their forward scatter and side scatter profiles; doublets were excluded from the analysis by investigating the pulse width. This is essential, as the stromal cells have long processes which express high levels of adhesion molecules to allow for the function of these cells, but which can confound the results. Once these structural elements have been accounted for, the cells were selected based on their lack of expression of CD45 and CD31, selecting the stromal cells compartment by excluding the hematopoietic and endothelial components. The expression of gp38, CD35 and BP-3 were then analysed on these CD45-CD31- cells.

A distinct population of gp38+BP3+ cells was robustly detected in unimmunised LN (figure 4.10b), that display low expression of CD35. We hypothesise that these gp38+BP3+CD35- cells are the B cell zone reticular cells that support the homeostatic B cell compartments. Following immune challenge, there is a significant expansion in the number of CD35+ cells (fig. 4.10c). The majority of CD35+ cells are also gp38+, as shown in figure 4.10c. The numbers of gp38+BP3+ cells are also expanded in the immunised lymph nodes, indicating an expansion in the size of the B cell zones. A large proportion of the gp38+CD35+ cells are also positive for BP-3. We hypothesise that these cells are the FDCs which

develop in response to inflammation and GC formation. Isotype controls for CD35 and BP3 are shown in figure 4.10d.

This analysis was then applied to the immunised CD248$^{-/-}$ lymph nodes (fig. 4.11). Expansion of the gp38+CD35+ and the gp38+BP3+ cell populations can also be observed in the CD248$^{-/-}$. There is no significant difference in the proportions of cells in these populations in the CD248$^{-/-}$ compared to the WT lymph nodes (fig.4.11b). The absolute numbers of these cells were also quantified using counting beads and revealed that again there is no significant difference in the numbers of these cells, as can be seen in figure 4.11c. When the expression of BP3 on gp38+CD35+ cells is analysed, many of these cells were identified as being BP3^{hi}. There appears to be a higher expression of BP3 on the CD35+ population in the CD248$^{-/-}$ cells as in the WT cells. This could indicate a difference in the proportions of the FDC population in the CD248$^{-/-}$ as in the WT lymph nodes.

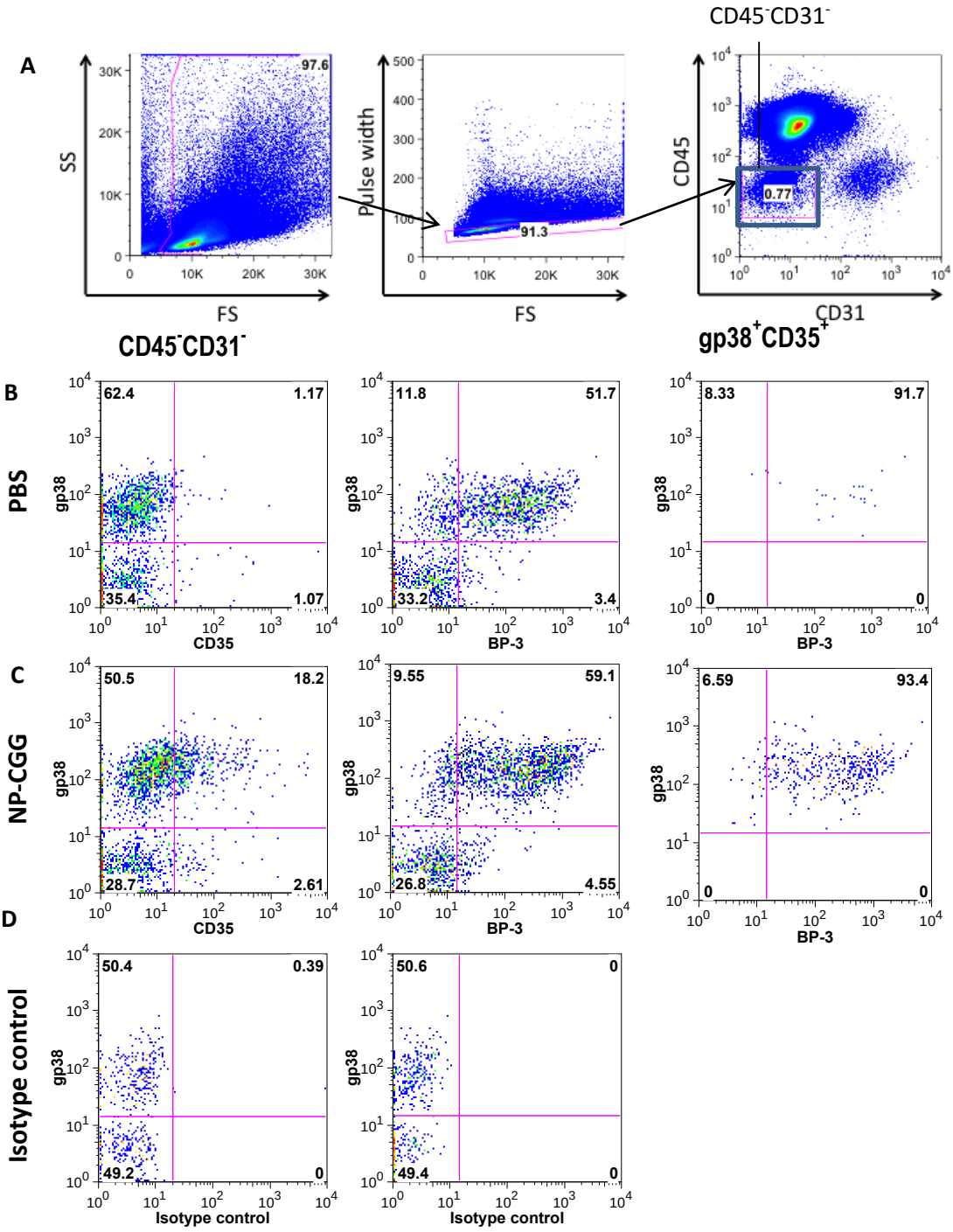

Figure 4.10 Establishing a novel method for analysing FDCs by flow cytometry. A) Gating strategy employed for the selection of the CD45- CD31- stromal cell population of brachial lymph nodes. **B)** lymph node stromal cells challenged with PBS were analysed for their expression of gp38, CD35 and BP3. **C)** lymph node stromal cells challenged with NP-CGG were analysed for their expression of gp38, CD35 and BP3. **D)** Isotype controls of the CD35 and BP3 antibodies on the CD45-CD31- stromal cell fraction.

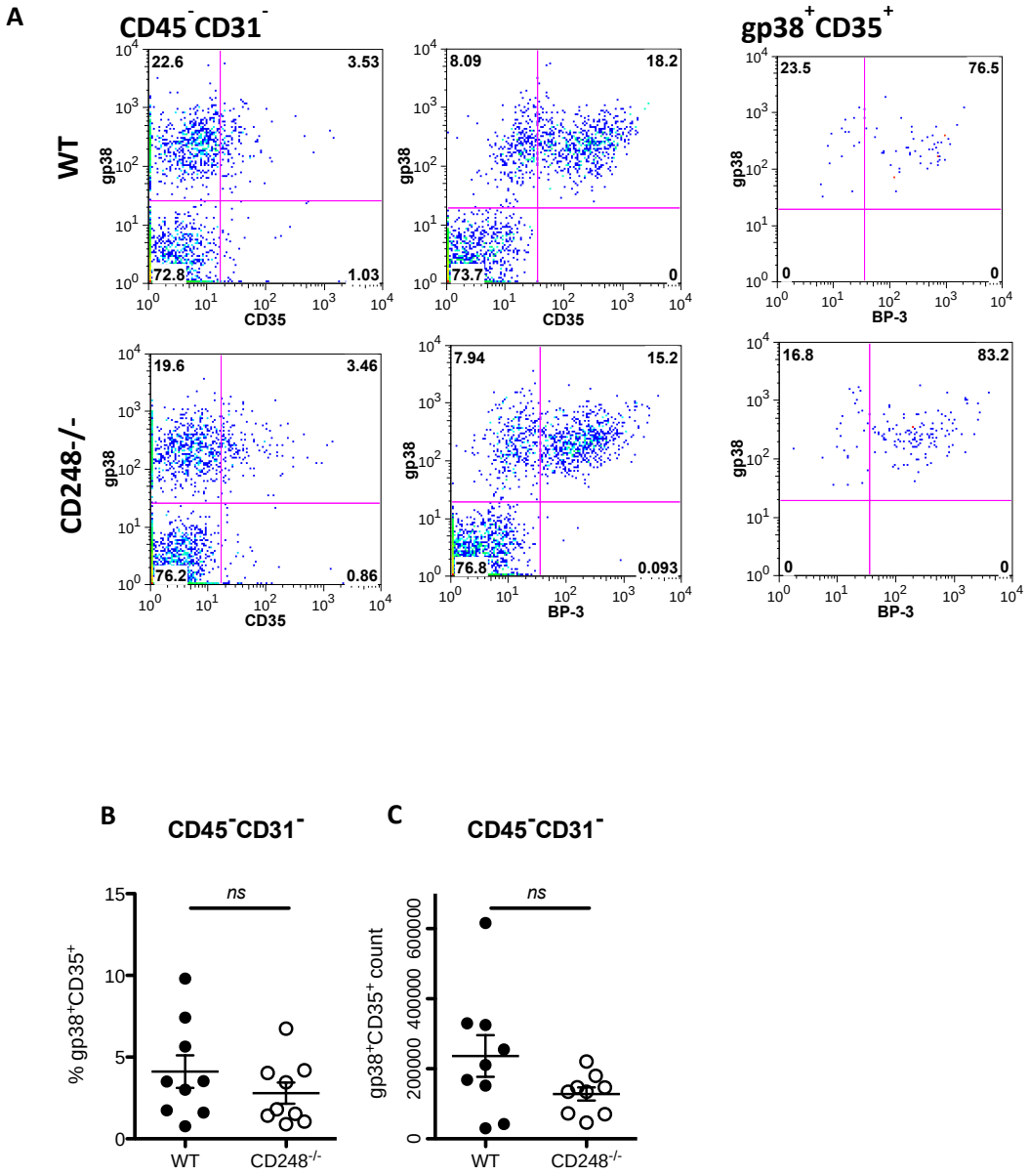

Figure 4.11 Investigating proportions of FDC in immunised WT and CD248-/- draining brachial lymph nodes. A) Gating strategy employed to analyse the FDCs in rechallenged WT and CD248-/- brachial lymph nodes. **B)** Quantification of the percentages of CD45-CD31-gp38+CD35+ in WT and CD248-/- lymph nodes. **C)** Quantification of the absolute numbers of CD45-CD31-gp38+CD35+ in WT and CD248-/- lymph nodes. Absolute numbers were quantified using counting beads. Data shown is representative of two independent experiments with n = 9. Error bars indicate mean ± SD with significance calculated using a Mann-Whitney Unpaired t test.

This analysis was also carried out in the mesenteric lymph node of the WT and CD248$^{-/-}$ challenged i.p. with NP-CGG. As can be seen in figure 4.12a, there is a significant expansion in the gp38+BP3+ population in the mesenteric lymph node compared to the brachial lymph node. This would lend yet more evidence to the hypothesis that the FDCs found in different lymphoid tissues are made up of multiple different lineages of cells. When the percentages of these cells following reimmunisation is quantified, as shown in figure 4.12b, there is a significant reduction in the number of gp38+ CD35+ cells in the CD248$^{-/-}$ mesenteric lymph nodes when compared to their WT counterparts. When the absolute numbers of the cells were quantified using counting beads, they also revealed a reduction in the numbers of these cells in the CD248$^{-/-}$ when compared to the WT organs. However, this reduction is not statistically significant, potentially because the absolute cell numbers were not normalised to organ weight.

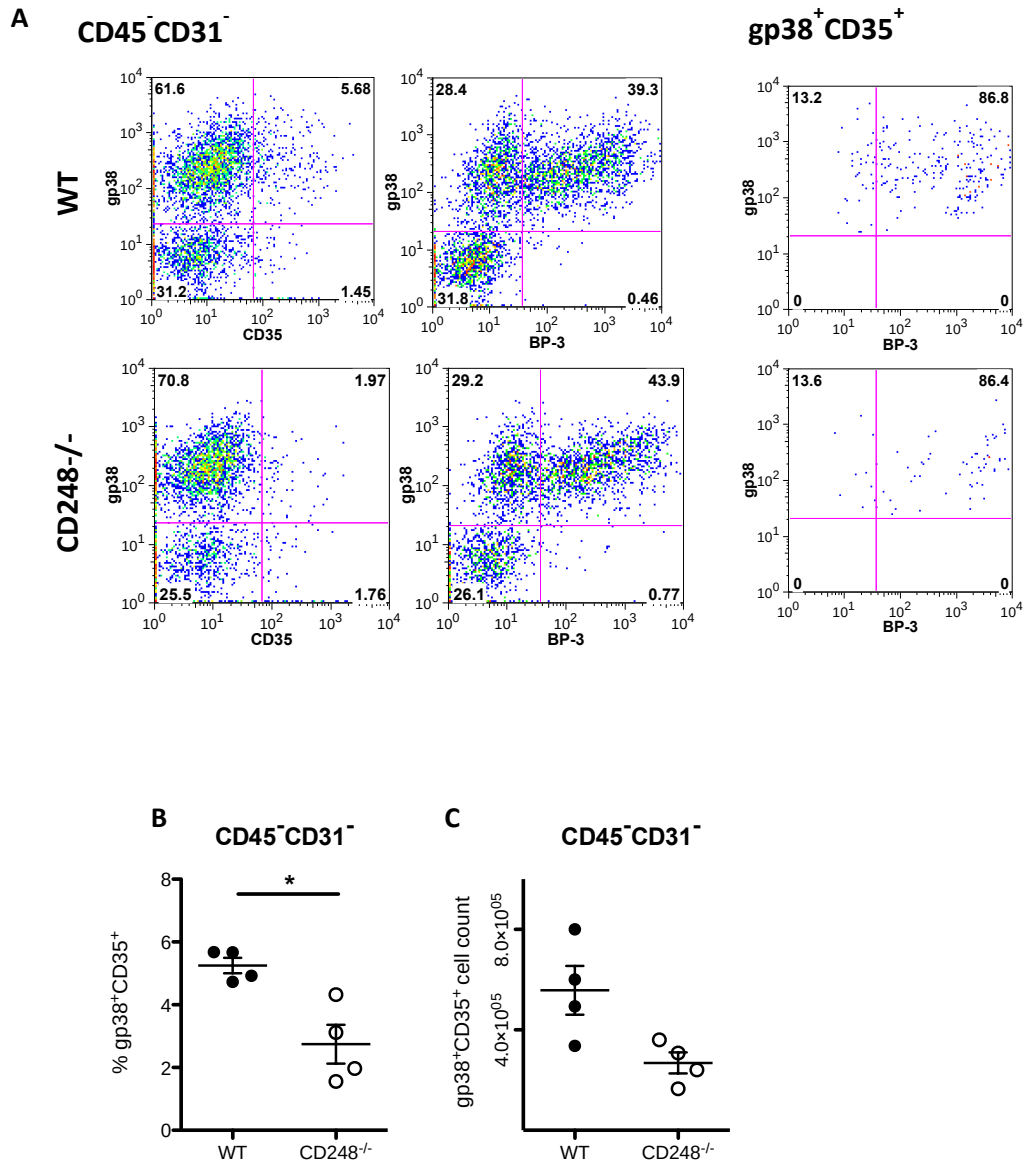

Figure 4.12 Investigating proportions of FDC in immunised WT and CD248-/- mesenteric lymph nodes. A) Gating strategy employed to analyse the FDCs in rechallenged WT and CD248-/- mesenteric lymph nodes. **B)** Quantification of the percentages of CD45-CD31-gp38+CD35+ in WT and CD248-/- lymph nodes. **C)** Quantification of the absolute numbers of CD45-CD31-gp38+CD35+ in WT and CD248-/- lymph nodes. Absolute numbers were quantified using counting beads. Data shown is representative of mean ± SD of n = 4, with significance calculated using a Mann-Whitney Unpaired t test with $p < 0.05$ = *.

According to the data outlined above, the defect previously observed in the CD248$^{-/-}$ appears to be more significant in the splenic immune response than in the brachial lymph node. This is further confirmed by the fact that there is no significant reduction in the number of FDCs in the immunised CD248$^{-/-}$ bLN. The defect observed is more significant by histology in the splenic immune response. Therefore, we attempted to separate the FDCs from the spleen. Due to the structure of the organ, which, as summarised in the introduction to this thesis, includes an increase in non-stromal cell types, such as endothelial cells and erythrocytes, and the increased "stickiness" of the organ compared to LN. Therefore, additional steps are required to separate out the stromal cell population accurately. As shown in figure 4.13a, the plots generated from single cell suspension from digested spleens appear significantly different from the plots generated in the LN. In particular, a large percentage of gp38-CD35- cells and a significant reduction in the percentage of CD45-CD31-CD11b-Ter119- cells that express gp38 and CD35 is observed. In order to remove some of these confounding factors and obtain clearer plots for analysis, MACS microbeads were used in different protocols to enrich the stromal cell population.

The removal of the CD45 fraction (figure 4.13b) already improved the detection of the CD45-CD31-CD11b-Ter119- stromal cell population, that increased from 2.04% to 18.8%. . We attempted to deplete erythrocytes using Ter119 beads in combination with CD45 beads and concluded that the former do not confound the staining panel as strongly as the leukocytes. Therefore, for subsequent analysis of the FDCs in the spleen, only lymphocytes were excluded using CD45+ beads. However, as shown in figure 4.13b & c, the number of cells in the gp38+CD35+ population and the separation of this population from the CD35- population is not as definite as in the lymph node, indicating that further steps are required to separate this population out of the total spleen for phenotypical analysis.

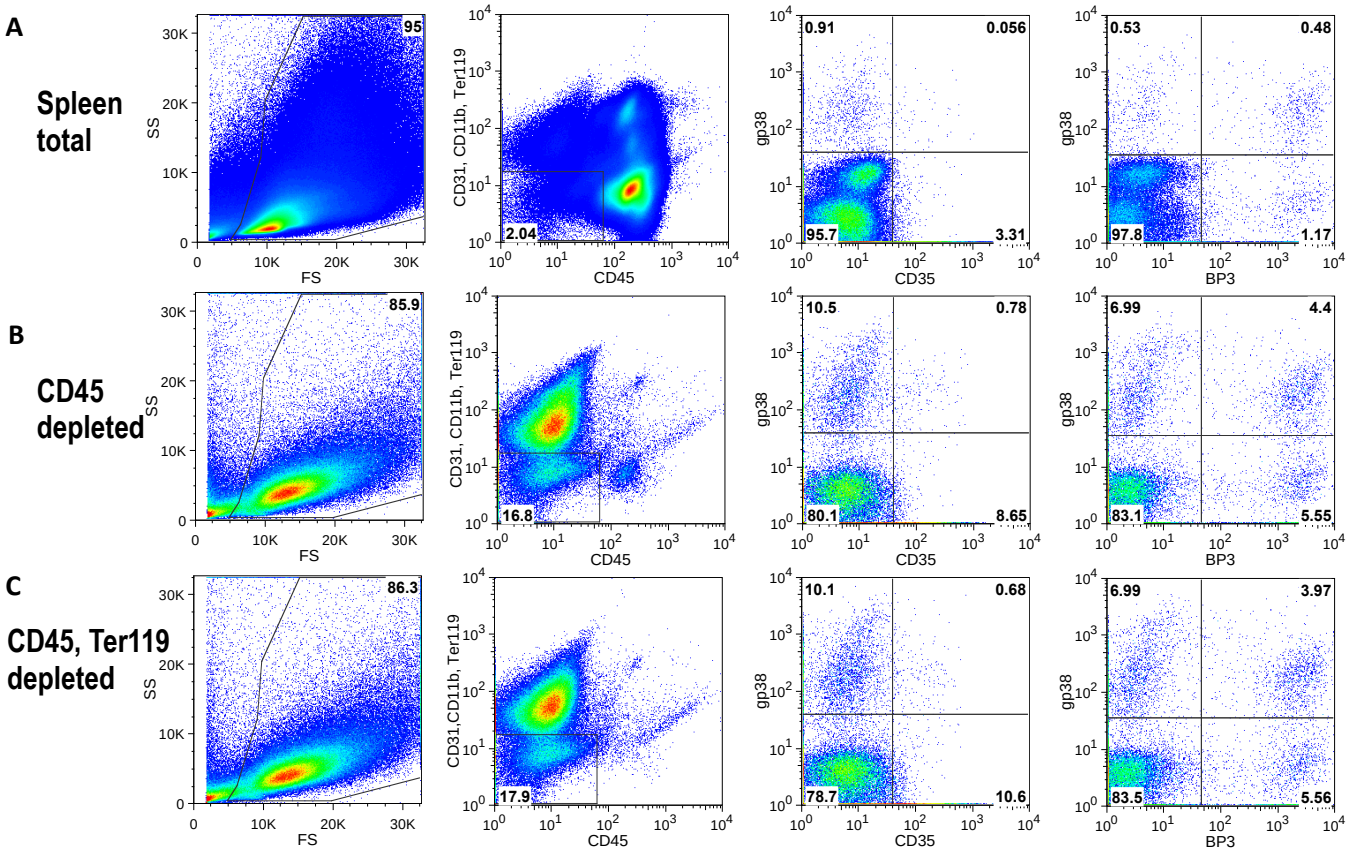

Figure 4.13 Establishing a method for analysing these stromal cells in spleen. Representative flow cytometry gating strategy to investigate the proportions of cells in digested spleens from the total spleen **(A),** after depletion of the lymphocytes using CD45+ MACS beads **(B)** and after exclusion of lymphocytes and erythrocytes using CD45+ and Ter119+ beads **(C)**

In order to fully confirm that the CD35+ cell population under investigation is, indeed, a population of FDC, the next step was to investigate the number of these cells in a system that is established to be completely lacking these cells. Therefore, we investigated whether these gp38+CD35+ cells were absent in the μMT mice. As examined in the introduction (chapter 1), the development of FDCs is dependent on the production of lymphotoxin by incoming B cells, therefore mice lacking B cells should also lack functional FDC development. This analysis was carried out in both immunisation procedures followed previously, in both the skin draining brachial lymph node and the central mesenteric lymph node. Representative plots can be seen in figure 4.14a & b and diagrams in figure 4.14 c-f that show how in both the brachial and mesenteric lymph nodes there is a lack of CD35 expression in response to immunisation. Nonetheless, a significant population of gp38+BP3+ cells is still present in the μMT mice, most likely the non FDC B cell stroma, BRCs.

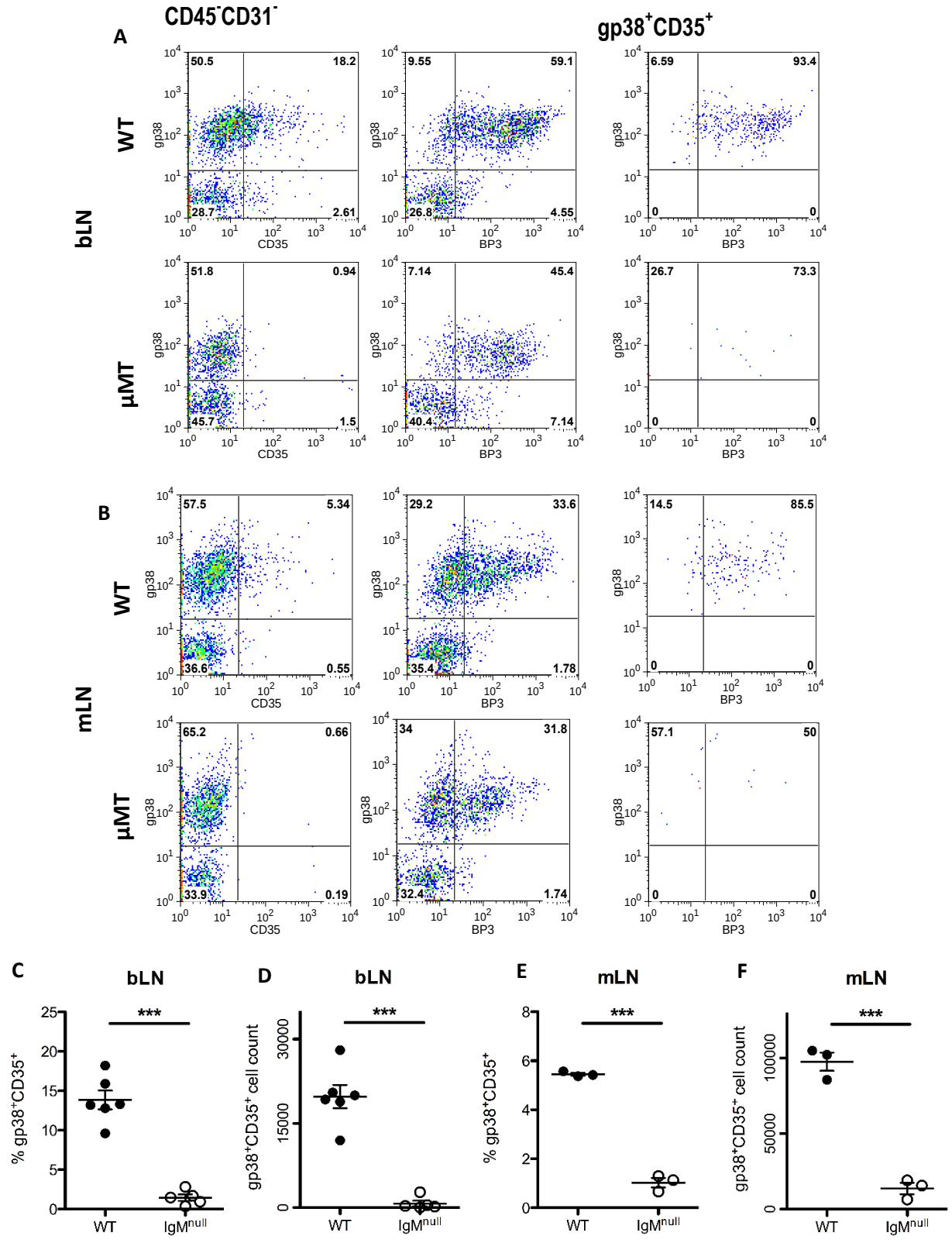

Figure 4.14 Confirming the identity of the potential FDCs using B cell knock out mice. Representative flow cytometry plots of the stromal cell populations in WT and B cell KO brachial **(A)** and mesenteric **(B)** lymph nodes. Quantification of the percentages of CD45-CD31-gp38+CD35+ in WT and B cell KO brachial **(C)** and mesenteric **(E)** lymph nodes. The absolute numbers of CD45-CD31-gp38+CD35+ cells were quantified in WT and B cell KO brachial **(D)** and mesenteric **(F)** lymph nodes. Absolute numbers were quantified using counting beads. Data shown is representative of mean ± SD of n = 3 - 6, with significance calculated using a Mann-Whitney Unpaired t test with $p < 0.0005$ = ***.

This data indicates that we were indeed able to separate the FDC from the other stromal cells in the lymphoid tissues. Therefore, we intended to use this opportunity to use fluorescence activated cell sorting techniques to isolate the populations for analysis by real-time quantitative PCR. The results of this analysis are shown in figure 4.15. This analysis demonstrated that both the gp38+CD35+ and gp38+CD35- populations express high level of the MFGE-8 gene, classically associated to FDC (fig. 4.15b). MFGE-8 is the antigen recognised by the FDC-M1 antibody used throughout this chapter to identify and analyse the FDC network.

FDCs are also known to express the B cell chemoattractants CXCL13, while CD21-/CD35- CRCs cells that inhabit the dark zone of the GC express CXCL12. As shown in figure 4.15c & d, the expression of CXCL13 was found to be higher in the CD35+ population as compared to the CD35- population. Conversely, CXCL12 expression was higher on the gp38+CD35- population, supporting the distribution of these 2 chemokines in FDC and CRCs (Allen and Cyster, 2008, Rodda et al., 2015). We could not detect a significant defect in the ability to produce these chemokines in $CD248^{-/-}$.

The T cell-attracting chemokines CCL19 and CCL21 were also investigated, and these results are shown in figure 4.15e & f. In accordance with previous reports the expression of both CCL19 and CCL21 was largely confined to the gp38+ populations. Interestingly, $CD248^{-/-}$ lymph nodes showed a slightly reduced expression of these chemokines, although this does not seem to be significant.

Other important FDC functional markers associated with activating B cell function were also analysed. APRIL and BAFF are both members of the TNF superfamily of signalling components and are known to be secreted by stromal cells and to act on B cells by inducing proliferation (APRIL) and activating the B cells (BAFF) (Hahne et al., 1998, Schneider et al., 1999). As observed in figures 4.15g & h, both of these factors are upregulated in the CD35+ populations. Interestingly, there appears to be an upregulation in the expression of APRIL in the $CD248^{-/-}$ gp38+CD35- population, which appears to be mirrored by a reduction in APRIL expression by the gp38+CD35+ population.

The detection of some T cell chemokines in our CD35 enriched population suggested the possibility that the sorting strategy used in our setting has to be refined and gating has to be set in more stringent manner. Given the difficulties posed in setting precise gates in the presence of a rather small population alternative techniques could be used, including sorting followed by positive beads selection.

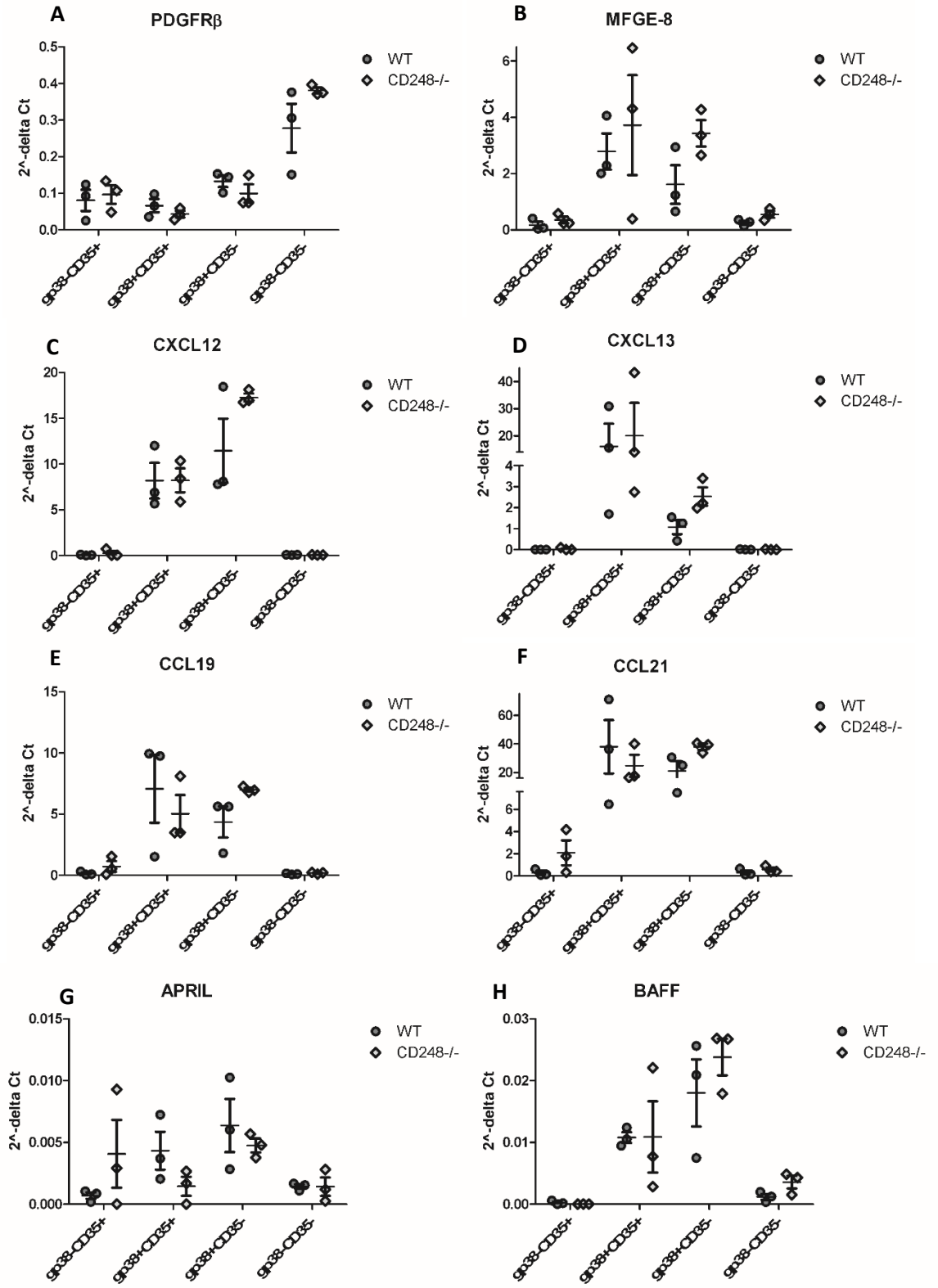

Figure 4.15 Genotyping of the CD45-CD31- stromal cell populations. Sorted stromal cell populations from WT and CD248-/- immunised lymph nodes were analysed by quantitative RT-PCR for their expression of **(A)** PDGFRβ **(B)** MFGE-8 **(C)** CXCL12 **(D)** CXCL13 **(E)** CCL19 **(F)** CCL21 **(G)** APRIL and **(H)** BAFF. These transcripts were normalised to either βactin expression (A, B, G & H) or PDGFRβ expression (C, D, E, F) and presented as $2^{\Delta Ct}$, with mean ± SD represented on the graph.

4.4 Discussion

4.4.1 Main findings

- CD248 is expressed on a subset of FDCs that dramatically expand in response to immune challenge.
- Lack of CD248 results in the formation of abnormal FDC networks.
- These CD248-expressing FDCs derive from a pool of pericytes in the lymphoid tissue.
- A novel method for separating FDCs from the other stromal cell compartments of lymphoid tissues has been established and allows for phenotyping of the subsets.

4.4.2 CD248 expression has been identified on follicular dendritic cells and indicates a differential developmental origin

In the spleen of immunised animals, this work has shown that CD248 can be detected on a stromal cell population within the B cell regions of the splenic white pulp. We demonstrated that these CD248+ stromal cells are follicular dendritic cells by counterstaining with an FDC-M1 antibody clone. The FDC-M1 clone is known to recognise Mfge-8, a factor essential for mediating the clearance of apoptotic B cells from the germinal centre, which is expressed by FDCs and binds to apoptotic B cells in order to facilitate their uptake by tingible body macrophages (Tumanov et al., 2004, Kranich et al., 2008). The $CD248^{+}$ cells have also been shown to be positive for other FDC markers such as CD21/35. The expansion of a CD248+ population in the spleen and lymph node following immunisation is a phenomenon that has previously been described by our group (Lax et al., 2007). However, the identity of the cells that upregulate this molecule was not established This work would indicate that this expansion is due to the expression of CD248 on FDCs, a subset of stromal cells known to respond to inflammation.

The FDCs in CD248$^{-/-}$ animals show a histological defect, preventing the FDCs from forming the classical reticular networks associated with these cells in WT conditions. Analysis of the formation of these networks during primary and secondary immune responses showed that both the size and interconnectedness of the cells is reduced in the CD248$^{-/-}$ animals during the secondary response. This defect is not significant following primary immunisation.

This novel observation of CD248 expression on FDCs is supported by evidence from the literature demonstrating that FDCs are derived from perivascular precursors. These finding were due to expression of the Mfge-8 FDC functional marker observed on pericytic cells, as defined by their expression of PDGFRβ (Krautler et al., 2012). Pericytes are a subtype of ubiquitous perivascular precursors which are well established as expressing CD248 (MacFadyen et al., 2007, Teicher, 2007, Tomkowicz et al., 2010, MacFadyen et al., 2005, Simonavicius et al., 2012, Smith et al., 2011). Therefore, I investigated whether I could identify further evidence for pericytes marker expression on the follicular dendritic cell networks in the spleens. As presented here, expression of the pericyte markers NG2 and α-SMA can be observed in the follicular dendritic cell networks in the spleen, with a reduction in the expression of these proteins in the CD248$^{-/-}$ mice. However, when the expression of these markers was analysed at the RNA level by RT-qPCR, there is no significant reduction in the number of transcripts of these genes in the CD248$^{-/-}$ germinal centres.

There is also evidence that splenic FDCs derive from a mesenchymal precursor of the Nkx2-5+Islet1+ lineages, in common with other splenic stromal cells (Castagnaro et al., 2013). Pericytes are an interesting cell type, and appear to be the major source of multipotent mesenchymal stem cells in the adult (Crisan et al., 2008). This evidence would therefore link the mesenchymal origin proposed by Castagnaro *et al*. (2013) and the perivascular origin suggested by Krautler *et al*. (2012).

Although in the spleen, the FDCs appear to develop from pericytes and express CD248, recent publications have indicated that FDCs in draining peripheral lymph nodes may have a different origin.

Jarjour *et al.* (Jarjour et al., 2014) have recently shown that in response to immune challenge, MRCs differentiate to give rise to FDCs. When the MRC in the CD248$^{-/-}$ organs are investigated, as I have done here, there does not seem to be a defect in the MRCs, despite the evidence presented in the previous chapter that developing CD248$^{-/-}$ lymph nodes have a significant reduction in the number of LTo cells. This is not as surprising as might be expected, as the evidence presented in the previous chapter indicates that the reduction in the numbers of these cells is overcome as development progresses. Influx of leukocytes following birth, especially B cells, is likely to bring with it increased expression of LTα1β2 which will bind to LTβR expressed on the stromal cells and may stimulate further maturation and differentiation of the stroma (Luther et al., 2002, Lorenz et al., 2003). Marginal reticular cells are known to play a functional role in the trafficking of antigen into the secondary lymphoid organs. Their localisation to the basal side of the subcapsular sinus, the location where afferent lymph vessels connect to the node indicates that these cells are involved in filtering the incoming lymph fluid and delivering the antigens appropriately throughout the lymph node (Katakai et al., 2008). RANKL+ cells in the spleen are also located to the blood endothelium surrounding the specialised sinuses that separate the blood circulating the spleen from the lymphoid tissue (Carrasco and Batista, 2007, Phan et al., 2009). There is no indication that the CD248$^{-/-}$ MRCs are functionally defective in any way from the evidence presented here. This would link to the fact that, as described here, the FDCs in the CD248$^{-/-}$ lymph nodes appear to be completely normal. This would indicate that the FDCs known to derive from MRCs in response to immunisation are completely normal in the CD248$^{-/-}$ lymph nodes.

Although all of this information points to FDCs deriving from a mesenchymal lineage, the exact steps in the differentiation of these cells have not been established. Taken together with the data presented here, it would appear that the FDCs which develop in response to immune challenge are a heterogeneous population derived from a number of different sources. The networks formed in CD248$^{-/-}$ draining brachial lymph nodes following multiple immune challenges are normal in

appearance, lending more evidence to the heterogeneity of these populations. Also, current knowledge of FDCs is based on their expression of various functional markers, such as FDC-M1 (Mfge-8) and CD21/35 (CR1/CR2). As there are no known origin or lineage markers associated with this population, unlike the MRCs which express many LTo-specific markers (Katakai, 2012), it is entirely possible that these cells are able to derive from any stromal precursors available in response to the production of LT by the incoming B cells. The evidence presented here would indicate that there are indeed different subtypes of FDCs, and that CD248 is able to mark these different lineages, opening up the opportunity for using CD248 as a marker to investigate the differences between the different subtypes.

Taken together, these data support the hypothesis that a subset of FDCs in the spleen differentiate from pericyte precursors as previously asserted in the literature (Krautler et al., 2012). The data presented here also supports the mesenchymal origin of FDCs proposed by Castagnaro *et al.* (2013). Further experiments are required to establish the steps involved in FDC development, which would help to resolve how closely linked the different subtypes of these cells are.

4.4.3 Establishing a novel method for digestion and flow cytometry analysis of follicular dendritic cells

FDCs have previously proved to be difficult to separate from the other surrounding stroma, due to their non-circulatory nature, the low numbers present in lymphoid organs, as well as their high expression of adhesion molecules and their long, thin and spindly structure with large networked processes that are difficult to separate (El Shikh and Pitzalis, 2012). As a result of all of these features, whilst other stromal cell populations have been widely examined by flow cytometry (Fletcher et al., 2011, Katakai et al., 2004, Katakai et al., 2008), FDCs have remained difficult to study directly.

Collagenase P is understood to be a milder enzyme than the collagenase D routinely used in our laboratory for stromal cell digestion (Barone et al., 2015, Nayar et al., 2016) and we attempted to use it to digest the delicate FDCs from the lymphoid organs. This digestion method was compared to the collagenase d digestion and was found to give comparable results, with an apparent improvement in the retention of cell surface markers (chapter 2). We believe that we were successfully able to separate out the stromal populations based on their expression of CD35, indicating that these cells are indeed FDCs.

I observed no significant numeric defect in the FDC as defined by CD35 and gp38 expression in the $CD248^{-/-}$ brachial lymph nodes. This agrees with the data observed by histology and the quantification of such as indicated previously. However, when the mesenteric lymph node was investigated, a significant defect in the number of these CD35+ cells was observed in the $CD248^{-/-}$ mice. The difference in the development of these organs has been explored previously, as indicated by certain mouse knock out studies investigating the different subunits of the canonical and non-canonical NF-κB pathways. The classical interaction required for lymph node development between LTβR and LTα1β2 has been investigated. Mice unable to produce LTβR completely lack the development of all lymph nodes and abnormal splenic microarchitecture. The B cells in these spleens are not restricted to the follicles, but could in fact be found spread throughout the white pulp, with a concurrent decrease in the number of T lymphocytes (De Togni et al., 1994). The effect of the heterodimer LTα1β2 was also investigated separately using mice either deficient in LTα or LTβ. $LT\alpha^{-/-}$ mice are unable to develop any lymph nodes or Peyer's patches. Also, the spleens of these mice do not exhibit separation between the T and B lymphocytes in the white pulp, these spleens are also unable to develop FDCs and functional germinal centres (Matsumoto et al., 1997). However, mice deficient in $LT\beta^{-/-}$ were able to develop both cervical and mesenteric lymph nodes, although these mice are still unable to develop Peyer's patches, peripheral lymph nodes, splenic germinal centres, and follicular dendritic cells. Other NF-κB signalling subunits that display a differential defect in lymph node development include NFκb1 and NFκb2 knock

out mice which display a defect in the development of inguinal lymph nodes only (Franzoso et al., 1998, Lo et al., 2006). FDC development is also dependant on the action of the chemokine CXCL13. This is also known to be important for lymph node development, as CXCL13-deficient mice lack peripheral lymph nodes, but present mesenteric and cervical lymph nodes (Luther et al., 2003). The lack of the receptor of this chemokine CXCR5 also results in only mesenteric and cervical lymph nodes developing (Ohl et al., 2003). For complete lack of all lymph nodes, the mice must be deficient in all chemokines (CXCL13, CCL21 and CCL19) or both of the receptors (CXCR5 and CCR7) (Ohl et al., 2003). This data also supports the histological analysis presented here, where a significant defect in the structure of FDCs is observable in the splenic immune response, but not in the skin-draining brachial lymph node response.

Investigation of the numbers of these potential CD35+ FDCs in the spleen presented a number of difficulties. The spleen is a much larger organ than the lymph node, with a higher level of heterogeneity in the cell populations found within the organ, although the white pulp presents similar structural components and functions to the lymph nodes. As the previous histological analysis has revealed a significant defect in the structure of the FDCs in the CD248$^{-/-}$ spleens, but not in the draining lymph nodes under the same immunisation conditions, we attempted to study the differences between the splenic FDCs and lymph node FDCs directly, in order to investigate whether a phenotypic difference could be observed. We intended to use to digestion protocol outlined in this thesis to separate the lymph node and splenic FDCs and then analyse the expression of classical FDC markers in order to identify any potential differences. Digestion of the FDCs from the lymph node was successful as presented here; however, this protocol was not as successful when applied to the spleen. Stromal cells are known to be a small cell population, only making up 1-5% of the cells in lymphoid organs (Malhotra et al., 2012). In the spleen, due to the larger size of the organ, the number of lymphocytes present is known to be greatly increased compared to the lymph node. The spleen also includes large areas of red pulp, containing many erythrocytes which also contribute to greater

heterogeneity in the digested cell populations. In order to attempt to overcome this, the stromal cell populations from digested spleens were enriched using MACS beads in order to exclude the lymphocytes and erythrocytes. This was successful in that it excluded these cells from our analysis, although the CD35+ FDC populations observed by flow cytometry still appeared markedly reduced compared to the populations observed in the lymph nodes. This is likely due to other factors at work in the spleen, including increased numbers of endothelial cells from the different vascular organisation and an increase in the "stickiness" of the cells thanks to an increase in the expression of adhesion molecules and Fc receptors. Further work is required to enable better separation of the FDC population from the other stromal compartments, for example by blocking the Fc receptors to prevent binding to other cells and therefore allowing better separation of the populations.

In order to confirm that these CD35+ stromal cells under investigation were, in fact, FDCs, the presence of these cells was investigated in mice understood to lack FDCs. As outlined in the introduction, the full development of adult lymphoid stromal cells is dependent on the influx of lymphocytes following birth. Full development of FDCs is dependent on the presence of B cells, and their production of LTα1β2 (Mackay and Browning, 1998, Gonzalez et al., 1998, Fu et al., 1998). In B cells lacking the chemokine receptor CXCR5, the B cells cannot travel into the B cell follicles following the CXCL13 gradient, and induce FDCs to develop in extrafollicular regions (Voigt et al., 2000). We therefore took advantage of the μMT mouse where the B cells are unable to develop past the bone-marrow located pre-B cell stage (Kitamura et al., 1991)unable to in order to validate whether our isolated population of gp38+CD35+ cells was indeed representative of FDCs. Use of this mouse was the most effective way to confirm that these cells are the FDCs that we expect, and our candidate population was indeed absent in the μMT mice.

Apart from FDCs, the other stromal cell type known to support the B cell follicle are the B cell zone reticular cells first observed in 1991 (McNagny et al., 1991). These cells are able to be identified as

different from the other lymphoid reticular cells thanks to their expression of the antigen BP-3. These cells are also found even in the absence of lymphocytes (McNagny et al., 1991). It appears that we can identify this cell population in our digestion protocol as there is a significant gp38+BP3+ population. There may be a slight reduction in the BP3+gp38+ stromal cells in the B cell knockout mice, although this does not appear to be a significant reduction. This would indicate that these cells are indeed the B cell reticular cells, which are not dependant of the presence of B cells to develop. However, the gp38hiBP3hi cells observed in the WT lymph nodes do seem to be absent in the B cell knockout mice. The evidence seems to indicate that these are FDCs, as they also seem to be CD35+. This is supported thanks to a study which concluded that the FDCs were closely associated with the B cell reticular cells thanks to the identification of around 90% of FDC-associated genes in the SCID mice lacking B cells in the B cell reticular zone cells (Wilke et al., 2010).

Once it was established that these cells under investigation were FDCs and could be separated successfully from the lymphoid organs, we used fluorescence activated cell sorting to isolate the cells and study their expression profile using real-time quantitative PCR analysis. The four populations; gp38-CD35-, gp38-CD35+, gp38+CD35- and gp38+CD35+, were analysed for the expression of a number of FDC markers. The expression of MFGE-8, the antigen recognised by the FDC-M1 antibody clone (Kranich et al., 2008), is higher in the gp38+CD35+ population, indicating strongly that these populations include FDCs. However, there is also expression of this marker in the gp38+CD35- population. MFGE-8 is known to only be expressed by FDCs in the stromal cell compartment (Kranich et al., 2008), and so this would indicate that the populations we have been able to identify are not able to be completely separated using this protocol. The FDCs may bind to other cells via their Fc receptors and other adhesion markers and so are sorted into another population. The CD35 marker may also have been cleaved from the cells by the digestion enzymes. Interestingly, we could not detect a significant reduction in the expression of this gene in the $CD248^{-/-}$ LNs, indicating that the structural defect observed in these mice is unlikely to be caused by a lack of MFGE-8. This result is different from

the expression indicated in the histological analysis carried out previously. This could indicate that the functional ability of these cells to produce this molecule is not significantly affected, but the defect observed in the CD248$^{-/-}$ spleens may be a structural defect in the development of the cells which affect this marker, rather than the inability to produce this molecule. A lack of MFGE-8 is known to result in development of splenomegaly and an expansion in the numbers of germinal centres and autoantibody production due to an inability of the tingible body macrophages to clear the apoptotic B cells (Hanayama et al., 2004). The defect observed in the CD248$^{-/-}$ mice is not a significant as this MFGE-8$^{-/-}$ phenotype; therefore, it is unlikely that the CD248$^{-/-}$ mice would completely lack the ability to produce MFGE-8.

CXCL13 is also known as B cell attracting chemokine (BCA-1) and, as the name suggests, is known to play an important role in attracting B cells to developing follicles, functioning via the chemokine receptor CXCR5 expressed on the B cells (Legler et al., 1998, Forster et al., 1996). The majority of CXCL13 in this system appears to be produced by the gp38+CD35+ cell population, indicating that our population of gp38+ CD35+ is a FDC enriched population. The expression of this chemokine is also increased in the gp38-CD35+ population, indicating that this population is also enriched in cells able to control the influx and retain B cells, evidence indicates that this would be the B cell zone reticular cells previously mentioned.

Interestingly, the expression of CXCL12 appears to be higher in the gp38+CD35- population than in the gp38+CD35+ population. A recent study has identified a novel population of CXCL12+ stromal cells (deemed CRCs) within the dark zone of the germinal centre. The study has indicated that these cells are not FDCs, due to their lack of FDC markers and independence of lymphotoxin or TNF signalling in order to develop (Rodda et al., 2015). These cells may be the gp38-CD35+population observed here, as the authors of this study reported that these CRCs express gp38, but not any classical FDC markers (Rodda et al., 2015). The fact that these CRCs are found in the dark zone of the germinal centre is also

interesting when the expression of BAFF (fig 4.13g) is taken into account. BAFF (B cell activating factor) is a member of the TNF superfamily of ligands. It is known to stimulate B cell growth and proliferation (Schneider et al., 1999, Kreuzaler et al., 2012). The dark zone of the germinal centre is so named because it is the site of intense proliferation of the centroblasts (the B cells in the dark zone), resulting in a dark area when examined histologically because of the dense collection of nuclei (Bannard et al., 2013). Therefore, if these gp38+CD35- cells are indeed these CRCs previously reported, one would expect significant expression of BAFF, although the authors have not examined the expression of BAFF on the population themselves. This marker is expressed in this cell population at even higher levels than the putative gp38+CD35+ FDCs, indicating that this analysis has, indeed been able to separate the light zone-located FDCs from the dark zone-associated CRCs.

Interestingly, there appears to be an upregulation in the expression of APRIL in the $CD248^{-/-}$ gp38+CD35- population, which appears to be mirrored by a reduction in APRIL expression by the gp38+CD35+ population, compared to the WT populations. APRIL is also known as tumour necrosis factor ligand superfamily member 13 (TNFSF13), and is known to contribute to B cell activation. Mice deficient in APRIL have been shown to have an increased number of germinal centres, and APRIL itself appears to promote IgA class switching (Castigli et al., 2004). The increased APRIL expression in the $CD248^{-/-}$ may contribute to promoting the germinal centre reaction and IgA class-switching in an attempt to overcome the abnormal FDC development observed.

There is also expression of the T cell chemokines CCL19 and CCL21 on the gp38+CD35+ and the gp38+CD35- populations. These chemokines are well understood to be expressed on TRCs, which are the predominant stromal cell population in the lymph node and which support T lymphocyte trafficking and homing through the organ (Fletcher et al., 2015). The expression of these 2 chemokines in the gp38+CD35- compartment is therefore reassuring. However, the expression of the former in FDC is not common and suggests a contamination with TRC into our FDC gate. T follicular helper (T_{FH})

cells are known to traffic into the germinal centre by upregulation of CXCR5, allowing the cells to respond to CXCL13, rather than following a CCL19 or CCL21 gradient established by the stromal cells (Arnold et al., 2007). Further work may therefore be required to try to tease apart the true FDCs and CRCs from their TRC associates and to guarantee the stringency of the gating strategy. The addition of other markers to our antibody cocktail might also be useful.

There does not seem to be a significant defect in the expression of any of these markers in the $CD248^{-/-}$ lymph nodes. This could be due to the fact that the histological defect observed in FDCS does impact on their function. Further work to analyse the functional defect in these cells is carried out in the next chapter, where the B cell response in the $CD248^{-/-}$ is thoroughly analysed.

These results indicate that separation of FDCs from the lymphoid tissue is indeed possible. Once these cells can be separated successfully and reproducibly from these organs, large scale analysis can be carried out on the cells in order to fully characterise the cells and investigate their potential origin in different lymphoid organs.

Chapter 5. Dissecting the functional effects of CD248 deficiency *in vivo*.

5.1 Chapter aims

- To exploit the CD248 deficient mice in order to understand the function of CD248 in the establishment and maintenance of an adaptive immune response.

5.2 Introduction

The germinal centre response is a critical feature of the humoral immune system. This reaction was conclusively proven to be the site of somatic hypermutation and the selection of high affinity B cell receptors (BCR), allowing for the development of long-lived B cell memory (Jacob et al., 1991, Berek et al., 1991, MacLennan, 1994, Nossal, 1994, Liu and Arpin, 1997, Coico et al., 1983). Naïve B cells expressing IgM are able to exit their site of development, the bone marrow, and circulate in the blood where they can traffic to the secondary lymphoid organs and enter the germinal centre reaction (Nossal, 1994). B cells which inhabit the GC are classified as centroblast and centrocytes. Centroblasts are IgD- PNA+ cells which rapidly proliferate within the dark zone (Kuppers et al., 1993, McHeyzer-Williams et al., 1993). Centroblasts undergo a strong induction of the processes involved in immunoglobulin class-switch recombination (Toellner et al., 1998). Once this is completed these rapidly dividing cells enter the light zone of the GC, downregulating CCR7 and moving toward the CXCL13 gradient via CXCR5. In the light zone the centroblasts lose their proliferative activity, engage with the FDCs and upregulate Bcl6 to become GC B cells or centrocytes (Linterman et al., 2010, Zotos et al., 2010, Lee et al., 2011, Ozaki et al., 2004). The main functions of the germinal centre reaction are somatic hypermutation (SHM) and class switch recombination (CSR). The enzyme AID (Activation induced cytidine deaminase) plays a key role in the GC reaction. AID is transiently active on highly proliferating B cells and determines DNA remodelling, causing somatic mutations in the variable chain

of the immunoglobulins (IgV) and class switch recombination of the heavy chains (Liu and Arpin, 1997, Xu et al., 2012, Stavnezer et al., 2008). Somatically mutated BCRs undergo successive tests to check the affinity and avidity for the antigen binding. These cells are understood to circulate from the light zone and re-enter the dark zone where further mutations occur to further increase the antibody affinity and avidity (Hauser et al., 2007). The B cell maturation and germinal centre reaction is further examined in the introduction to this thesis (chapter 1).

FDCs are responsible for the correct presentation of antigen in the context of immune complexes (ICs) to naïve B cells (Ogata et al., 1996). Expression of CD21/35, otherwise known as complement receptors 1 and 2 (CR-1 and CR-2), by FDCs is required for this process and enable the binding of the immune complexes (ICs) on the cell surface. FDCs are also responsible for marking apoptotic B cells for destruction by the tingible body macrophages (Kranich et al., 2008, Aguzzi et al., 2014). FDCs also provide a number of factors required for full B cell activation and maturation to plasma cells and memory B cells. These factors include the adhesion molecules VCAM-1, ICAM-1 and MAdCAM-1, involved in retaining the B cells in contact with the FDCs, allowing for sufficient activation of the BCR via the IC (El Shikh and Pitzalis, 2012, Allen et al., 2004) It is well established that the presence of FDCs is essential for the maintenance of the germinal centre response (Kosco et al., 1992, Wang et al., 2011)

FDCs are unable to phagocytose and process antigen. Antigens displayed by FDCs are presented in the native form, and can be displayed across multimerised ICs mainly via CD21/35. Additional, low affinity Fc receptors FcγRIIB (CD32) and FCεRII (CD23) and factors such as iC3b, C3d and C3dg from complement 3 are also involved in this process (El Shikh and Pitzalis, 2012). Presentation of these large structures allow for cross-linking of the B cell receptors (BCRs) resulting in more efficient B cell activation and initiation of the germinal centre response (Sukumar et al., 2008).

Naïve circulating B cells that have not undergone class switching naturally express IgM, as the segment giving rise to this isotype is the first section encountered when the heavy chain is transcribed. Once

AID has been activated to induced class-switch recombination, the isotypes that are produced are dependent on the activity of different cytokines. For example, the classical T-helper cell (Th2) induced class switching is dependent on production of IL-4 and other Th2 cytokines, such as IL-13, results in a switch of the BCR to the IgG1subtype (Toellner et al., 1998, Cunningham et al., 2002, Cunningham et al., 2004).

In the previous chapter, I have demonstrated that absence of CD248 induces profound morphological changes in the spleen FDCs and therefore the GC. In order to investigate potential functional effects of those we dissected the B cell response elicited in the CD248$^{-/-}$ mice.

5.3 Results

5.3.1 Investigating the B cell response in CD248$^{-/-}$ mice

As discussed previously, CD248$^{-/-}$ mice develop abnormal FDC networks in response to immune challenge (chapter 4). Given the critical role of FDC in the process of induction and maintenance of the germinal centre response, I investigated the effects that CD248 deletion might play in the generation of an antigen specific B cell response. I concentrated this part of analysis to the spleen, the organ that showed the most significant changes in terms of FDC morphology in our mutants.

Firstly, I evaluated whether the size of B cell follicles was affected in the CD248$^{-/-}$ spleen. These follicles were quantified by analysing the size of the B cell zones as a factor of the total area of the spleen to give a percentage of the total B cells within the whole spleen. Figure 5.1a illustrates a representative image with the CD19 positive B cell follicular areas encircled in red to indicate how the images were quantified. The total area was calculated as ratio between the B cell area and the total area of the spleens, two cutting levels were quantified per spleen, and three biological replicates were analysed per group (Figure 5.1b) shows the summary of the areas calculated as a ratio between of the spleens. As can be seen in figure 5.1b, there is a significant reduction in the size of the B cell areas and therefore the number of B cells in CD248$^{-/-}$ animals when compared to WT counterparts. The number of B cells was also quantified by flow cytometry on total spleens, cells were extracted by mechanical disruption from the whole spleen and then the flow cytometry analysis was carried out as described in chapter 2. This quantification revealed no significant difference in the total number of B cells in the spleens of CD248$^{-/-}$ animals compared to WT mice (fig. 5.1c). This could be due to the different markers used to analyse the B cells by immunofluorescence (CD19) and flow cytometry (B220).

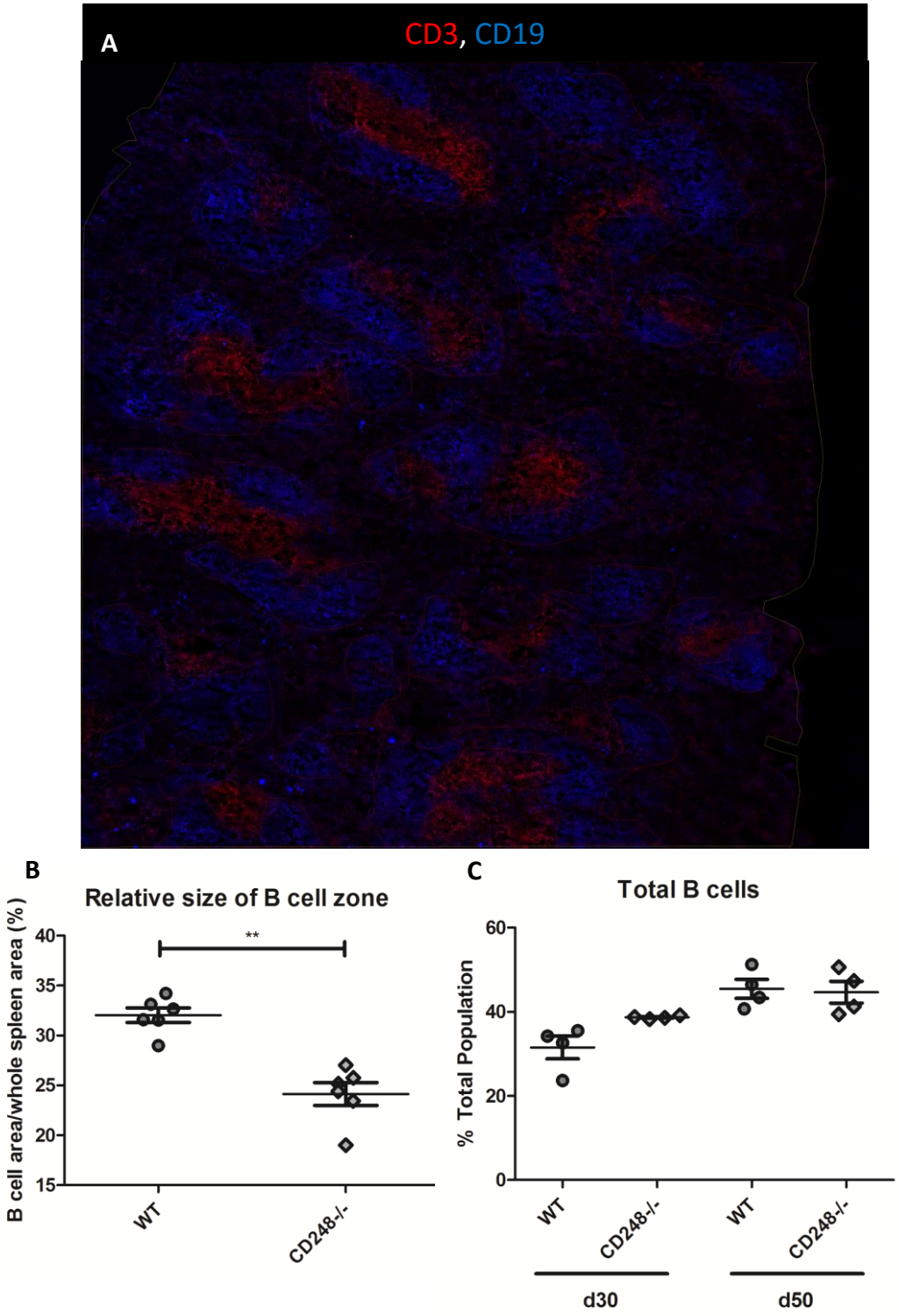

Figure 5.1 Quantification of the number of B cells in CD248$^{-/-}$ spleens compared to WT. A) Representative image of WT spleen used for quantification, stained with CD3 (red) and CD19 (blue). The B cell zones are shown circled in red. Image taken at x10 magnification. **B)** Quantification of the percentage of total splenic area covered by B cell positive staining in the WT and CD248$^{-/-}$ spleens. Images used for quantification were all at x10 magnification, with 2 cutting levels imaged per biological replicate, which was averaged to be represented on the graph, number of mice per group = 3 with mean ± SEM represented on the graph. **C)** Total numbers of B cells in immunised spleens analysed by flow cytometry, with n=4. Graph indicated mean ± SD. Significance was calculated using Mann-Witney unpaired t test, with ** indicating $p<0.005$.

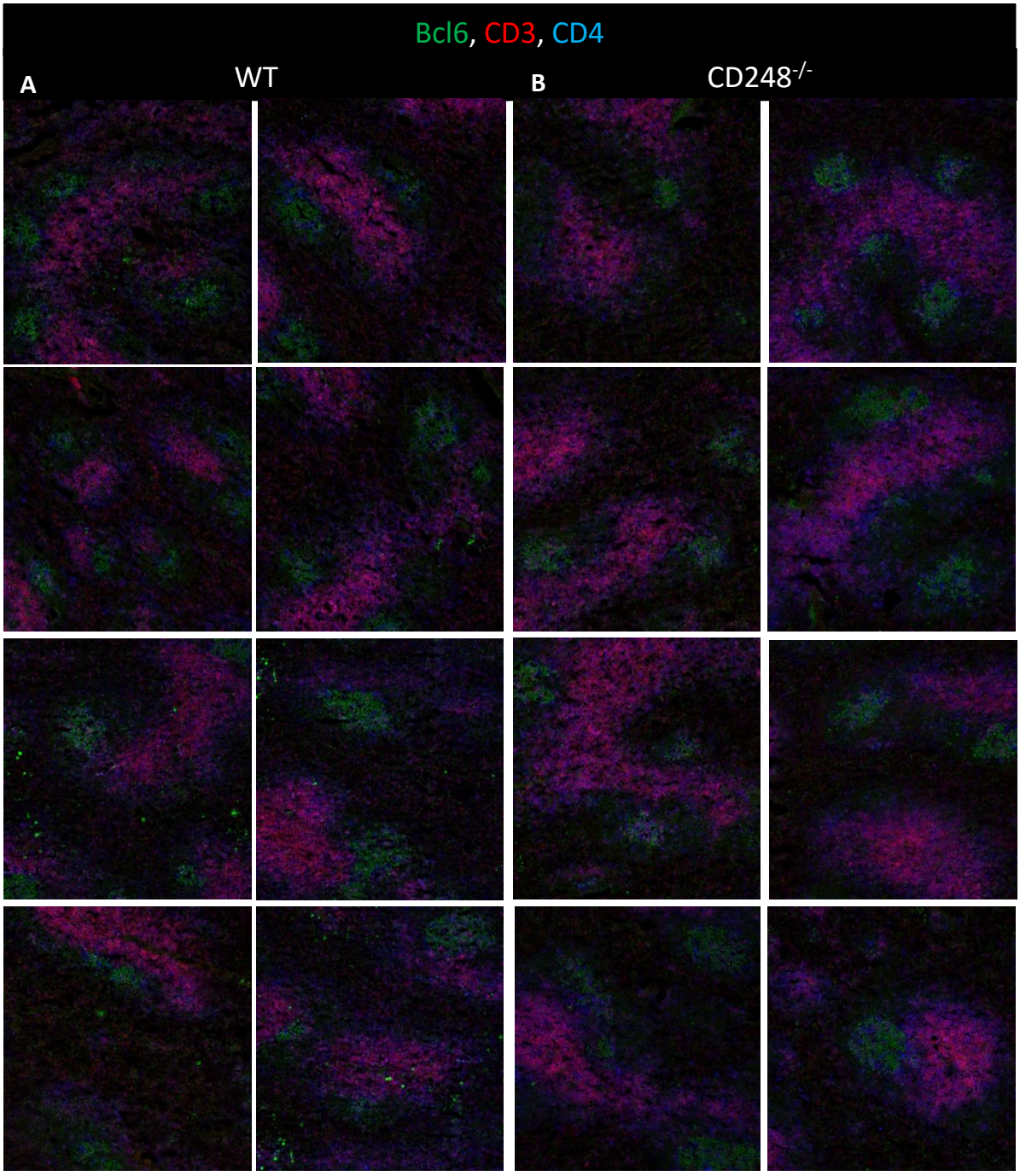

Figure 5.2 Analysis of the number and size of active germinal centres in the CD248$^{-/-}$ and WT spleens. Images of WT (**A**) and CD248$^{-/-}$ (**B**) spleens, stained with Bcl6 (green), CD3 (red) and CD4 (blue). All images taken at x10 magnification and from multiple cutting levels within the spleens.

A reduction in the number of germinal centre B cells was also observed when investigated by Bcl6 staining (figure 5.2). This defect was then also quantified by analysing the average size of the GC (fig. 5.3b) and the number of GCs as a factor of the total area of the spleen (fig. 5.3c). All images were quantified across three whole spleens per group, each at two cutting levels. This analysis demonstrated the presence of a reduction in the average size of germinal centres formed in the $CD248^{-/-}$ spleens in response to immune challenge when compared to WT spleens (fig. 5.3b). The number of germinal centres within the immunised spleens was also quantified and normalised to the size of the spleen, as shown in figure 5.3c. There was a reduction in the number of germinal centres that formed, although this was not a significant reduction when a Mann-Whitney unpaired t test was performed.

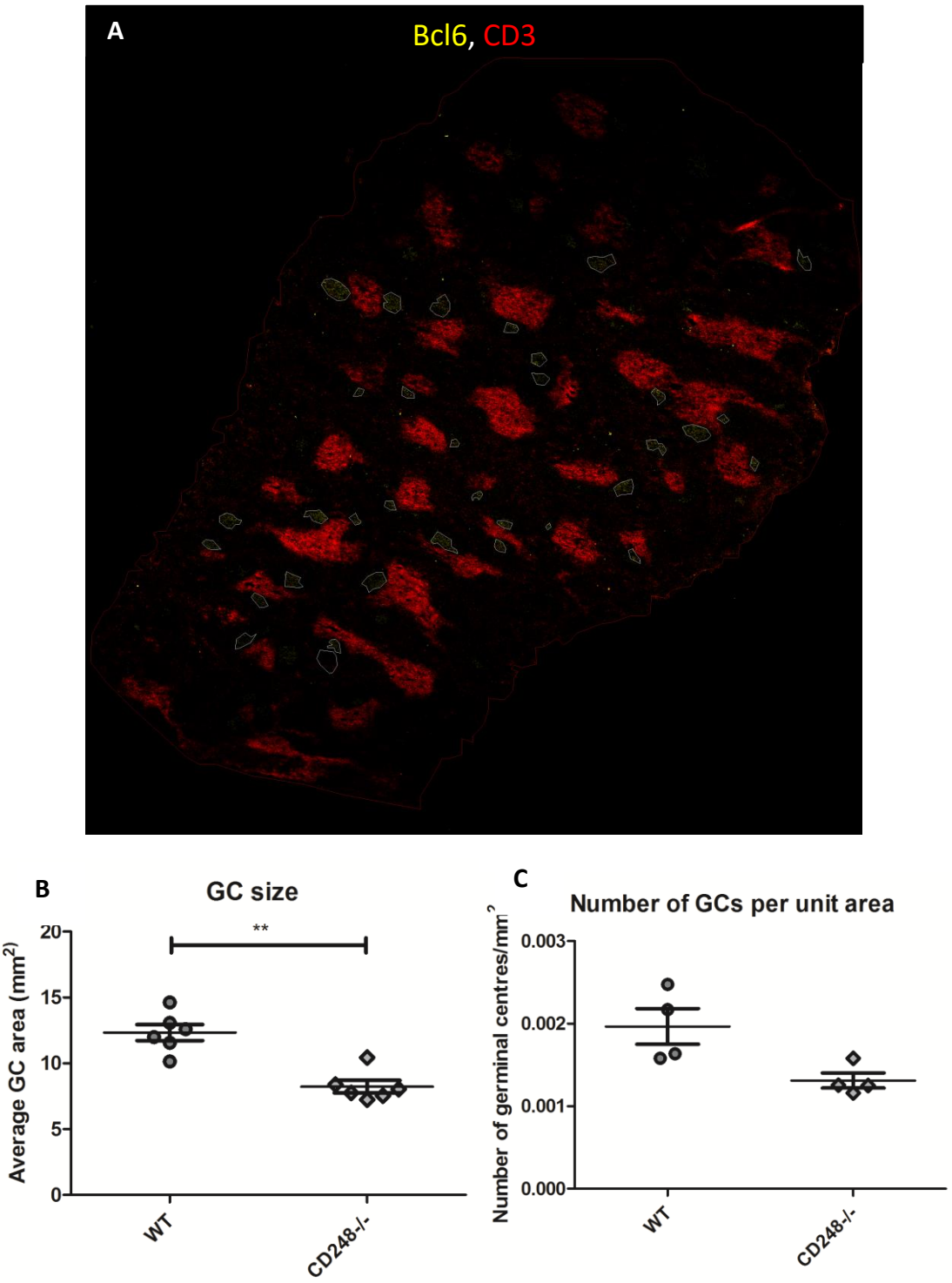

Figure 5.3 Analysis of the number and size of active germinal centres in the CD248$^{-/-}$ and WT spleens. A) Representative image of WT spleen used for quantification, stained with CD3 (red) and Bcl6 (yellow). The GC zones are shown circled in white. Image taken at x10 magnification. **B)** Quantification of the average area of the GC in WT and CD248$^{-/-}$ spleens. **C)** Quantification of the average number of germinal centres per unit of area in WT and CD248$^{-/-}$ spleens. Images used for quantification were all at x10 magnification, with with 2 cutting levels imaged per biological replicate, which was averaged to be represented on the graph, n = 4 - 6 with mean ± SEM represented on the graph. Significance calculated using Mann-Witney unpaired t test.

This defect in B cell number and distributions in CD248$^{-/-}$ mice was further investigated by flow cytometry upon digestion of the whole spleens from WT and CD248$^{-/-}$ mice. The populations of lymphocytes were expanded by NP-CGG immunisation as described in chapter 2. The mice were immunised i.p. with NP-CGG in alum on day 0 and then the spleens were analysed at day 8 for the primary immunisations. The rechallenged mice were immunised subsequently on day 21 and analysed for the secondary immune response. Other mice were immunised on day 0, day 21 and day 42 and were then analysed at day 50 for the tertiary immune response. Germinal centre B cells were identified as being lymphocytes, which were then separated from T cells by selecting B220+CD3- cells. These cells were then gated based on their expression of GL7 and Fas. These two markers have been shown to mark the GC B cells alone, with follicular B cells known to be B220+GL7-Fas-, whereas GC B cells are B220+GL7+Fas+ (Zaheen et al., 2009). From previous data, it appears that the total B cell numbers are unaffected (fig. 5.1c), although the GC appears to be affected (chapter 4), therefore we exploited these markers in order to analyse the GC B cells specifically. The gating strategy is outlined in figure 5.4a. Germinal centre B cells were defined as being GL7+Fas+. The proportion of GL7+Fas+ germinal centre B cells was then calculated as various time points following immunisation. As shown in figure 5.4b, 8 days after initial immunisation, no significant difference could be observed in the proportion of B cells that were germinal centre positive between the WT and the CD248$^{-/-}$ spleens. However, when an immunisation schedule including re-challenges was followed, the number of germinal centre B cells in the CD248$^{-/-}$ was significantly reduced compared to WT. This reduction was observed after two immunisations, and was more significant following three immunisations (fig. 5.4b). The GL7+Fas+ germinal centre B cells were then also analysed for their specificity for the antigen NP using an NP-specific antibody (fig. 5.4c). The number of GC B cells was also quantified following three immunisations, with the results shown in figure 5.4d. As can be seen, the percentage of NP-specific germinal centre B cells in the CD248$^{-/-}$ spleens appears to have increased when compared to the WT.

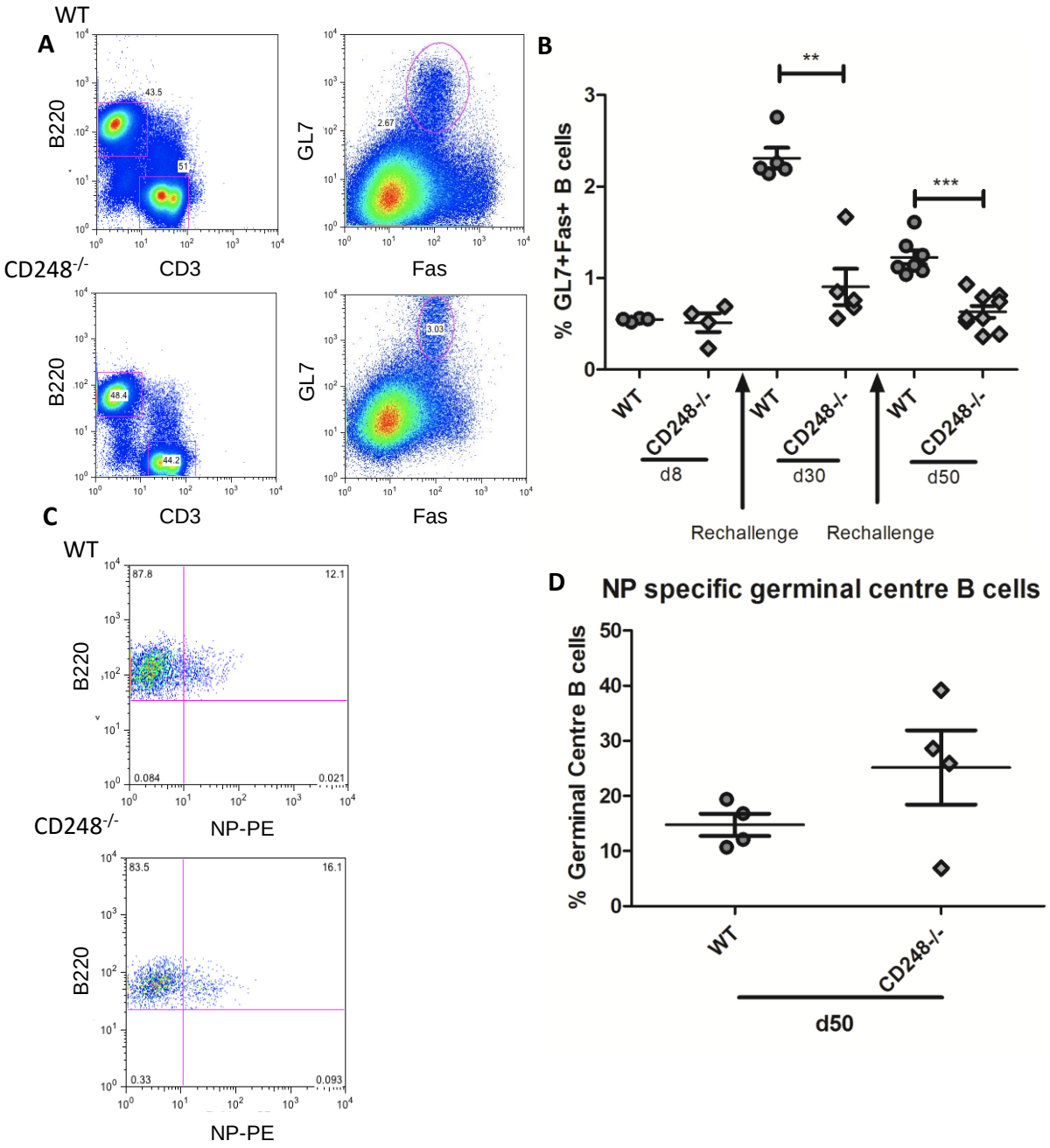

Figure 5.4 Understanding the effect of defective FDCs on splenic germinal centre B cell formation. Whole spleens were disrupted and germinal centre B cells were quantified using the gating strategy outlined in **(A)**. Germinal centre B cells are described as $B220^{+}CD3^{-}$ and $GL7^{+}Fas^{+}$. Quantification of the number of germinal centre B cells expressed as a % of the total number of B cells in different lymphoid organs is shown in **(B)**. Numbers of B cells were quantified over a time course, with immunisations carried out at d0, d21 and d41. **C)** The GC B cells were analysed for their expression of NP as antigen-specific GC B cells. These cells were quantified and these results are shown in **(D).** Graphs represent the mean ± SD of the data with n = 4 – 8 from two independent experiments. Significance was calculated using a Mann-Witney unpaired t test, with a Bonferroni correction for multiple comparisons. $p > 0.005$ is represented as **.

In order to investigate whether the same defect in the GC reaction was present in the lymph node we performed paw pad immunisation in CD248$^{-/-}$ according to the protocol described in Chapter 2 at the time points previously described, where NP-CGG was injected subcutaneously into the paw pad of the mice. As shown in figure 5.5a, the gating strategy employed in this instance was identical to that employed for investigating the spleens. The number of germinal centre B cells in the draining lymph node following immunisation was quantified, and the results are displayed in figure 5.5b. Differently from the spleen, no significant differences in the percentage of GL7+Fas+ B cells was observed, across the whole time course, in the lymph nodes of CD248$^{-/-}$ regardless of the number of immunisations administered.

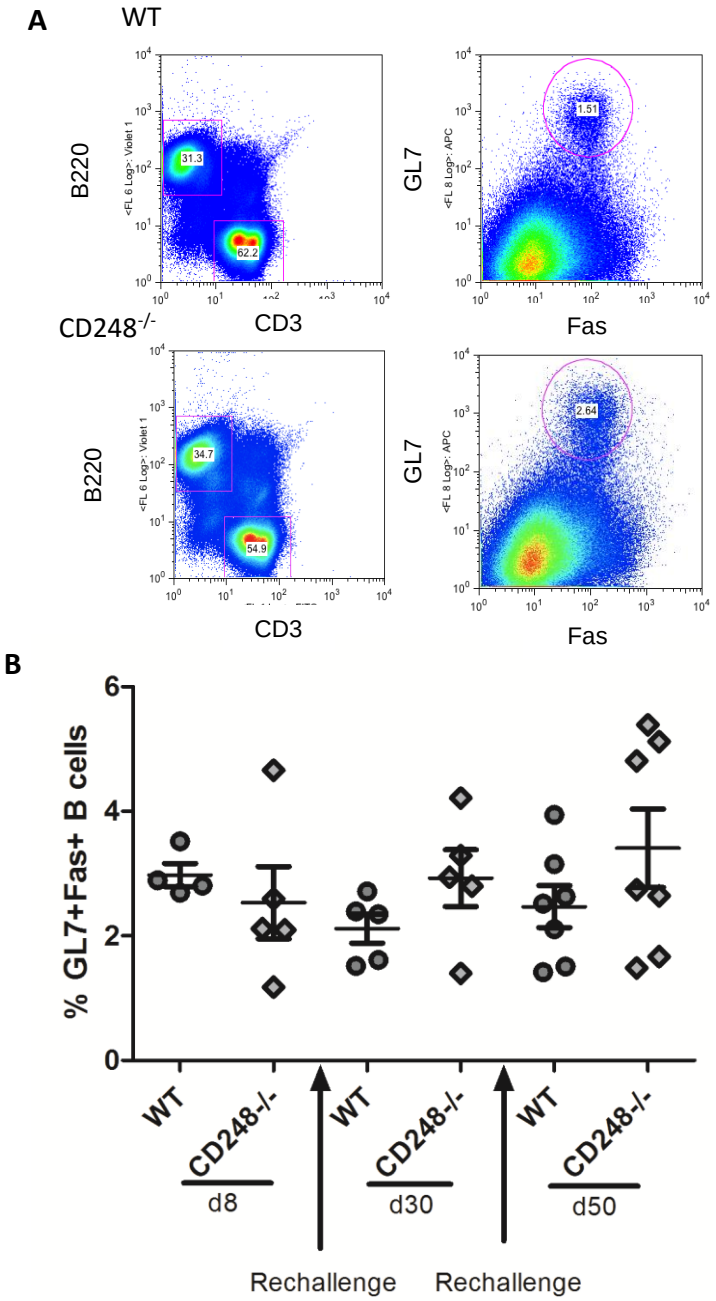

Figure 5.5 Understanding the effect of defective FDCs on lymph node germinal centre B cell formation. Whole spleens were disrupted and germinal centre B cells were quantified using the gating strategy outlined in **(A)**. Germinal centre B cells are described as $B220^{+}CD3^{-}$ and $GL7^{+}Fas^{+}$. Quantification of the number of germinal centre B cells expressed as a % of the total number of B cells in different lymphoid organs is shown in **(B)**. Numbers of B cells were quantified over a time course, with immunisations carried out at d0, d21 and d41. Graphs represent the mean ± SD of the data with n = 4 – 8 from two independent experiments. Significance was calculated using a Mann-Witney unpaired t test, with a Bonferroni correction for multiple comparisons.

5.3.2 CD248-/- B cells maintain their ability to produce high affinity, class-switched antibodies

In order to investigate whether the B cell defect impacted on the antibody production, ELISA assays were carried out to analyse the amount of antigen specific antibody generated upon immunization. Blood was harvested weekly over the course of the spleen immunisation protocol, and the total amount of NP-specific IgG and IgM was quantified, with results shown in fig 5.6a and fig. 5.6b. The amount of high affinity, class switched antibody IgG was also quantified to provide further information about the effectiveness of the germinal centres formed in the CD248$^{-/-}$ mice, as shown in figure 5.6c. The amount of antigen specific, germinal centre independent, IgM is shown in figure 5.6a. The amount of NP-specific IgM produced varies at different time points during the immunisation protocol, with peaks observed following rechallenge. The amount of antibody produced is highly variable, and seems slightly reduced in the CD248$^{-/-}$ mice compared to their WT controls, although these difference are not significant.

The amount of class-switched, germinal centre dependant IgG produced in response to immunisation was then quantified to analyse whether the reduction in germinal centre B cells observed lead to a defect in the ability of these cells to respond to immune challenge (fig.5.6b). As can be seen in figure 5.6b, at d30, following second immunisation, there is a significant reduction in the amount of antigen-specific antibody produced by the CD248$^{-/-}$ compared to the WT. However, at further time points following immunisation, including at d50, following a third immunisation, there does not appear to be any differences between the production of IgG in the CD248$^{-/-}$ or WT mice. As can be seen in figure 5.6c, at d30, following two immunisations, there is a significant reduction in the amount of high affinity IgG produced by the CD248$^{-/-}$ mice, but this difference is lost after another challenge, at d50.

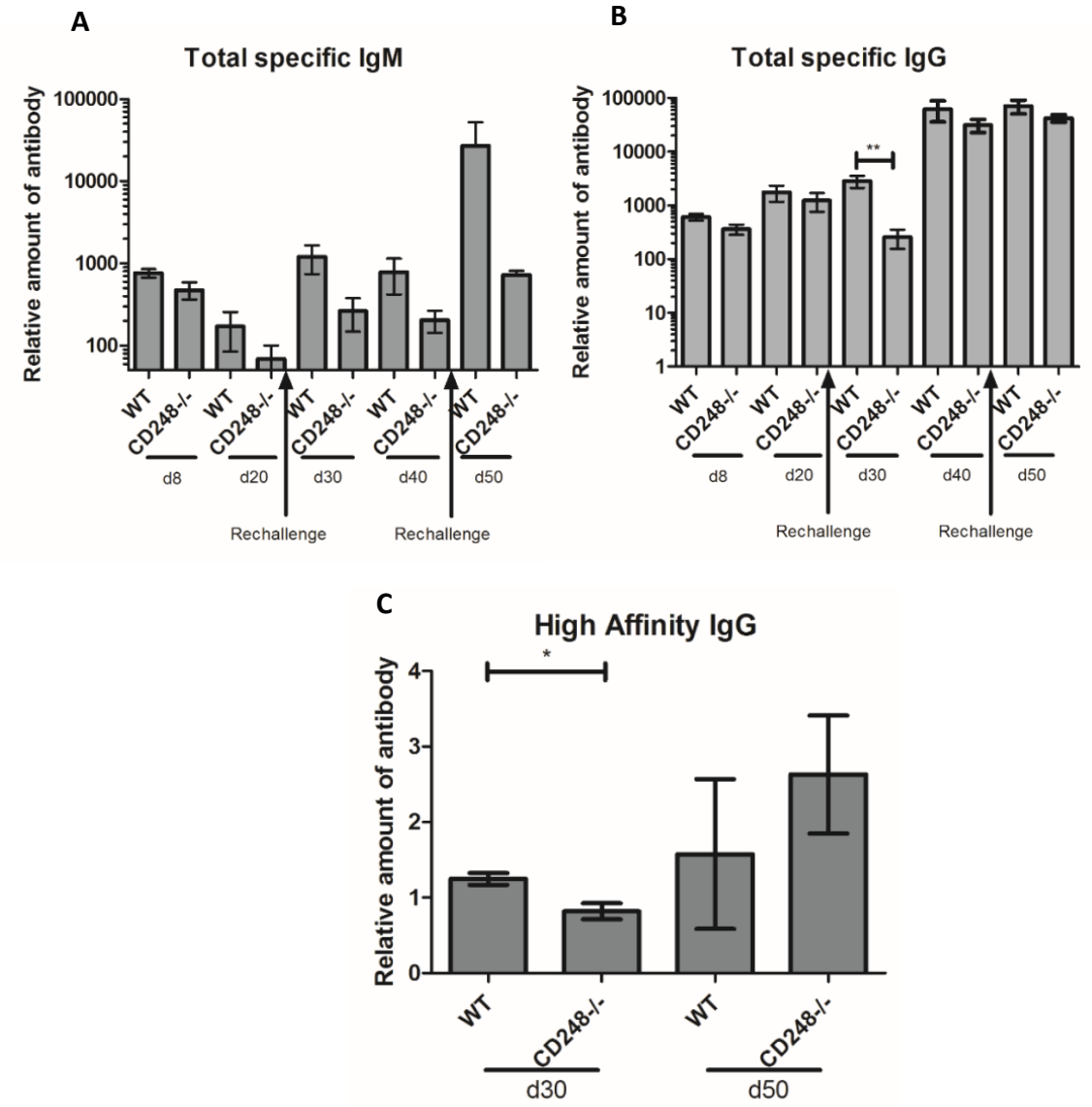

Figure 5.6 Analysis of the antigen-specific antibody response generated in response to ip immunisation in WT and CD248$^{-/-}$ spleens. Sera was collected from mice at weekly intervals and analysed using ELISAs to investigate the antigen-specific antibodies produced. **A)** The total amount of NP-specific IgM present in the serum across the whole time course. **B)** The total amount of NP-specific IgG present in the serum across the whole time course C) The amount of high affinity NP-specific IgG present in the serum at specific points during the immune response. Graphs represent the mean ± SD of the data with n = 6 – 8 from two independent experiments. Significance was calculated using a Mann-Witney unpaired t test, with a Bonferroni correction for multiple comparisons. p>0.05 represented as * and p > 0.005 represented as **.

This ELISA analysis was also carried out for the antibodies produced in response to paw pad immunisation. As shown in figure 5.7a, the amount of NP-specific IgM produced by B cells primed in $CD248^{-/-}$ lymph nodes is not significantly reduced when compared to the antibody produced by WT. The amount of class switched IgG antibody produced was also not significantly reduced in the $CD248^{-/-}$ lymph nodes when compared to their WT counterparts (fig. 5.7b). As well as being no significant difference in the total amount of IgG produced, the amount of high affinity IgG was also not significantly different from $CD248^{-/-}$ lymph nodes when compared to WT lymph nodes (fig.5.7c).

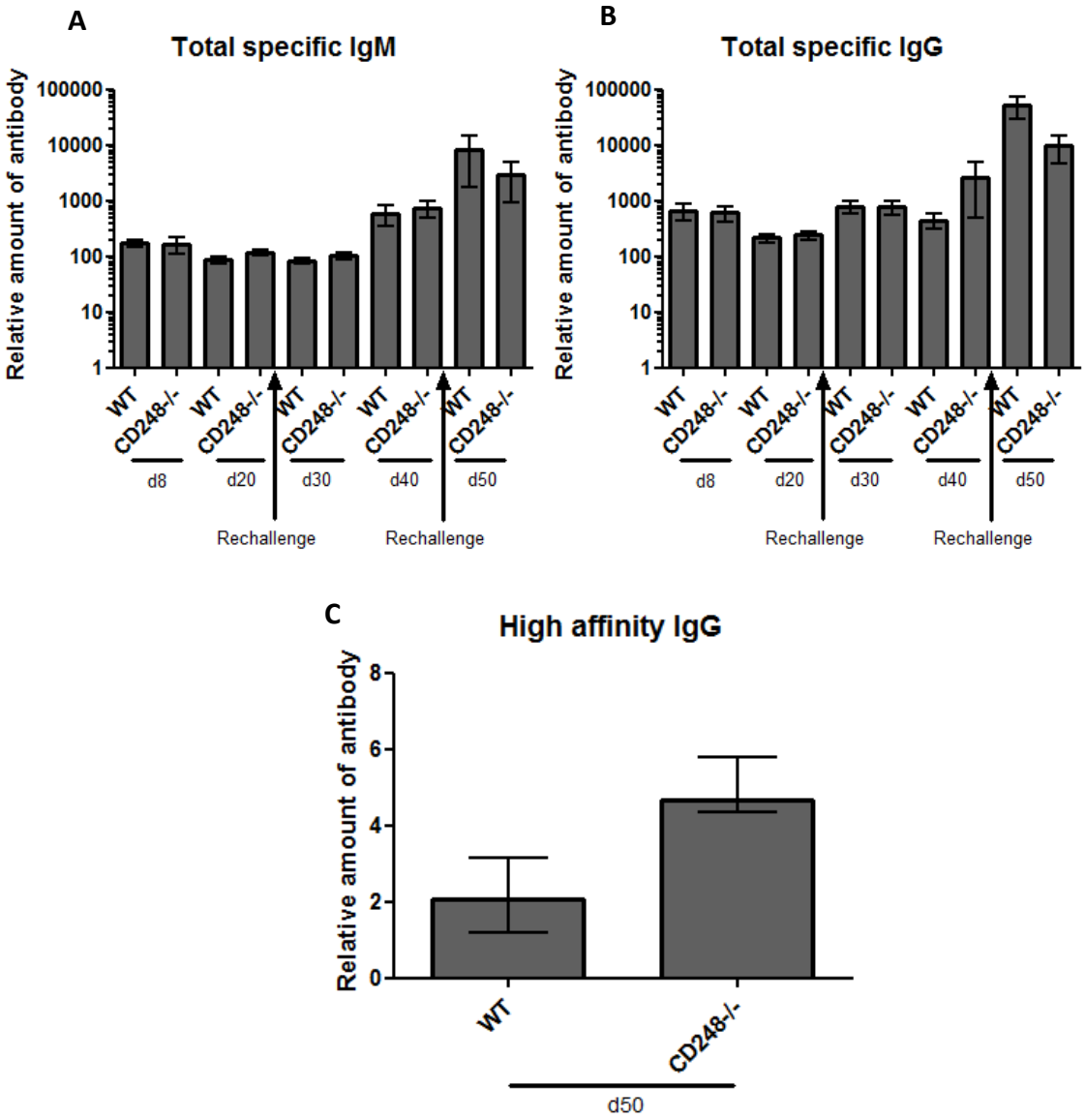

Figure 5.7 Analysis of the antigen-specific antibody response generated in response to paw pad immunisation in WT and CD248$^{-/-}$ lymph nodes. Sera was collected from mice at weekly intervals and analysed using ELISAs to investigate the antigen-specific antibodies produced. **A)** The total amount of NP-specific IgM present in the serum across the whole time course. **B)** The total amount of NP-specific IgG present in the serum across the whole time course C) The amount of high affinity NP-specific IgG present in the serum at specific points during the immune response. Graphs represent the mean ± SD of the data with n = 6 – 8 from two independent experiments. Significance was calculated using a Mann Witney unpaired t test with a Bonferroni correction for multiple comparisons.

5.3.3 Blocking PDGFRβ signalling appears to recapitulate the effects seen in the CD248$^{-/-}$ mice in vivo.

As established in previous chapters, CD248 functions via PDGFRβsignalling and PDGFR inhibition largely mimics CD248 defects. As shown in chapter 3, inhibition of PDGFRβ signalling by imatinib mesylate can mimic the reduction in the ability of MSCs to respond to stimulation observed in the absence of CD248. In order to investigate whether the defective formation of FDC network and aberrant B cell response observed in CD248$^{-/-}$ is partially attributable to defective PDGFRβ signalling the immunisation protocol was repeated in WT mice treated daily with imatinib mesylate. This treatment regime was carried out from one day before the final immune challenge (day 39) and continued for one week until the mice were sacrificed for investigation. This treatment regime was followed in order to analyse whether the lack of FDCs and abnormal GC formation is specific to the inflammatory challenge.

As shown in figure 5.8a, the FDC networks formed in the spleens of imatinib treated mice were disrupted, with their abnormal histology reminiscent of the abnormal distribution observed in the CD248$^{-/-}$ spleens. This results in punctate cells, lacking the processes which connect the networks and are responsible for displaying antigen to the B cells. The number of germinal centre B cells in both the spleens and lymph nodes in imatinib treated mice was also analysed. As can be seen in figure 5.8b, a reduction in the number of germinal centre B cells was observed when comparing imatinib treated mice with untreated controls. On the contrary, no significant difference between the number of germinal centre B cells in the treated mice compared to the untreated controls was observed in immunised lymph nodes.

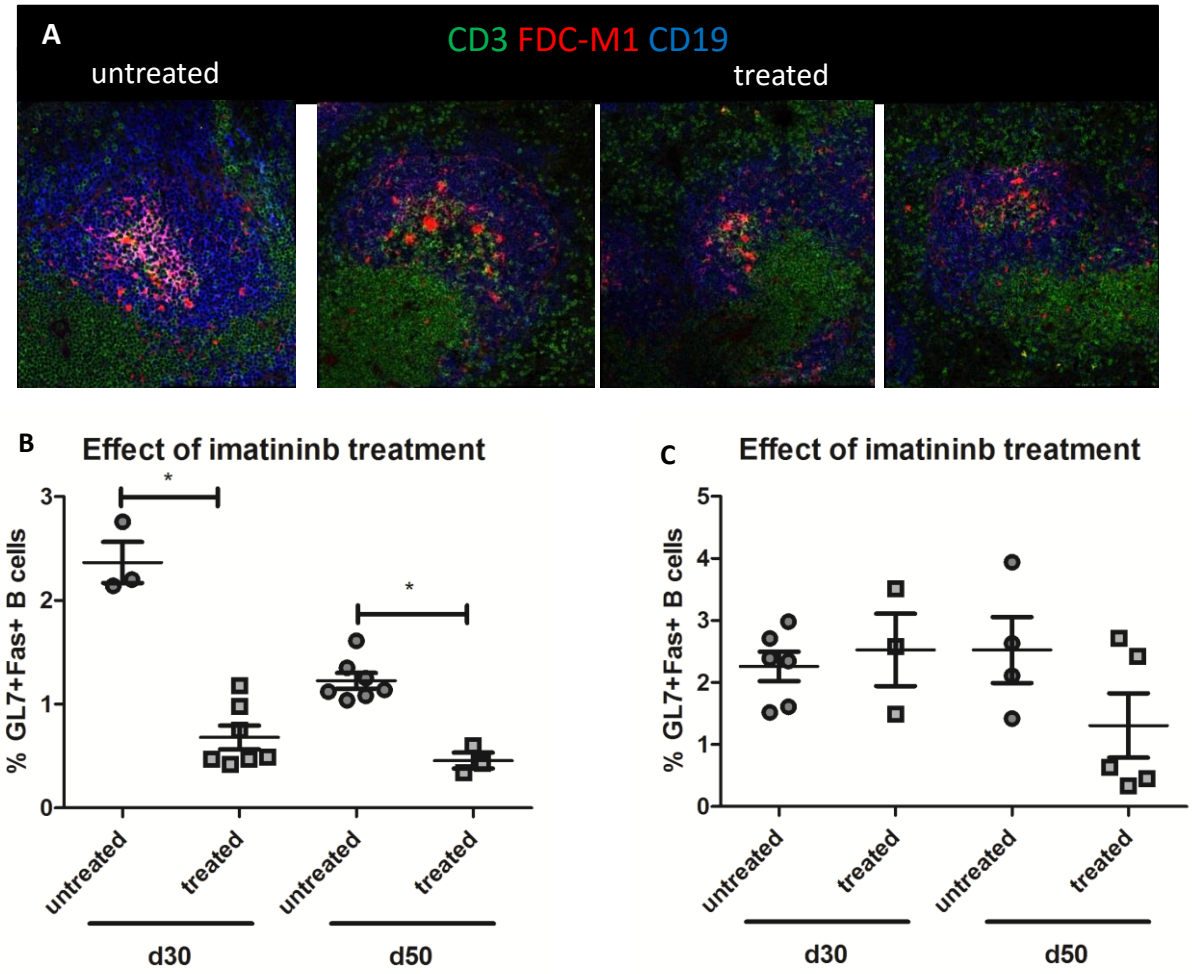

Figure 5.8 Investigating whether PDGFRβ plays a role in differentiation of FDCs. A) Tile scans of WT spleens immunised ip at d50 and treated with imatinib mesylate by gavage from d40 to d50. 6µm sections were stained with CD3 (green), FDC-M1 (red) and CD19 (blue). The spleens were disrupted and the germinal centre B cells were analysed by flow cytometry as previously. Germinal centre B cells are described as $B220^{+}CD3^{-}$ and $GL7^{+}Fas^{+}$. Quantification of the number of germinal centre B cells in immunised spleens expressed as a % of the total number of B cells in different lymphoid organs is shown in **(B)**. Quantification of the number of germinal centre B cells in immunised lymph nodes expressed as a % of the total number of B cells in different lymphoid organs is shown in **(C)**. Numbers of B cells were quantified over a time course, with immunisations carried out at d0, d21 and d41. Graphs represent the mean ± SD of the data with n = 3 – 8 from two independent experiments. Significance was calculated using a Mann-Witney unpaired t test, with a Bonferroni correction for multiple comparisons. $p > 0.05$ is represented as *.

5.3.4 CD248$^{-/-}$ germinal centres do not appear to be functionally defective in terms of their ability to produce chemokines and maintain segregation between T/B cell zones

As the segregation of T and B cell zones is known to be essential for the correct function of secondary lymphoid organs (Butcher and Picker, 1996), it is pertinent to investigate whether these abnormal follicles present in CD248 deficient animals present this organizational defect. T/B cell segregation is defined both in spleen and lymph nodes by specific chemokine distribution. Both those parameters were investigated in immunised WT and CD248$^{-/-}$ spleens and LNs.

Histological analysis of the distribution of the chemokines by immunofluorescence revealed that the distribution of these proteins is largely conserved in CD248$^{-/-}$ spleens as shown in figure 5.9. There appears to be a wider distribution of CXCL13 outside of the B cells follicles in the CD248$^{-/-}$ spleen (fig. 5.9b), although there is no evidence for this being related to increased or decreased B cell homing to the B cell zones (as previously demonstrated in figure 5.1). Accordingly, T/B cell segregation was conserved in CD248 mice.

In order to validate these data at the mRNA level, the number of transcripts of the chemokines CCL19, CCL21, CCXCL12 and CXCL13, along with lymphotoxin-alpha (LTα) and LTβR were analysed by quantitative RT-PCR. Splenic white pulp was identified by cresyl violet staining and microdissected, mRNA was then isolated only from relevant follicular areas, lymph node mRNA was isolated from whole tissue sections. Sample analysis is shown in figure 5.10 for the spleen and figure 5.11 for lymph nodes.

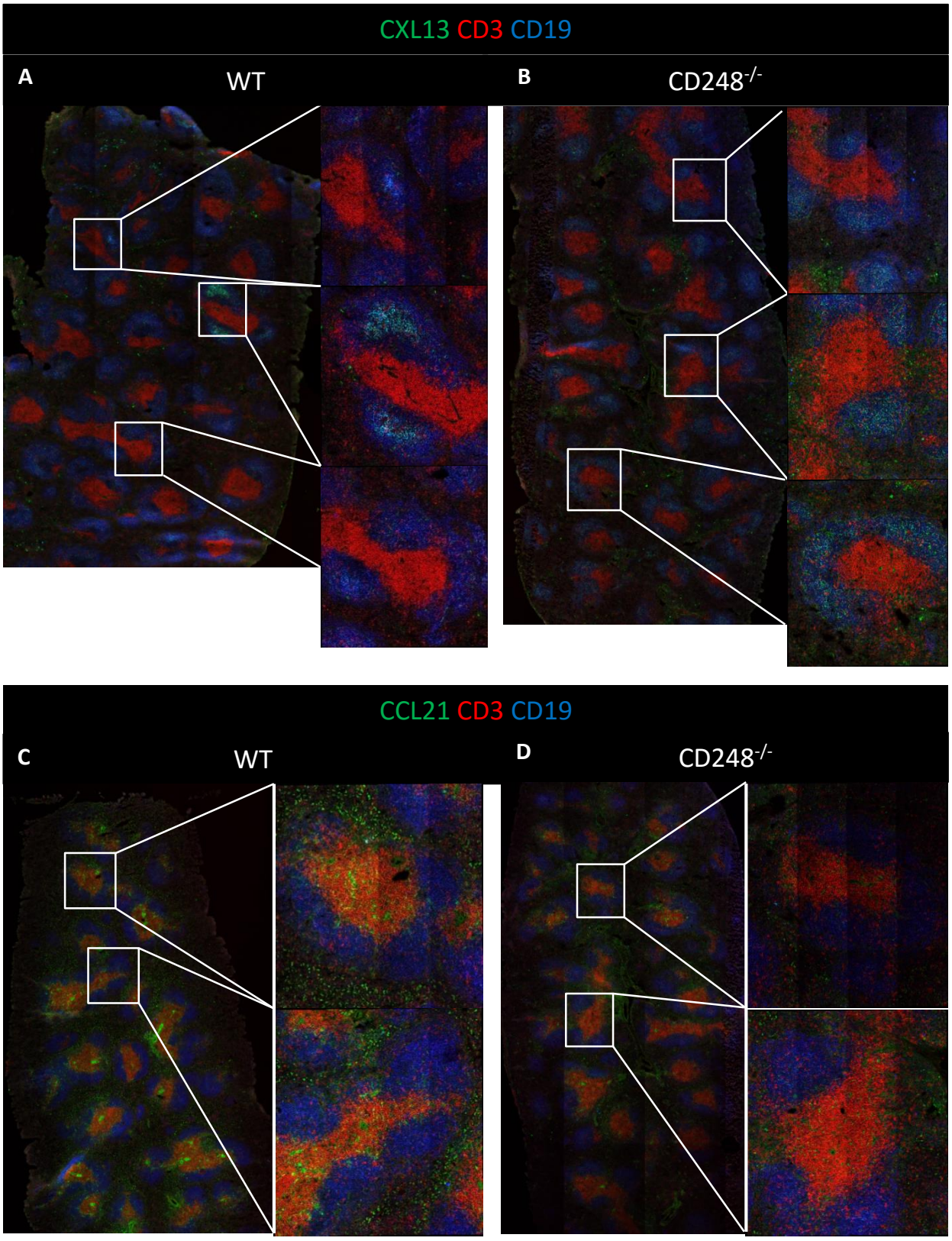

Figure 5.9 Analysis of the chemokine gradients in CD248$^{-/-}$ and WT spleens. Images of WT (**A**) and CD248$^{-/-}$ (**B**) spleens, stained with CXCL13 (green), CD3 (red) and CD19 (blue). **.** Images of WT (**C**) and CD248$^{-/-}$ (**D**) spleens, stained with CCL21 (green), CD3 (red) and CD19 (blue). Overview images taken at x10 magnification, with tile scan insets taken at x40.

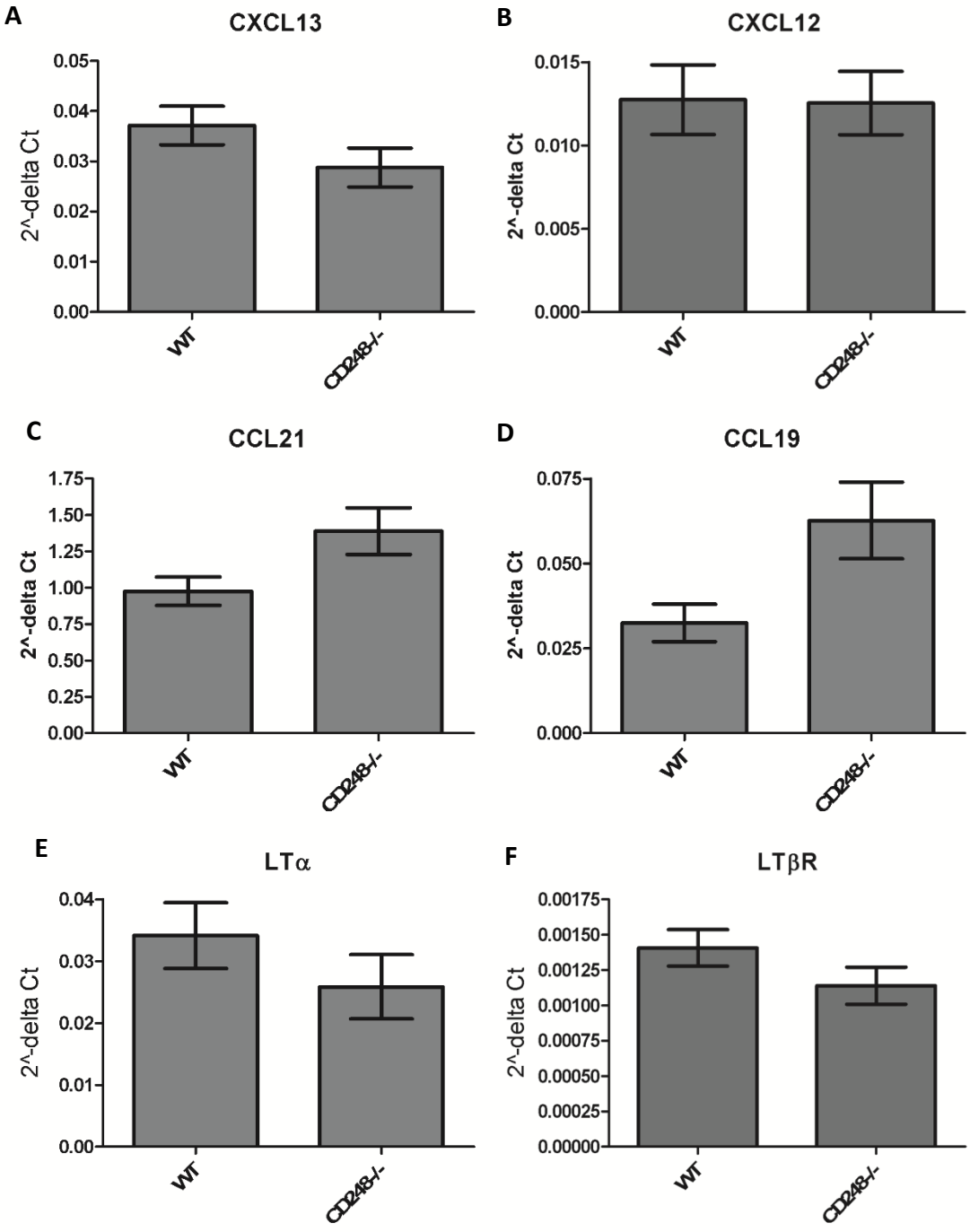

Figure 5.10 Analysis of the chemokine expression in CD248$^{-/-}$ and WT microdissected spleens. White pulp regions were microdissected out of immunised WT and CD248$^{-/-}$ spleens and analysed by quantitative RT-PCR. The mRNA extracted from the samples were analysed for a range of lymphoid stromal chemokines including **(A)** CXCL13, **(B)** CXCL12, **(C)** CCL21, **(D)** CCL19, **(E)** LTα and **(F)** LTβR. These transcripts were normalised to PDGFRβ expression and presented as $2^{\Delta Ct}$, with mean ± SD represented on the graph, n = 6. Significance was analysed by Mann-Witney Unpaired t test.

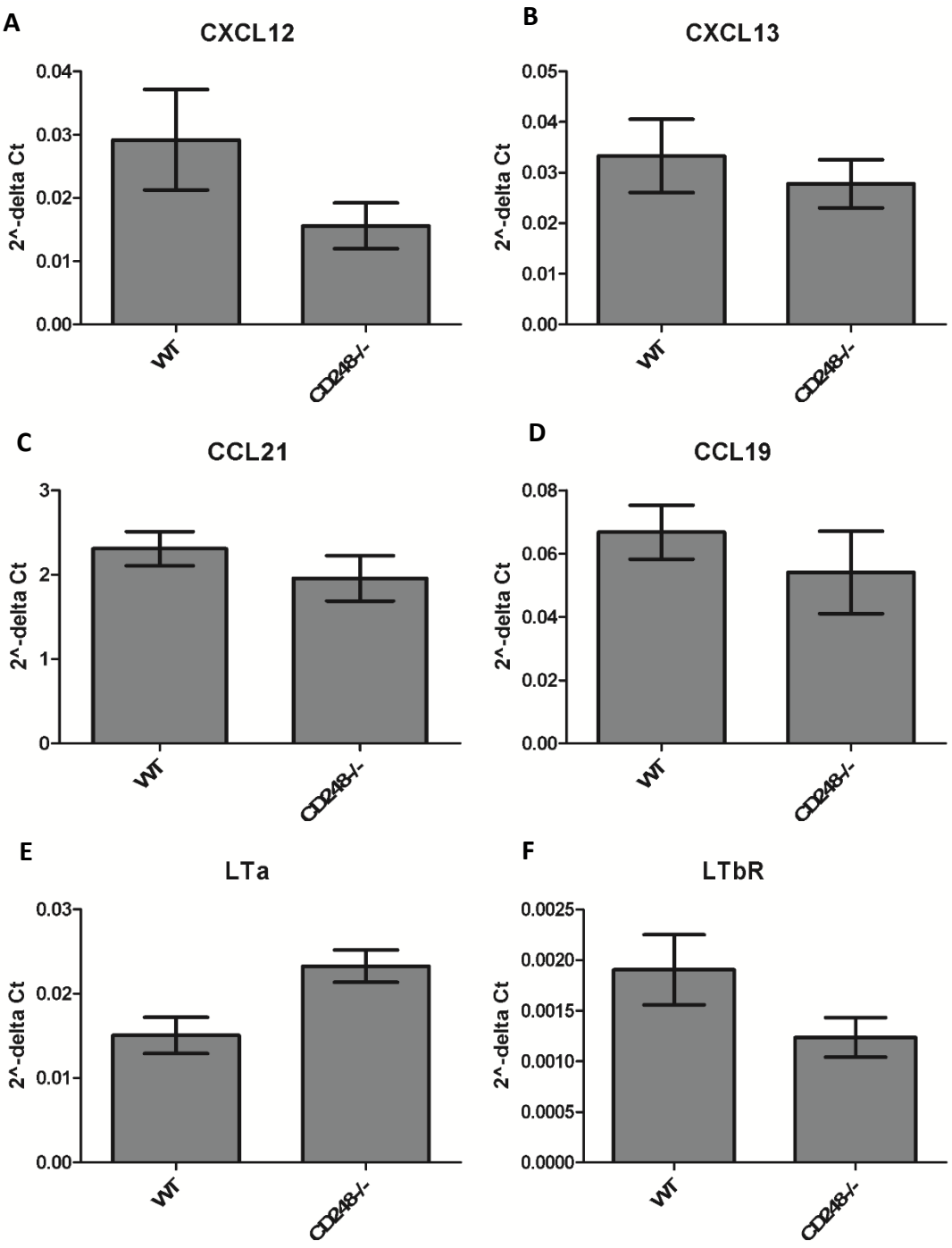

Figure 5.11 Analysis of the chemokine expression in CD248$^{-/-}$ and WT lymph nodes. **I**mmunised WT and CD248$^{-/-}$ sbrachial lymph nodes were analysed by quantitative RT-PCR. The mRNA extracted from the samples were analysed for a range of lymphoid stromal chemokines including **(A)** CXCL13, **(B)** CXCL12, **(C)** CCL21, **(D)** CCL19, **(E)** LTα and **(F)** LTβR. These transcripts were normalised to PDGFRβ expression and presented as $2^{\Delta Ct}$, with mean ± SD represented on the graph. Significance was analysed by Mann-Witney Unpaired t test.

As demonstrated in both figure 5.10 and 5.11, the transcript level of the classical B cell chemokines CXCL13 and CXCL12 is reduced in the CD248$^{-/-}$ lymphoid organs than in the WT organs (fig. 5.10a, 5.10b, 5.11a & 5.11b). However, this reduction is not significant when the data is analysed using a Mann-Witney Unpaired t test. There also appears to a concurrent increased in the expression of T cell chemokine such as CCL21 and CCL19 in the CD248$^{-/-}$ spleens, although again this result is not significant.

LTα and LTβR are responsible for the cross-talk between FDCs and B cells within the B cell follicles. From this analysis, there appears to be a reduction in the production of the LTβR on the stromal cells in the CD248$^{-/-}$ lymphoid organs (fig. 5.10f & 5.11f). The engagement of LTβR on the FDCs by LTα1β2 produced by B cells is essential for full maturation and development of the germinal centre and so this reduction may result in defective GC formation. However, there is some indication that the brachial lymph nodes may overcome this reduction in LTβR expression, increasing LTα production 5.11e. A similar effect might occur in our setting.

5.4 Discussion

5.4.1 Main findings

- In the primary immune response, there is no significant difference in the number of germinal centre B cells in the absence of the CD248-expressing FDCs, although the numbers of these cells are significantly reduced following repeated immune challenge.
- The reduction in germinal centre B cells following multiple immune challenges does not translate into a reduction in the amount of high affinity class-switched antibody produced by these mice.
- The lack of the CD248+ subpopulation of FDCs does not adversely affect the ability of the stromal cells in the CD248$^{-/-}$ spleens to maintain segregation between the lymphocyte zones, maintaining the function of these cell types.

5.4.2 Germinal centre B cell responses are maintained in CD248$^{-/-}$ spleens

Data presented previously in this thesis has indicated that in the absence of CD248, the stromal cell compartments which develop in response to inflammatory challenge, notably the follicular dendritic cells are abnormal, with the apparent loss of a subtype of the cells. As GC function is dependent on the presence of functional FDCs (Boulianne et al., 2013), I then examined the output of the GC in terms of B cell functionality.

The role of the CD248+ FDCs during response to immune challenge was studied by immunising wild type CD248+/+ and knock out CD248$^{-/-}$ mice with NP-CGG via intra-peritoneal and sub-cutaneous paw pad injection.

It is known that NP-CGG injection together with alum adjuvant immunisation is able to elicit a robust germinal centre response, with strong T-cell engagement (Barry and Ruddle, 1983, Toellner et al., 1996). Therefore, this model provides an appropriate tool to study the effect of the lack of the CD248+ FDCs on the ability of naïve B cells to undergo high affinity maturation within the germinal centre reaction and produce a mature B cell response. A number of readouts of the efficacy of the germinal centre response were measured in order to analyse this response.

By immunofluorescence, there is evidence that the size of the B cell zones as a proportion of the total spleen is significantly reduced in CD248$^{-/-}$ mice as compared to WT. However, when the number of B cells is analysed by flow cytometry, there is no significant difference in the numbers of the cells in the CD248$^{-/-}$ spleens compared to the WT. These data were generated using two different B cell markers; the FACS data looked at B220+ cells and the immunofluorescence studied CD19+ cells. These markers are differentially expressed by B cell populations, possibly accounting for the discrepancy in the data. For example, B220 is known to be expressed by subtypes of marginal zone B cells. This could indicate that the observed defect affects only some of the B cell subtypes, rather than the whole population. This is unsurprising, as we have previously observed no defect in the B cell development, or with the bone marrow in the CD248$^{-/-}$ mice (Naylor et al., 2012, Lax et al., 2010) indicating that any defect is unlikely to be intrinsic to the B cells.

Germinal centre B cells are characterised by their expression of the transcription factor Bcl6. This protein has been conclusively shown to be essential for the induction and maintenance of the GC (Basso and Dalla-Favera, 2012). Bcl6 maintains B cells in a GC phenotype, controlling the cell cycle and differentiation and limits DNA damage, allowing the cells to survive the stress of the high levels of mutation and BCR rearrangement (Klein et al., 2003, Shaffer et al., 2000, Ranuncolo et al., 2007, Reljic et al., 2000, Vasanwala et al., 2002, Phan et al., 2007). Intracellular staining for this molecule is complex and requires cell permeabilisation post digestion, whilst can be used successfully in IF. We

therefore used a different approach to investigate GC B cell distribution and numbers by flow cytometry and IF. Single cell suspension derived from spleen and lymph nodes were stained with a cocktail of antibodies that contained both GL7 (a marker of leukocyte activation) and Fas (a critical regulator of the germinal centre), whilst tissue sections were stained using Blc6 in combination with T cell markers; CD4 or CD3 and the B cell marker CD19. Flow cytometry analysis of GL7 and Fas as markers of germinal centre B cells is a well-established method, which has been used to characterise these cells for many years (Hao et al., 2008, Kitano et al., 2011).

Our analysis showed that, following primary immune challenge, the number of germinal centre B cells in the CD248$^{-/-}$ spleens is maintained, re-enforcing our previous morphological observation of intact FDC network formation upon primary challenge in CD248 $^{-/-}$ mice. During the secondary immune response, the number of germinal centre B cells as observed by flow cytometry is significantly reduced in the CD248$^{-/-}$, with a modest reduction in size and number of GC confirmed by IF. This further supports the flow cytometry analysis and shows that the CD248$^{-/-}$ spleens have a reduced ability to respond to immune challenges. On the contrary, the lymph node responses show no effect on the formation of germinal centres and the number of GC B cells in the LN of CD248$^{-/-}$ mice is normal.

The differences between the total number of B cells as calculated by immunofluorescence and flow cytometry may also be due to the fact that the two different methods take different features of the B cell zones into account. The quantification method used to analyse the size of the B cell zones is not commonly used as representative of the total numbers of B cells. This could be affected by a number of different factors, for example; the increase in number of germinal centres could increase the total size of the B cell zones without increasing the absolute numbers of B cells as GCs contain a number of other cells types. The presence of FDCs and T follicular helper cells within the germinal centre, as well as the reduced density of B cell within the light zone of the B cell follicle could all contribute to a difference in the area of the zones without affecting the absolute number of cells (Gatto and Brink,

2010). The significant reduction in the size of the B cell zone in CD248$^{-/-}$ shown in figure 5.1b could therefore give further evidence that the size and number of germinal centres are affected in the CD248$^{-/-}$ animals. The FACS analysis method used was only investigating single cell suspensions for their expression of the activation markers as discussed, and so does not take the histological differences in density and heterogeneity of the population into account.

5.4.3 CD248$^{-/-}$ B cells maintain their ability to produce high affinity, class-switched antibodies

As there is a difference in the appearance of the B cell zones, I also investigated whether the mature B cells resulting from the defective germinal centres, were able to functionally respond to immune challenge. This was analysed by investigating the production of high affinity antibodies by the B cells.

IgM is a natural antibody, and so B cells are able to produce this immunoglobulin independently on the GC (Stavnezer et al., 2008). Conversely, production of IgG is only possible as a result of the B cells undergoing CSR during the GC (Xu et al., 2012). Production of IgM following rechallenge is slightly decreased in the CD248$^{-/-}$ animals when compared to the wild type, although this is not significant. This may indicate that there is some defect in the ability of the B cells to produce antibodies, which may be due to abnormal CXCL12 and CXCL13 expression. This may contribute to defective B cell trafficking around the lymph node and therefore a defect in the engagement of the BCR on naïve B cells resulting in a reduction in the number of short-lived IgM producing plasmablasts which inhabit the splenic marginal zone and produce IgM early on during the immune response (William et al., 2005).

The total production of IgG by both groups of mice is significantly increased in the secondary immune response, as expected, due to the existence of memory B cells that can instantly give rise to antigen specific plasma cells. The production of NP-specific IgG in response to secondary immune challenge is

also modestly reduced in the CD248$^{-/-}$ compared to the wild type animals. Interestingly, these levels returned to normal following a further immunisation step. Similarly, a modest defect in the amount of high affinity IgG was compensated after the third round of immunisation. When investigating the production of the same antibodies in response to a subcutaneous paw pad injection, no differences were found between the antibody titres in the WT or the CD248$^{-/-}$ sera.

Taken together, this data indicates that the defective FDC networks observed in the CD248$^{-/-}$ may have a modest impairment in the ability to form effective germinal centres and to produce antibodies to fight infection. However, there is no difference in the early immune response, and it appears that the GC defect may be overcome during a chronic antigen specific response, for example, thanks to long-lived plasma cells continuing to produce antigen-specific class-switched antibodies (Gatto and Brink, 2010). This data seems to agree to some extent with a report previously published by our group (Lax et al., 2010). In this work, the responses were analysed in the CD248$^{-/-}$ draining lymph nodes during the primary immune response alone, and found no difference in the production of antibodies between the CD248$^{-/-}$ and WT animals. This concurs with the results presented here. However, the responses were not analysed in the spleen, which is where we see the main defect. This appears to link the absent FDCs with the subtype of splenic FDCs identified by Krautler *et al.* (2012), which derive from perivascular precursors believed to be pericytes. There is no evidence that lymph node FDCs derive from pericytes, in fact the source of these cells appears to be the marginal reticular cells (Jarjour et al., 2014).

The observation that the FDCs in the CD248$^{-/-}$ spleens are abnormal only following repeated immune challenge would indicate that the affected FDCs are of a specific subtype formed in response to inflammatory challenge. Evidence is building that FDCs can develop both during normal embryological development of lymphoid organs and also in response to immunological challenge (Fletcher et al., 2015). These subpopulations appear to derive from mesenchymal precursors, but from slightly

different precursors at different developmental stages. This would indicate that loss of CD248 is able to abrogate the development of, or completely delete, a population of FDCs which is specific to the secondary immune response in the spleen.

5.4.4 PDGFRβ signalling is important in the formation and function of FDCs

As previously established in this piece of work, CD248 is able to function via manipulating the pathway of PDFG receptor β. Although the data previously presented has indicated the importance of this pathway in the development of lymphoid like stromal cells *in vitro*, the importance of this pathway in the development of follicular dendritic cells *in vivo* warranted further investigation, most notably due to the demonstrated effects of the lack of CD248, and the link between the PDGFR-expressing pericytes and MSCs, and the fully developed FDCs which has previously been established (Krautler et al., 2012, Castagnaro et al., 2013).

We are able to assess the function of this pathway *in vivo* by administration of imatinib mesylate as previously used *in vitro*. The dosing strategy was based on an established protocol previously published (Schultheis et al., 2012). As the main morphological defect observed appeared to be following multiple immunisation challenges, the inhibitor was only administered from one day prior to the final immunisation until the experiment was completed. Indeed, both the flow analysis and the IF staining on the spleen confirm that imatninb tratemt in WT mice phenocopies the results seen in the $CD248^{-/-}$, with the treated spleens demonstrating a significant reduction in the number of GC B cells compared to the unmanipulated organs. However, the lymph nodes do not demonstrate this defect. This data would indicate that in the spleen there is a population of CD248+ FDCs that is reliant on PDGFRβ signalling in order to form in response to immune challenge. These signals are not important for FDC development in the lymph node.

5.4.5 CD248$^{-/-}$ germinal centres do not appear to be functionally defective in terms of their ability to produce chemokines and maintain segregation between T/B cell zones

FDCs produce CXCL13 in order to maintain the segregation of the B and T cell zones within lymphoid organs. CD248$^{-/-}$ animals appear to have no defect in producing this chemokine, although expression does not appear to be as restricted to the B cell follicles as in the wild type animals. CXCL13 is known to be important in regulating the movement of B cells into the GC, potentially indicating how the CD248$^{-/-}$ GCs have a reduced number of GC B cells (Bannard et al., 2013). The interactions between FDCs and B cells have been shown to be essential for the development of the germinal centre. This interaction is known to be dependent on LTβR and LTα1β2 engagement (Fu et al., 1998, Tumanov et al., 2004). In this context, a small reduction in the expression of LTβR was observed. Interestingly, this reduction in receptor expression appears to be compensated by over-expression of LTα, required for LT heterodimer assembly. This attempt to overcome the defect in LTβR only occurs in the lymph nodes and may potentially justify the normal phenotype observed in CD248$^{-/-}$ Lymph nodes.

This atypical chemokine localisation does not appear to be reflected in the expression of CCL21, the chemokine responsible for maintaining the T cell zone. By immunofluorescence there appears to be very little difference between the WT and the CD248$^{-/-}$ animals, although there is a suggestion that the expression of this chemokine is also less restricted to the typical T cells zones, just as the CXCL13 expression is disrupted. This may indicate that different subtypes of FDCs perform different functions, for example, some may produce more chemokines, whereas some may display more immune complexes. This hypothesis would require further testing and refinement of the FDC digestion protocol established in chapter 4 in order to allow analysis of the phenotypes of the different FDC subtypes.

Chapter 6. General discussion and future work

CD248 is a C-type lectin membrane receptor, thought to be related to the CD93 family of proteins (Christian et al., 2001). It is understood to be expressed in the rheumatoid arthritis synovium, in chronic kidney disease and in a variety of human tumours (MacFadyen et al., 2005, Nanda et al., 2006, Maia et al., 2010, Smith et al., 2011). CD248 is also expressed on mesenchymal stem cells and adult pericytes, among other, less well-defined cell types (MacFadyen et al., 2005, MacFadyen et al., 2007, Christian et al., 2008, Tomkowicz et al., 2010). CD248 expression on pericytes surrounding the tumour vasculature has been shown to play an interesting role in controlling the growth and invasiveness of tumours (Valdez et al., 2012). This expression has been shown to have no effect on pericyte functions in other conditions, such as wound healing (Nanda et al., 2006), indicating that there is a differential role of CD248 on this population in homeostatic condition and in different pathogenic settings. Another notable expression of CD248 is in lymphoid organ development and homeostasis. As shown within this laboratory, CD248 is strongly upregulated in the lymph node, spleen and thymus during embryological development (Lax et al., 2007). This expression becomes increasingly restricted as the organs develop, and after birth, CD248 can only be detected in specific regions of lymphoid tissue, notably on the capsule of the lymph nodes and in pathogenic condition. Notably this expression is limited to the stromal cells and in mice, CD248 is absent on leucocytes, although a population of CD248+ CD8+ cytotoxic T cells can be observed in humans (Hardie et al., 2011).

The evidence that CD248 is able to control the differentiation of mesenchymal stem cells to osteoblasts and adipocytes (Naylor et al., 2012), the expression of CD248 on embryonic lymph node stroma and the strong link between fat and development of the lymphoid tissue (Pond and Mattacks, 2002, Pond, 2003) raised the possibility that CD248 expression is involved in the development of lymphoid stromal cells. Moreover, data suggesting the upregulation of CD248 in the context of stroma

cell expansion in immunised lymphoid organs, suggests that CD248 is involved in the regulation of some stromal cell function in response to immune challenge.

The work presented in this thesis establishes that in the absence of CD248, the differentiation of MSC to lymphoid stromal precursors expressing high levels of VCAM-1 and ICAM-1 is impaired (Benezech et al., 2012). This translates *in vivo* into a reduction in the number of LTi and LTo cells in the developing mesenteric lymph nodes in the CD248-/- in the latest phases of LN assembly in embryonic life.

I have also shown that the upregulation of the CD248 observed in response to immunisation (Lax et al., 2007, Lax et al., 2010) is largely due to the upregulation of this marker on a subset of follicular dendritic cells which develop following immune challenge. This finding, in the context of preferential expression of CD248 on pericytes reinforces published observations that splenic FDCs derive from ubiquitous perivascular precursors (Krautler et al., 2012). As established here, CD248 is able to control the differentiation of mesenchymal stem cells in the embryonic life, linking the observations in the embryonic life with the adult lymphoid organs. There are indications in the literature available that pericytes are the source of adult mesenchymal stem cells able to respond to both adipogenic and osteogenic signals (Crisan et al., 2008). The osteogenic properties of these cells are also hypothesised to be responsible for the calcification of blood vessels and heart valves associated with severe pathogenicity (Collett and Canfield, 2005). Pericytes are understood to be a heterogenic population, especially displaying variable α-SMA expression which contributes to the ability of the cells to control the contractility of the microvasculature (Nehls and Drenckhahn, 1991, Boado and Pardridge, 1994). The heterogeneity of the potential precursor population would lend further support to the hypothesis proposed here that the FDCs are a heterogenic population, which varies in different lymphoid organs in terms of origin and dependency on homeostatic signals.

The hypothesis proposed by Fletcher *et al.* (2015), whereby lymph node fibroblastic cells derive from two different sources – (1) the LTo cells during initial embryological development and (2) mesenchymal precursors that migrate into the lymph node in response to inflammation, may therefore also apply to FDCs. The evidence presented in this thesis would therefore indicate that these two origins of these cells give rise to distinct populations of mature FDCs, which can be discriminated by their expression of CD248. The indication is that although these FDCs are developmentally distinct, the roles in the adult overlap to the extent that the lack of one subtype of FDC (CD248+) is not able to completely abrogate B cell responses. Although use of the CD248-/- mouse is only able to investigate the effects of gene deletion, the lack of CD248 appears to completely abrogate a population of FDCs, potentially maintaining the precursors in an immature state. The evidence suggests a lack of these cells due to a reduction in the number of dendrites. However, due to the 3D structure of the FDC networks, we were unable to show a reduction in these cells by describing a reduction in the number of nuclei. Investigation of the cell numbers by flow cytometry indicates that there is a reduction in these cell populations, although further work may be required to conclusively demonstrate that the abrogation of this population.

Lymph node development is dependent on the interaction between LTβR (LTβR-/- mice lack all lymph nodes) and LTα1β2 (LTα-/- mice are unable to develop lymph nodes or Peyer's patches, although LTβ-/- mice are able to develop both cervical and mesenteric lymph nodes) (Matsumoto et al., 1997, Koni et al., 1997). This is dependent on signalling via two NF-κB pathways (Mebius, 2003). The data presented in this thesis, however, unveils a selective role for CD248 and in turn for the PDGFRβ signalling cascade in the development and maturation of the stromal cell compartment. This suggests a potential cross-talk or relative modulation of these 3 signalling cascades. Unfortunately, this link was not conclusively investigated in this thesis. Further work is required to establish whether there is an interaction between the any of the subunits featured in the two signalling pathways. Investigation is being carried out into the extracellular binding of CD248, and it has been shown to possibly function

as an intermediate in the binding between clec-14A and MMRN2, and extracellular matrix components (Noy et al., 2016) & personal communication). However, establishing the intracellular binding has proved difficult thanks to the short cytoplasmic tail lacking classical binding domains (Valdez et al., 2012). Investigation of the binding of this domain to subunits of the PDGFRβ signalling pathway by immunoprecipitation may be able to indicate how and whether CD248 interact with this pathway. A similar approach could be also applied to the investigation on the potential interaction of CD248 and PDGFRB with the subunits of the NF-κB signalling pathway

Mice deficient in the CD248+ FDC subset appear to have abnormal germinal centre development, but a reduction in B cell number. However, there is no defect in the ability of the B cells to access the germinal centre to mature into antigen-specific IgG producing plasma cells. The CD248-/- germinal centres in the spleen appear to have a reduction in the number of transcripts of chemokines, although this data does not seem to be relevant in the lymph nodes when analysed by microdissection, or in the sorted FDC population. This latter data has to be carefully evaluated as the transcripts detected in the allegedly purified FDC population suggest cross contamination from other fibroblastic reticular cell populations.

Further work is also required in order to fully characterise the role of CD248 in the development of lymph node stromal cells. The manner in which CD248 is able to modulate signalling pathways must be resolved, potentially investigating the interactions between CD248 and the subunits of the PDGFRβ signalling pathway. This will also contribute to the understanding of the interactions between this signalling pathway and the NF-κB signalling pathways. It is known that interactions between LTβR and LTα1β2 are important in lymphoid tissue stromal development both in the embryo and in the adult in response to inflammation (Mebius, 2003, Benezech et al., 2012, Fletcher et al., 2015). Identification of the role of PDGFRβ signalling subunits in assisting this interaction would be an interesting and novel finding. Interestingly, administration of the PDGFRβ inhibitor, imatinib mesylate, is capable of

phenocopying the defective FDC development observed in the CD248-/- spleens. This is observed when the mice are treated for only a short time, for 1 week, only 1 day prior to booster immunisation. this would indicate that imatinib is able to elicit a strong response in a limited time, therefore, the role of imatinib in controlling inflammation needs to be further investigated. This is especially poignant as imatinib mesylate is used widely in humans to treat a number of cancers (Demetri et al., 2002, Wang and Li, 2015).

In the spleen, the source of pre-FDC MSCs is likely to be provided by pericyte precursors as observed by Krautler *et al.* (2012). In the absence of CD248, there is a reduction in pericytes (Naylor et al., 2014), and so there is a reduction in the pool of FDC precursors in the CD248-/- spleens, resulting in the reduced FDC development in response to repeated immunisations characterised in this thesis.

The FDC digestion established in this thesis is very promising, whilst presenting a number of questions and challenges. Further work is required in order to accurately separate the cells from the tissue and characterise them. Once these cells can be reliably separated from different lymphoid tissues, such as lymph node, the spleen, Peyer's patches and possibly from inducible tertiary lymphoid structures (TLSs), the FDCs from different origins can then be fully phenotypically analysed in order to assess whether there are observable differences in the FDCs present in different organs. Follicular dendritic cells are currently being investigated by a number of different groups as the knowledge of the cells is limited compared to a number of different lymphoid stromal cells. The protocols established here offer a novel method for investigating these cells, as well as evidence for different subpopulations of the cells which can be further investigated for different functions.

This project establishes CD248 as a novel molecule involved in the development and differentiation of lymphoid stromal cells both in embryonic and adult life. CD248 is shown to be able to mark a subset of FDCs which develop in response to inflammatory challenge. Further work is required to characterise the phenotypes of the different FDC subtypes proposed here, but this provides exciting evidence of

the presence of separate subtypes and the possibility of using this model to investigate the nature of these cells to a greater extent.

List of References

ACTON, S. E. & REIS E SOUSA, C. 2016. Dendritic cells in remodeling of lymph nodes during immune responses. *Immunol Rev,* 271**,** 221-9.

ADACHI, S., YOSHIDA, H., HONDA, K., MAKI, K., SAIJO, K., IKUTA, K., SAITO, T. & NISHIKAWA, S. I. 1998. Essential role of IL-7 receptor alpha in the formation of Peyer's patch anlage. *Int Immunol,* 10**,** 1-6.

ADACHI, S., YOSHIDA, H., KATAOKA, H. & NISHIKAWA, S. 1997. Three distinctive steps in Peyer's patch formation of murine embryo. *Int Immunol,* 9**,** 507-14.

AGUZZI, A., KRANICH, J. & KRAUTLER, N. J. 2014. Follicular dendritic cells: origin, phenotype, and function in health and disease. *Trends Immunol,* 35**,** 105-13.

AGUZZI, A. & KRAUTLER, N. J. 2010. Characterizing follicular dendritic cells: A progress report. *Eur J Immunol,* 40**,** 2134-8.

AKUNE, T., OHBA, S., KAMEKURA, S., YAMAGUCHI, M., CHUNG, U. I., KUBOTA, N., TERAUCHI, Y., HARADA, Y., AZUMA, Y., NAKAMURA, K., KADOWAKI, T. & KAWAGUCHI, H. 2004. PPARgamma insufficiency enhances osteogenesis through osteoblast formation from bone marrow progenitors. *J Clin Invest,* 113**,** 846-55.

ALCAMO, E., HACOHEN, N., SCHULTE, L. C., RENNERT, P. D., HYNES, R. O. & BALTIMORE, D. 2002. Requirement for the NF-kappaB family member RelA in the development of secondary lymphoid organs. *J Exp Med,* 195**,** 233-44.

ALI, A. A., WEINSTEIN, R. S., STEWART, S. A., PARFITT, A. M., MANOLAGAS, S. C. & JILKA, R. L. 2005. Rosiglitazone causes bone loss in mice by suppressing osteoblast differentiation and bone formation. *Endocrinology,* 146**,** 1226-35.

ALIAHMAD, P., DE LA TORRE, B. & KAYE, J. 2010. Shared dependence on the DNA-binding factor TOX for the development of lymphoid tissue-inducer cell and NK cell lineages. *Nat Immunol,* 11**,** 945-52.

ALIMZHANOV, M. B., KUPRASH, D. V., KOSCO-VILBOIS, M. H., LUZ, A., TURETSKAYA, R. L., TARAKHOVSKY, A., RAJEWSKY, K., NEDOSPASOV, S. A. & PFEFFER, K. 1997. Abnormal development of secondary lymphoid tissues in lymphotoxin beta-deficient mice. *Proc Natl Acad Sci U S A,* 94**,** 9302-7.

ALLEN, C. D., ANSEL, K. M., LOW, C., LESLEY, R., TAMAMURA, H., FUJII, N. & CYSTER, J. G. 2004. Germinal center dark and light zone organization is mediated by CXCR4 and CXCR5. *Nat Immunol,* 5**,** 943-52.

ALLEN, C. D. & CYSTER, J. G. 2008. Follicular dendritic cell networks of primary follicles and germinal centers: phenotype and function. *Semin Immunol,* 20**,** 14-25.

ALOISI, F. & PUJOL-BORRELL, R. 2006. Lymphoid neogenesis in chronic inflammatory diseases. *Nat Rev Immunol,* 6**,** 205-17.

ANGELIN-DUCLOS, C., CATTORETTI, G., LIN, K. I. & CALAME, K. 2000. Commitment of B lymphocytes to a plasma cell fate is associated with Blimp-1 expression in vivo. *J Immunol,* 165**,** 5462-71.

ANSEL, K. M., NGO, V. N., HYMAN, P. L., LUTHER, S. A., FORSTER, R., SEDGWICK, J. D., BROWNING, J. L., LIPP, M. & CYSTER, J. G. 2000. A chemokine-driven positive feedback loop organizes lymphoid follicles. *Nature,* 406**,** 309-14.

ARMULIK, A., GENOVE, G. & BETSHOLTZ, C. 2011. Pericytes: developmental, physiological, and pathological perspectives, problems, and promises. *Dev Cell,* 21**,** 193-215.

ARNOLD, C. N., CAMPBELL, D. J., LIPP, M. & BUTCHER, E. C. 2007. The germinal center response is impaired in the absence of T cell-expressed CXCR5. *Eur J Immunol,* 37**,** 100-9.

ARNON, T. I., HORTON, R. M., GRIGOROVA, I. L. & CYSTER, J. G. 2013. Visualization of splenic marginal zone B-cell shuttling and follicular B-cell egress. *Nature,* 493**,** 684-8.

ASAYESH, A., SHARPE, J., WATSON, R. P., HECKSHER-SORENSEN, J., HASTIE, N. D., HILL, R. E. & AHLGREN, U. 2006. Spleen versus pancreas: strict control of organ interrelationship revealed by analyses of Bapx1-/- mice. *Genes Dev,* 20**,** 2208-13.

BAGLEY, R. G., WEBER, W., ROULEAU, C., YAO, M., HONMA, N., KATAOKA, S., ISHIDA, I., ROBERTS, B. L. & TEICHER, B. A. 2009. Human mesenchymal stem cells from bone marrow express tumor endothelial and stromal markers. *Int J Oncol,* 34**,** 619-27.

BAILEY, R. P. & WEISS, L. 1975. Ontogeny of human fetal lymph nodes. *Am J Anat,* 142**,** 15-27.

BAJENOFF, M., EGEN, J. G., KOO, L. Y., LAUGIER, J. P., BRAU, F., GLAICHENHAUS, N. & GERMAIN, R. N. 2006. Stromal cell networks regulate lymphocyte entry, migration, and territoriality in lymph nodes. *Immunity,* 25**,** 989-1001.

BAJENOFF, M. & GERMAIN, R. N. 2009. B-cell follicle development remodels the conduit system and allows soluble antigen delivery to follicular dendritic cells. *Blood,* 114**,** 4989-97.

BANKS, T. A., RICKERT, S., BENEDICT, C. A., MA, L., KO, M., MEIER, J., HA, W., SCHNEIDER, K., GRANGER, S. W., TUROVSKAYA, O., ELEWAUT, D., OTERO, D., FRENCH, A. R., HENRY, S. C., HAMILTON, J. D., SCHEU, S., PFEFFER, K. & WARE, C. F. 2005. A lymphotoxin-IFN-beta axis essential for lymphocyte survival revealed during cytomegalovirus infection. *J Immunol,* 174**,** 7217-25.

BANKS, T. A., ROUSE, B. T., KERLEY, M. K., BLAIR, P. J., GODFREY, V. L., KUKLIN, N. A., BOULEY, D. M., THOMAS, J., KANANGAT, S. & MUCENSKI, M. L. 1995. Lymphotoxin-alpha-deficient mice. Effects on secondary lymphoid organ development and humoral immune responsiveness. *J Immunol,* 155**,** 1685-93.

BANNARD, O., HORTON, R. M., ALLEN, C. D., AN, J., NAGASAWA, T. & CYSTER, J. G. 2013. Germinal center centroblasts transition to a centrocyte phenotype according to a timed program and depend on the dark zone for effective selection. *Immunity,* 39**,** 912-24.

BARONE, F., NAYAR, S., CAMPOS, J., CLOAKE, T., WITHERS, D. R., TOELLNER, K. M., ZHANG, Y., FOUSER, L., FISHER, B., BOWMAN, S., RANGEL-MORENO, J., GARCIA-HERNANDEZ MDE, L., RANDALL, T. D., LUCCHESI, D., BOMBARDIERI, M., PITZALIS, C., LUTHER, S. A. & BUCKLEY, C. D. 2015. IL-22 regulates lymphoid chemokine production and assembly of tertiary lymphoid organs. *Proc Natl Acad Sci U S A,* 112**,** 11024-9.

BARRINGTON, R. A., POZDNYAKOVA, O., ZAFARI, M. R., BENJAMIN, C. D. & CARROLL, M. C. 2002. B lymphocyte memory: role of stromal cell complement and FcgammaRIIB receptors. *J Exp Med,* 196**,** 1189-99.

BARRY, W. C. & RUDDLE, N. H. 1983. The delayed-type hypersensitivity response to (4-hydroxy-3-nitrophenyl) acetyl- (NP) coupled proteins is carrier-specific: in vivo and in vitro demonstrations. *J Immunol,* 131**,** 70-6.

BASSO, K. & DALLA-FAVERA, R. 2012. Roles of BCL6 in normal and transformed germinal center B cells. *Immunol Rev,* 247**,** 172-83.

BATISTA, F. D. & HARWOOD, N. E. 2009. The who, how and where of antigen presentation to B cells. *Nat Rev Immunol,* 9**,** 15-27.

BAUMJOHANN, D., OKADA, T. & ANSEL, K. M. 2011. Cutting Edge: Distinct waves of BCL6 expression during T follicular helper cell development. *J Immunol,* 187**,** 2089-92.

BECHAR, J. A. 2012. The role of CD248 in mesenchymal stem cell differentiation into adipocytes. *BMedSc Clinical Science Thesis, University of Birmingham*.

BECKER, R., LENTER, M. C., VOLLKOMMER, T., BOOS, A. M., PFAFF, D., AUGUSTIN, H. G. & CHRISTIAN, S. 2008. Tumor stroma marker endosialin (Tem1) is a binding partner of metastasis-related protein Mac-2 BP/90K. *FASEB J,* 22**,** 3059-67.

BENEZECH, C. & CAAMANO, J. H. 2013. Generation of lymph node-fat pad chimeras for the study of lymph node stromal cell origin. *J Vis Exp***,** e50952.

BENEZECH, C., LUU, N. T., WALKER, J. A., KRUGLOV, A. A., LOO, Y., NAKAMURA, K., ZHANG, Y., NAYAR, S., JONES, L. H., FLORES-LANGARICA, A., MCINTOSH, A., MARSHALL, J., BARONE, F., BESRA, G., MILES, K., ALLEN, J. E., GRAY, M., KOLLIAS, G., CUNNINGHAM, A. F., WITHERS, D. R., TOELLNER, K. M., JONES, N. D., VELDHOEN, M., NEDOSPASOV, S. A., MCKENZIE, A. N. & CAAMANO, J. H. 2015. Inflammation-induced formation of fat-associated lymphoid clusters. *Nat Immunol,* 16**,** 819-28.

BENEZECH, C., MADER, E., DESANTI, G., KHAN, M., NAKAMURA, K., WHITE, A., WARE, C. F., ANDERSON, G. & CAAMANO, J. H. 2012. Lymphotoxin-beta receptor signaling through NF-kappaB2-RelB pathway reprograms adipocyte precursors as lymph node stromal cells. *Immunity,* 37**,** 721-34.

BENEZECH, C., NAYAR, S., FINNEY, B. A., WITHERS, D. R., LOWE, K., DESANTI, G. E., MARRIOTT, C. L., WATSON, S. P., CAAMANO, J. H., BUCKLEY, C. D. & BARONE, F. 2014. CLEC-2 is required for development and maintenance of lymph nodes. *Blood,* 123**,** 3200-7.

BENEZECH, C., WHITE, A., MADER, E., SERRE, K., PARNELL, S., PFEFFER, K., WARE, C. F., ANDERSON, G. & CAAMANO, J. H. 2010. Ontogeny of stromal organizer cells during lymph node development. *J Immunol,* 184**,** 4521-30.

BEREK, C., BERGER, A. & APEL, M. 1991. Maturation of the immune response in germinal centers. *Cell,* 67**,** 1121-9.

BERGERS, G. & SONG, S. 2005. The role of pericytes in blood-vessel formation and maintenance. *Neuro Oncol,* 7**,** 452-64.

BLUM, K. S. & PABST, R. 2006. Keystones in lymph node development. *J Anat,* 209**,** 585-95.

BOADO, R. J. & PARDRIDGE, W. M. 1994. Differential expression of alpha-actin mRNA and immunoreactive protein in brain microvascular pericytes and smooth muscle cells. *J Neurosci Res,* 39**,** 430-5.

BOEHM, T., HESS, I. & SWANN, J. B. 2012. Evolution of lymphoid tissues. *Trends Immunol,* 33**,** 315-21.

BOEHM, T., SCHEU, S., PFEFFER, K. & BLEUL, C. C. 2003. Thymic medullary epithelial cell differentiation, thymocyte emigration, and the control of autoimmunity require lympho-epithelial cross talk via LTbetaR. *J Exp Med,* 198**,** 757-69.

BONFIELD, T. L. & CAPLAN, A. I. 2010. Adult mesenchymal stem cells: an innovative therapeutic for lung diseases. *Discov Med,* 9**,** 337-45.

BOOS, M. D., YOKOTA, Y., EBERL, G. & KEE, B. L. 2007. Mature natural killer cell and lymphoid tissue-inducing cell development requires Id2-mediated suppression of E protein activity. *J Exp Med,* 204**,** 1119-30.

BOULIANNE, B., LE, M. X., WARD, L. A., MENG, L., HADDAD, D., LI, C., MARTIN, A. & GOMMERMAN, J. L. 2013. AID-expressing germinal center B cells cluster normally within lymph node follicles in the absence of FDC-M1+ CD35+ follicular dendritic cells but dissipate prematurely. *J Immunol,* 191**,** 4521-30.

BRENDOLAN, A., FERRETTI, E., SALSI, V., MOSES, K., QUAGGIN, S., BLASI, F., CLEARY, M. L. & SELLERI, L. 2005. A Pbx1-dependent genetic and transcriptional network regulates spleen ontogeny. *Development,* 132**,** 3113-26.

BRENDOLAN, A., ROSADO, M. M., CARSETTI, R., SELLERI, L. & DEAR, T. N. 2007. Development and function of the mammalian spleen. *Bioessays,* 29**,** 166-77.

BROWN, F. D. & TURLEY, S. J. 2015. Fibroblastic reticular cells: organization and regulation of the T lymphocyte life cycle. *J Immunol,* 194**,** 1389-94.

BROWNING, J. L., ALLAIRE, N., NGAM-EK, A., NOTIDIS, E., HUNT, J., PERRIN, S. & FAVA, R. A. 2005. Lymphotoxin-beta receptor signaling is required for the homeostatic control of HEV differentiation and function. *Immunity,* 23**,** 539-50.

BUCKLEY, C. D. 2011. Why does chronic inflammation persist: An unexpected role for fibroblasts. *Immunol Lett,* 138**,** 12-4.

BUTCHER, E. C. & PICKER, L. J. 1996. Lymphocyte homing and homeostasis. *Science,* 272**,** 60-6.

BUTCHER, E. C., WILLIAMS, M., YOUNGMAN, K., ROTT, L. & BRISKIN, M. 1999. Lymphocyte trafficking and regional immunity. *Adv Immunol,* 72**,** 209-53.

CAO, R., BJORNDAHL, M. A., RELIGA, P., CLASPER, S., GARVIN, S., GALTER, D., MEISTER, B., IKOMI, F., TRITSARIS, K., DISSING, S., OHHASHI, T., JACKSON, D. G. & CAO, Y. 2004. PDGF-BB induces intratumoral lymphangiogenesis and promotes lymphatic metastasis. *Cancer Cell,* 6**,** 333-45.

CAO, X., SHORES, E. W., HU-LI, J., ANVER, M. R., KELSALL, B. L., RUSSELL, S. M., DRAGO, J., NOGUCHI, M., GRINBERG, A., BLOOM, E. T. & ET AL. 1995. Defective lymphoid development in mice lacking expression of the common cytokine receptor gamma chain. *Immunity,* 2**,** 223-38.

CAPLAN, A. I. 2008. All MSCs are pericytes? *Cell Stem Cell,* 3**,** 229-30.

CARON, G., LE GALLOU, S., LAMY, T., TARTE, K. & FEST, T. 2009. CXCR4 expression functionally discriminates centroblasts versus centrocytes within human germinal center B cells. *J Immunol,* 182**,** 7595-602.

CARRAGHER, D., JOHAL, R., BUTTON, A., WHITE, A., ELIOPOULOS, A., JENKINSON, E., ANDERSON, G. & CAAMANO, J. 2004. A stroma-derived defect in NF-kappaB2-/- mice causes impaired lymph node development and lymphocyte recruitment. *J Immunol,* 173**,** 2271-9.

CARRASCO, Y. R. & BATISTA, F. D. 2007. B cells acquire particulate antigen in a macrophage-rich area at the boundary between the follicle and the subcapsular sinus of the lymph node. *Immunity,* 27**,** 160-71.

CARSON-WALTER, E. B., WINANS, B. N., WHITEMAN, M. C., LIU, Y., JARVELA, S., HAAPASALO, H., TYLER, B. M., HUSO, D. L., JOHNSON, M. D. & WALTER, K. A. 2009. Characterization of TEM1/endosialin in human and murine brain tumors. *BMC Cancer,* 9**,** 417.

CASAMAYOR-PALLEJA, M., FEUILLARD, J., BALL, J., DREW, M. & MACLENNAN, I. C. 1996. Centrocytes rapidly adopt a memory B cell phenotype on co-culture with autologous germinal centre T cell-enriched preparations. *Int Immunol,* 8**,** 737-44.

CASTAGNARO, L., LENTI, E., MARUZZELLI, S., SPINARDI, L., MIGLIORI, E., FARINELLO, D., SITIA, G., HARRELSON, Z., EVANS, S. M., GUIDOTTI, L. G., HARVEY, R. P. & BRENDOLAN, A. 2013. Nkx2-5(+)islet1(+) mesenchymal precursors generate distinct spleen stromal cell subsets and participate in restoring stromal network integrity. *Immunity,* 38**,** 782-91.

CASTIGLI, E., SCOTT, S., DEDEOGLU, F., BRYCE, P., JABARA, H., BHAN, A. K., MIZOGUCHI, E. & GEHA, R. S. 2004. Impaired IgA class switching in APRIL-deficient mice. *Proc Natl Acad Sci U S A,* 101**,** 3903-8.

CAVANAGH, T. J., LAKEY, J. R., WRIGHT, M. J., FETTERHOFF, T. & WILE, K. 1997. Crude collagenase loses islet-isolating efficacy regardless of storage conditions. *Transplant Proc,* 29**,** 1942-4.

CHAI, Q., ONDER, L., SCANDELLA, E., GIL-CRUZ, C., PEREZ-SHIBAYAMA, C., CUPOVIC, J., DANUSER, R., SPARWASSER, T., LUTHER, S. A., THIEL, V., RULICKE, T., STEIN, J. V., HEHLGANS, T. & LUDEWIG, B. 2013. Maturation of lymph node fibroblastic reticular cells from myofibroblastic precursors is critical for antiviral immunity. *Immunity,* 38**,** 1013-24.

CHAN, T. D., GATTO, D., WOOD, K., CAMIDGE, T., BASTEN, A. & BRINK, R. 2009. Antigen affinity controls rapid T-dependent antibody production by driving the expansion rather than the differentiation or extrafollicular migration of early plasmablasts. *J Immunol,* 183**,** 3139-49.

CHANG, H. Y., CHI, J. T., DUDOIT, S., BONDRE, C., VAN DE RIJN, M., BOTSTEIN, D. & BROWN, P. O. 2002. Diversity, topographic differentiation, and positional memory in human fibroblasts. *Proceedings of the National Academy of Sciences of the United States of America,* 99**,** 12877-82.

CHANG, J. E. & TURLEY, S. J. 2015. Stromal infrastructure of the lymph node and coordination of immunity. *Trends Immunol,* 36**,** 30-9.

CHAUDHURI, J., TIAN, M., KHUONG, C., CHUA, K., PINAUD, E. & ALT, F. W. 2003. Transcription-targeted DNA deamination by the AID antibody diversification enzyme. *Nature,* 422**,** 726-30.

CHEN, S. C., VASSILEVA, G., KINSLEY, D., HOLZMANN, S., MANFRA, D., WIEKOWSKI, M. T., ROMANI, N. & LIRA, S. A. 2002. Ectopic expression of the murine chemokines CCL21a and CCL21b induces the formation of lymph node-like structures in pancreas, but not skin, of transgenic mice. *J Immunol,* 168**,** 1001-8.

CHEN, W. W., WU, X. L., NIE, W. M., XIE, Y. X., WANG, L. & ZHAO, M. 2012. [Characteristics of gammadelta T cell subsets induced from peripheral blood mononuclear cells of HIV/AIDS patients in vitro]. *Xi Bao Yu Fen Zi Mian Yi Xue Za Zhi,* 28**,** 285-7.

CHENG, N., BRANTLEY, D. M. & CHEN, J. 2002. The ephrins and Eph receptors in angiogenesis. *Cytokine Growth Factor Rev,* 13**,** 75-85.

CHERRIER, M., SAWA, S. & EBERL, G. 2012. Notch, Id2, and RORgammat sequentially orchestrate the fetal development of lymphoid tissue inducer cells. *J Exp Med,* 209**,** 729-40.

CHRISTIAN, S., AHORN, H., KOEHLER, A., EISENHABER, F., RODI, H. P., GARIN-CHESA, P., PARK, J. E., RETTIG, W. J. & LENTER, M. C. 2001. Molecular cloning and characterization of endosialin, a C-type lectin-like cell surface receptor of tumor endothelium. *J Biol Chem,* 276**,** 7408-14.

CHRISTIAN, S., WINKLER, R., HELFRICH, I., BOOS, A. M., BESEMFELDER, E., SCHADENDORF, D. & AUGUSTIN, H. G. 2008. Endosialin (Tem1) is a marker of tumor-associated myofibroblasts and tumor vessel-associated mural cells. *Am J Pathol,* 172**,** 486-94.

CHU, S., HOLTZ, M., GUPTA, M. & BHATIA, R. 2004. BCR/ABL kinase inhibition by imatinib mesylate enhances MAP kinase activity in chronic myelogenous leukemia CD34+ cells. *Blood,* 103**,** 3167-74.

CHUNG, C.-H., LIN, K.-T., CHANG, C.-H., PENG, H.-C. & HUANG, T.-F. 2009. The integrin α2β1 agonist, aggretin, promotes proliferation and migration of VSMC through NF-kB translocation and PDGF production. *British Journal of Pharmacology,* 156**,** 846-856.

COHEN, J. N., TEWALT, E. F., ROUHANI, S. J., BUONOMO, E. L., BRUCE, A. N., XU, X., BEKIRANOV, S., FU, Y. X. & ENGELHARD, V. H. 2014. Tolerogenic properties of lymphatic endothelial cells are controlled by the lymph node microenvironment. *PLoS One,* 9**,** e87740.

COICO, R. F., BHOGAL, B. S. & THORBECKE, G. J. 1983. Relationship of germinal centers in lymphoid tissue to immunologic memory. VI. Transfer of B cell memory with lymph node cells fractionated according to their receptors for peanut agglutinin. *J Immunol,* 131**,** 2254-7.

COLES, M., KIOUSSIS, D. & VEIGA-FERNANDES, H. 2010. Cellular and Molecular Requirements in Lymph Node and Peyer's Patch Development. 92**,** 177-205.

COLES, M. & VEIGA-FERNANDES, H. 2013. Insight into lymphoid tissue morphogenesis. *Immunology Letters,* 156**,** 46-53.

COLES, M. C., VEIGA-FERNANDES, H., FOSTER, K. E., NORTON, T., PAGAKIS, S. N., SEDDON, B. & KIOUSSIS, D. 2006. Role of T and NK cells and IL7/IL7r interactions during neonatal maturation of lymph nodes. *Proc Natl Acad Sci U S A,* 103**,** 13457-62.

COLLETT, G. D. & CANFIELD, A. E. 2005. Angiogenesis and pericytes in the initiation of ectopic calcification. *Circ Res,* 96**,** 930-8.

COOK, M. C., KORNER, H., RIMINTON, D. S., LEMCKERT, F. A., HASBOLD, J., AMESBURY, M., HODGKIN, P. D., CYSTER, J. G., SEDGWICK, J. D. & BASTEN, A. 1998. Generation of splenic follicular structure and B cell movement in tumor necrosis factor-deficient mice. *J Exp Med,* 188**,** 1503-10.

CREMASCO, V., WOODRUFF, M. C., ONDER, L., CUPOVIC, J., NIEVES-BONILLA, J. M., SCHILDBERG, F. A., CHANG, J., CREMASCO, F., HARVEY, C. J., WUCHERPFENNIG, K., LUDEWIG, B., CARROLL, M. C. & TURLEY, S. J. 2014. B cell homeostasis and follicle confines are governed by fibroblastic reticular cells. *Nat Immunol,* 15**,** 973-81.

CRISAN, M., YAP, S., CASTEILLA, L., CHEN, C. W., CORSELLI, M., PARK, T. S., ANDRIOLO, G., SUN, B., ZHENG, B., ZHANG, L., NOROTTE, C., TENG, P. N., TRAAS, J., SCHUGAR, R., DEASY, B. M., BADYLAK, S., BUHRING, H. J., GIACOBINO, J. P., LAZZARI, L., HUARD, J. & PEAULT, B. 2008. A perivascular origin for mesenchymal stem cells in multiple human organs. *Cell Stem Cell,* 3**,** 301-13.

CUNNINGHAM, A. F., FALLON, P. G., KHAN, M., VACHERON, S., ACHA-ORBEA, H., MACLENNAN, I. C., MCKENZIE, A. N. & TOELLNER, K. M. 2002. Th2 activities induced during virgin T cell priming in the absence of IL-4, IL-13, and B cells. *J Immunol,* 169**,** 2900-6.

CUNNINGHAM, A. F., SERRE, K., TOELLNER, K. M., KHAN, M., ALEXANDER, J., BROMBACHER, F. & MACLENNAN, I. C. 2004. Pinpointing IL-4-independent acquisition and IL-4-influenced maintenance of Th2 activity by CD4 T cells. *Eur J Immunol,* 34**,** 686-94.

CUPEDO, T., CRELLIN, N. K., PAPAZIAN, N., ROMBOUTS, E. J., WEIJER, K., GROGAN, J. L., FIBBE, W. E., CORNELISSEN, J. J. & SPITS, H. 2009. Human fetal lymphoid tissue-inducer cells are interleukin 17-producing precursors to RORC+ CD127+ natural killer-like cells. *Nat Immunol,* 10**,** 66-74.

CUPEDO, T. & MEBIUS, R. E. 2005. Cellular interactions in lymph node development. *J Immunol,* 174**,** 21-5.

CUPEDO, T., VONDENHOFF, M. F., HEEREGRAVE, E. J., DE WEERD, A. E., JANSEN, W., JACKSON, D. G., KRAAL, G. & MEBIUS, R. E. 2004. Presumptive lymph node organizers are differentially represented in developing mesenteric and peripheral nodes. *J Immunol,* 173**,** 2968-75.

CYSTER, J. G. 2010. B cell follicles and antigen encounters of the third kind. *Nat Immunol,* 11**,** 989-96.

CYSTER, J. G., ANSEL, K. M., REIF, K., EKLAND, E. H., HYMAN, P. L., TANG, H. L., LUTHER, S. A. & NGO, V. N. 2000. Follicular stromal cells and lymphocyte homing to follicles. *Immunol Rev,* 176**,** 181-93.

DAL PORTO, J. M., HABERMAN, A. M., KELSOE, G. & SHLOMCHIK, M. J. 2002. Very low affinity B cells form germinal centers, become memory B cells, and participate in secondary immune responses when higher affinity competition is reduced. *J Exp Med,* 195**,** 1215-21.

DE SILVA, N. S. & KLEIN, U. 2015. Dynamics of B cells in germinal centres. *Nat Rev Immunol,* 15**,** 137-48.

DE TOGNI, P., GOELLNER, J., RUDDLE, N. H., STREETER, P. R., FICK, A., MARIATHASAN, S., SMITH, S. C., CARLSON, R., SHORNICK, L. P., STRAUSS-SCHOENBERGER, J. & ET AL. 1994. Abnormal development of peripheral lymphoid organs in mice deficient in lymphotoxin. *Science,* 264**,** 703-7.

DEAR, T. N., COLLEDGE, W. H., CARLTON, M. B., LAVENIR, I., LARSON, T., SMITH, A. J., WARREN, A. J., EVANS, M. J., SOFRONIEW, M. V. & RABBITTS, T. H. 1995. The Hox11 gene is essential for cell survival during spleen development. *Development,* 121**,** 2909-15.

DEJARDIN, E., DROIN, N. M., DELHASE, M., HAAS, E., CAO, Y., MAKRIS, C., LI, Z. W., KARIN, M., WARE, C. F. & GREEN, D. R. 2002. The lymphotoxin-beta receptor induces different patterns of gene expression via two NF-kappaB pathways. *Immunity,* 17**,** 525-35.

DEMETRI, G. D., VON MEHREN, M., BLANKE, C. D., VAN DEN ABBEELE, A. D., EISENBERG, B., ROBERTS, P. J., HEINRICH, M. C., TUVESON, D. A., SINGER, S., JANICEK, M., FLETCHER, J. A., SILVERMAN, S. G., SILBERMAN, S. L., CAPDEVILLE, R., KIESE, B., PENG, B., DIMITRIJEVIC, S., DRUKER, B. J., CORLESS, C., FLETCHER, C. D. & JOENSUU, H. 2002. Efficacy and safety of imatinib mesylate in advanced gastrointestinal stromal tumors. *N Engl J Med,* 347**,** 472-80.

DEMOULIN, J. B. 2010. No PDGF receptor signal in pericytes without endosialin? *Cancer Biol Ther,* 9**,** 916-8.

DENNIS, J. E., HAYNESWORTH, S. E., YOUNG, R. G. & CAPLAN, A. I. 1992. Osteogenesis in marrow-derived mesenchymal cell porous ceramic composites transplanted subcutaneously: effect of fibronectin and laminin on cell retention and rate of osteogenic expression. *Cell Transplant,* 1**,** 23-32.

DENTON, A. E., ROBERTS, E. W., LINTERMAN, M. A. & FEARON, D. T. 2014. Fibroblastic reticular cells of the lymph node are required for retention of resting but not activated CD8+ T cells. *Proc Natl Acad Sci U S A,* 111**,** 12139-44.

DI NOIA, J. M. & NEUBERGER, M. S. 2007. Molecular mechanisms of antibody somatic hypermutation. *Annu Rev Biochem,* 76**,** 1-22.

DIAMOND, L. K. 1969. Splenectomy in childhood and the hazard of overwhelming infection. *Pediatrics,* 43**,** 886-9.

DICKERSON, S. K., MARKET, E., BESMER, E. & PAPAVASILIOU, F. N. 2003. AID mediates hypermutation by deaminating single stranded DNA. *J Exp Med,* 197**,** 1291-6.

DIMARINO, A. M., CAPLAN, A. I. & BONFIELD, T. L. 2013. Mesenchymal stem cells in tissue repair. *Front Immunol,* 4**,** 201.

DOGAN, I., BERTOCCI, B., VILMONT, V., DELBOS, F., MEGRET, J., STORCK, S., REYNAUD, C. A. & WEILL, J. C. 2009. Multiple layers of B cell memory with different effector functions. *Nat Immunol,* 10**,** 1292-9.

DOUGALL, W. C., GLACCUM, M., CHARRIER, K., ROHRBACH, K., BRASEL, K., DE SMEDT, T., DARO, E., SMITH, J., TOMETSKO, M. E., MALISZEWSKI, C. R., ARMSTRONG, A., SHEN, V., BAIN, S.,

COSMAN, D., ANDERSON, D., MORRISSEY, P. J., PESCHON, J. J. & SCHUH, J. 1999. RANK is essential for osteoclast and lymph node development. *Genes Dev,* 13**,** 2412-24.

DRAYTON, D. L., BONIZZI, G., YING, X., LIAO, S., KARIN, M. & RUDDLE, N. H. 2004. I kappa B kinase complex alpha kinase activity controls chemokine and high endothelial venule gene expression in lymph nodes and nasal-associated lymphoid tissue. *J Immunol,* 173**,** 6161-8.

DRAYTON, D. L., LIAO, S., MOUNZER, R. H. & RUDDLE, N. H. 2006. Lymphoid organ development: from ontogeny to neogenesis. *Nature Immunology,* 7**,** 344-353.

DURANDY, A. 2003. Activation-induced cytidine deaminase: a dual role in class-switch recombination and somatic hypermutation. *Eur J Immunol,* 33**,** 2069-73.

EBERL, G. 2007. From induced to programmed lymphoid tissues: the long road to preempt pathogens. *Trends Immunol,* 28**,** 423-8.

EBERL, G., MARMON, S., SUNSHINE, M. J., RENNERT, P. D., CHOI, Y. & LITTMAN, D. R. 2004. An essential function for the nuclear receptor RORgamma(t) in the generation of fetal lymphoid tissue inducer cells. *Nat Immunol,* 5**,** 64-73.

ECKHARDT, T., JAHR, H., FEDERLIN, K. & BRETZEL, R. G. 1999. Endotoxin impairs the engraftment of rat islets transplanted beneath the kidney capsule of C57BL/6-mice. *J Mol Med (Berl),* 77**,** 123-5.

EIKELENBOOM, P., NASSY, J. J., POST, J., VERSTEEG, J. C. & LANGEVOORT, H. L. 1978. The histogenesis of lymph nodes in rat and rabbit. *Anat Rec,* 190**,** 201-15.

EL SHIKH, M. E. & PITZALIS, C. 2012. Follicular dendritic cells in health and disease. *Front Immunol,* 3**,** 292.

ENDRES, R., ALIMZHANOV, M. B., PLITZ, T., FUTTERER, A., KOSCO-VILBOIS, M. H., NEDOSPASOV, S. A., RAJEWSKY, K. & PFEFFER, K. 1999. Mature follicular dendritic cell networks depend on expression of lymphotoxin beta receptor by radioresistant stromal cells and of lymphotoxin beta and tumor necrosis factor by B cells. *J Exp Med,* 189**,** 159-68.

EVANS, D. I. 1985. Postsplenectomy sepsis 10 years or more after operation. *J Clin Pathol,* 38**,** 309-11.

FAN, L., REILLY, C. R., LUO, Y., DORF, M. E. & LO, D. 2000. Cutting edge: ectopic expression of the chemokine TCA4/SLC is sufficient to trigger lymphoid neogenesis. *J Immunol,* 164**,** 3955-9.

FASNACHT, N., HUANG, H. Y., KOCH, U., FAVRE, S., AUDERSET, F., CHAI, Q., ONDER, L., KALLERT, S., PINSCHEWER, D. D., MACDONALD, H. R., TACCHINI-COTTIER, F., LUDEWIG, B., LUTHER, S. A. & RADTKE, F. 2014. Specific fibroblastic niches in secondary lymphoid organs orchestrate distinct Notch-regulated immune responses. *J Exp Med,* 211**,** 2265-79.

FINKE, D., ACHA-ORBEA, H., MATTIS, A., LIPP, M. & KRAEHENBUHL, J. 2002. CD4+CD3- cells induce Peyer's patch development: role of alpha4beta1 integrin activation by CXCR5. *Immunity,* 17**,** 363-73.

FLETCHER, A. L., ACTON, S. E. & KNOBLICH, K. 2015. Lymph node fibroblastic reticular cells in health and disease. *Nat Rev Immunol,* 15**,** 350-61.

FLETCHER, A. L., LUKACS-KORNEK, V., REYNOSO, E. D., PINNER, S. E., BELLEMARE-PELLETIER, A., CURRY, M. S., COLLIER, A. R., BOYD, R. L. & TURLEY, S. J. 2010. Lymph node fibroblastic reticular cells directly present peripheral tissue antigen under steady-state and inflammatory conditions. *J Exp Med,* 207**,** 689-97.

FLETCHER, A. L., MALHOTRA, D., ACTON, S. E., LUKACS-KORNEK, V., BELLEMARE-PELLETIER, A., CURRY, M., ARMANT, M. & TURLEY, S. J. 2011. Reproducible isolation of lymph node stromal cells reveals site-dependent differences in fibroblastic reticular cells. *Front Immunol,* 2**,** 35.

FORSTER, R., MATTIS, A. E., KREMMER, E., WOLF, E., BREM, G. & LIPP, M. 1996. A putative chemokine receptor, BLR1, directs B cell migration to defined lymphoid organs and specific anatomic compartments of the spleen. *Cell,* 87**,** 1037-47.

FORSTER, R., SCHUBEL, A., BREITFELD, D., KREMMER, E., RENNER-MULLER, I., WOLF, E. & LIPP, M. 1999. CCR7 coordinates the primary immune response by establishing functional microenvironments in secondary lymphoid organs. *Cell,* 99**,** 23-33.

FOY, T. M., LAMAN, J. D., LEDBETTER, J. A., ARUFFO, A., CLAASSEN, E. & NOELLE, R. J. 1994. gp39-CD40 interactions are essential for germinal center formation and the development of B cell memory. *J Exp Med,* 180**,** 157-63.

FRANZOSO, G., CARLSON, L., POLJAK, L., SHORES, E. W., EPSTEIN, S., LEONARDI, A., GRINBERG, A., TRAN, T., SCHARTON-KERSTEN, T., ANVER, M., LOVE, P., BROWN, K. & SIEBENLIST, U. 1998. Mice deficient in nuclear factor (NF)-kappa B/p52 present with defects in humoral responses, germinal center reactions, and splenic microarchitecture. *J Exp Med,* 187**,** 147-59.

FU, Y. X., HUANG, G., WANG, Y. & CHAPLIN, D. D. 1998. B lymphocytes induce the formation of follicular dendritic cell clusters in a lymphotoxin alpha-dependent fashion. *J Exp Med,* 187**,** 1009-18.

FU, Y. X., HUANG, G., WANG, Y. & CHAPLIN, D. D. 2000. Lymphotoxin-alpha-dependent spleen microenvironment supports the generation of memory B cells and is required for their subsequent antigen-induced activation. *J Immunol,* 164**,** 2508-14.

FU, Y. X., MOLINA, H., MATSUMOTO, M., HUANG, G., MIN, J. & CHAPLIN, D. D. 1997. Lymphotoxin-alpha (LTalpha) supports development of splenic follicular structure that is required for IgG responses. *J Exp Med,* 185**,** 2111-20.

FUTTERER, A., MINK, K., LUZ, A., KOSCO-VILBOIS, M. H. & PFEFFER, K. 1998. The lymphotoxin beta receptor controls organogenesis and affinity maturation in peripheral lymphoid tissues. *Immunity,* 9**,** 59-70.

GARSIDE, P., INGULLI, E., MERICA, R. R., JOHNSON, J. G., NOELLE, R. J. & JENKINS, M. K. 1998. Visualization of specific B and T lymphocyte interactions in the lymph node. *Science,* 281**,** 96-9.

GATTO, D. & BRINK, R. 2010. The germinal center reaction. *J Allergy Clin Immunol,* 126**,** 898-907; quiz 908-9.

GATTO, D., PAUS, D., BASTEN, A., MACKAY, C. R. & BRINK, R. 2009. Guidance of B cells by the orphan G protein-coupled receptor EBI2 shapes humoral immune responses. *Immunity,* 31**,** 259-69.

GATTO, D., PFISTER, T., JEGERLEHNER, A., MARTIN, S. W., KOPF, M. & BACHMANN, M. F. 2005. Complement receptors regulate differentiation of bone marrow plasma cell precursors expressing transcription factors Blimp-1 and XBP-1. *J Exp Med,* 201**,** 993-1005.

GEARHART, P. J. & WOOD, R. D. 2001. Emerging links between hypermutation of antibody genes and DNA polymerases. *Nat Rev Immunol,* 1**,** 187-92.

GIRARD, J. P. & SPRINGER, T. A. 1995. High endothelial venules (HEVs): specialized endothelium for lymphocyte migration. *Immunol Today,* 16**,** 449-57.

GITLIN, A. D., SHULMAN, Z. & NUSSENZWEIG, M. C. 2014. Clonal selection in the germinal centre by regulated proliferation and hypermutation. *Nature,* 509**,** 637-40.

GONZALEZ, M., MACKAY, F., BROWNING, J. L., KOSCO-VILBOIS, M. H. & NOELLE, R. J. 1998. The sequential role of lymphotoxin and B cells in the development of splenic follicles. *J Exp Med,* 187**,** 997-1007.

GONZALEZ, S. F., DEGN, S. E., PITCHER, L. A., WOODRUFF, M., HEESTERS, B. A. & CARROLL, M. C. 2011. Trafficking of B cell antigen in lymph nodes. *Annu Rev Immunol,* 29**,** 215-33.

GOODNOW, C. C. 1997. Chance encounters and organized rendezvous. *Immunol Rev,* 156**,** 5-10.

GRAY, E. E. & CYSTER, J. G. 2012. Lymph node macrophages. *J Innate Immun,* 4**,** 424-36.

GRETER, M., HOFMANN, J. & BECHER, B. 2009. Neo-lymphoid aggregates in the adult liver can initiate potent cell-mediated immunity. *PLoS Biol,* 7**,** e1000109.

GRETZ, J. E., NORBURY, C. C., ANDERSON, A. O., PROUDFOOT, A. E. & SHAW, S. 2000. Lymph-borne chemokines and other low molecular weight molecules reach high endothelial venules via specialized conduits while a functional barrier limits access to the lymphocyte microenvironments in lymph node cortex. *J Exp Med,* 192**,** 1425-40.

GRIGOROVA, I. L., PANTELEEV, M. & CYSTER, J. G. 2010. Lymph node cortical sinus organization and relationship to lymphocyte egress dynamics and antigen exposure. *Proc Natl Acad Sci U S A,* 107**,** 20447-52.

GUNN, M. D., KYUWA, S., TAM, C., KAKIUCHI, T., MATSUZAWA, A., WILLIAMS, L. T. & NAKANO, H. 1999. Mice lacking expression of secondary lymphoid organ chemokine have defects in lymphocyte homing and dendritic cell localization. *J Exp Med,* 189**,** 451-60.

HAHNE, M., KATAOKA, T., SCHROTER, M., HOFMANN, K., IRMLER, M., BODMER, J. L., SCHNEIDER, P., BORNAND, T., HOLLER, N., FRENCH, L. E., SORDAT, B., RIMOLDI, D. & TSCHOPP, J. 1998. APRIL, a new ligand of the tumor necrosis factor family, stimulates tumor cell growth. *J Exp Med,* 188**,** 1185-90.

HAN, S., HATHCOCK, K., ZHENG, B., KEPLER, T. B., HODES, R. & KELSOE, G. 1995. Cellular interaction in germinal centers. Roles of CD40 ligand and B7-2 in established germinal centers. *J Immunol,* 155**,** 556-67.

HANAYAMA, R., TANAKA, M., MIYASAKA, K., AOZASA, K., KOIKE, M., UCHIYAMA, Y. & NAGATA, S. 2004. Autoimmune disease and impaired uptake of apoptotic cells in MFG-E8-deficient mice. *Science,* 304**,** 1147-50.

HAO, Z., DUNCAN, G. S., SEAGAL, J., SU, Y. W., HONG, C., HAIGHT, J., CHEN, N. J., ELIA, A., WAKEHAM, A., LI, W. Y., LIEPA, J., WOOD, G. A., CASOLA, S., RAJEWSKY, K. & MAK, T. W. 2008. Fas receptor expression in germinal-center B cells is essential for T and B lymphocyte homeostasis. *Immunity,* 29**,** 615-27.

HARDIE, D. L., BALDWIN, M. J., NAYLOR, A., HAWORTH, O. J., HOU, T. Z., LAX, S., CURNOW, S. J., WILLCOX, N., MACFADYEN, J., ISACKE, C. M. & BUCKLEY, C. D. 2011. The stromal cell antigen CD248 (endosialin) is expressed on naive CD8+ human T cells and regulates proliferation. *Immunology,* 133**,** 288-95.

HARGREAVES, D. C., HYMAN, P. L., LU, T. T., NGO, V. N., BIDGOL, A., SUZUKI, G., ZOU, Y. R., LITTMAN, D. R. & CYSTER, J. G. 2001. A coordinated change in chemokine responsiveness guides plasma cell movements. *J Exp Med,* 194**,** 45-56.

HARMSEN, A., KUSSER, K., HARTSON, L., TIGHE, M., SUNSHINE, M. J., SEDGWICK, J. D., CHOI, Y., LITTMAN, D. R. & RANDALL, T. D. 2002. Cutting edge: organogenesis of nasal-associated lymphoid tissue (NALT) occurs independently of lymphotoxin-alpha (LT alpha) and

retinoic acid receptor-related orphan receptor-gamma, but the organization of NALT is LT alpha dependent. *J Immunol,* 168**,** 986-90.

HAUSER, A. E., JUNT, T., MEMPEL, T. R., SNEDDON, M. W., KLEINSTEIN, S. H., HENRICKSON, S. E., VON ANDRIAN, U. H., SHLOMCHIK, M. J. & HABERMAN, A. M. 2007. Definition of germinal-center B cell migration in vivo reveals predominant intrazonal circulation patterns. *Immunity,* 26**,** 655-67.

HECKSHER-SORENSEN, J., WATSON, R. P., LETTICE, L. A., SERUP, P., ELEY, L., DE ANGELIS, C., AHLGREN, U. & HILL, R. E. 2004. The splanchnic mesodermal plate directs spleen and pancreatic laterality, and is regulated by Bapx1/Nkx3.2. *Development,* 131**,** 4665-75.

HEESTERS, B. A., CHATTERJEE, P., KIM, Y. A., GONZALEZ, S. F., KULIGOWSKI, M. P., KIRCHHAUSEN, T. & CARROLL, M. C. 2013. Endocytosis and recycling of immune complexes by follicular dendritic cells enhances B cell antigen binding and activation. *Immunity,* 38**,** 1164-75.

HEESTERS, B. A., MYERS, R. C. & CARROLL, M. C. 2014. Follicular dendritic cells: dynamic antigen libraries. *Nat Rev Immunol,* 14**,** 495-504.

HOFMANN, J., GRETER, M., DU PASQUIER, L. & BECHER, B. 2010. B-cells need a proper house, whereas T-cells are happy in a cave: the dependence of lymphocytes on secondary lymphoid tissues during evolution. *Trends Immunol,* 31**,** 144-53.

HONDA, K., NAKANO, H., YOSHIDA, H., NISHIKAWA, S., RENNERT, P., IKUTA, K., TAMECHIKA, M., YAMAGUCHI, K., FUKUMOTO, T., CHIBA, T. & NISHIKAWA, S. I. 2001. Molecular basis for hematopoietic/mesenchymal interaction during initiation of Peyer's patch organogenesis. *J Exp Med,* 193**,** 621-30.

HOULIHAN, D. D., MABUCHI, Y., MORIKAWA, S., NIIBE, K., ARAKI, D., SUZUKI, S., OKANO, H. & MATSUZAKI, Y. 2012. Isolation of mouse mesenchymal stem cells on the basis of expression of Sca-1 and PDGFR-alpha. *Nat Protoc,* 7**,** 2103-11.

HUANG, H. P., HONG, C. L., KAO, C. Y., LIN, S. W., LIN, S. R., WU, H. L., SHI, G. Y., YOU, L. R., WU, C. L. & YU, I. S. 2011. Gene targeting and expression analysis of mouse Tem1/endosialin using a lacZ reporter. *Gene Expr Patterns,* 11**,** 316-26.

IMAZEKI, N., SENOO, A. & FUSE, Y. 1992. Is the follicular dendritic cell a primarily stationary cell? *Immunology,* 76**,** 508-10.

ITANO, A. A., MCSORLEY, S. J., REINHARDT, R. L., EHST, B. D., INGULLI, E., RUDENSKY, A. Y. & JENKINS, M. K. 2003. Distinct dendritic cell populations sequentially present antigen to CD4 T cells and stimulate different aspects of cell-mediated immunity. *Immunity,* 19**,** 47-57.

JACOB, J. & KELSOE, G. 1992. In situ studies of the primary immune response to (4-hydroxy-3-nitrophenyl)acetyl. II. A common clonal origin for periarteriolar lymphoid sheath-associated foci and germinal centers. *J Exp Med,* 176**,** 679-87.

JACOB, J., KELSOE, G., RAJEWSKY, K. & WEISS, U. 1991. Intraclonal generation of antibody mutants in germinal centres. *Nature,* 354**,** 389-92.

JARJOUR, M., JORQUERA, A., MONDOR, I., WIENERT, S., NARANG, P., COLES, M. C., KLAUSCHEN, F. & BAJENOFF, M. 2014. Fate mapping reveals origin and dynamics of lymph node follicular dendritic cells. *J Exp Med,* 211**,** 1109-22.

JUNT, T., MOSEMAN, E. A., IANNACONE, M., MASSBERG, S., LANG, P. A., BOES, M., FINK, K., HENRICKSON, S. E., SHAYAKHMETOV, D. M., DI PAOLO, N. C., VAN ROOIJEN, N., MEMPEL, T. R., WHELAN, S. P. & VON ANDRIAN, U. H. 2007. Subcapsular sinus macrophages in lymph nodes clear lymph-borne viruses and present them to antiviral B cells. *Nature,* 450**,** 110-4.

JUNT, T., NAKANO, H., DUMRESE, T., KAKIUCHI, T., ODERMATT, B., ZINKERNAGEL, R. M., HENGARTNER, H. & LUDEWIG, B. 2002. Antiviral immune responses in the absence of organized lymphoid T cell zones in plt/plt mice. *J Immunol,* 168**,** 6032-40.

KABASHIMA, K., SHIRAISHI, N., SUGITA, K., MORI, T., ONOUE, A., KOBAYASHI, M., SAKABE, J., YOSHIKI, R., TAMAMURA, H., FUJII, N., INABA, K. & TOKURA, Y. 2007. CXCL12-CXCR4 engagement is required for migration of cutaneous dendritic cells. *Am J Pathol,* 171**,** 1249-57.

KANZLER, B. & DEAR, T. N. 2001. Hox11 acts cell autonomously in spleen development and its absence results in altered cell fate of mesenchymal spleen precursors. *Dev Biol,* 234**,** 231-43.

KASAJIMA-AKATSUKA, N. & MAEDA, K. 2006. Development, maturation and subsequent activation of follicular dendritic cells (FDC): immunohistochemical observation of human fetal and adult lymph nodes. *Histochem Cell Biol,* 126**,** 261-73.

KATAKAI, T. 2012. Marginal reticular cells: a stromal subset directly descended from the lymphoid tissue organizer. *Front Immunol,* 3**,** 200.

KATAKAI, T., HARA, T., SUGAI, M., GONDA, H. & SHIMIZU, A. 2004. Lymph node fibroblastic reticular cells construct the stromal reticulum via contact with lymphocytes. *J Exp Med,* 200**,** 783-95.

KATAKAI, T., SUTO, H., SUGAI, M., GONDA, H., TOGAWA, A., SUEMATSU, S., EBISUNO, Y., KATAGIRI, K., KINASHI, T. & SHIMIZU, A. 2008. Organizer-like reticular stromal cell layer common to adult secondary lymphoid organs. *J Immunol,* 181**,** 6189-200.

KAWAGUCHI, H., AKUNE, T., YAMAGUCHI, M., OHBA, S., OGATA, N., CHUNG, U. I., KUBOTA, N., TERAUCHI, Y., KADOWAKI, T. & NAKAMURA, K. 2005. Distinct effects of PPARgamma insufficiency on bone marrow cells, osteoblasts, and osteoclastic cells. *J Bone Miner Metab,* 23**,** 275-9.

KEDL, R. M. & TAMBURINI, B. A. 2015. Antigen archiving by lymph node stroma: A novel function for the lymphatic endothelium. *Eur J Immunol,* 45**,** 2721-9.

KERFOOT, S. M., YAARI, G., PATEL, J. R., JOHNSON, K. L., GONZALEZ, D. G., KLEINSTEIN, S. H. & HABERMAN, A. M. 2011. Germinal center B cell and T follicular helper cell development initiates in the interfollicular zone. *Immunity,* 34**,** 947-60.

KIM, D., MEBIUS, R. E., MACMICKING, J. D., JUNG, S., CUPEDO, T., CASTELLANOS, Y., RHO, J., WONG, B. R., JOSIEN, R., KIM, N., RENNERT, P. D. & CHOI, Y. 2000. Regulation of peripheral lymph node genesis by the tumor necrosis factor family member TRANCE. *J Exp Med,* 192**,** 1467-78.

KIM, M. Y., GASPAL, F. M., WIGGETT, H. E., MCCONNELL, F. M., GULBRANSON-JUDGE, A., RAYKUNDALIA, C., WALKER, L. S., GOODALL, M. D. & LANE, P. J. 2003. CD4(+)CD3(-) accessory cells costimulate primed CD4 T cells through OX40 and CD30 at sites where T cells collaborate with B cells. *Immunity,* 18**,** 643-54.

KITAMURA, D., ROES, J., KUHN, R. & RAJEWSKY, K. 1991. A B cell-deficient mouse by targeted disruption of the membrane exon of the immunoglobulin mu chain gene. *Nature,* 350**,** 423-6.

KITANO, M., MORIYAMA, S., ANDO, Y., HIKIDA, M., MORI, Y., KUROSAKI, T. & OKADA, T. 2011. Bcl6 protein expression shapes pre-germinal center B cell dynamics and follicular helper T cell heterogeneity. *Immunity,* 34**,** 961-72.

KLEIN, U., TU, Y., STOLOVITZKY, G. A., KELLER, J. L., HADDAD, J., JR., MILJKOVIC, V., CATTORETTI, G., CALIFANO, A. & DALLA-FAVERA, R. 2003. Transcriptional analysis of the B cell germinal center reaction. *Proc Natl Acad Sci U S A,* 100**,** 2639-44.

KNOOP, K. A., KUMAR, N., BUTLER, B. R., SAKTHIVEL, S. K., TAYLOR, R. T., NOCHI, T., AKIBA, H., YAGITA, H., KIYONO, H. & WILLIAMS, I. R. 2009. RANKL is necessary and sufficient to initiate development of antigen-sampling M cells in the intestinal epithelium. *J Immunol,* 183**,** 5738-47.

KOK, H. M., FALKE, L. L., GOLDSCHMEDING, R. & NGUYEN, T. Q. 2014. Targeting CTGF, EGF and PDGF pathways to prevent progression of kidney disease. *Nat Rev Nephrol,* 10**,** 700-11.

KONDO, M. 2010. Lymphoid and myeloid lineage commitment in multipotent hematopoietic progenitors. *Immunol Rev,* 238**,** 37-46.

KONG, Y. Y., YOSHIDA, H., SAROSI, I., TAN, H. L., TIMMS, E., CAPPARELLI, C., MORONY, S., OLIVEIRA-DOS-SANTOS, A. J., VAN, G., ITIE, A., KHOO, W., WAKEHAM, A., DUNSTAN, C. R., LACEY, D. L., MAK, T. W., BOYLE, W. J. & PENNINGER, J. M. 1999. OPGL is a key regulator of osteoclastogenesis, lymphocyte development and lymph-node organogenesis. *Nature,* 397**,** 315-23.

KONI, P. A., SACCA, R., LAWTON, P., BROWNING, J. L., RUDDLE, N. H. & FLAVELL, R. A. 1997. Distinct roles in lymphoid organogenesis for lymphotoxins alpha and beta revealed in lymphotoxin beta-deficient mice. *Immunity,* 6**,** 491-500.

KOSCO, M. H., PFLUGFELDER, E. & GRAY, D. 1992. Follicular dendritic cell-dependent adhesion and proliferation of B cells in vitro. *J Immunol,* 148**,** 2331-9.

KRACKER, S. & DURANDY, A. 2011. Insights into the B cell specific process of immunoglobulin class switch recombination. *Immunol Lett,* 138**,** 97-103.

KRANICH, J., KRAUTLER, N. J., HEINEN, E., POLYMENIDOU, M., BRIDEL, C., SCHILDKNECHT, A., HUBER, C., KOSCO-VILBOIS, M. H., ZINKERNAGEL, R., MIELE, G. & AGUZZI, A. 2008. Follicular dendritic cells control engulfment of apoptotic bodies by secreting Mfge8. *J Exp Med,* 205**,** 1293-302.

KRATZ, A., CAMPOS-NETO, A., HANSON, M. S. & RUDDLE, N. H. 1996. Chronic inflammation caused by lymphotoxin is lymphoid neogenesis. *J Exp Med,* 183**,** 1461-72.

KRAUTLER, N. J., KANA, V., KRANICH, J., TIAN, Y., PERERA, D., LEMM, D., SCHWARZ, P., ARMULIK, A., BROWNING, J. L., TALLQUIST, M., BUCH, T., OLIVEIRA-MARTINS, J. B., ZHU, C., HERMANN, M., WAGNER, U., BRINK, R., HEIKENWALDER, M. & AGUZZI, A. 2012. Follicular dendritic cells emerge from ubiquitous perivascular precursors. *Cell,* 150**,** 194-206.

KREUZALER, M., RAUCH, M., SALZER, U., BIRMELIN, J., RIZZI, M., GRIMBACHER, B., PLEBANI, A., LOUGARIS, V., QUINTI, I., THON, V., LITZMAN, J., SCHLESIER, M., WARNATZ, K., THIEL, J., ROLINK, A. G. & EIBEL, H. 2012. Soluble BAFF levels inversely correlate with peripheral B cell numbers and the expression of BAFF receptors. *J Immunol,* 188**,** 497-503.

KUKA, M. & IANNACONE, M. 2014. The role of lymph node sinus macrophages in host defense. *Ann N Y Acad Sci,* 1319**,** 38-46.

KUPPERS, R., ZHAO, M., HANSMANN, M. L. & RAJEWSKY, K. 1993. Tracing B cell development in human germinal centres by molecular analysis of single cells picked from histological sections. *EMBO J,* 12**,** 4955-67.

LAKY, K., LEFRANCOIS, L., LINGENHELD, E. G., ISHIKAWA, H., LEWIS, J. M., OLSON, S., SUZUKI, K., TIGELAAR, R. E. & PUDDINGTON, L. 2000. Enterocyte expression of interleukin 7 induces development of gammadelta T cells and Peyer's patches. *J Exp Med,* 191**,** 1569-80.

LAX, S., HARDIE, D. L., WILSON, A., DOUGLAS, M. R., ANDERSON, G., HUSO, D., ISACKE, C. M. & BUCKLEY, C. D. 2010. The pericyte and stromal cell marker CD248 (endosialin) is required for efficient lymph node expansion. *Eur J Immunol,* 40**,** 1884-9.

LAX, S., HOU, T. Z., JENKINSON, E., SALMON, M., MACFADYEN, J. R., ISACKE, C. M., ANDERSON, G., CUNNINGHAM, A. F. & BUCKLEY, C. D. 2007. CD248/Endosialin is dynamically expressed on a subset of stromal cells during lymphoid tissue development, splenic remodeling and repair. *FEBS Lett,* 581**,** 3550-6.

LEBIEN, T. W. & TEDDER, T. F. 2008. B lymphocytes: how they develop and function. *Blood,* 112**,** 1570-80.

LEE, B. J., SANTEE, S., VON GESJEN, S., WARE, C. F. & SARAWAR, S. R. 2000. Lymphotoxin-alpha-deficient mice can clear a productive infection with murine gammaherpesvirus 68 but fail to develop splenomegaly or lymphocytosis. *J Virol,* 74**,** 2786-92.

LEE, S. K., RIGBY, R. J., ZOTOS, D., TSAI, L. M., KAWAMOTO, S., MARSHALL, J. L., RAMISCAL, R. R., CHAN, T. D., GATTO, D., BRINK, R., YU, D., FAGARASAN, S., TARLINTON, D. M., CUNNINGHAM, A. F. & VINUESA, C. G. 2011. B cell priming for extrafollicular antibody responses requires Bcl-6 expression by T cells. *J Exp Med,* 208**,** 1377-88.

LEGLER, D. F., LOETSCHER, M., ROOS, R. S., CLARK-LEWIS, I., BAGGIOLINI, M. & MOSER, B. 1998. B cell-attracting chemokine 1, a human CXC chemokine expressed in lymphoid tissues, selectively attracts B lymphocytes via BLR1/CXCR5. *J Exp Med,* 187**,** 655-60.

LENTI, E., FARINELLO, D., YOKOYAMA, K. K., PENKOV, D., CASTAGNARO, L., LAVORGNA, G., WUPUTRA, K., SANDELL, L. L., TJADEN, N. E., BERNASSOLA, F., CARIDI, N., DE ANTONI, A., WAGNER, M., KOZINC, K., NIEDERREITHER, K., BLASI, F., PASINI, D., MAJDIC, G., TONON, G., TRAINOR, P. A. & BRENDOLAN, A. 2016. Transcription factor TLX1 controls retinoic acid signaling to ensure spleen development. *J Clin Invest,* 126**,** 2452-64.

LEVEEN, P., PEKNY, M., GEBRE-MEDHIN, S., SWOLIN, B., LARSSON, E. & BETSHOLTZ, C. 1994. Mice deficient for PDGF B show renal, cardiovascular, and hematological abnormalities. *Genes Dev,* 8**,** 1875-87.

LINK, A., VOGT, T. K., FAVRE, S., BRITSCHGI, M. R., ACHA-ORBEA, H., HINZ, B., CYSTER, J. G. & LUTHER, S. A. 2007. Fibroblastic reticular cells in lymph nodes regulate the homeostasis of naive T cells. *Nat Immunol,* 8**,** 1255-65.

LINTERMAN, M. A., BEATON, L., YU, D., RAMISCAL, R. R., SRIVASTAVA, M., HOGAN, J. J., VERMA, N. K., SMYTH, M. J., RIGBY, R. J. & VINUESA, C. G. 2010. IL-21 acts directly on B cells to regulate Bcl-6 expression and germinal center responses. *J Exp Med,* 207**,** 353-63.

LIU, Y. J. & ARPIN, C. 1997. Germinal center development. *Immunol Rev,* 156**,** 111-26.

LO, J. C., BASAK, S., JAMES, E. S., QUIAMBO, R. S., KINSELLA, M. C., ALEGRE, M. L., WEIH, F., FRANZOSO, G., HOFFMANN, A. & FU, Y. X. 2006. Coordination between NF-kappaB family members p50 and p52 is essential for mediating LTbetaR signals in the development and organization of secondary lymphoid tissues. *Blood,* 107**,** 1048-55.

LORENZ, R. G., CHAPLIN, D. D., MCDONALD, K. G., MCDONOUGH, J. S. & NEWBERRY, R. D. 2003. Isolated lymphoid follicle formation is inducible and dependent upon lymphotoxin-sufficient B lymphocytes, lymphotoxin beta receptor, and TNF receptor I function. *J Immunol,* 170**,** 5475-82.

LUND, F. E., PARTIDA-SANCHEZ, S., LEE, B. O., KUSSER, K. L., HARTSON, L., HOGAN, R. J., WOODLAND, D. L. & RANDALL, T. D. 2002. Lymphotoxin-alpha-deficient mice make delayed, but effective, T and B cell responses to influenza. *J Immunol,* 169**,** 5236-43.

LUTHER, S. A., ANSEL, K. M. & CYSTER, J. G. 2003. Overlapping roles of CXCL13, interleukin 7 receptor alpha, and CCR7 ligands in lymph node development. *J Exp Med,* 197**,** 1191-8.

LUTHER, S. A., BIDGOL, A., HARGREAVES, D. C., SCHMIDT, A., XU, Y., PANIYADI, J., MATLOUBIAN, M. & CYSTER, J. G. 2002. Differing activities of homeostatic chemokines CCL19, CCL21, and CXCL12 in lymphocyte and dendritic cell recruitment and lymphoid neogenesis. *J Immunol,* 169**,** 424-33.

LUTHER, S. A., GULBRANSON-JUDGE, A., ACHA-ORBEA, H. & MACLENNAN, I. C. 1997. Viral superantigen drives extrafollicular and follicular B cell differentiation leading to virus-specific antibody production. *J Exp Med,* 185**,** 551-62.

LUTHER, S. A., LOPEZ, T., BAI, W., HANAHAN, D. & CYSTER, J. G. 2000. BLC expression in pancreatic islets causes B cell recruitment and lymphotoxin-dependent lymphoid neogenesis. *Immunity,* 12**,** 471-81.

MABBOTT, N. A., KENNETH BAILLIE, J., KOBAYASHI, A., DONALDSON, D. S., OHMORI, H., YOON, S. O., FREEDMAN, A. S., FREEMAN, T. C. & SUMMERS, K. M. 2011. Expression of mesenchyme-specific gene signatures by follicular dendritic cells: insights from the meta-analysis of microarray data from multiple mouse cell populations. *Immunology,* 133**,** 482-98.

MACFADYEN, J., SAVAGE, K., WIENKE, D. & ISACKE, C. M. 2007. Endosialin is expressed on stromal fibroblasts and CNS pericytes in mouse embryos and is downregulated during development. *Gene Expr Patterns,* 7**,** 363-9.

MACFADYEN, J. R., HAWORTH, O., ROBERSTON, D., HARDIE, D., WEBSTER, M. T., MORRIS, H. R., PANICO, M., SUTTON-SMITH, M., DELL, A., VAN DER GEER, P., WIENKE, D., BUCKLEY, C. D. & ISACKE, C. M. 2005. Endosialin (TEM1, CD248) is a marker of stromal fibroblasts and is not selectively expressed on tumour endothelium. *FEBS Lett,* 579**,** 2569-75.

MACKAY, F. & BROWNING, J. L. 1998. Turning off follicular dendritic cells. *Nature,* 395**,** 26-7.

MACLENNAN, I. C. 1994. Germinal centers. *Annu Rev Immunol,* 12**,** 117-39.

MAIA, M., DE VRIESE, A., JANSSENS, T., MOONS, M., VAN LANDUYT, K., TAVERNIER, J., LORIES, R. J. & CONWAY, E. M. 2010. CD248 and its cytoplasmic domain: a therapeutic target for arthritis. *Arthritis Rheum,* 62**,** 3595-606.

MAIA, M., DEVRIESE, A., JANSSENS, T., MOONS, M., LORIES, R. J., TAVERNIER, J. & CONWAY, E. M. 2011. CD248 facilitates tumor growth via its cytoplasmic domain. *BMC Cancer,* 11**,** 162.

MALHOTRA, D., FLETCHER, A. L., ASTARITA, J., LUKACS-KORNEK, V., TAYALIA, P., GONZALEZ, S. F., ELPEK, K. G., CHANG, S. K., KNOBLICH, K., HEMLER, M. E., BRENNER, M. B., CARROLL, M. C., MOONEY, D. J., TURLEY, S. J. & IMMUNOLOGICAL GENOME PROJECT, C. 2012. Transcriptional profiling of stroma from inflamed and resting lymph nodes defines immunological hallmarks. *Nat Immunol,* 13**,** 499-510.

MALHOTRA, D., FLETCHER, A. L. & TURLEY, S. J. 2013. Stromal and hematopoietic cells in secondary lymphoid organs: partners in immunity. *Immunol Rev,* 251**,** 160-76.

MANZ, R. A., THIEL, A. & RADBRUCH, A. 1997. Lifetime of plasma cells in the bone marrow. *Nature,* 388**,** 133-4.

MARSLAND, B. J., BATTIG, P., BAUER, M., RUEDL, C., LASSING, U., BEERLI, R. R., DIETMEIER, K., IVANOVA, L., PFISTER, T., VOGT, L., NAKANO, H., NEMBRINI, C., SAUDAN, P., KOPF, M. & BACHMANN, M. F. 2005. CCL19 and CCL21 induce a potent proinflammatory differentiation program in licensed dendritic cells. *Immunity,* 22**,** 493-505.

MARTENSSON, I. L., ALMQVIST, N., GRIMSHOLM, O. & BERNARDI, A. I. 2010. The pre-B cell receptor checkpoint. *FEBS Lett,* 584**,** 2572-9.

MATLOUBIAN, M., LO, C. G., CINAMON, G., LESNESKI, M. J., XU, Y., BRINKMANN, V., ALLENDE, M. L., PROIA, R. L. & CYSTER, J. G. 2004. Lymphocyte egress from thymus and peripheral lymphoid organs is dependent on S1P receptor 1. *Nature,* 427**,** 355-60.

MATSUMOTO, M., FU, Y. X., MOLINA, H. & CHAPLIN, D. D. 1997. Lymphotoxin-alpha-deficient and TNF receptor-I-deficient mice define developmental and functional characteristics of germinal centers. *Immunol Rev,* 156**,** 137-44.

MCHEYZER-WILLIAMS, M. G., MCLEAN, M. J., LALOR, P. A. & NOSSAL, G. J. 1993. Antigen-driven B cell differentiation in vivo. *J Exp Med,* 178**,** 295-307.

MCHEYZER-WILLIAMS, M. G., NOSSAL, G. J. & LALOR, P. A. 1991. Molecular characterization of single memory B cells. *Nature,* 350**,** 502-5.

MCNAGNY, K. M., BUCY, R. P. & COOPER, M. D. 1991. Reticular cells in peripheral lymphoid tissues express the phosphatidylinositol-linked BP-3 antigen. *Eur J Immunol,* 21**,** 509-15.

MEBIUS, R. E. 2003. Organogenesis of lymphoid tissues. *Nat Rev Immunol,* 3**,** 292-303.

MEBIUS, R. E., MIYAMOTO, T., CHRISTENSEN, J., DOMEN, J., CUPEDO, T., WEISSMAN, I. L. & AKASHI, K. 2001. The fetal liver counterpart of adult common lymphoid progenitors gives rise to all lymphoid lineages, CD45+CD4+CD3- cells, as well as macrophages. *J Immunol,* 166**,** 6593-601.

MEBIUS, R. E., STREETER, P. R., MICHIE, S., BUTCHER, E. C. & WEISSMAN, I. L. 1996. A developmental switch in lymphocyte homing receptor and endothelial vascular addressin expression regulates lymphocyte homing and permits CD4+ CD3- cells to colonize lymph nodes. *Proc Natl Acad Sci U S A,* 93**,** 11019-24.

MIONNET, C., MONDOR, I., JORQUERA, A., LOOSVELD, M., MAURIZIO, J., ARCANGELI, M. L., RUDDLE, N. H., NOWAK, J., AURRAND-LIONS, M., LUCHE, H. & BAJENOFF, M. 2013. Identification of a new stromal cell type involved in the regulation of inflamed B cell follicles. *PLoS Biol,* 11**,** e1001672.

MIYAWAKI, S., NAKAMURA, Y., SUZUKA, H., KOBA, M., YASUMIZU, R., IKEHARA, S. & SHIBATA, Y. 1994. A new mutation, aly, that induces a generalized lack of lymph nodes accompanied by immunodeficiency in mice. *Eur J Immunol,* 24**,** 429-34.

MORI, S., NAKANO, H., ARITOMI, K., WANG, C. R., GUNN, M. D. & KAKIUCHI, T. 2001. Mice lacking expression of the chemokines CCL21-ser and CCL19 (plt mice) demonstrate delayed but enhanced T cell immune responses. *J Exp Med,* 193**,** 207-18.

MOUSSION, C. & GIRARD, J. P. 2011. Dendritic cells control lymphocyte entry to lymph nodes through high endothelial venules. *Nature,* 479**,** 542-6.

MOYRON-QUIROZ, J. E., RANGEL-MORENO, J., KUSSER, K., HARTSON, L., SPRAGUE, F., GOODRICH, S., WOODLAND, D. L., LUND, F. E. & RANDALL, T. D. 2004. Role of inducible bronchus associated lymphoid tissue (iBALT) in respiratory immunity. *Nat Med,* 10**,** 927-34.

MUELLER, S. N. & GERMAIN, R. N. 2009. Stromal cell contributions to the homeostasis and functionality of the immune system. *Nat Rev Immunol,* 9**,** 618-29.

MULLER, G., HOPKEN, U. E. & LIPP, M. 2003. The impact of CCR7 and CXCR5 on lymphoid organ development and systemic immunity. *Immunol Rev,* 195**,** 117-35.

MUNOZ-FERNANDEZ, R., BLANCO, F. J., FRECHA, C., MARTIN, F., KIMATRAI, M., ABADIA-MOLINA, A. C., GARCIA-PACHECO, J. M. & OLIVARES, E. G. 2006. Follicular dendritic cells are related to bone marrow stromal cell progenitors and to myofibroblasts. *J Immunol,* 177**,** 280-9.

MURAKAMI, T., CHEN, X., HASE, K., SAKAMOTO, A., NISHIGAKI, C. & OHNO, H. 2007. Splenic CD19-CD35+B220+ cells function as an inducer of follicular dendritic cell network formation. *Blood,* 110**,** 1215-24.

MURAMATSU, M., KINOSHITA, K., FAGARASAN, S., YAMADA, S., SHINKAI, Y. & HONJO, T. 2000. Class switch recombination and hypermutation require activation-induced cytidine deaminase (AID), a potential RNA editing enzyme. *Cell,* 102**,** 553-63.

NAITO, A., AZUMA, S., TANAKA, S., MIYAZAKI, T., TAKAKI, S., TAKATSU, K., NAKAO, K., NAKAMURA, K., KATSUKI, M., YAMAMOTO, T. & INOUE, J. 1999. Severe osteopetrosis, defective interleukin-1 signalling and lymph node organogenesis in TRAF6-deficient mice. *Genes Cells,* 4**,** 353-62.

NAKANO, H., TAMURA, T., YOSHIMOTO, T., YAGITA, H., MIYASAKA, M., BUTCHER, E. C., NARIUCHI, H., KAKIUCHI, T. & MATSUZAWA, A. 1997. Genetic defect in T lymphocyte-specific homing into peripheral lymph nodes. *Eur J Immunol,* 27**,** 215-21.

NANDA, A., KARIM, B., PENG, Z., LIU, G., QIU, W., GAN, C., VOGELSTEIN, B., ST CROIX, B., KINZLER, K. W. & HUSO, D. L. 2006. Tumor endothelial marker 1 (Tem1) functions in the growth and progression of abdominal tumors. *Proc Natl Acad Sci U S A,* 103**,** 3351-6.

NAYAR, S., CAMPOS, J., CHUNG, M. M., NAVARRO-NUNEZ, L., CHACHLANI, M., STEINTHAL, N., GARDNER, D. H., RANKIN, P., CLOAKE, T., CAAMANO, J. H., MCGETTRICK, H. M., WATSON, S. P., LUTHER, S., BUCKLEY, C. D. & BARONE, F. 2016. Bimodal Expansion of the Lymphatic Vessels Is Regulated by the Sequential Expression of IL-7 and Lymphotoxin alpha1beta2 in Newly Formed Tertiary Lymphoid Structures. *J Immunol*.

NAYLOR, A. J., AZZAM, E., SMITH, S., CROFT, A., POYSER, C., DUFFIELD, J. S., HUSO, D. L., GAY, S., OSPELT, C., COOPER, M. S., ISACKE, C., GOODYEAR, S. R., ROGERS, M. J. & BUCKLEY, C. D. 2012. The mesenchymal stem cell marker CD248 (endosialin) is a negative regulator of bone formation in mice. *Arthritis Rheum,* 64**,** 3334-43.

NAYLOR, A. J., MCGETTRICK, H. M., MAYNARD, W. D., MAY, P., BARONE, F., CROFT, A. P., EGGINTON, S. & BUCKLEY, C. D. 2014. A differential role for CD248 (Endosialin) in PDGF-mediated skeletal muscle angiogenesis. *PLoS One,* 9**,** e107146.

NEHLS, V. & DRENCKHAHN, D. 1991. Heterogeneity of microvascular pericytes for smooth muscle type alpha-actin. *J Cell Biol,* 113**,** 147-54.

NGO, V. N., CORNALL, R. J. & CYSTER, J. G. 2001. Splenic T zone development is B cell dependent. *J Exp Med,* 194**,** 1649-60.

NGO, V. N., KORNER, H., GUNN, M. D., SCHMIDT, K. N., RIMINTON, D. S., COOPER, M. D., BROWNING, J. L., SEDGWICK, J. D. & CYSTER, J. G. 1999. Lymphotoxin alpha/beta and tumor necrosis factor are required for stromal cell expression of homing chemokines in B and T cell areas of the spleen. *J Exp Med,* 189**,** 403-12.

NIEUWENHUIS, P. & OPSTELTEN, D. 1984. Functional anatomy of germinal centers. *Am J Anat,* 170**,** 421-35.

NISHIMURA, M., MURAKAMI, A., HARA, Y. & AZUMA, T. 2011. Characterization of memory B cells responsible for affinity maturation of anti- (4-hydroxy-3-nitrophenyl)acetyl (NP) antibodies. *Int Immunol,* 23**,** 271-85.

NOSSAL, G. J. 1994. Differentiation of the secondary B-lymphocyte repertoire: the germinal center reaction. *Immunol Rev,* 137**,** 173-83.

NOY, P. J., SWAIN, R. K., KHAN, K., LODHIA, P. & BICKNELL, R. 2016. Sprouting angiogenesis is regulated by shedding of the C-type lectin family 14, member A (CLEC14A) ectodomain, catalyzed by rhomboid-like 2 protein (RHBDL2). *FASEB J,* 30**,** 2311-23.

O'CONNOR, B. P., VOGEL, L. A., ZHANG, W., LOO, W., SHNIDER, D., LIND, E. F., RATLIFF, M., NOELLE, R. J. & ERICKSON, L. D. 2006. Imprinting the fate of antigen-reactive B cells through the affinity of the B cell receptor. *J Immunol,* 177**,** 7723-32.

OCHSENBEIN, A. F., SIERRO, S., ODERMATT, B., PERICIN, M., KARRER, U., HERMANS, J., HEMMI, S., HENGARTNER, H. & ZINKERNAGEL, R. M. 2001. Roles of tumour localization, second signals and cross priming in cytotoxic T-cell induction. *Nature,* 411**,** 1058-64.

OECKINGHAUS, A., HAYDEN, M. S. & GHOSH, S. 2011. Crosstalk in NF-kappaB signaling pathways. *Nat Immunol,* 12**,** 695-708.

OGATA, T., YAMAKAWA, M., IMAI, Y. & TAKAHASHI, T. 1996. Follicular dendritic cells adhere to fibronectin and laminin fibers via their respective receptors. *Blood,* 88**,** 2995-3003.

OHL, L., HENNING, G., KRAUTWALD, S., LIPP, M., HARDTKE, S., BERNHARDT, G., PABST, O. & FORSTER, R. 2003. Cooperating mechanisms of CXCR5 and CCR7 in development and organization of secondary lymphoid organs. *J Exp Med,* 197**,** 1199-204.

OKADA, T., MILLER, M. J., PARKER, I., KRUMMEL, M. F., NEIGHBORS, M., HARTLEY, S. B., O'GARRA, A., CAHALAN, M. D. & CYSTER, J. G. 2005. Antigen-engaged B cells undergo chemotaxis toward the T zone and form motile conjugates with helper T cells. *PLoS Biol,* 3**,** e150.

ONDER, L., DANUSER, R., SCANDELLA, E., FIRNER, S., CHAI, Q., HEHLGANS, T., STEIN, J. V. & LUDEWIG, B. 2013. Endothelial cell-specific lymphotoxin-beta receptor signaling is critical for lymph node and high endothelial venule formation. *J Exp Med,* 210**,** 465-73.

OPAVSKY, R., HAVIERNIK, P., JURKOVICOVA, D., GARIN, M. T., COPELAND, N. G., GILBERT, D. J., JENKINS, N. A., BIES, J., GARFIELD, S., PASTOREKOVA, S., OUE, A. & WOLFF, L. 2001. Molecular characterization of the mouse Tem1/endosialin gene regulated by cell density in vitro and expressed in normal tissues in vivo. *J Biol Chem,* 276**,** 38795-807.

OZAKI, K., SPOLSKI, R., ETTINGER, R., KIM, H. P., WANG, G., QI, C. F., HWU, P., SHAFFER, D. J., AKILESH, S., ROOPENIAN, D. C., MORSE, H. C., 3RD, LIPSKY, P. E. & LEONARD, W. J. 2004. Regulation of B cell differentiation and plasma cell generation by IL-21, a novel inducer of Blimp-1 and Bcl-6. *J Immunol,* 173**,** 5361-71.

PARK, S. Y., SAIJO, K., TAKAHASHI, T., OSAWA, M., ARASE, H., HIRAYAMA, N., MIYAKE, K., NAKAUCHI, H., SHIRASAWA, T. & SAITO, T. 1995. Developmental defects of lymphoid cells in Jak3 kinase-deficient mice. *Immunity,* 3**,** 771-82.

PAUS, D., PHAN, T. G., CHAN, T. D., GARDAM, S., BASTEN, A. & BRINK, R. 2006. Antigen recognition strength regulates the choice between extrafollicular plasma cell and germinal center B cell differentiation. *J Exp Med,* 203**,** 1081-91.

PEDUTO, L., DULAUROY, S., LOCHNER, M., SPATH, G. F., MORALES, M. A., CUMANO, A. & EBERL, G. 2009. Inflammation recapitulates the ontogeny of lymphoid stromal cells. *J Immunol,* 182**,** 5789-99.

PEREIRA, J. P., KELLY, L. M., XU, Y. & CYSTER, J. G. 2009. EBI2 mediates B cell segregation between the outer and centre follicle. *Nature,* 460**,** 1122-6.

PHAM, P., BRANSTEITTER, R., PETRUSKA, J. & GOODMAN, M. F. 2003. Processive AID-catalysed cytosine deamination on single-stranded DNA simulates somatic hypermutation. *Nature,* 424**,** 103-7.

PHAM, T. H., BALUK, P., XU, Y., GRIGOROVA, I., BANKOVICH, A. J., PAPPU, R., COUGHLIN, S. R., MCDONALD, D. M., SCHWAB, S. R. & CYSTER, J. G. 2010. Lymphatic endothelial cell sphingosine kinase activity is required for lymphocyte egress and lymphatic patterning. *J Exp Med,* 207**,** 17-27.

PHAN, R. T., SAITO, M., KITAGAWA, Y., MEANS, A. R. & DALLA-FAVERA, R. 2007a. Genotoxic stress regulates expression of the proto-oncogene Bcl6 in germinal center B cells. *Nat Immunol,* 8**,** 1132-9.

PHAN, T. G., GREEN, J. A., GRAY, E. E., XU, Y. & CYSTER, J. G. 2009. Immune complex relay by subcapsular sinus macrophages and noncognate B cells drives antibody affinity maturation. *Nat Immunol,* 10**,** 786-93.

PHAN, T. G., GRIGOROVA, I., OKADA, T. & CYSTER, J. G. 2007b. Subcapsular encounter and complement-dependent transport of immune complexes by lymph node B cells. *Nat Immunol,* 8**,** 992-1000.

PHAN, T. G., PAUS, D., CHAN, T. D., TURNER, M. L., NUTT, S. L., BASTEN, A. & BRINK, R. 2006. High affinity germinal center B cells are actively selected into the plasma cell compartment. *J Exp Med,* 203**,** 2419-24.

PISKURICH, J. F., LIN, K. I., LIN, Y., WANG, Y., TING, J. P. & CALAME, K. 2000. BLIMP-I mediates extinction of major histocompatibility class II transactivator expression in plasma cells. *Nat Immunol,* 1**,** 526-32.

PITTENGER, M. F., MACKAY, A. M., BECK, S. C., JAISWAL, R. K., DOUGLAS, R., MOSCA, J. D., MOORMAN, M. A., SIMONETTI, D. W., CRAIG, S. & MARSHAK, D. R. 1999. Multilineage potential of adult human mesenchymal stem cells. *Science,* 284**,** 143-7.

POND, C. M. 2003. Paracrine relationships between adipose and lymphoid tissues: implications for the mechanism of HIV-associated adipose redistribution syndrome. *Trends Immunol,* 24**,** 13-8.

POND, C. M. & MATTACKS, C. A. 2002. The activation of the adipose tissue associated with lymph nodes during the early stages of an immune response. *Cytokine,* 17**,** 131-9.

QI, H., CANNONS, J. L., KLAUSCHEN, F., SCHWARTZBERG, P. L. & GERMAIN, R. N. 2008. SAP-controlled T-B cell interactions underlie germinal centre formation. *Nature,* 455**,** 764-9.

QU, C., EDWARDS, E. W., TACKE, F., ANGELI, V., LLODRA, J., SANCHEZ-SCHMITZ, G., GARIN, A., HAQUE, N. S., PETERS, W., VAN ROOIJEN, N., SANCHEZ-TORRES, C., BROMBERG, J., CHARO, I. F., JUNG, S., LIRA, S. A. & RANDOLPH, G. J. 2004. Role of CCR8 and other chemokine pathways in the migration of monocyte-derived dendritic cells to lymph nodes. *J Exp Med,* 200**,** 1231-41.

RANDALL, T. D., CARRAGHER, D. M. & RANGEL-MORENO, J. 2008. Development of secondary lymphoid organs. *Annu Rev Immunol,* 26**,** 627-50.

RANUNCOLO, S. M., POLO, J. M., DIEROV, J., SINGER, M., KUO, T., GREALLY, J., GREEN, R., CARROLL, M. & MELNICK, A. 2007. Bcl-6 mediates the germinal center B cell phenotype and lymphomagenesis through transcriptional repression of the DNA-damage sensor ATR. *Nat Immunol,* 8**,** 705-14.

REIF, K., EKLAND, E. H., OHL, L., NAKANO, H., LIPP, M., FORSTER, R. & CYSTER, J. G. 2002. Balanced responsiveness to chemoattractants from adjacent zones determines B-cell position. *Nature,* 416**,** 94-9.

RELJIC, R., WAGNER, S. D., PEAKMAN, L. J. & FEARON, D. T. 2000. Suppression of signal transducer and activator of transcription 3-dependent B lymphocyte terminal differentiation by BCL-6. *J Exp Med,* 192**,** 1841-8.

RENNERT, P. D., BROWNING, J. L. & HOCHMAN, P. S. 1997. Selective disruption of lymphotoxin ligands reveals a novel set of mucosal lymph nodes and unique effects on lymph node cellular organization. *Int Immunol,* 9**,** 1627-39.

RENNERT, P. D., BROWNING, J. L., MEBIUS, R., MACKAY, F. & HOCHMAN, P. S. 1996. Surface lymphotoxin alpha/beta complex is required for the development of peripheral lymphoid organs. *J Exp Med,* 184**,** 1999-2006.

RENNERT, P. D., HOCHMAN, P. S., FLAVELL, R. A., CHAPLIN, D. D., JAYARAMAN, S., BROWNING, J. L. & FU, Y. X. 2001. Essential role of lymph nodes in contact hypersensitivity revealed in lymphotoxin-alpha-deficient mice. *J Exp Med,* 193**,** 1227-38.

RENNERT, P. D., JAMES, D., MACKAY, F., BROWNING, J. L. & HOCHMAN, P. S. 1998. Lymph node genesis is induced by signaling through the lymphotoxin beta receptor. *Immunity,* 9**,** 71-9.

RETTIG, W. J., GARIN-CHESA, P., HEALEY, J. H., SU, S. L., JAFFE, E. A. & OLD, L. J. 1992. Identification of endosialin, a cell surface glycoprotein of vascular endothelial cells in human cancer. *Proc Natl Acad Sci U S A,* 89**,** 10832-6.

REVY, P., MUTO, T., LEVY, Y., GEISSMANN, F., PLEBANI, A., SANAL, O., CATALAN, N., FORVEILLE, M., DUFOURCQ-LABELOUSE, R., GENNERY, A., TEZCAN, I., ERSOY, F., KAYSERILI, H., UGAZIO, A. G., BROUSSE, N., MURAMATSU, M., NOTARANGELO, L. D., KINOSHITA, K., HONJO, T., FISCHER, A. & DURANDY, A. 2000. Activation-induced cytidine deaminase (AID) deficiency causes the autosomal recessive form of the Hyper-IgM syndrome (HIGM2). *Cell,* 102**,** 565-75.

RINN, J. L., KERTESZ, M., WANG, J. K., SQUAZZO, S. L., XU, X., BRUGMANN, S. A., GOODNOUGH, L. H., HELMS, J. A., FARNHAM, P. J., SEGAL, E. & CHANG, H. Y. 2007. Functional demarcation of active and silent chromatin domains in human HOX loci by noncoding RNAs. *Cell,* 129**,** 1311-23.

ROBERTS, C. W., SHUTTER, J. R. & KORSMEYER, S. J. 1994. Hox11 controls the genesis of the spleen. *Nature,* 368**,** 747-9.

RODDA, L. B., BANNARD, O., LUDEWIG, B., NAGASAWA, T. & CYSTER, J. G. 2015. Phenotypic and Morphological Properties of Germinal Center Dark Zone Cxcl12-Expressing Reticular Cells. *J Immunol,* 195**,** 4781-91.

ROOZENDAAL, R. & CARROLL, M. C. 2007. Complement receptors CD21 and CD35 in humoral immunity. *Immunol Rev,* 219**,** 157-66.

ROOZENDAAL, R. & MEBIUS, R. E. 2011. Stromal cell-immune cell interactions. *Annu Rev Immunol,* 29**,** 23-43.

ROOZENDAAL, R., MEBIUS, R. E. & KRAAL, G. 2008. The conduit system of the lymph node. *Int Immunol,* 20**,** 1483-7.

ROOZENDAAL, R., MEMPEL, T. R., PITCHER, L. A., GONZALEZ, S. F., VERSCHOOR, A., MEBIUS, R. E., VON ANDRIAN, U. H. & CARROLL, M. C. 2009. Conduits mediate transport of low-molecular-weight antigen to lymph node follicles. *Immunity,* 30**,** 264-76.

ROSEN, E. D. & MACDOUGALD, O. A. 2006. Adipocyte differentiation from the inside out. *Nat Rev Mol Cell Biol,* 7**,** 885-96.

RUDDLE, N. H. & AKIRAV, E. M. 2009. Secondary lymphoid organs: responding to genetic and environmental cues in ontogeny and the immune response. *J Immunol,* 183**,** 2205-12.

RUPP, C., DOLZNIG, H., PURI, C., SOMMERGRUBER, W., KERJASCHKI, D., RETTIG, W. J. & GARIN-CHESA, P. 2006. Mouse endosialin, a C-type lectin-like cell surface receptor: expression during embryonic development and induction in experimental cancer neoangiogenesis. *Cancer Immun,* 6**,** 10.

SABIN, F. R. 1902. On the origin of the lymphatic system from the veins and the development of the lymph hearts and thoracic duct in the pig. *American Journal of Anatomy,* 1**,** 367-389.

SABIN, F. R. 1904. On the development of the superficial lymphatics in the skin of the pig. *American Journal of Anatomy,* 3**,** 183-195.

SABOURI, Z., SCHOFIELD, P., HORIKAWA, K., SPIERINGS, E., KIPLING, D., RANDALL, K. L., LANGLEY, D., ROOME, B., VAZQUEZ-LOMBARDI, R., ROUET, R., HERMES, J., CHAN, T. D., BRINK, R., DUNN-WALTERS, D. K., CHRIST, D. & GOODNOW, C. C. 2014. Redemption of autoantibodies on anergic B cells by variable-region glycosylation and mutation away from self-reactivity. *Proc Natl Acad Sci U S A,* 111**,** E2567-75.

SCANDELLA, E., BOLINGER, B., LATTMANN, E., MILLER, S., FAVRE, S., LITTMAN, D. R., FINKE, D., LUTHER, S. A., JUNT, T. & LUDEWIG, B. 2008. Restoration of lymphoid organ integrity through the interaction of lymphoid tissue-inducer cells with stroma of the T cell zone. *Nat Immunol,* 9**,** 667-75.

SCHACHT, V., RAMIREZ, M. I., HONG, Y. K., HIRAKAWA, S., FENG, D., HARVEY, N., WILLIAMS, M., DVORAK, A. M., DVORAK, H. F., OLIVER, G. & DETMAR, M. 2003. T1alpha/podoplanin deficiency disrupts normal lymphatic vasculature formation and causes lymphedema. *EMBO J,* 22**,** 3546-56.

SCHEU, S., ALFERINK, J., POTZEL, T., BARCHET, W., KALINKE, U. & PFEFFER, K. 2002. Targeted disruption of LIGHT causes defects in costimulatory T cell activation and reveals cooperation with lymphotoxin beta in mesenteric lymph node genesis. *J Exp Med,* 195**,** 1613-24.

SCHLIEPHAKE, D. E. & SCHIMPL, A. 1996. Blimp-1 overcomes the block in IgM secretion in lipopolysaccharide/anti-mu F(ab')2-co-stimulated B lymphocytes. *Eur J Immunol,* 26**,** 268-71.

SCHNEIDER, P., MACKAY, F., STEINER, V., HOFMANN, K., BODMER, J. L., HOLLER, N., AMBROSE, C., LAWTON, P., BIXLER, S., ACHA-ORBEA, H., VALMORI, D., ROMERO, P., WERNER-FAVRE, C., ZUBLER, R. H., BROWNING, J. L. & TSCHOPP, J. 1999. BAFF, a novel ligand of the tumor necrosis factor family, stimulates B cell growth. *J Exp Med,* 189**,** 1747-56.

SCHULTHEIS, B., NIJMEIJER, B. A., YIN, H., GOSDEN, R. G. & MELO, J. V. 2012. Imatinib mesylate at therapeutic doses has no impact on folliculogenesis or spermatogenesis in a leukaemic mouse model. *Leuk Res,* 36**,** 271-4.

SCHUMANN, K., LAMMERMANN, T., BRUCKNER, M., LEGLER, D. F., POLLEUX, J., SPATZ, J. P., SCHULER, G., FORSTER, R., LUTZ, M. B., SOROKIN, L. & SIXT, M. 2010. Immobilized chemokine fields and soluble chemokine gradients cooperatively shape migration patterns of dendritic cells. *Immunity,* 32**,** 703-13.

SCHWICKERT, T. A., VICTORA, G. D., FOOKSMAN, D. R., KAMPHORST, A. O., MUGNIER, M. R., GITLIN, A. D., DUSTIN, M. L. & NUSSENZWEIG, M. C. 2011. A dynamic T cell-limited checkpoint regulates affinity-dependent B cell entry into the germinal center. *J Exp Med,* 208**,** 1243-52.

SHAFFER, A. L., YU, X., HE, Y., BOLDRICK, J., CHAN, E. P. & STAUDT, L. M. 2000. BCL-6 represses genes that function in lymphocyte differentiation, inflammation, and cell cycle control. *Immunity,* 13**,** 199-212.

SHIH, T. A., MEFFRE, E., ROEDERER, M. & NUSSENZWEIG, M. C. 2002. Role of BCR affinity in T cell dependent antibody responses in vivo. *Nat Immunol,* 3**,** 570-5.

SHULMAN, Z., GITLIN, A. D., WEINSTEIN, J. S., LAINEZ, B., ESPLUGUES, E., FLAVELL, R. A., CRAFT, J. E. & NUSSENZWEIG, M. C. 2014. Dynamic signaling by T follicular helper cells during germinal center B cell selection. *Science,* 345**,** 1058-62.

SIMONAVICIUS, N., ASHENDEN, M., VAN WEVERWIJK, A., LAX, S., HUSO, D. L., BUCKLEY, C. D., HUIJBERS, I. J., YARWOOD, H. & ISACKE, C. M. 2012. Pericytes promote selective vessel regression to regulate vascular patterning. *Blood,* 120**,** 1516-27.

SIMONAVICIUS, N., ROBERTSON, D., BAX, D. A., JONES, C., HUIJBERS, I. J. & ISACKE, C. M. 2008. Endosialin (CD248) is a marker of tumor-associated pericytes in high-grade glioma. *Mod Pathol,* 21**,** 308-15.

SINGER, D. B. 1973. Postsplenectomy sepsis. *Perspect Pediatr Pathol,* 1**,** 285-311.

SINHA, R. K., PARK, C., HWANG, I. Y., DAVIS, M. D. & KEHRL, J. H. 2009. B lymphocytes exit lymph nodes through cortical lymphatic sinusoids by a mechanism independent of sphingosine-1-phosphate-mediated chemotaxis. *Immunity,* 30**,** 434-46.

SIXT, M., KANAZAWA, N., SELG, M., SAMSON, T., ROOS, G., REINHARDT, D. P., PABST, R., LUTZ, M. B. & SOROKIN, L. 2005. The conduit system transports soluble antigens from the afferent lymph to resident dendritic cells in the T cell area of the lymph node. *Immunity,* 22**,** 19-29.

SMITH, K. G., LIGHT, A., NOSSAL, G. J. & TARLINTON, D. M. 1997. The extent of affinity maturation differs between the memory and antibody-forming cell compartments in the primary immune response. *EMBO J,* 16**,** 2996-3006.

SMITH, S. W., EARDLEY, K. S., CROFT, A. P., NWOSU, J., HOWIE, A. J., COCKWELL, P., ISACKE, C. M., BUCKLEY, C. D. & SAVAGE, C. O. 2011. CD248+ stromal cells are associated with progressive chronic kidney disease. *Kidney Int,* 80**,** 199-207.

SONNENBERG, G. F. & ARTIS, D. 2015. Innate lymphoid cells in the initiation, regulation and resolution of inflammation. *Nat Med,* 21**,** 698-708.

SPITS, H. & DI SANTO, J. P. 2011. The expanding family of innate lymphoid cells: regulators and effectors of immunity and tissue remodeling. *Nat Immunol,* 12**,** 21-7.

STAVNEZER, J., GUIKEMA, J. E. & SCHRADER, C. E. 2008. Mechanism and regulation of class switch recombination. *Annu Rev Immunol,* 26**,** 261-92.

SUH, J. M., GAO, X., MCKAY, J., MCKAY, R., SALO, Z. & GRAFF, J. M. 2006. Hedgehog signaling plays a conserved role in inhibiting fat formation. *Cell Metab,* 3**,** 25-34.

SUKUMAR, S., EL SHIKH, M. E., TEW, J. G. & SZAKAL, A. K. 2008. Ultrastructural study of highly enriched follicular dendritic cells reveals their morphology and the periodicity of immune complex binding. *Cell Tissue Res,* 332**,** 89-99.

SUKUMAR, S., SZAKAL, A. K. & TEW, J. G. 2006. Isolation of functionally active murine follicular dendritic cells. *J Immunol Methods,* 313**,** 81-95.

SUN, Z., UNUTMAZ, D., ZOU, Y. R., SUNSHINE, M. J., PIERANI, A., BRENNER-MORTON, S., MEBIUS, R. E. & LITTMAN, D. R. 2000. Requirement for RORgamma in thymocyte survival and lymphoid organ development. *Science,* 288**,** 2369-73.

TACHIBANA, M., TENNO, M., TEZUKA, C., SUGIYAMA, M., YOSHIDA, H. & TANIUCHI, I. 2011. Runx1/Cbfbeta2 complexes are required for lymphoid tissue inducer cell differentiation at two developmental stages. *J Immunol,* 186**,** 1450-7.

TAKEMORI, T., KAJI, T., TAKAHASHI, Y., SHIMODA, M. & RAJEWSKY, K. 2014. Generation of memory B cells inside and outside germinal centers. *Eur J Immunol,* 44**,** 1258-64.

TAMBURINI, B. A., BURCHILL, M. A. & KEDL, R. M. 2014. Antigen capture and archiving by lymphatic endothelial cells following vaccination or viral infection. *Nat Commun,* 5**,** 3989.

TEICHER, B. A. 2007. Newer vascular targets: endosialin (review). *Int J Oncol,* 30**,** 305-12.

TEWALT, E. F., COHEN, J. N., ROUHANI, S. J. & ENGELHARD, V. H. 2012. Lymphatic endothelial cells - key players in regulation of tolerance and immunity. *Front Immunol,* 3**,** 305.

THIEL, G. A. & DOWNEY, H. 1921. The development of the mammalian spleen, with special reference to its hematopoietic activity. *American Journal of Anatomy,* 28**,** 279-339.

TIMENS, W., ROZEBOOM, T. & POPPEMA, S. 1987. Fetal and neonatal development of human spleen: an immunohistological study. *Immunology,* 60**,** 603-9.

TOELLNER, K. M., GULBRANSON-JUDGE, A., TAYLOR, D. R., SZE, D. M. & MACLENNAN, I. C. 1996. Immunoglobulin switch transcript production in vivo related to the site and time of antigen-specific B cell activation. *J Exp Med,* 183**,** 2303-12.

TOELLNER, K. M., LUTHER, S. A., SZE, D. M., CHOY, R. K., TAYLOR, D. R., MACLENNAN, I. C. & ACHA-ORBEA, H. 1998. T helper 1 (Th1) and Th2 characteristics start to develop during T cell priming and are associated with an immediate ability to induce immunoglobulin class switching. *J Exp Med,* 187**,** 1193-204.

TOMKOWICZ, B., RYBINSKI, K., FOLEY, B., EBEL, W., KLINE, B., ROUTHIER, E., SASS, P., NICOLAIDES, N. C., GRASSO, L. & ZHOU, Y. 2007. Interaction of endosialin/TEM1 with extracellular matrix proteins mediates cell adhesion and migration. *Proc Natl Acad Sci U S A,* 104**,** 17965-70.

TOMKOWICZ, B., RYBINSKI, K., SEBECK, D., SASS, P., NICOLAIDES, N. C., GRASSO, L. & ZHOU, Y. 2010. Endosialin/TEM-1/CD248 regulates pericyte proliferation through PDGF receptor signaling. *Cancer Biol Ther,* 9**,** 908-15.

TRIBIOLI, C., FRASCH, M. & LUFKIN, T. 1997. Bapx1: an evolutionary conserved homologue of the Drosophila bagpipe homeobox gene is expressed in splanchnic mesoderm and the embryonic skeleton. *Mech Dev,* 65**,** 145-62.

TRIBIOLI, C. & LUFKIN, T. 1999. The murine Bapx1 homeobox gene plays a critical role in embryonic development of the axial skeleton and spleen. *Development,* 126**,** 5699-711.

TUMANOV, A. V., KUPRASH, D. V., MACH, J. A., NEDOSPASOV, S. A. & CHERVONSKY, A. V. 2004. Lymphotoxin and TNF produced by B cells are dispensable for maintenance of the follicle-associated epithelium but are required for development of lymphoid follicles in the Peyer's patches. *J Immunol,* 173**,** 86-91.

USUI, K., HONDA, S., YOSHIZAWA, Y., NAKAHASHI-ODA, C., TAHARA-HANAOKA, S., SHIBUYA, K. & SHIBUYA, A. 2012. Isolation and characterization of naive follicular dendritic cells. *Mol Immunol,* 50**,** 172-6.

VALDEZ, Y., MAIA, M. & CONWAY, E. M. 2012. CD248: reviewing its role in health and disease. *Curr Drug Targets,* 13**,** 432-9.

VAN DE PAVERT, S. A. & MEBIUS, R. E. 2010. New insights into the development of lymphoid tissues. *Nat Rev Immunol,* 10**,** 664-74.

VAN DE PAVERT, S. A., OLIVIER, B. J., GOVERSE, G., VONDENHOFF, M. F., GREUTER, M., BEKE, P., KUSSER, K., HÖPKEN, U. E., LIPP, M., NIEDERREITHER, K., BLOMHOFF, R., SITNIK, K., AGACE, W. W., RANDALL, T. D., DE JONGE, W. J. & MEBIUS, R. E. 2009. Chemokine CXCL13 is essential for lymph node initiation and is induced by retinoic acid and neuronal stimulation. *Nature Immunology,* 10**,** 1193-1199.

VAN DELFT, M. A., HUITEMA, L. F. & TAS, S. W. 2015. The contribution of NF-kappaB signalling to immune regulation and tolerance. *Eur J Clin Invest,* 45**,** 529-39.

VARGAS, F., VIVES-PI, M., SOMOZA, N., ARMENGOL, P., ALCALDE, L., MARTI, M., COSTA, M., SERRADELL, L., DOMINGUEZ, O., FERNANDEZ-LLAMAZARES, J., JULIAN, J. F., SANMARTI, A. & PUJOL-BORRELL, R. 1998. Endotoxin contamination may be responsible for the

unexplained failure of human pancreatic islet transplantation. *Transplantation,* 65**,** 722-7.

VARGAS, F., VIVES-PI, M., SOMOZA, N., FERNANDEZ-LLAMAZARES, J. & PUJOL-BORRELL, R. 1997. Endotoxin activity of collagenase and human islet transplantation. *Lancet,* 350**,** 641.

VASANWALA, F. H., KUSAM, S., TONEY, L. M. & DENT, A. L. 2002. Repression of AP-1 function: a mechanism for the regulation of Blimp-1 expression and B lymphocyte differentiation by the B cell lymphoma-6 protooncogene. *J Immunol,* 169**,** 1922-9.

VASSILEVA, G., SOTO, H., ZLOTNIK, A., NAKANO, H., KAKIUCHI, T., HEDRICK, J. A. & LIRA, S. A. 1999. The reduced expression of 6Ckine in the plt mouse results from the deletion of one of two 6Ckine genes. *J Exp Med,* 190**,** 1183-8.

VEIGA-FERNANDES, H., COLES, M. C., FOSTER, K. E., PATEL, A., WILLIAMS, A., NATARAJAN, D., BARLOW, A., PACHNIS, V. & KIOUSSIS, D. 2007. Tyrosine kinase receptor RET is a key regulator of Peyer's patch organogenesis. *Nature,* 446**,** 547-51.

VENANZI, E. S., GRAY, D. H., BENOIST, C. & MATHIS, D. 2007. Lymphotoxin pathway and Aire influences on thymic medullary epithelial cells are unconnected. *J Immunol,* 179**,** 5693-700.

VICTORA, G. D., DOMINGUEZ-SOLA, D., HOLMES, A. B., DEROUBAIX, S., DALLA-FAVERA, R. & NUSSENZWEIG, M. C. 2012. Identification of human germinal center light and dark zone cells and their relationship to human B-cell lymphomas. *Blood,* 120**,** 2240-8.

VICTORA, G. D. & NUSSENZWEIG, M. C. 2012. Germinal centers. *Annu Rev Immunol,* 30**,** 429-57.

VICTORA, G. D., SCHWICKERT, T. A., FOOKSMAN, D. R., KAMPHORST, A. O., MEYER-HERMANN, M., DUSTIN, M. L. & NUSSENZWEIG, M. C. 2010. Germinal center dynamics revealed by multiphoton microscopy with a photoactivatable fluorescent reporter. *Cell,* 143**,** 592-605.

VIRGINTINO, D., GIROLAMO, F., ERREDE, M., CAPOBIANCO, C., ROBERTSON, D., STALLCUP, W. B., PERRIS, R. & RONCALI, L. 2007. An intimate interplay between precocious, migrating pericytes and endothelial cells governs human fetal brain angiogenesis. *Angiogenesis,* 10**,** 35-45.

VISSERS, J. L., HARTGERS, F. C., LINDHOUT, E., FIGDOR, C. G. & ADEMA, G. J. 2001. BLC (CXCL13) is expressed by different dendritic cell subsets in vitro and in vivo. *Eur J Immunol,* 31**,** 1544-9.

VOIGT, I., CAMACHO, S. A., DE BOER, B. A., LIPP, M., FORSTER, R. & BEREK, C. 2000. CXCR5-deficient mice develop functional germinal centers in the splenic T cell zone. *Eur J Immunol,* 30**,** 560-7.

VON ANDRIAN, U. H. & MEMPEL, T. R. 2003. Homing and cellular traffic in lymph nodes. *Nat Rev Immunol,* 3**,** 867-78.

VONDENHOFF, M. F., DESANTI, G. E., CUPEDO, T., BERTRAND, J. Y., CUMANO, A., KRAAL, G., MEBIUS, R. E. & GOLUB, R. 2008a. Separation of splenic red and white pulp occurs before birth in a LTalphabeta-independent manner. *J Leukoc Biol,* 84**,** 152-61.

VONDENHOFF, M. F., GREUTER, M., GOVERSE, G., ELEWAUT, D., DEWINT, P., WARE, C. F., HOORWEG, K., KRAAL, G. & MEBIUS, R. E. 2009. LTbetaR signaling induces cytokine expression and up-regulates lymphangiogenic factors in lymph node anlagen. *J Immunol,* 182**,** 5439-45.

VONDENHOFF, M. F., VAN DE PAVERT, S. A., DILLARD, M. E., GREUTER, M., GOVERSE, G., OLIVER, G. & MEBIUS, R. E. 2008b. Lymph sacs are not required for the initiation of lymph node formation. *Development,* 136**,** 29-34.

WANG, X., CHO, B., SUZUKI, K., XU, Y., GREEN, J. A., AN, J. & CYSTER, J. G. 2011. Follicular dendritic cells help establish follicle identity and promote B cell retention in germinal centers. *J Exp Med,* 208**,** 2497-510.

WANG, X. J. & LI, Y. H. 2015. Inhibition of human chronic myelogenous leukemia K562 cell growth following combination treatment with resveratrol and imatinib mesylate. *Genet Mol Res,* 14**,** 6413-8.

WARE, C. F. 2005. Network communications: lymphotoxins, LIGHT, and TNF. *Annu Rev Immunol,* 23**,** 787-819.

WEIH, F., CARRASCO, D., DURHAM, S. K., BARTON, D. S., RIZZO, C. A., RYSECK, R. P., LIRA, S. A. & BRAVO, R. 1995. Multiorgan inflammation and hematopoietic abnormalities in mice with a targeted disruption of RelB, a member of the NF-kappa B/Rel family. *Cell,* 80**,** 331-40.

WHITE, A., CARRAGHER, D., PARNELL, S., MSAKI, A., PERKINS, N., LANE, P., JENKINSON, E., ANDERSON, G. & CAAMANO, J. H. 2007. Lymphotoxin a-dependent and -independent signals regulate stromal organizer cell homeostasis during lymph node organogenesis. *Blood,* 110**,** 1950-9.

WIGLE, J. T. & OLIVER, G. 1999. Prox1 function is required for the development of the murine lymphatic system. *Cell,* 98**,** 769-78.

WILHELM, A., ALDRIDGE, V., HALDAR, D., NAYLOR, A. J., WESTON, C. J., HEDEGAARD, D., GARG, A., FEAR, J., REYNOLDS, G. M., CROFT, A. P., HENDERSON, N. C., BUCKLEY, C. D. & NEWSOME, P. N. 2016. CD248/endosialin critically regulates hepatic stellate cell proliferation during chronic liver injury via a PDGF-regulated mechanism. *Gut,* 65**,** 1175-85.

WILKE, G., STEINHAUSER, G., GRUN, J. & BEREK, C. 2010. In silico subtraction approach reveals a close lineage relationship between follicular dendritic cells and BP3(hi) stromal cells isolated from SCID mice. *Eur J Immunol,* 40**,** 2165-73.

WILLIAM, J., EULER, C. & SHLOMCHIK, M. J. 2005. Short-lived plasmablasts dominate the early spontaneous rheumatoid factor response: differentiation pathways, hypermutating cell types, and affinity maturation outside the germinal center. *J Immunol,* 174**,** 6879-87.

XU, Z., ZAN, H., PONE, E. J., MAI, T. & CASALI, P. 2012. Immunoglobulin class-switch DNA recombination: induction, targeting and beyond. *Nat Rev Immunol,* 12**,** 517-31.

YANG, C. Y., VOGT, T. K., FAVRE, S., SCARPELLINO, L., HUANG, H. Y., TACCHINI-COTTIER, F. & LUTHER, S. A. 2014. Trapping of naive lymphocytes triggers rapid growth and remodeling of the fibroblast network in reactive murine lymph nodes. *Proc Natl Acad Sci U S A,* 111**,** E109-18.

YASUDA, T., KUWABARA, T., NAKANO, H., ARITOMI, K., ONODERA, T., LIPP, M., TAKAHAMA, Y. & KAKIUCHI, T. 2007. Chemokines CCL19 and CCL21 promote activation-induced cell death of antigen-responding T cells. *Blood,* 109**,** 449-56.

YI, T., WANG, X., KELLY, L. M., AN, J., XU, Y., SAILER, A. W., GUSTAFSSON, J. A., RUSSELL, D. W. & CYSTER, J. G. 2012. Oxysterol gradient generation by lymphoid stromal cells guides activated B cell movement during humoral responses. *Immunity,* 37**,** 535-48.

YIN, L., WU, L., WESCHE, H., ARTHUR, C. D., WHITE, J. M., GOEDDEL, D. V. & SCHREIBER, R. D. 2001. Defective lymphotoxin-beta receptor-induced NF-kappaB transcriptional activity in NIK-deficient mice. *Science,* 291**,** 2162-5.

YOKOTA, Y., MANSOURI, A., MORI, S., SUGAWARA, S., ADACHI, S., NISHIKAWA, S. & GRUSS, P. 1999. Development of peripheral lymphoid organs and natural killer cells depends on the helix-loop-helix inhibitor Id2. *Nature,* 397**,** 702-6.

YOSHIDA, H., HONDA, K., SHINKURA, R., ADACHI, S., NISHIKAWA, S., MAKI, K., IKUTA, K. & NISHIKAWA, S. I. 1999. IL-7 receptor alpha+ CD3(-) cells in the embryonic intestine induces the organizing center of Peyer's patches. *Int Immunol,* 11**,** 643-55.

YOSHIDA, H., KAWAMOTO, H., SANTEE, S. M., HASHI, H., HONDA, K., NISHIKAWA, S., WARE, C. F., KATSURA, Y. & NISHIKAWA, S. I. 2001. Expression of alpha(4)beta(7) integrin defines a distinct pathway of lymphoid progenitors committed to T cells, fetal intestinal lymphotoxin producer, NK, and dendritic cells. *J Immunol,* 167**,** 2511-21.

YOSHIDA, H., NAITO, A., INOUE, J., SATOH, M., SANTEE-COOPER, S. M., WARE, C. F., TOGAWA, A., NISHIKAWA, S. & NISHIKAWA, S. 2002. Different cytokines induce surface lymphotoxin-alphabeta on IL-7 receptor-alpha cells that differentially engender lymph nodes and Peyer's patches. *Immunity,* 17**,** 823-33.

ZAHEEN, A., BOULIANNE, B., PARSA, J. Y., RAMACHANDRAN, S., GOMMERMAN, J. L. & MARTIN, A. 2009. AID constrains germinal center size by rendering B cells susceptible to apoptosis. *Blood,* 114**,** 547-54.

ZAHEEN, A. & MARTIN, A. 2011. Activation-induced cytidine deaminase and aberrant germinal center selection in the development of humoral autoimmunities. *Am J Pathol,* 178**,** 462-71.

ZHANG, Y., GARCIA-IBANEZ, L. & TOELLNER, K. M. 2016. Regulation of germinal center B-cell differentiation. *Immunol Rev,* 270**,** 8-19.

ZHANG, Y., MEYER-HERMANN, M., GEORGE, L. A., FIGGE, M. T., KHAN, M., GOODALL, M., YOUNG, S. P., REYNOLDS, A., FALCIANI, F., WAISMAN, A., NOTLEY, C. A., EHRENSTEIN, M. R., KOSCO-VILBOIS, M. & TOELLNER, K. M. 2013. Germinal center B cells govern their own fate via antibody feedback. *J Exp Med,* 210**,** 457-64.

ZOTOS, D., COQUET, J. M., ZHANG, Y., LIGHT, A., D'COSTA, K., KALLIES, A., CORCORAN, L. M., GODFREY, D. I., TOELLNER, K. M., SMYTH, M. J., NUTT, S. L. & TARLINTON, D. M. 2010. IL-21 regulates germinal center B cell differentiation and proliferation through a B cell-intrinsic mechanism. *J Exp Med,* 207**,** 365-78.

ZUCCARINO-CATANIA, G. V., SADANAND, S., WEISEL, F. J., TOMAYKO, M. M., MENG, H., KLEINSTEIN, S. H., GOOD-JACOBSON, K. L. & SHLOMCHIK, M. J. 2014. CD80 and PD-L2 define functionally distinct memory B cell subsets that are independent of antibody isotype. *Nat Immunol,* 15**,** 631-7.